2038-5625

Italian Journal of Agrometeorology

Rivista Italiana di Agrometeorologia

n. 2 – 2024

SCIENTIFIC DIRECTOR

Simone Orlandini
Department of Agriculture, Food, Environment and Forestry (DAGRI)
University of Florence
Piazzale delle Cascine 18 – 50144, Firenze (FI), Italia
Tel. +39 055 2755755
simone.orlandini@unifi.it

PUBLICATION DIRECTOR

Francesca Ventura
Department of Agricultural and Food Sciences
University of Bologna
Via Fanin, 44 – 40127 Bologna (BO), Italia
Tel. +39 051 20 96 658
francesca.ventura@unibo.it

EDITORIAL BOARD

Filiberto Altobelli - Orcid 0000-0002-2499-8640 -Council for Agricultural Research and Economics (CREA), Research Centre for Agricultural Policies and Bioeconomy, Rome, Italy
economic sustainability, ecosystem services, water resource

Pierluigi Calanca - Orcid 0000-0003-3113-2885 - Department of Agroecology and Environment, Agroscope, Zurich, Switzerland
climate change, micrometeorology, evapotranspiration, extreme events, downscaling

Gabriele Cola - Orcid 0000-0003-2561-0908 - Department of Agricultural and Environmental Sciences, University of Milan, Italy
phenology, crop modelling, agroecology

Simona Consoli - Orcid 0000-0003-1100-654X - Department Agriculture, Food and Environment, University of Catania, Italy
micrometeorology, evapotranspiration, irrigation, remote sensing

Anna Dalla Marta - Orcid 0000-0002-4606-7521 - Department of Agriculture, Food, Environment and Forestry (DAGRI), University of Florence, Italy
cropping systems, crop growth and production, crop management

Joseph Eitzinger - Orcid 0000-0001-6155-2886 - Institute of Meteorology and Climatology (BOKU-Met), WG Agrometeorology Department of Water, Atmosphere and Environment (WAU), University of Natural Resources and Life Sciences, Vienna, Austria
agrometeorology, crop modelling, climate change impacts on agriculture

Branislava Lalic - Orcid 0000-0001-5790-7533 - Faculty of Agriculture, Meteorology and Biophysics, University of Novi Sad, Serbia
biosphere-atmosphere feedback, plant-atmosphere physical processes parameterisation, plant-related weather and climate indices

Carmelo Maucieri - Orcid 0000-0003-4004-6612 - Department of Agronomy, Food, Natural resources, Animals and Environment (DAFNAE), University of Padova, Italy
climate change, adaptation, crops irrigation, crops fertilization

Marco Napoli - Orcid 0000-0002-7454-9341 - Department of Agriculture, Food, Environment and Forestry (DAGRI) - University of Florence, Italy
field crops, soil hydrology and crop water requirements, soil tillage and management

Park Eunwoo - Orcid 0000-0001-8305-5709 - Field Support Education Division, Epinet Co., Ltd, Seoul National University, Gangwon-do, South Korea
agrometeorology, crop protection, plant disease modelling

Valentina Pavan - Orcid 0000-0002-9608-1903 - ARPAE-SIMC Emilia-Romagna, Bologna, Italy
climatology, climate variability, climate impacts, climate change

Federica Rossi - Orcid 0000-0003-4428-4749 - CNR – Institute of Bioeconomy, Bologna, Italy
sustainable orchard management, ecophysiology, micrometeorology

Levent Şaylan - Orcid 0000-0003-3233-0277 - Faculty of Aeronautics and Astronautics, Department of Meteorological Engineering, Istanbul Technical University, Turkey
agrometeorology, evapotranspiration and drought, micrometeorology, impacts of climate change on agriculture

Vesselin A. Alexandrov - Institute of Climate, Atmosphere and Water Research, Bulgarian Academy of Science
climate variability and change, extreme events, vulnerability and adaptation, statistical and dynamic simulation models of climate and ecosystems

Domenico Ventrella - Orcid 0000-0001-8761-028X - Council for Agricultural Research and Economics (CREA), Research Center Agriculture and Environment, Bari, Italy
climate change impact, climate change adaptation and mitigation, cropping system modelling, sustainable agriculture

Fabio Zottele - Orcid 0000-0002-1015-5511 - Fondazione Edmund Mach, San Michele all'Adige, Italy
agrometeorology, GIS, remote sensing

Cover photo by Maurizio Borin

Italian Journal of Agrometeorology

n. 2 - 2024

Firenze University Press

The ***Italian Journal of Agrometeorology*** (***IJAm - Rivista Italiana di Agrometeorologia***) is the official periodical of the Italian Association of Agrometeorology (AIAM) and aims to publish original scientific contributions in English on agrometerology, as a science that studies the interactions of hydrological and meteorological factors with the agricultural and forest ecosystems, and with agriculture in its broadest sense (including livestock and fisheries).

https://riviste.fupress.net/index.php/IJAm
ISSN 2038-5625 (print)

Italian Association of Agrometeorology (AIAM)
Presidente: Francesca Ventura (francesca.ventura@unibo.it)
Vicepresidente: Gabriele Cola
Consiglieri: Filiberto Altobelli, Anna dalla Marta, Chiara Epifani, Federica Rossi, Emanuele Scalcione, Danilo Tognetti
Revisori dei conti: Simone Ugo Maria Bregaglio, Bruno Di Lena, Marco Secondo Gerardi
Segreteria: Simone Falzoi, Emanuela Forni, Tiziana La Iacona, Mattia Sanna, Irene Vercellino
e-mail AIAM: segreteria@agrometeorologia.it
Sede legale: via Caproni, 8 - 50144 Firenze
web: www.agrometeorologia.it
e-mail Italian Journal of Agrometeorology: ijagrometeorology@agrometeorologia.it

SUBSCRIPTION INFORMATION
IJAm articles are freely available online, but print editions are available to paying subscribers. Subscription rates are in Eur and are applicable worldwide.
Annual Subscription: € 50,00 Single Issue: € 25,00

CONTACT INFORMATION
Please contact ordini@fupress.com, if you have any questions about your subscription or if you would like to place an order for the print edition. Information on payment methods will be provided after your initial correspondence.

OPEN ACCESS

© 2024 Author(s)

Content license: except where otherwise noted, the present work is released under Creative Commons Attribution 4.0 International license (CC BY 4.0: https://creativecommons.org/licenses/by/4.0/legalcode). This license allows you to share any part of the work by any means and format, modify it for any purpose, including commercial, as long as appropriate credit is given to the author, any changes made to the work are indicated and a URL link is provided to the license.

Metadata license: all the metadata are released under the Public Domain Dedication license (CC0 1.0 Universal: https://creativecommons.org/publicdomain/zero/1.0/legalcode).

Published by Firenze University Press

Firenze University Press
Università degli Studi di Firenze
via Cittadella, 7, 50144 Firenze, Italy
www.fupress.com

Italian Journal of Agrometeorology
Rivista Italiana di Agrometeorologia

Firenze University Press
https://riviste.fupress.net/index.php/IJAm

OPEN ACCESS

Citation: Sarfaraz, S., Asgharzadeh, A., & Zabihi, H. (2024). Assessing the effects of water stress and bio-organic fertilizers on English and French Lavandula species in different locations. *Italian Journal of Agrometeorology* (2): 3-22. doi: 10.36253/ijam-2878

Received: July 21, 2024

Accepted: November 22, 2024

Published: December 30, 2024

© 2024 Author(s). This is an open access, peer-reviewed article published by Firenze University Press (https://www.fupress.com) and distributed, except where otherwise noted, under the terms of the CC BY 4.0 License for content and CC0 1.0 Universal for metadata.

Data Availability Statement: All relevant data are within the paper and its Supporting Information files.

Competing Interests: The Author(s) declare(s) no conflict of interest.

Assessing the effects of water stress and bio-organic fertilizers on English and French Lavandula species in different locations

Somayeh Sarfaraz[1], Ahmad Asgharzadeh[1,*], Hamidreza Zabihi[2]

[1] *Department of Agriculture, Shirvan Branch, Islamic Azad University, North Khorasan, Iran*
[2] *Assistant Professor, Khorasan Razavi Agricultural and Natural Resources Research and Education Center, Iran*
*Corresponding author. E-mail: ah.asgharzadeh@iau.ac.ir

Abstract. A study was conducted utilizing a factorial split-plot design within complete randomized blocks to evaluate the effects of water stress (at 95±5, 75±5, 50±5, and 25±5% of the field capacity (FC)) and various fertilizer sources (Azotobacter-Psedomonas Bacterial (APB), arbuscular mycorrhizal fungi (AMFs), and biochar (BI), applied individually and in combination, along with a control treatment on the two species of lavender (French and English) in two distinct climates (Fars and Hamedan) in Iran. The results revealed that severe water deficit stress reduced the growth, yield, and essential oil content in both lavender species. APB+AMFs+BI and APB+BI led to the highest flower yield for French lavender in Fars and Hamedan while subjected to well-watered conditions. The essential oil yield significantly decreased in both experimental regions under 25% FC. Employing APB+BI under 75 and 50% FC treatments led to the highest essential oil content (4.23 and 1.56%, respectively) in English lavender. Linalool showed the highest average (22.46 to 30.06%) in both species. French and English lavender in Fars showed significant differences in fatty acid compositions, but no such differences were reported in Hamedan. APB+BI emerged as the most effective fertilizer combination in terms of total fatty acids and rank index. Simultaneous use of bio-organic fertilizers yielded appropriate results under water-deficient conditions. Finally, the study underscored the strong correlation between climatic parameters such as rainfall and temperature, as well as the efficacy of different fertilizer sources, emphasizing that climatic condition and plant species can significantly impact the effectiveness of fertilizer use.

Keywords: Azotobacter-Psedomonas Bacterial, biochar, essential oil content, fatty acid compositions, irrigation regimes.

HIGHLIGHT

- English and French lavender species varied in biochemistry and quality traits across climates.
- Water stress conditions (25% FC) reduced yield attributes, including flower yield and total biomass.

– Linalool, a fatty acid composition in the essential oil, had the highest average in both species.
– Azotobacter-Psedomonas Bacterial + Biochar proved most effective in total fatty acid content.

INTRODUCTION

Lavandula spp., as a member of the Lamiaceae family, is considered as a distinguished genus of flowering plants commonly related to aromatic herbs such as mint, basil, and thyme. The above-mentioned perennial plant, originally native to the Mediterranean region, has garnered global recognition due to its diverse applications in horticulture, medicine, and gastronomy (Pokajewicz *et al*. 2021; Özsevinç and Alkan 2023). *Lavandula angustifolia* (English lavender) and *L. stoechas* (French lavender) are regarded as two notably cultivated and commercially significant varieties of lavender species (Crişan *et al*. 2023). *L. angustifolia*, which is native to the Mediterranean region, is extensively grown for its aromatic flowers and essential oil. In addition, *L. stoechas*, known as Spanish lavender or butterfly lavender, is found in specific regions of Southern Europe and North Africa. "French lavender", which is cultivated in French gardens, is widely used in French perfumes and soaps, despite its nomenclature. It is worth noting that French lavender differs from the lavender species native to France such as *L. angustifolia* (Du and Rennenberg 2018; Peçanha *et al*. 2023). Studies conducted in various climatic conditions can provide valuable insights due to the significance of this medicinal plant and distinct characteristics of its two main species in terms of essential oil quality.

Water scarcity significantly impacts the growth and yield of agricultural, horticultural, and medicinal plants, particularly in arid and semi-arid regions (Nouri *et al*. 2023). It directly affects processes like leaf reduction, stomatal closure, diminished stomatal conductance, and decreased chloroplast and protoplasmic components, leading to reduced photosynthetic efficiency (Wahab *et al*. 2022; Nouri *et al*. 2023). Water stress also affects biochemical processes related to photosynthesis and indirectly reduces carbon dioxide entry into closed stomata (Afshari *et al*. 2022). Furthermore, it hampers the transport of photosynthetic materials, saturating leaves and limiting photosynthesis, ultimately impairing plant growth and yield (Li *et al*. 2024).

Various strategies are used including employing arbuscular mycorrhizal fungi (AMFs) and plant growth-promoting rhizobacteria (PGPRs) to mitigate the adverse effects of drought stress on plants (Begum *et al*. 2022). Biofertilizers, which contain beneficial microorganisms, are generated for specific objectives such as nitrogen fixation (Soumare *et al*. 2020), phosphate ion release (Kumar *et al*. 2022), mobilization of potassium and iron from their insoluble compounds, and the like (Jiao *et al*., 2024). AMFs, which can increase plant growth hormones such as cytokinins, gibberellins, and auxins, play a crucial role in stimulating plant growth (Liu *et al*. 2023). Such enhancement is achieved through increased water conductivity in the roots, leading to elevated rates of transpiration and evaporation (Liu *et al*. 2023), improved plant nutritional conditions by enhancing water and nutrient absorption, especially for less mobile elements such as phosphorus (Wahab *et al*. 2023), better plant establishment (Mitra *et al*., 2021), and raised water use efficiency (Sun and Shahrajabian 2023). Biological fertilizers, which contain beneficial bacteria and fungi, are applied for specific objectives such as nitrogen fixation, phosphate ion release, and mobilization of iron and potassium from their insoluble compounds (Singh *et al*. 2021). Such bacteria, which are typically established in the root environment, contribute to nutrient absorption by the plant (Singh *et al*. 2021). Some sources indicate the positive impact of biological fertilizers on the growth of medicinal plants such as *Thymus vulgaris* L. (Nadjafi *et al*. 2014), *Catharanthus roseus* L. (Sharma *et al*. 2023), and *Mentha aquatic* L. (Javanmard *et al*. 2022). Furthermore, the synergistic combination of AMFs and PGPRs enhances the quantity and quality of various plants such as *Melissa officinalis* L. (Eshaghi Gorgi *et al*. 2022), tobacco (Begum *et al*. 2022), soybean (Sheteiwy *et al*. 2021), and common myrtle (Azizi *et al*., 2021) under environmentally stressful conditions such as drought.

Biochar (BI), which is considered as a soil organic amendment, improves the physical and chemical traits of soil, increases nutrient availability, diminishes leaching of elements, and enhances agricultural production (Allohverdi *et al*. 2021; Saha *et al*. 2022). BI can potentially enhance plant growth by improving the chemical, physical, and biological traits of soil such as increasing soil moisture availability, leading to higher crop yields (Diatta *et al*. 2020). Adding BI can increase water retention capacity in the soil. In other words, soil amendment with BI can improve crop production by conserving more rainwater in arid regions (Allohverdi *et al*. 2021), as well as reducing the frequency or amount of irrigation water required (Zhang *et al*. 2020).

Lavender, valued for its medicinal essential oil, is grown for pharmaceutical, perfumery, and cosmetic purposes. Research on cultivating and comparing English and French varieties, of interest to farmers and producers, is limited. Additionally, there's a lack of studies on lavender's growth and physiology under different irri-

gation regimes in field cultivation, crucial due to water crises worldwide and the importance of medicinal plant cultivation. Organic fertilizers, known for their environmental friendliness, are gaining traction. They improve plant stress tolerance and alter metabolites and physiological processes positively. This study aims to explore the morphological and biochemical responses of English and French lavender to AMFs, PGPRs, and BI under varied irrigation and climate conditions in Hamedan and Fars.

MATERIALS AND METHODS

Experimental design and study area

This study followed a split-plot factorial scheme implemented in randomized complete block design layouts with three replications in two regions including Firuzabad (Fars) and Hamedan (Hamedan). The present study was conducted during the 2022-23. The maximum, minimum, and average air temperature in Hamedan equaled 36.8, 3.6, and 9.6 °C, respectively. The annual rainfall totaled 317.7 mm, indicating variability across different months. Hamedan with geographical coordinates of 34.80°N and 48.52°E is situated at an altitude of 1741 m above sea level. Firuzabad in Fars, which is located at an altitude of 1600 m above sea level, has an annual average temperature and precipitation equal to 21.78°C and 522 mm, respectively. The location of Fars is specified by coordinates 36.85°N and 54.44°E (Table 1).

Table 1. Geographical and climatic characteristics of investigated experimental sites (Fars and Hamedan) in Iran.

Experimental sites	Latitude	Longitude	Elevation (m a.s.l.)	Avg. Precipitation (mm)	Avg. Temperature (°C)
Fars	36.85° N	54.44° E	1600	522	21.78
Hamedan	34.80°N	48.52°E	1741	317.7	9.6

Table 2. Soil characteristics in experimental sites (Fars and Hamedan, Iran) - 0-30 cm depth,

Characteristic	Fars	Hamedan
Texture	Loam	Sandy-Loam
Sand (2-0.05 mm, %)	30.1	41
Silt (0.05-0.002 mm, %)	43.3	28
Clay (< 0.002 mm, %)	25.4	31
pH	7.44	7.9
Electrical conductivity in saturated extract (dS/m)	1.54	1.88
Organic matter (%)	0.78	0.78
Nitrogen (ppm of soil)	1.88	1.48
Phosphorus extractable with sodium bicarbonate (ppm of soil)	8.71	11.25
Potassium extractable (ppm of soil)	318	281
Iron extractable with DTPA (ppm of soil)	1.87	1.21
Manganese extractable with DTPA (ppm of soil)	3.28	2.79
Copper extractable with DTPA (ppm of soil)	0.50	0.71
Zinc extractable with DTPA (ppm of soil)	0.49	0.59

Experimental treatments and setup

The initial factor in this experiment involved inducing irrigation regimes at four levels, especially at 95 ± 5, 75 ± 5, 50 ± 5, and 25 ± 5% of the field capacity (FC). The second factor comprised diverse combinations of Azotobacter-Psedomonas Bacterial (APB), AMFs (*Funneliformis mosseae* and *Funneliformis intraradices*), and BI, applied individually and in combinations, along with a control treatment (no application), resulting in forming a total of 96 experimental plots. The third factor assessed the responses of English (*L. angustifolia*) and French lavender (*L. angustifolia*) which serve as the focal plant species under investigation.

The soil structure and concentration of macro- and micro-nutrients were reviewed in both study areas prior to planting (Table 2). The procedure proposed by Carter and Gregorich (2007) was applied to ascertain the concentration of soil elements and various soil characteristics. All of the essential micro- and macro-nutrients were present at levels deemed adequate to support the growth of plants.

The APB and AMFs isolated from the rhizosphere of maize and wheat plants were obtained from the Soil and Water Research Institute in Karaj, Iran. The fungal inoculum and roots, comprising spores, and colonized root fragments were incorporated into the sandy substrate at a rate of 50 g kg^{-1} of soil around the root zone (Agnihotri *et al*., 2021). The root colonization percentage was measured employing the method proposed by Campo *et al*. (2020), indicating that the colonization level in fungal treatments was above 50%. The aforementioned value was below 10% in other treatments, indicating proper inoculation of fungi with plant roots. Concurrently, a bacterial inoculum with an approximate population of 10^7 colony-forming units (CFU/ml) at the time of planting was employed (Yadav *et al*. 2020). A combination of *Azotobacter* sp. strain 5 and *Pseudomonas fluorescens* strain 168 was used here. Biochar application as a BI fer-

tilizer was achieved from the Fifth Season Company and utilized at a rate of 3 tons per ha (wood BI) following the recommendations provided by the manufacturer. All of the fertilizers were applied simultaneously with planting and inoculated into the soil.

Seedlings for both lavender species were cultivated in seedling trays and transplanted to the field after selecting nearly uniform seedlings (approximately 5 cm in height). Each experimental plot, measuring 6 × 3 m (18 m^2), had six planting rows with 50-cm spacing and 40-cm intervals between plants. Plot and block spacing were designated as one and two meters, respectively (Hadipour *et al*. 2013). Planting was conducted in Fars and Hamedan during late March and early April, respectively.

It is noteworthy that the irrigation treatments commenced two weeks after the seedlings were fully established in the field. The irrigation was performed employing a drip irrigation system with regulated water output. For each irrigation cycle, the soil moisture samples were taken from the root development depth, and its content was computed based on dry weight. The soil moisture was measured using a weight-based method, and the relationship between water potential and soil moisture at specific potential points was determined utilizing the soil moisture characteristic curve. The required water amount was calculated applying the Optiwat software and the irrigation process was executed after determining the soil moisture levels and identifying the optimal irrigation timing (Siahbidi and Rrezaizad 2018). The number of irrigations employed in all of the irrigation treatments was 7 times, and no rainfall occurred during the entire growth period. Totally, 7500, 5842, 3910, and 3050 m^3 ha^{-1} of water were used for irrigation treatments at 95, 75, 50, and 25% of FC, respectively.

Assessing the growth and yield characteristics

Totally, three plants were randomly selected to mitigate marginal effects after four months of cultivation following the completion of vegetative and generative growth, along with achieving 100% flowering. Diverse characteristics including plant height, number of leaves per plant, root volume, dry root weight, and root length were documented (Aghighi Shahverdi *et al*. 2020). Then, a half-square meter from each plot was harvested to assess the biomass and yield. Measurements and records were taken for the total leaf biomass, flower yield, and total biomass (or biological yield calculated by summing leaf, flower, and root weight) (Aghighi Shahverdi *et al*. 2018).

Evaluating the essential oil content and components

Totally, 100 g samples (leaf and flower) were collected from each replicate of each treatment. The essential oil was extracted from the whole plant using a Clevenger apparatus (steam distillation method). The yield of the essential oil was determined utilizing biomass calculation.

Essential oil components were identified via Gas Chromatography-Mass Spectrometry (GC-MS) using a ThermoQuest-Finnigan TRACE MS model equipped with a 30-meter HP-5MS column (0.25 mL inner diameter, 0.25 µm layer thickness). The temperature regimen included an initial oven temperature of 60 °C for five min, a thermal gradient of 3 °C per min to 250 °C, held for five min. Injection column temperature was 290 °C, and helium gas flowed at 1.1 mm per min. Mass spectrometer utilized electron ionization (EI) at 220 °C with 70 electron volts. Spectra were compared with standards and mass spectra of standard compounds, further confirmed via computerized libraries (Pokajewicz *et al*. 2021). Essential oil components were measured in one trial by combining samples from three replicates (Fig. 1). Rank indices were assigned based on the highest and lowest mean for each compound in each treatment. Sum of ranks for each treatment level determined the rank index.

Statistical analysis

The Statistical Analysis Software, 9.2 (SAS software) was utilized following the assessment of data distribution normality applying Kolmogorov-Smirnov and Shapiro-Wilk tests to examine all of the gathered data from Fars and Hamedan. A three-factor factorial ANOVA was independently conducted for each experimental location employing a split-plot design to investigate the variance components related to the impacts of irrigation regimes, fertilizer sources, species, and their interactions. Treatment differences were studied using Duncan's Multiple Range Test (DMRT) when the ANOVA F-test showed a significance level of 0.05. Pearson correlation between characteristics and Stepwise regression (where essential oil content was considered as a dependent variable and other growth and yield traits as independent variables) was performed utilizing Microsoft Excel 2013 and Minitab 18 software.

RESULTS

Effect of experimental treatments on plant height

Severe water deficit stress decreased the plant height by 37.9 and 40.5% in Fars and Hamedan compared to

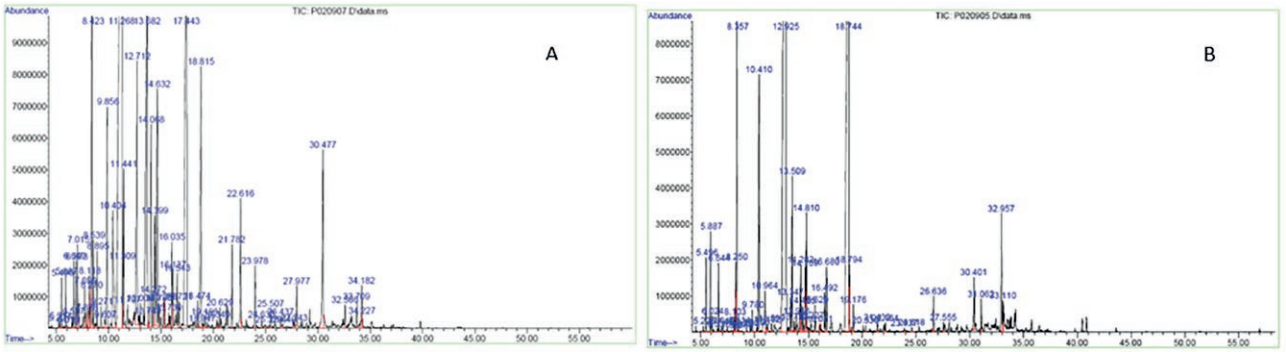

Figure 1. GC-Mass chromatogram of the essential oil of English species (A) and French species (B) of lavender.

well-watered conditions. Additionally, using various fertilizer sources increased the average plant height. Utilizing AMFs+BI and all of the fertilizer sources (APB+AMFs+BI) demonstrated the tallest plant height with average heights of 36.06 and 30.5 cm for Fars and Hamedan, respectively. The average plant height in the French species exceeded that of the English ones in both climatic conditions, showing 17.9 and 37.2% higher averages in Fars and Hamedan, respectively (Table 3).

Effect of experimental treatments on number of leaves

As indicated in Table 3, the number of leaves per plant is significantly influenced by irrigation regimes and fertilizer sources in both experimental regions. An increase in the severity of water deficit stress decreased the number of leaves per plant significantly. The reduction was 50 and 48.9% in Fars and Hamedan compared to well-watered conditions. Applying various fertilizer sources increased the number of leaves per plant compared to the no-fertilizer treatment. Employing APB+BI in Fars and APB+AMFs in Hamedan led to the highest number of leaves per plant (22.76 and 29.23, respectively). No significant difference was reported in the number of leaves per plant between the two lavender species in Fars. However, the French species exhibited a 38.54% higher number of leaves in Hamedan compared to the English ones.

Effect of experimental treatments on total leaves biomass

A significant decrease in total leaf biomass was observed with increasing severity of water deficit stress similar to other growth and morphological traits (plant height and leaf number). At the 25% FC level, the total leaf biomass reduced in Fars and Hamedan by 29.8 and 43.0% compared to well-watered conditions. Using AMFs+BI in Fars and APB+AMFs+BI in Hamedan led to the highest total leaf biomass, reaching 2588.1 and 2401.2 kg ha^{-1}, respectively. The lowest mean for the aforementioned trait was related to the non-application of fertilizer in both regions (1526.5 and 1284.6 kg ha^{-1}, respectively). The French species demonstrated a significantly higher total leaf biomass compared to the English ones with a 9.33 and 14.7% average superiority in Fars and Hamedan, respectively (Table 3).

Effect of experimental treatments on flower yield

Based on the results, the irrigation regimes, fertilizer sources, plant species, and their interactions affected the flower yield considerably at a 1% significance level. Severe water deficit stress reduced the flower yield 2.17 and 1.93 times in Fars and Hamedan compared to well-irrigated conditions. The flower yield in both regions was higher for the French species than the English ones, reaching more than 2.5 times in Hamedan. Utilizing all of the fertilizer sources in the French species under non-stress conditions in Fars showed the highest flower yield (1402 kg ha^{-1}). In addition, applying ABP+BI in the French species under non-stress conditions led to the highest flower yield with an average of 1991.3 kg ha^{-1}. The lowest flower yield was related to the non-application of fertilizer, as well as the use of ABP AMFs in both plant species under severe water deficit stress conditions in Fars. The absence of fertilizer application in the English species under severe water deficit stress conditions in Hamedan showed the lowest flower yield with an average of 252.1 kg ha^{-1} (Fig. 2A).

Effect of experimental treatments on total biomass yield

Severe water deficit stress reduced the total biomass yield in Fars and Hamedan by 36.62 and 44.4% com-

Table 3. ANOVA and mean compassion of growth and yield characteristics of two lavender species (English and French) under effect of irrigation regimes and different fertilizers sources in two experimental sites in Fars and Hamedan, Iran.

Treatments	Plant height (cm)		Number of leaves (per plant)		Total leaf biomass (kg ha^{-1})		Flower yield (kg ha^{-1})		Total biomass yield (kg ha^{-1})	
	Fars	Hamedan	Fars	Hamedan	Fars	Hamedan	Fars	Hamedan	Fars	Hamedan
Irrigation (I) (%FC)										
95 ± 5	50.39±11.1	46.38±19.09	26.4±7.88	32.09±15.79	2233.92±595.18	2425.07±1281.45	871.85±268.3	861.95±756.9	3882.24±948.06	4108.79±2181.68
75 ± 5	39.46±7.13	34.61±12.24	23.31±6.92	22.71±11.6	2042.09±1118.63	2190.54±823.69	768.6±335.63	734±533.73	3513.37±1657.83	3655.68±1511.45
50 ± 5	38.08±8.26	32.9±7.81	18.4±7.34	18.72±8.37	1924.27±554	1823.72±825.79	557.15±375.23	624.76±483.49	3101.79±1035.7	3060.6±1191.11
25 ± 5	31.26±5.14	27.56±6.56	13.2±3.03	16.39±6.39	1567.15±923.68	1380.88±687.16	401.1±87.99	444.32±330.73	2460.32±1175.29	2281.51±1039.98
Fertilizers (F)										
CK	36.06±11.37	30.5±11.53	16.92±3.58	16.04±9	1526.52±679.94	1284.67±602.18	544.98±194.76	442.88±428.51	2589.38±960.27	2159.44±1165.56
APB	40.82±10.6	34.5±9.99	18.95±4.56	22.99±12.07	1947.91±877.41	1545.91±783.34	603.81±227.05	507.83±365.77	3189.67±1171.78	2567.19±1141.21
AMF	38.82±7.59	35.77±12.52	19.99±10.41	20.46±7	1668.63±615.46	1681.98±623.82	574.95±360	594.06±388.69	2804.5±601.97	2845.06±908.39
BI	40.08±11.96	36.94±13.61	20.51±6.26	22.48±10.19	1983.95±1125.06	2024.36±823.87	589.79±375.86	621.56±553.81	3217.18±1786.08	3307.4±1429.55
APB + AMF	39.82±11.12	32.54±11.18	21.35±7.03	19.96±10.44	1685.48±979.76	2285.39±798.18	658.88±453.88	965.95±499.34	2930.47±1733.61	4064.19±1346.08
APB + BI	40.29±11.97	37.06±17.51	20.67±6.31	29.23±19.62	1756.4±820.73	2345.97±986.21	673.8±328.06	868.23±977.24	3037.77±1202.67	4017.76±2268.36
AMF+ BI	41.28±12.48	37.34±17.52	22.76±13.11	21.75±10.01	2588.17±631.55	2094.93±1432.41	757.13±325.04	564.13±456.51	3964.83±978.53	3323.83±2187.64
APB+AMF+BI	41.21±7.47	38.22±17.09	21.48±9.86	26.91±14.62	2377.78±486.57	2401.2±1220.43	794.08±350.47	765.42±467.7	4181.64±1130.07	3928.28±1565.72
Species (S)										
English	35.87±6.88	27.26±4.59	19.7±7.33	17.11±7.52	1846.81±844.36	1799.3±788.81	579.15±270.26	397.64±242.79	3032.46±1245.67	2746.18±1128.47
French	43.72±12.23	43.47±15.73	20.95±9.03	27.84±14.23	2036.9±869.69	2110.8±1167.36	720.2±386.48	934.87±660.89	3446.39±1393.99	3807.11±1956.09
Interaction effects										
I × F	**	**	**	**	**	**	**	**	**	**
I × S	**	**	**	**	ns	**	**	**	ns	**
F × S	ns	**	*	ns	ns	ns	**	*	ns	ns
I × F × S	ns	**	ns	ns	ns	ns	**	**	**	*

NS, *, and ** are respectively non-significant, significant at the 5% probability level, and significant at the 1% probability level. Non-application (CK), Azotobacter-Psedomonas Bacterial (APB), Arbuscular mycorrhiza fungi (AMF), Biochar (BI).

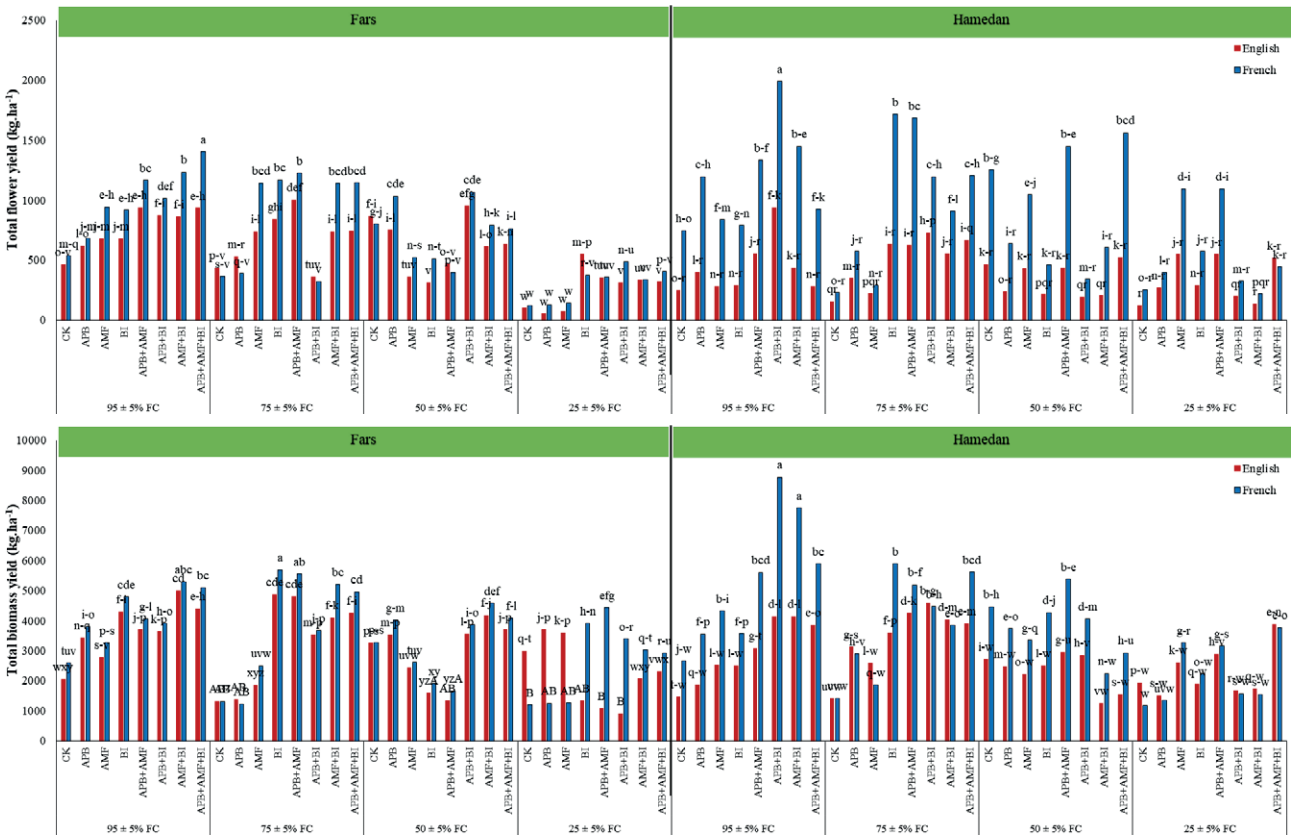

Figure 2. The interaction effect of irrigation regimes and fertilizer treatments on the total flower yield (A) and total biomass yield (B) of two Lavandula species (English and French) was investigated in two different climates, Fars and Hamadan, Iran. The averages presented in each column, sharing similar letters, do not have a statistically significant difference based on the Duncan's multiple range test at the 1% significance level. The two experimental sites were analyzed separately. Non-application (CK); Azotobacter-Psedomonas Bacterial (APB); Arbuscular mycorrhiza fungi (AMF); Biochar (BI).

pared to well-irrigated conditions. Employing various fertilizer sources increased the average total biomass yield. The French species consistently exhibited a higher average total biomass yield compared to the English ones in both experimental sites (Table 3). As illustrated in Fig. 2B, the highest total biomass yield in Fars is related to using BI in the French species under 75% FC irrigation (5686 kg ha^{-1}). Utilizing ABP+BI and AMFs+BI in the French species under non-stress conditions in Hamedan led to the highest total biomass yield (8770.6 and 7752.5 kg ha^{-1}, respectively). The non-application of fertilizer in both experimental sites led to the lowest total biomass yield in the French species under severe water deficit stress conditions (1196.6 and 1175.9 kg ha^{-1}, respectively).

Effect of experimental treatments on root traits

The results indicated that the 75% FC irrigation treatment reduced the root-related traits significantly compared to the control with a substantial decrease in root volume (36.93 and 31.7%), root dry weight (60.5 and 39.7%), and root length (50.3 and 30.5%) in Fars and Hamedan, respectively. All of the fertilizer sources increased the average of all of the measured parameters in both experimental sites compared to the absence of fertilizer application. Generally, applying fertilizer sources demonstrated superior root traits performance compared to their individual use. ABP+BI and AMFs+BI were considered as the most appropriate fertilizer sources based on the overall three root traits in both experimental sites. English species exhibited higher averages in most cases, except for root volume in Fars (Table 4).

The highest root dry weight was related to employing all of the fertilizer sources in the English species under 50% FC irrigation treatment with an average of 32.88 g plant^{-1} in Fars. Meanwhile, using ABP+BI in the English species under 75% FC treatment in Hamedan showed the highest average for the above-mentioned trait (41 g plant^{-1}). The non-application of fertilizer under severe

Table 4. ANOVA and mean compassion of root attributes and essential oil content of two lavender species (English and French) under effect of irrigation regimes and different fertilizers sources in two experimental sites in Fars and Hamedan, Iran.

Treatments	Root volume (cm^3)		Root dry weight ($g\ plant^{-1}$)		Root length (cm)		Essential oil content (%)		Essential oil yield ($g.ha^{-1}$)	
	Fars	Hamedan	Fars	Hamedan	Fars	Hamedan	Fars	Hamedan	Fars	Hamedan
Irrigation (I) (%FC)										
95 ± 5	56.1±6.98	73.39±55.96	21.8±4.8	24.38±6.02	19.41±4.27	21.7±5.36	1.34±0.87	1.22±0.16	41.15±30.25	39.46±19.56
75 ± 5	53.35±7.44	71.28±21.92	21.61±4.58	21.39±11.26	19.23±4.07	19.04±10.02	1.98±1.07	1.31±0.16	56.34±44.21	38.23±16.06
50 ± 5	49.23±14.03	62.79±26.5	18.29±8.65	19.25±6.57	16.28±7.7	17.14±5.85	1.73±0.8	1.33±0.13	45.26±27.75	32.48±12.79
25 ± 5	35.38±8.98	50.06±26.17	8.59±2.01	14.68±6.96	9.64±1.79	15.07±6.19	1.57±0.94	0.65±0.05	28.5±17.01	11.77±5.37
Fertilizers (F)										
CK	44.35±12.53	46.75±24.26	15.39±7.26	16.8±7.74	13.7±6.46	14.95±6.89	1.45±0.61	1.08±0.29	30.6±18.81	19.41±13.52
APB	48.02±12.77	57.52±32.35	16.75±9.13	18.83±9.2	14.91±8.12	16.76±8.19	1.55±0.77	1.13±0.32	36.56±20.41	24.48±13.54
AMF	44.99±13.75	59.78±34.92	17.33±6.39	18.96±9.93	15.43±5.68	16.88±8.84	1.55±0.68	1.14±0.32	33.87±14.77	25.28±9.35
BI	47.98±11.44	62.4±18.27	15.75±8.61	19.63±7.21	14.02±7.66	17.47±6.42	1.62±1.05	1.12±0.31	39.4±35.22	31.65±18.77
APB + AMF	52.7±11.22	62.63±16.65	18.94±7.24	20.41±6.36	16.85±6.44	18.17±5.66	1.39±0.7	1.14±0.34	33.65±28.03	38.18±17.54
APB + BI	49.47±13.38	80.55±39.76	18.93±7.67	21.6±10.86	16.85±6.83	19.23±9.66	1.88±1.05	1.15±0.33	47.88±34.99	38.82±22.56
AMF+ BI	50.52±12.69	80.05±51.2	18.19±7.29	21.62±7.3	16.19±6.49	19.25±6.5	1.91±1.45	1.15±0.32	62.71±53.3	31.78±22.11
APB+AMF+BI	50.05±12.1	65.34±48.15	19.3±7.74	21.56±9.8	17.18±6.89	19.19±8.73	1.9±0.95	1.1±0.3	57.82±26.85	34.25±16.66
Species (S)										
English	48.39±11.73	67.51±14.36	19.55±8.28	24.3±8.97	17.4±7.37	21.63±7.99	1.99±1.05	1.16±0.32	48.97±37	25.91±13.52
French	48.63±13.4	61.24±49.17	15.59±6.52	15.55±5.65	13.88±5.8	13.84±5.03	1.32±0.7	1.1±0.3	36.65±26.42	35.06±20.9
Interaction effects										
I × F	**	**	**	**	**	**	**	*	**	**
I × S	ns	**	**	**	**	**	**	**	**	**
F × S	ns	**	ns	*	ns	*	**	**	**	ns
I × F × S	ns	**	**	**	**	**	**	**	**	ns

NS, *, and ** are respectively non-significant, significant at the 5% probability level, and significant at the 1% probability level. Non-application (CK), Azotobacter-Psedomonas Bacterial (APB), Arbuscular mycorrhiza fungi (AMF), Biochar (BI).

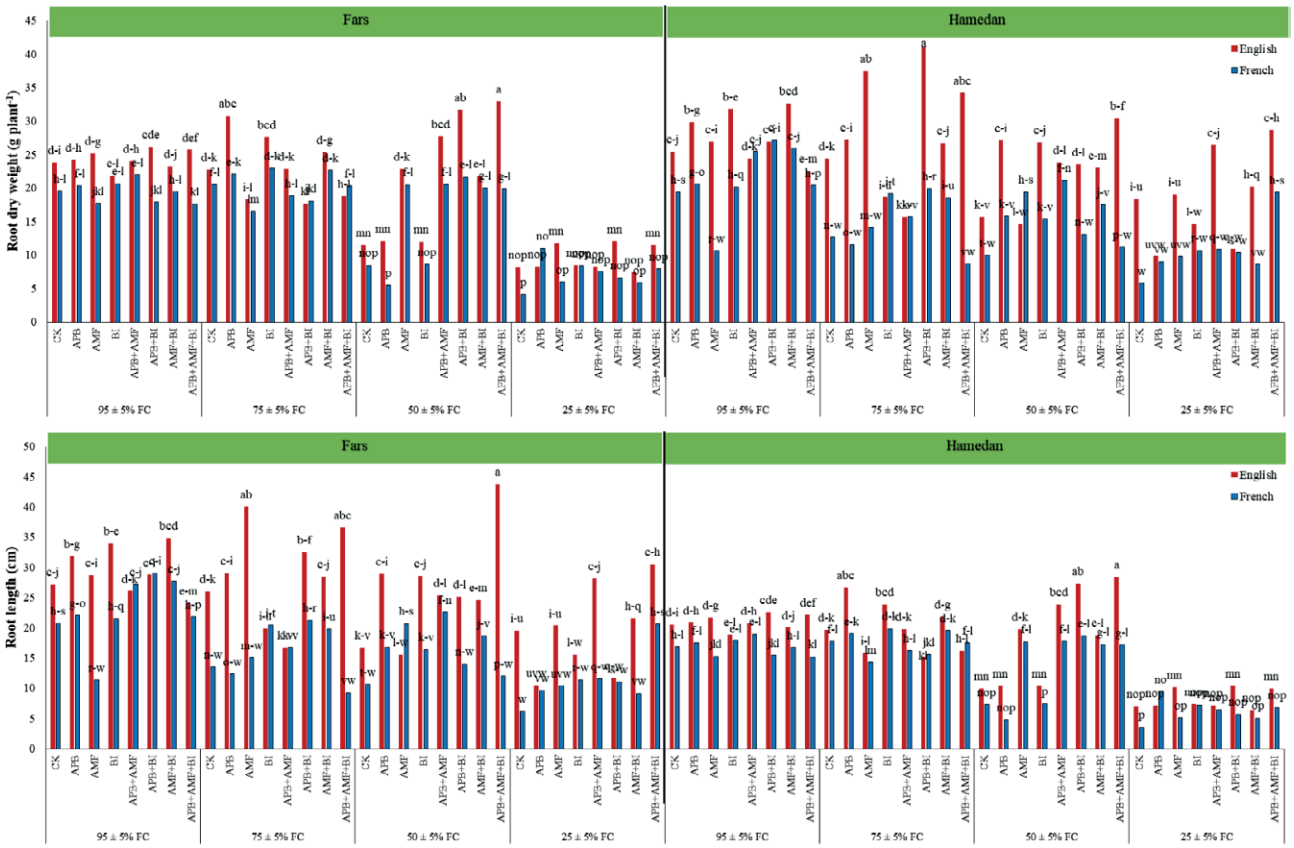

Figure 3. The interaction effect of irrigation regimes and fertilizer treatments on the root dry weight (A) and root length (B) of two Lavandula species (English and French) was investigated in two different climates, Fars and Hamadan, Iran. The averages presented in each column, sharing similar letters, do not have a statistically significant difference based on the Duncan's multiple range test at the 1% significance level. The two experimental sites were analyzed separately. Non-application (CK); Azotobacter-Psedomonas Bacterial (APB); Arbuscular mycorrhiza fungi (AMF); Biochar (BI).

water deficit stress conditions in the French species led to the lowest average root dry weight (4.13 and 5.76 g plant^{-1} for Fars and Hamedan, respectively) (Fig. 3A).

Using all of the fertilizer sources in English species under 50% FC irrigation treatment demonstrated the highest root length in Fars and Hamedan with lengths of 43.78 and 28.38 cm, respectively. The lowest root length in both experimental sites was related to the non-application of fertilizer in the French species under severe water deficit stress treatment with average lengths of 6.15 and 3.56 cm, respectively (Fig. 3B).

Effect of experimental treatments on essential oil content and yield

The results represented that the irrigation regime and fertilizer treatments influenced the essential oil content and yield significantly. Partial water deficit stress (75 and 50% FC) increased the essential oil content compared to the control irrigation in both experimental regions. Severe water deficit stress led to an increase in essential oil content in Fars and a decrease in Hamedan compared to the control irrigation treatment. However, the essential oil yield in both experimental regions significantly decreased under severe water deficit stress (1.44- and 3.33-times reduction, respectively). Some fertilizer treatments decreased the essential oil content significantly compared to the non-fertilized treatment, while most of the fertilizer treatments increased the average content.

Applying AMFs and BI in Fars, as well as APB+AMFs and APB+BI in Hamedan led to the highest average essential oil yield (62.71, 38.18, and 38.82 g ha^{-1}, respectively). The lowest essential oil yield was related to the non-fertilized treatment in both experimental sites (30.6 and 19.41 g ha^{-1}). The English species exhibited a higher average than the French ones in both experimental regions with this difference being statistically non-

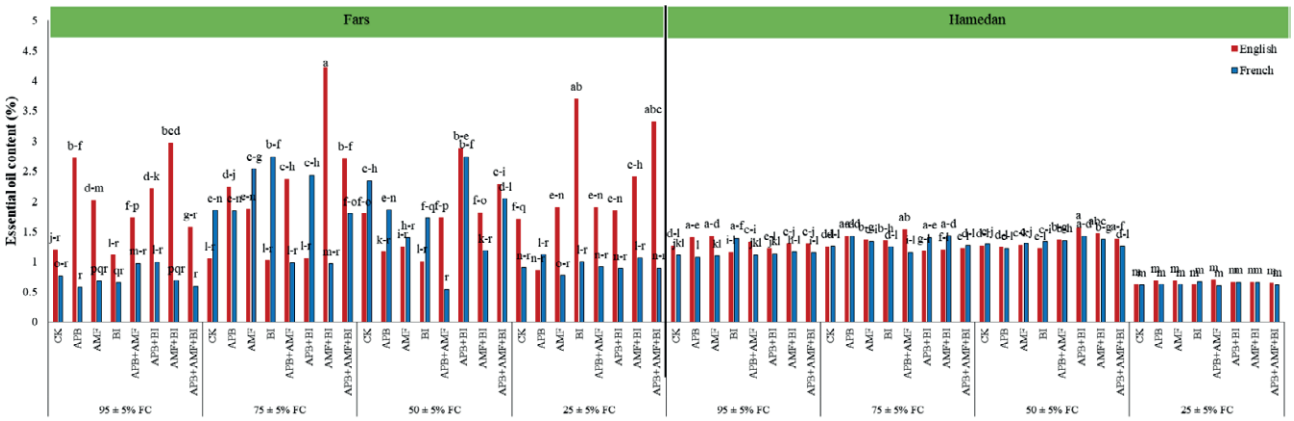

Figure 4. The interaction effect of irrigation regimes and fertilizer treatments on the essential oil content of two Lavandula species (English and French) was investigated in two different climates, Fars and Hamadan, Iran. The averages presented in each column, sharing similar letters, do not have a statistically significant difference based on the Duncan's multiple range test at the 1% significance level. The two experimental sites were analyzed separately. Non-application (CK); Azotobacter-Psedomonas Bacterial (APB); Arbuscular mycorrhiza fungi (AMF); Biochar (BI).

significant in Hamedan. The essential oil yield varied based on the climatic conditions of the experiment site in two lavender species. The highest essential oil yield in Fars (48.97 g ha^{-1}) was related to the English species, while the French species exhibited the highest yield in Hamedan (35.09 g ha^{-1}) (Table 4).

The essential oil content in employing APB+BI in the English species under 75% FC irrigation treatment showed the highest average (4.23%) in Fars. Meanwhile, the highest average of this trait in Hamedan was related to using APB+BI under 50% FC irrigation treatment in the English species with an average of 1.56%. All of the fertilizer levels in both lavender species under 25% FC irrigation treatment demonstrated the lowest essential oil content in Hamedan. Utilizing APB, fertilizer sources in the French species under control irrigation treatment, and APB+AMFs in the French species under 50% FC irrigation treatment exhibited the lowest essential oil content (0.57, 0.59, and 0.54%, respectively) (Fig. 4).

Effect of experimental treatments on fatty acids composition

Analyzing GC-MS on the essential oil indicated that eight compounds were identified in all of the treatment levels, plant species, and experimental sites. The aforementioned compounds included α-Pinene, B-Pinene, Linalool, Camphor, Borneol, Terpinen, Linalyl acetate, and Caryophyllene Oxide. As demonstrated in Fig. 5, Linalool shows the highest average in both experimental sites and plant species (22.46 to 30.06%). Linalyl acetate and Caryophyllene Oxide exhibited the highest averages in Fars after the above-mentioned compound, while Borneol and Terpinen showed the highest averages in Hamedan. No significant difference was reported in the measured compounds in Hamedan. However, significant differences were observed in Fars in the levels of Linalool, Terpinen, and Caryophyllene Oxid with the English species excelling in the first and the French ones in the second and third compounds.

Table 5 shows the results related to the effect of irrigation treatments and fertilizer sources in Fars on the composition of essential oil fatty acids. As represented, severe water stress (except for Terpinen) exhibits the lowest average in most of the identified compounds, meaning a reduction in the average compounds. Meanwhile, irrigation levels of 75 and 50% FC allocated the highest averages in most of the compounds. The control irrigation treatment showed superiority in terms of the Borneol compound. The 75% FC treatment demonstrated the highest average (91.83%), while the lowest average was related to severe water stress (76.91%) in terms of the total compounds. Similar results were obtained with the highest and lowest indices reported in the 75 and 25% FC treatment, respectively. Different fertilizer sources affected the amount of compounds differently. Utilizing BI led to the highest averages in α-Pinene, Camphor, and Terpinen (2.93, 6.88, and 8.94%, respectively). Applying APB+BI led to the highest averages for Linalool and Linalyl acetate (29.8 and 26.88%, respectively). In addition, employing all of the fertilizer sources showed the highest averages for B-Pinene and Caryophyllene Oxide (5.75 and 13%). The fertilizer sources APB+BI and APB+AMFs+BI exhibited the highest averages (89.14 and 88.97%, respectively),

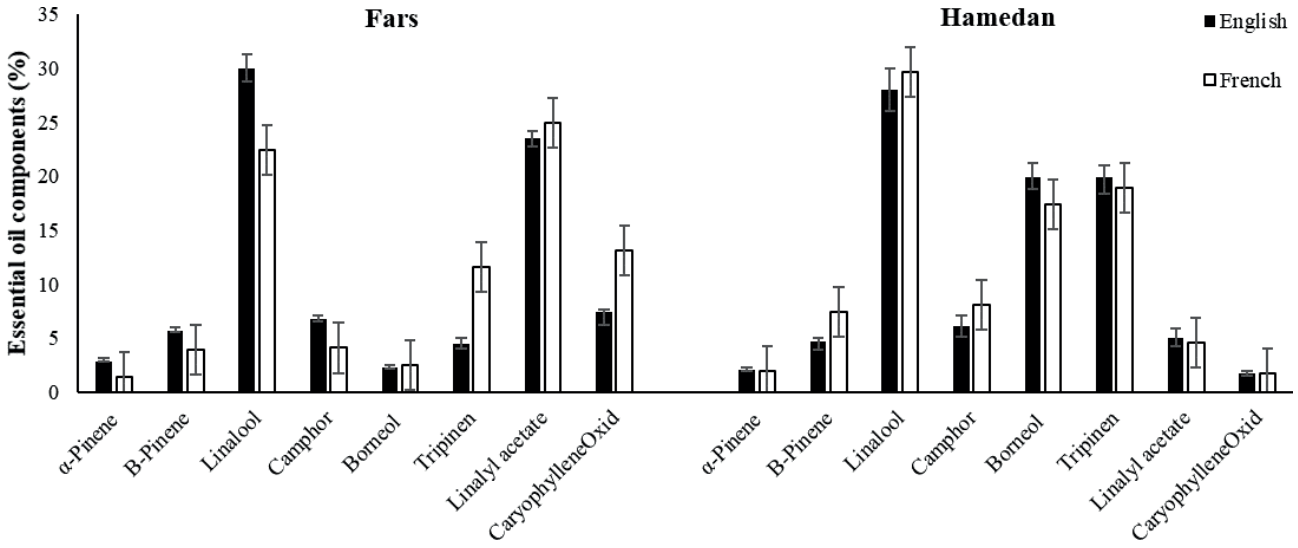

Figure 5. The variations in the essential oil fatty acid content of two lavender species (French and English) in the climates of Fars and Hamedan, Iran.

while the lowest total compounds were observed in the non-application and AMFs application treatments (76.87 and 76.77%, respectively). Non-application of fertilizer and combined use of the fertilizer sources demonstrated the lowest and highest-ranking indices, respectively.

As presented in Table 6, the highest average of α-Pinene and Linalool is reported in the 95% FC irrigation treatment in Hamedan. In addition, the highest averages of Camphor, Borneol, Terpinen, and Linalyl acetate are observed in the 75 and 50% FC irrigation levels, while the highest averages of β-Pinene and Caryophyllene Oxide are reported in the 25% FC irrigation level. Irrigation at 50 and 25% FC exhibited the highest averages, while irrigation at 75% FC showed the lowest average. Such classification was observed in the ranking index. Using the sources led to the highest averages of β-Pinene (8.1%), Linalool (33.23%), Borneol (19.91%), and Caryophyllene Oxide (2.85%). Further, the highest averages of α-Pinene and Linalyl acetate were reported in the treatment without fertilizer (2.44 and 8.47%, respectively). Utilizing AMFs and APB+BI showed the highest total compound averages (90.39 and 89.79%, respectively). However, the lowest total compound average was related to applying all of the fertilizer sources (87.11%). The highest index was related to APB, and the lowest one was observed in employing all of the fertilizer sources.

Correlation analysis

Table 7 and 8 indicate the results related to simple correlations between measured traits for Fars and Hamedan, respectively. No significant correlation was observed between the physiological, biochemical, growth, morphological, and yield parameters with essential oil content in Fars. However, a positive correlation was reported between the percentage of essential oil with traits such as RWC, chlorophyll b content, root dry weight, and root length in Hamedan. Additionally, a negative and significant correlation was observed between the aforementioned traits with proline content and activities of antioxidant enzymes such as CAT, POX, SOD, and APX. Further, no significant correlation was reported between Linalool, as the most indicative fatty acid compound, with the growth, yield, physiological, biochemical, or morphological traits in Hamedan. However, a positive correlation was observed between the above-mentioned traits with root dry weight and length at a 5% significance level in Fars.

DISCUSSION

This study seeks to review the efficiency of different fertilizer sources under various irrigation regimes. The results indicated that severe water scarcity (25% FC) decreased the average plant height, leaf number, leaf biomass, flower yield, and total biomass compared to the control irrigation treatment. In addition, employing different fertilizer sources increased the aforementioned traits. Water scarcity reduces the growth parameters such as leaf area and number, as well as alterations in physiological parameters (Afshari *et al.* 2022), resulting in

Table 5. The content of essential oil fatty acids in the lavender influenced by various irrigation levels and different fertilizer treatments under the climatic conditions of Fars, Iran.

	α-Pinene	B-Pinene	Linalool	Camphor	Borneol	Tripinen	Linalyl acetate	Caryophyllene Oxide	Cumulative	Rank index
RI	930	960	1089	1117	1141	1156	1244	1557		
Irrigation (I) (%FC)										
95 ± 5	2.12±1.06	5.27±1.79	24.94±8.9	5.6±2.2	**2.52±0.72**	7.85±5.03	24.21±3.15	8.9±3.21	81.41	22
75 ± 5	**2.56±1.6**	**5.44±1.52**	28.24±6.23	5.55±2.97	2.47±0.72	6.96±4.95	**26.63±2.74**	**14±9.07**	91.83	25
50 ± 5	**2.56±1.86**	4.82±1.9	**29.82±8.13**	**6.13±1.96**	2.4±0.95	*6.1±4.23*	23.8±5.32	*8.02±1.6*	83.66	20
25 ± 5	*1.28±0.13*	*3.73±0.53*	*21.96±6.13*	*4.38±0.94*	*2.13±1.31*	**11.2±2.37**	*22.16±4.44*	10.07±2.46	76.91	13
Fertilizers (F)										
Non-application (CK)	1.74±0.57	4.5±0.84	26.06±4.87	5.35±1.47	2.24±0.87	*7.11±4.89*	*21.76±3.65*	8.1±2.97	76.87	23
Azotobacter-Psedomonas Bacterial (APB)	2.59±1.86	4.97±1.36	27.58±4.82	5.98±2.26	2.21±0.88	8.17±4.26	23.24±5.74	*8.02±3.55*	82.76	38
Arbuscular mycorrhiza fungi (AMF)	1.62±0.6	5.16±1.67	*23.05±8.9*	5.13±1.06	2.31±0.7	7.56±5.59	22.5±5.96	9.44±2.86	76.77	27
Biochar (BI)	**2.93±2.48**	4.73±2.54	26.41±9.6	**6.88±2.9**	2.3±0.93	**8.94±4.73**	24.37±2.91	9.37±4.25	85.92	45
APB + AMF	1.65±0.61	4.64±1.75	28.79±8.1	*4.8±1.83*	*2.13±0.74*	7.41±4.89	23.63±3.5	10.84±3.85	83.89	26
APB + BI	2.29±1.39	*4.02±1.08*	**29.08±6.86**	4.84±2.03	2.32±0.89	7.95±4.04	**26.88±3.5**	11.77±7.62	89.14	41
AMF + BI	*1.61±0.49*	4.78±1.45	24.02±8.08	5.18±2.59	**2.94±1.61**	8.15±5.53	25.16±3.79	11.44±6.75	83.28	38
APB + AMF + BI	2.59±1.63	**5.75±2.02**	24.92±11.18	5.17±2.89	2.58±0.8	8.92±4.64	26.04±3.13	**13±8.51**	88.97	50

These traits were analyzed in a single replication and from the combination of samples over two years. The highest mean for each combination is in bold, and the lowest is in italics.

Table 6. The content of essential oil fatty acids in the lavender influenced by various irrigation levels and different fertilizer treatments under the climatic conditions of Hamadan, Iran.

	α-Pinene	B-Pinene	Linalool	Camphor	Borneol	Tripinen	Linalyl acetate	Caryophyllene Oxide	Total identified compounds	Rank indices
RI	930	960	1089	1117	1141	1156	1244	1557		
Irrigation (I) (%FC)										
95 ± 5	**2.21±0.87**	6.61±3.16	**31.06±12.7**	7.57±5.14	*17.04±7.21*	18.79±5.02	4.39±6.34	*1.14±0.59*	88.81	20
75 ± 5	*1.81±0.49*	*4.32±1.74*	27.53±10.47	**8.66±6.67**	19.08±8.09	20.07±9.69	*2.81±1.51*	1.96±0.63	86.23	18
50 ± 5	2.11±0.84	5.66±2.41	*27.34±11.98*	*5.31±5.52*	**19.88±5.61**	**20.96±8.07**	**6.45±5.93**	1.64±1.08	89.34	21
25 ± 5	1.85±0.86	**7.69±5.59**	29.27±8.55	6.77±4.72	18.69±7.24	*17.63±5.85*	5.5±2.78	**2.03±2.25**	89.43	21
Fertilizers (F)										
Non-application (CK)	**2.44±1.16**	5.16±1.98	26.16±17.25	*4.77±4.23*	*16.18±7.26*	23.36±11.67	**8.47±10.38**	1.18±0.73	87.72	33
Azotobacter-Psedomonas Bacterial (APB)	2.1±0.97	5.56±2.23	24.82±14.47	9.55±8.06	18.95±7.43	19.7±7.04	6.63±4.33	1.51±0.58	88.8	41
Arbuscular mycorrhiza fungi (AMF)	2.06±0.84	5.08±2.16	*24.53±9.17*	**9.72±7.63**	19.19±8.17	**23.88±5.01**	4.3±2.3	1.63±0.64	90.39	40
Biochar (BI)	1.89±0.53	7.08±4.16	28.37±4.38	5.29±5.23	19.46±6.44	20.13±5.27	4.79±3.38	1.37±0.31	88.38	37
APB + AMF	1.9±0.61	7.41±6.12	29.88±5.57	8.88±4.96	17.92±3.46	*15.85±3.21*	4.46±3.5	1.81±0.86	88.1	35
APB + BI	*1.66±0.32*	**8.1±4.96**	**33.23±9.94**	4.84±2.92	18.75±8.62	17.37±3.47	2.99±1.89	**2.85±3.14**	89.79	35
AMF + BI	2±0.74	*5.02±3.26*	32.37±11.57	5.79±4.54	**19.91±7.36**	17.84±7.82	*2.52±1.45*	1.9±1.3	87.34	37
APB + AMF + BI	1.91±0.9	5.14±2.26	31.07±9.99	7.76±4.46	19.02±8.6	16.77±9.44	4.15±2.97	*1.3±0.47*	87.11	30

These traits were analyzed in a single replication and from the combination of samples over two years. The highest mean for each combination is in bold, and the lowest is in italics.

Table 7. The simple correlation coefficients between growth and yield attributes as well as essential oil content and components of two lavender species (English and French) under effect of irrigation regimes and different fertilizers sources in Fars, Iran.

	1	2	3	4	5	6	7	8	9	10	11	12	13	14	15	16	17	18
1	1	*	*	**	*	*	*	*	ns	ns	ns	ns	ns	ns	ns	ns	ns	ns
2	0.5	1	*	**	*	*	*	*	ns	*	ns	ns	ns	ns	ns	ns	ns	ns
3	0.37	0.35	1	*	**	ns	ns	ns	ns	**	ns	ns	ns	ns	ns	ns	ns	ns
4	0.52	0.7	0.5	1	**	**	*	*	ns	*	ns	ns	ns	ns	ns	ns	ns	ns
5	0.46	0.5	0.96	0.72	1	*	ns	ns	ns	**	ns	ns	ns	ns	ns	ns	ns	ns
6	0.43	0.5	0.29	0.53	0.4	1	**	**	ns	ns	ns	ns	ns	ns	ns	ns	ns	ns
7	0.35	0.31	0.22	0.32	0.28	0.68	1	**	ns	*	*	**	*	*	ns	*	ns	ns
8	0.35	0.31	0.22	0.32	0.28	0.68	0.99	1	ns	*	*	**	*	*	ns	*	ns	ns
9	-0.2	0.09	-0.07	0.07	-0.03	0.01	0.2	0.2	1	**	ns	ns	ns	ns	ns	ns	ns	ns
10	0.09	0.37	0.52	0.43	0.56	0.26	0.34	0.34	0.76	1	ns	ns	ns	ns	ns	ns	ns	ns
11	-0.23	0.01	0.06	-0.03	0.04	0.21	0.47	0.47	0.05	0.07	1	**	**	**	ns	**	ns	ns
12	-0.08	0.09	0.13	-0.01	0.1	0.29	0.54	0.54	0.06	0.13	0.64	1	*	**	ns	**	ns	ns
13	-0.22	0.06	-0.04	-0.06	-0.05	0.09	0.36	0.36	0.17	0.15	0.6	0.44	1	*	ns	**	ns	*
14	-0.19	-0.02	0.06	-0.13	0.01	0.22	0.37	0.37	0.05	0.07	0.71	0.65	0.41	1	ns	**	ns	**
15	0.15	-0.03	0.13	0.09	0.13	0.08	0.19	0.19	-0.16	-0.04	0.26	0.15	0.1	0.03	1	ns	ns	ns
16	0.25	-0.08	-0.04	0.09	-0.01	-0.16	-0.46	-0.46	-0.26	-0.29	-0.57	-0.67	-0.67	-0.61	0.06	1	ns	*
17	0.24	0.21	-0.03	0.26	0.06	0.23	0.28	0.28	0.14	0.13	0.01	-0.09	-0.06	-0.2	0.05	0.08	1	ns
18	0.14	0.18	0.15	0.22	0.19	0.04	-0.07	-0.07	-0.07	0.04	-0.28	-0.27	-0.31	-0.57	0.11	0.44	0.24	1

Table 8. The simple correlation coefficients between growth and yield attributes as well as essential oil content and components of two lavender species (English and French) under effect of irrigation regimes and different fertilizers sources in Hamedan, Iran.

	1	2	3	4	5	6	7	8	9	10	11	12	13	14	15	16	17	18
1	1	**	**	**	**	*	ns	ns	ns	**	ns	ns	ns	ns	ns	ns	ns	ns
2	0.71	1	**	**	**	*	ns	ns	ns	**	ns	ns	ns	ns	ns	ns	ns	ns
3	0.57	0.53	1	**	**	**	ns	ns	ns	**	ns	ns	ns	ns	ns	ns	ns	ns
4	0.68	0.6	0.54	1	**	ns	ns	ns	ns	**	ns	ns	ns	ns	ns	ns	ns	ns
5	0.69	0.63	0.94	0.8	1	*	ns	ns	ns	**	ns	ns	ns	ns	ns	ns	ns	ns
6	0.33	0.44	0.55	0.27	0.5	1	*	*	ns	*	ns	ns	ns	ns	ns	ns	ns	ns
7	-0.11	0.03	0.28	-0.04	0.18	0.3	1	**	*	ns	ns	ns	ns	ns	ns	ns	ns	ns
8	-0.11	0.03	0.28	-0.04	0.18	0.3	0.99	1	*	ns	ns	ns	ns	ns	ns	ns	ns	ns
9	0.17	0.2	0.28	0.1	0.24	0.22	0.35	0.35	1	**	ns	ns	ns	ns	ns	ns	ns	ns
10	0.64	0.6	0.89	0.7	0.93	0.49	0.24	0.24	0.56	1	ns	ns	ns	ns	ns	ns	ns	ns
11	0.06	-0.12	-0.11	-0.03	-0.09	-0.09	0.01	0.01	0.06	-0.06	1	ns	*	ns	ns	ns	*	ns
12	0.19	0.13	-0.05	0.26	0.07	-0.13	-0.25	-0.25	-0.29	-0.05	-0.09	1	ns	ns	ns	ns	ns	ns
13	0.09	0.21	0.12	0.17	0.16	0.01	-0.01	-0.01	0.06	0.17	-0.33	-0.12	1	ns	*	**	*	ns
14	0.11	0.14	-0.08	0.09	-0.02	-0.02	-0.1	-0.1	0.03	-0.01	-0.13	-0.11	-0.07	1	*	ns	ns	ns
15	-0.14	-0.2	0.06	-0.08	0.01	0.02	0.21	0.21	0.01	0.01	0.29	-0.05	-0.37	-0.4	1	ns	ns	ns
16	-0.05	-0.13	-0.05	-0.13	-0.09	-0.04	0.04	0.04	0.07	-0.1	0.08	0.03	-0.63	-0.25	0.01	1	ns	ns
17	0.01	-0.1	-0.17	-0.15	-0.19	-0.09	-0.1	-0.1	-0.14	-0.22	0.43	0.05	-0.48	-0.18	0.25	0.25	1	ns
18	-0.13	-0.05	0.01	-0.04	-0.01	0.13	-0.11	-0.11	-0.12	-0.02	-0.14	-0.1	-0.16	0.13	0.07	-0.03	-0.25	1

ns: non-significant; * and **: significant at 5 and 1% probably level, respectively.
1. Plant height, 2. Number of leaves, 3. Total leaves biomass, 7. Total flower yield, 8. Total biomass yield, 9. Root volume, 7. Root dry weight, 8. Root length, 9. EOC, 10. EOY, 11. α-Pinene, 12. B-Pinene, 13. Linalool, 14. Camphor, 15. Borneol, 16. Tripinen, 17. Linalyl acetate, 18. Caryophyllene Oxide.

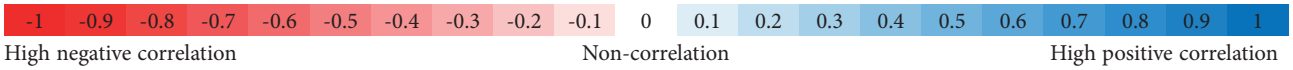

declining the yield-related traits such as flower and biomass yield. Further, water scarcity diminishes solar energy absorption and nutrient uptake by reducing leaf number and area, as well as shortening the plant growth period, resulting in affecting the quantitative and qualitative aspects of plant yield negatively (Benadjaoud *et al*. 2022). For example, Chrysargyris *et al* (2016) argued that water stress declined the growth and chemical composition of lavender (*L. angustifolia*) compared to plants subjected to regular irrigation. In addition, Zollinger *et al* (2006) observed a reduction in leaf number and total dry weight under water stress conditions in *L. stoechas*, as another lavender species. The impact of water deficit on growth inhibition has been extensively documented in various plant species including *Stellaria dichotoma* L. (Zhang *et al*. 2017), *Stevia rebaudiana* (Afshari *et al*. 2022), and *Foeniculum vulgare* Mill (Peymaei *et al*. 2024). Some others (e.g. García-Caparrós *et al*. 2019; Salata *et al*. 2020) claimed that the exposure of medicinal plants including *L. latifolia*, *M. piperita*, and *T. capitatus* to drought stress decreased their aerial fresh weight and yield.

The plant responds by increasing the activity of antioxidant enzymes, as well as the synthesis of osmolytes under severe water deficit conditions, which leads to a higher consumption of photosynthetic materials by the plant to cope with drought stress, resulting in decreasing the growth and yield parameters (Mahajan and Pal 2023).

The distribution of biomass in plants, specifically root and shoot dry weights, was significantly affected under water stress conditions. Water stress altered the allocation of biomass to roots, resulting in impacting photosynthetic efficiency, nutrient absorption, and overall growth parameters (Begum *et al*. 2022). The alterations in biomass composition and structure were related to varying water availability, resulting in influencing plant adaptation strategies and productivity. Severe water stress induced modifications in water use efficiency, root-shoot ratios, and physiological processes, indicating the ability of plant to adapt to limited water conditions (Rodríguez-Pérez *et al*. 2017; Afshari *et al*. 2022; Peymaei *et al*. 2024).

The results represented that using fertilizers including APB, AMFs, and BI increased the average yield traits of the plant under well-irrigated and low irrigation conditions. Apparently, utilizing BOFs enhanced the growth and yield parameters by reducing soil acidity and providing appropriate conditions for absorbing essential nutrients, especially nitrogen, phosphorus, and trace elements such as iron, zinc, and copper (El-Attar *et al*. 2023). Sharma *et al* (2023) reported that the highest mean values for plant height, number of branches, pod length and weight, seed number, and total plant yield of *Pisum sativum* L. were achieved by using BOFs.

Utilizing APB and BI in both regions under irrigation treatments of 75 and 50% FC showed the highest essential oil content, indicating that partial water stress increases the essential oil content compared to normal irrigation conditions. However, severe water stress or drought reduced the essential oil content significantly. The essential oil content reduces under severe water stress due to the decrease in the activity of enzymes and biochemical pathways related to the synthesis of essential oils in plants, which diminishes by water stress (Mohammadi *et al*. 2018). Additionally, severe water deficit declines the quality and quantity of the essential oil by weakening the plant to absorb and transport water and essential nutrients (Asghari *et al*. 2020). According to other researchers, moderate water stress in *L. angustifolia* increases the essential oil content compared to the control treatment (Sałata *et al*. 2020). The stress induced by drought decreases the production of secondary metabolites significantly, resulting in impacting the accumulation of essential oils in plants (Kleinwächter *et al*., 2015). Comparable results were reported in cultivating *L. latifolia* (García-Caparrós *et al*. 2019), and *Thymus vulgaris* (Kleinwächter *et al*. 2015).

Applying APB + BI increased the essential oil content in both species of lavender. Employing the aforementioned fertilizers elevates the synthesis of secondary metabolites by enhancing plant growth and yield (Ullah *et al*. 2020), improving nutrient uptake (Phares *et al*., 2022), and increasing resistance to environmental stresses (Lalay *et al*. 2022). In addition, enhancing the nutrient balance using the above-mentioned fertilizers empowers the plant to absorb elements, resulting in augmenting enzyme activity and biochemical pathways involved in essential oil synthesis (Kari *et al*. 2021). No report was found on employing APB + BI regarding the essential oils of medicinal plants. However, several studies have been conducted on using the aforementioned substances in enhancing the quantitative and qualitative yield of maize plants under low-water irrigation stress (Ullah *et al*. 2020) and increasing the microbial population in acidic soils (Kari *et al*. 2021). Utilizing organic fertilizer with nitrogen-fixing bacteria (Azetobacter) in a similar experiment was regarded as the most effective fertilizer combination in enhancing the quality of lavender essential oil under conditions of moderate salinity stress (Khatami *et al*. 2023).

Applying Bi and APB improved the root characteristics significantly, resulting in increasing nutrient absorption and enhancements in quantitative and qualitative parameters. Ethylene, as a well-known stress hormone, is recognized for its inhibitory effect on root growth

(Ullah *et al*. 2020). APB promotes root growth through the activity of 1-aminocyclopropane-1-carboxylate (ACC) deaminase, which aids in ethylene reduction within the root zone (Bechtaoui *et al*. 2021). The bacteria involved in the above-mentioned process possess ACC deaminase, resulting in enabling the conversion of ACC, as an ethylene precursor, into ammonia and α-ketobutyrate. The aforementioned enzymatic activity reduces ethylene-induced stress, resulting in fostering root growth (Ahmad *et al*. 2024). The synergistic effect of rhizobacteria and BI application was further pronounced because BI served as a nutrient source for bacteria and enhanced the physicochemical characteristics of soil. Therefore, bacterial growth was amplified, resulting in augmenting the root parameters (Ullah *et al*. 2020).

The results represented that employing BI, especially in combination with APB and AMFs, increased physiological parameters, resulting in enhancing the quantitative and qualitative yield in both lavender species. Thus, BI increases the growth parameters, as well as the quantitative and qualitative yield by improving the physical, chemical, and biological characteristics of the soil such as moisture availability (Allohverdi *et al*. 2021). Fascella *et al* (2020) asserted that the highest plant height, leaf area, leaf, and flower yield in lavender were recorded in substrates with 25-75% BI content. In addition, the increase in BI content improved the several chemical and physical characteristics such as electrical conductivity, pH, apparent density, and total porosity, as well as reducing the water holding capacity and increasing the availability of nutrients such as phosphorus, magnesium, and calcium (Fascella *et al*. 2020).

BOFs can elicit various responses in various crops under different environmental conditions (Januškaitienė *et al*. 2022). This phenomenon was observed in the present experiment. The flower and total biomass yield were observed in Fars by using APB, AFMs, and BI, while utilizing APB and AFMs demonstrated the highest average for such traits in Hamedan. Even the fertilizer treatments showed differences in both regions while combined with other factors such as irrigation and plant species. For instance, the total biomass yield in the English species under the treatment with BI alone under 75% FC irrigation exhibited the highest average in Fars. However, applying fertilizers such as APB+BI under control irrigation in the French species showed the highest average in Hamedan. Such variations can be ascribed to discrepancies in climatic factors including geographical dimensions, elevation, mean temperature, and precipitation. The climatic data underscores the lower average temperatures and precipitation levels in Hamedan unlike Fars. The less appropriate conditions concerning the above-mentioned parameters necessitate an augmentation in metabolite production to counteract the imposed stress conditions. In addition, the overall inhospitable conditions influence the growth and performance by modifying physiological and biochemical parameters compared to Fars (Aghighi Shahverdi *et al*. 2018; Farrokhi *et al*. 2021). Farrokhi *et al* (2021) found that temperature variations and precipitation levels are among the key climatic factors, which can influence the quantitative and qualitative performance of plants. The microbial activity of BOFs is highly influenced by temperature and soil moisture levels. Similarly, the presence of appropriate environmental conditions in terms of precipitation and elevated temperatures can enhance their activity, resulting in increasing efficiency in fertilizer utilization (Cui *et al*. 2016; Kumar *et al*. 2022). Therefore, employing fewer fertilizer sources can be highly effective under appropriate environmental conditions. However, multiple fertilizer sources should be used to meet the nutritional requirements of plant in inappropriate environmental conditions (Kumar *et al*. 2022). Thus, utilizing all of the fertilizer sources showed the highest average performance in flower-related traits and total biomass under the climatic conditions in Hamedan. The efficiency of fertilizer use is significantly impacted by the type and frequency of fertilizer application, with organic fertilizer and single applications generally exhibiting low values (Zhu *et al*. 2023). According to Yu *et al* (2022), the rise in the growing season temperature for rice and wheat increased nitrogen use efficiency significantly.

The physical and chemical condition of the fields is among the reasons for the difference in fertilizer compositions between Fars and Hamedan. As presented in Table 2, the levels of nitrogen, potassium, iron, and magnesium in Fars are higher than those in Hamedan. Therefore, higher concentrations of resources should be applied compared to Fars to meet the intended plant nutrient requirements in Hamedan. The results indicate the influence of soil physicochemical characteristics on the quantity and efficiency of fertilizer utilization (Yu *et al*. 2022).

Based on the results, linalool was considered as the predominant compound in both species at both experimental sites. Others (e.g. Crișan *et al*. 2023; Khatami *et al*. 2023) reported similar results regarding the lavender plant. No significant difference was reported between the English and French lavender species in terms of fatty acid content in Hamedan. However, some variations were observed in compounds such as Linalool, Terpinen, and Caryophyllene Oxide in Hamedan. The English species exhibited higher levels of the first compound, while the French ones excelled in the second and third compounds. Differences in the GC-MS composition of

the essential oil of English and French lavender varieties may be attributed to various factors. Environmental factors such as diverse climatic conditions in Hamadan and Fars, distinct soil characteristics in these areas, and genetic variations between the two varieties could contribute to differences in the essential oil composition (Détár *et al*. 2020). Environmental factors such as precipitation, temperature, sunlight, and soil characteristics can influence physiological processes in plants, resulting in altering the essential oil composition (Özsevinç and Alkan 2023). Additionally, genetic differences between the species play a crucial role in the aforementioned variations. Further studies should be conducted in the fields of plant physiology, genetics, and ecology for a more comprehensive understanding of the above-mentioned differences (Détár *et al*. 2020).

The results indicated that severe water deficit stress (25% FC) reduced the average content of most fatty acid compounds in the essential oil of both species, while moderate stress levels (75 and 50% FC) increased the average compound content compared to the well-watered treatment. The levels of borneol, camphor, linalyl acetate, gamma-cadinene, caryophyllene oxide, and muurolol identified in the essential oil of Lavandula under water stress conditions increased compared to the control, which differed from the obtained results (Sałata *et al*. 2020). The variation in irrigation treatment levels in the aforementioned study and this experiment appears to be the main reason for the above-mentioned difference since two irrigation treatment levels were employed in the aforementioned study, while four levels were implemented here, and the highest stress level reduced the average content. The results indicated that utilizing APB+BI and APB+AMFs+BI in Fars led to the highest total fatty acids and rank index. However, the non-application of fertilizer led to the lowest total fatty acids and rank index. In addition, applying three fertilizer sources in Hamedan led to the lowest rank index and total fatty acids. Employing the combined fertilizer APB+BI in both experimental regions affected the fatty acid content positively. Finally, the composition of essential oils in aromatic-medicinal plants may vary based on the genotype, ecological conditions, and fertilizer treatments (Giannoulis *et al*. 2020).

CONCLUSION

The following conclusions emerge from the conducted experiment in line with the predefined objectives: Severe water stress (25% FC) resulted in diminished growth and yield characteristics, consequently reducing the quantity and quality of essential oil in both French and English lavender varieties. Application of various fertilizers, especially in combination (AMFs, APB, BI), demonstrated a notable enhancement in growth, yield, and essential oil content compared to non-fertilized plants. Essential oil content, fatty acid quality, and yield exhibited variations among lavender species and experimental sites. Notably, Fars exhibited the highest total fatty acids when treated with combined fertilizers, while Hamedan showcased the lowest. The combination of APB + BI emerged as the most effective fertilizer blend. French lavender displayed a higher average yield, whereas English lavender exhibited superior essential oil content, particularly in the Fars region. Parameters associated with root development exhibited a positive correlation with essential oil content. The composition of essential oils encompassed α-Pinene, β-Pinene, Linalool, Camphor, Borneol, Terpinen, Linalyl acetate, and Caryophyllene Oxide, with Linalool being particularly prominent across both species and sites. Climatic factors and soil characteristics significantly influenced the efficacy of fertilizers and the responses of Lavandula species, particularly in the climates of Fars and Hamedan. Future investigations should delve into these influences concerning qualitative traits in both species.

REFERENCE

Afshari, F., Nakhaei, F., Mosavi, S., Seghatoleslami, M. 2022. Physiological and biochemical responses of Stevia rebaudiana Bertoni to nutri-priming and foliar nutrition under water supply restrictions. Industrial Crops and Products, 176, 114399. https://doi.org/10.1016/j.indcrop.2021.114399

Aghighi Shahverdi, M., Omidi, H., Damalas, C.A. 2020. Foliar fertilization with micronutrients improves *Stevia rebaudiana* tolerance to salinity stress by improving root characteristics. Brazilian Journal of Botany, 43, 55-65. https://doi.org/10.1007/s40415-020-00588-6

Aghighi Shahverdi, M., Omidi, H., Tabatabaei, S.J. 2018. Plant growth and steviol glycosides as affected by foliar application of selenium, boron, and iron under NaCl stress in *Stevia rebaudiana* Bertoni. Industrial Crops and Products, 125, 408-415. https://doi.org/10.1016/j.indcrop.2018.09.029

Agnihotri, R., Pandey, A., Bharti, A., Chourasiya, D., Maheshwari, H.S., Ramesh, A., Billore, S.D., Sharma, M.P. 2021. Soybean processing mill waste plus vermicompost enhances arbuscular mycorrhizal fungus inoculum production. Current Microbiology, 78, 2595-2607. https://doi.org/10.1007/s00284-021-02532-7

Ahmad, S., Ni, S.Q., Safdar, H., Javeria, F., Haider, M., Khan, Z. 2024. ACC deaminase produced by PGPB and their role in stress management.' in, *Bacterial Secondary Metabolites* (Elsevier). https://doi.org/10.1016/B978-0-323-95251-4.00014-4

Allohverdi, T., Mohanty, A.K., Roy, P., Misra, M. 2021. A review on current status of biochar uses in agriculture. Molecules, 26, 5584. https://doi.org/10.3390/molecules26185584

Asghari, B., Khademian, R., Sedaghati, B. 2020. Plant growth promoting rhizobacteria (PGPR) confer drought resistance and stimulate biosynthesis of secondary metabolites in pennyroyal (*Mentha pulegium* L.) under water shortage condition. Scientia Horticulturae, 263, 109132. https://doi.org/10.1016/j.scienta.2019.109132

Azizi, S., Kouchaksaraei, M.T., Hadian, J., Abad, A.R.F.N., Sanavi, S.A.M.M., Ammer, C., Bader, M.K.F. 2021. Dual inoculations of arbuscular mycorrhizal fungi and plant growth-promoting rhizobacteria boost drought resistance and essential oil yield of common myrtle. Forest Ecology and Management, 497, 119478. https://doi.org/10.1016/j.foreco.2021.119478

Bechtaoui, N., Rabiu, M.K., Raklami, A., Oufdou, K., Hafidi, M., Jemo, M. 2021. Phosphate-dependent regulation of growth and stresses management in plants. Frontiers in Plant Science, 12, 679916. https://doi.org/10.3389/fpls.2021.679916

Begum, N., Wang, L., Ahmad, H., Akhtar, K., Roy, R., Khan, M.I., Zhao, T. 2022. Co-inoculation of arbuscular mycorrhizal fungi and the plant growth-promoting rhizobacteria improve growth and photosynthesis in tobacco under drought stress by up-regulating antioxidant and mineral nutrition metabolism. Microbial Ecology, 83(4), 971-988. https://doi.org/10.1007/s00248-021-01815-7

Benadjaoud, A., Dadach, M., El-Keblawy, A., Mehdadi, Z. 2022. Impacts of osmopriming on mitigation of the negative effects of salinity and water stress in seed germination of the aromatic plant *Lavandula stoechas* L. Journal of Applied Research on Medicinal and Aromatic Plants, 31, 100407. https://doi.org/10.1016/j.jarmap.2022.100407

Campo, S., Martín-Cardoso, H., Olivé, M., Pla, E., Catala-Forner, M., Martínez-Eixarch, M., San Segundo, B. 2020. Effect of root colonization by arbuscular mycorrhizal fungi on growth, productivity and blast resistance in rice. Rice, 13, 1-14. https://doi.org/10.1186/s12284-020-00402-7

Carter, M.R.,Gregorich, E.G. 2007. Soil sampling and methods of analysis (CRC press).

Chrysargyris, A., Laoutari, S., Litskas, V.D., Stavrinides, M.C., Tzortzakis, N. 2016. Effects of water stress on lavender and sage biomass production, essential oil composition and biocidal properties against Tetranychus urticae (Koch). Scientia Horticulturae, 213, 96-103. https://doi.org/10.1016/j.scienta.2016.10.024

Crişan, I., Ona, A., Vârban, D., Muntean, L., Vârban, R., Stoie, A., Mihăiescu, T., Morea, A. 2023. Current trends for lavender (*lavandula angustifolia* Mill.) crops and products with emphasis on essential oil quality. Plants, 12, 357. https://doi.org/10.3390/plants12020357

Cui, P., Fan, F., Yin, C., Song, A., Huang, P., Tang, Y., Zhu, P., Peng, C., Li, T., Wakelin, S.A. 2016. Long-term organic and inorganic fertilization alters temperature sensitivity of potential N_2O emissions and associated microbes. Soil Biology and Biochemistry, 93, 131-141. https://doi.org/10.1016/j.soilbio.2015.11.005

Détár, E., Németh, É.Z., Gosztola, B., Demján, I., Pluhár, Z. 2020. Effects of variety and growth year on the essential oil properties of lavender (*Lavandula angustifolia* Mill.) and lavandin (*Lavandula* x *intermedia* Emeric ex Loisel.). Biochemical Systematics and Ecology, 90, 104020. https://doi.org/10.1016/j.bse.2020.104020

Diatta, A.A., Fike, J.H., Battaglia, M.L., Galbraith, J.M., Baig, M.B. 2020. Effects of biochar on soil fertility and crop productivity in arid regions: a review. Arabian Journal of Geosciences, 13, 1-17. https://doi.org/10.1007/s12517-020-05586-2

Du, B., Rennenberg, H. 2018. Physiological responses of lavender (*Lavandula angustifolia* Mill.) towater deficit and recovery. South African Journal of Botany, 119: 212-218. https://doi.org/10.1016/j.sajb.2018.09.002

El-Attar, A.B., Othman, E.Z., El-Bahbohy, R.M., Mahmoud, A.W.M. 2023. Efficiency of different potassium sources, and soil bio-fertilizers for growth, productivity, and biochemical constituents of Narcissus (*Narcissus tazetta* L.). Journal of Plant Nutrition, 46, 2416-2433. https://doi.org/10.1080/01904167.2022.2155552

Eshaghi Gorgi, O., Fallah, H., Niknejad, Y., Barari Tari, D. 2022. Effect of plant growth promoting rhizobacteria (PGPR) and mycorrhizal fungi inoculations on essential oil in *Melissa officinalis* L. under drought stress. Biologia, 77, 11-20. https://doi.org/10.1007/s11756-021-00919-2

Farrokhi, H., Asgharzadeh, A., Samadi, M.K. 2021. Yield and qualitative and biochemical characteristics of saffron (*Crocus sativus* L.) cultivated in different soil, water, and climate conditions. Italian Journal of Agrometeorology, 2, 43-55. https://doi.org/10.36253/ijam-1216

Fascella, G., D'Angiolillo, F., Ruberto, G., Napoli, E. 2020. Agronomic performance, essential oils and hydrodistillation wastewaters of *Lavandula angustifolia* grown on biochar-based substrates. Industrial Crops and Products, 154, 112733. https://doi.org/10.1016/j.indcrop.2020.112733

Fascella, G., Mammano, M.M., D'Angiolillo, F., Pannico, A., Rouphael, Y. 2020. Coniferous wood biochar as substrate component of two containerized Lavender species: Effects on morpho-physiological traits and nutrients partitioning. Scientia Horticulturae, 267, 109356. https://doi.org/10.1016/j.scienta.2020.109356

García-Caparrós, P., Romero, M.J., Llanderal, A., Cermeño, P., Lao, M.T., Segura, M.L. 2019. Effects of drought stress on biomass, essential oil content, nutritional parameters, and costs of production in six Lamiaceae species. Water, 11, 573. https://doi.org/10.3390/w11030573

Giannoulis, K.D., Evangelopoulos, V., Gougoulias, N., Wogiatzi, E. 2020. Could bio-stimulators affect flower, essential oil yield, and its composition in organic lavender (*Lavandula angustifolia*) cultivation? Industrial Crops and Products, 154, 112611. https://doi.org/10.1016/j.indcrop.2020.112611

Hadipour, A., Hoseini Mazinani, M., Mehrafarin, A. 2013. Changes in essential oil content/composition and shoot aerial yield of lavender (*Lavandula officinalis* L.) affected by different treatments of nitrogen. Journal of Medicinal Plants, 12, 156-169

Januškaitienė, I., Dikšaitytė, A., Kunigiškytė, J. 2022. Organic fertilizers reduce negative effect of drought in barely (C3) and millet (C4) under warmed climate conditions. Archives of Agronomy and Soil Science, 68, 1810-1825. https://doi.org/10.1080/03650340.2021.1928648

Javanmard, A., Amani Machiani, M., Haghaninia, M., Pistelli, L., Najar, B. 2022. Effects of green manures (in the form of monoculture and intercropping), biofertilizer and organic manure on the productivity and phytochemical properties of peppermint (*Mentha piperita* L.). Plants, 11, 2941. https://doi.org/10.3390/plants11212941

Jiao, H., Wang, R., Qin, W., Yang, J. 2024. Screening of rhizosphere nitrogen fixing, phosphorus and potassium solubilizing bacteria of Malus sieversii (Ldb.) Roem. and the effect on apple growth. Journal of Plant Physiology, 292, 154142. https://doi.org/10.1016/j.jplph.2023.154142

Kari, A., Nagymáté, Z., Romsics, C., Vajna, B., Tóth, E., Lazanyi-Kovács, R., Rizó, B., Kutasi, J., Bernhardt, B., Farkas, É. 2021. Evaluating the combined effect of biochar and PGPR inoculants on the bacterial community in acidic sandy soil. Applied Soil Ecology, 160, 103856. https://doi.org/10.1016/j.apsoil.2020.103856

Khatami, S.A., Kasraie, P., Oveysi, M., Tohidi Moghadam, H.R., Ghooshchi, F. 2023. Impacts of plant growth-promoting bacteria, compost and biodynamic compost preparations for alleviating the harmful effects of salinity on essential oil characteristics of lavender. Chemical and Biological Technologies in Agriculture, 10, 110. https://doi.org/10.1186/s40538-023-00485-6

Kleinwächter, M., Paulsen, J., Bloem, E., Schnug, E., Selmar, D. 2015. Moderate drought and signal transducer induced biosynthesis of relevant secondary metabolites in thyme (*Thymus vulgaris*), greater celandine (*Chelidonium majus*) and parsley (*Petroselinum crispum*). Industrial Crops and Products, 64, 158-166. https://doi.org/10.1016/j.indcrop.2014.10.062

Kumar, A., Bhattacharya, T., Mukherjee, S., Sarkar, B. 2022. A perspective on biochar for repairing damages in the soil–plant system caused by climate change-driven extreme weather events. Biochar, 4, 22. https://doi.org/10.1007/s42773-022-00148-z

Kumar, S., Sindhu, S.S., Kumar, R. 2022. Biofertilizers: An ecofriendly technology for nutrient recycling and environmental sustainability. Current Research in Microbial Sciences, 3, 100094. https://doi.org/10.1016/j.crmicr.2021.100094

Lalay, G., Ullah, A., Iqbal, N., Raza, A., Asghar, M.A., Ullah, S. 2022. The alleviation of drought-induced damage to growth and physio-biochemical parameters of *Brassica napus* L. genotypes using an integrated approach of biochar amendment and PGPR application. Environment, Development and Sustainability, 26, 3457-3480. https://doi.org/10.1007/s10668-022-02841-2

Li, Y., Wei, J., Ma, L., Wu, X., Zheng, F., Cui, R., Tan, D. 2024. Enhancing wheat yield through microbial organic fertilizer substitution for partial chemical fertilization: regulation of nitrogen conversion and utilization. Journal of Soil Science and Plant Nutrition, 1-9. https://doi.org/10.1007/s42729-023-01597-6

Liu, C.Y., Hao, Y., Wu, X.L., Dai, F.J., Abd-Allah, E.F., Wu, Q.S., Liu, S.R. 2023. Arbuscular mycorrhizal fungi improve drought tolerance of tea plants via modulating root architecture and hormones. Plant Growth Regulation, 102,13-22. https://doi.org/10.1007/s10725-023-00972-8

Mahajan, M., Pal, P.K. 2023. Chapter Five - Drought and salinity stress in medicinal and aromatic plants: Physiological response, adaptive mechanism, management/amelioration strategies, and an opportunity for production of bioactive compounds.' in Sparks

DL (ed.), *Advances in agronomy* (Academic Press). https://doi.org/10.1016/bs.agron.2023.06.005

Mohammadi, H., Ghorbanpour, M., Brestic, M. 2018. Exogenous putrescine changes redox regulations and essential oil constituents in field-grown *Thymus vulgaris* L. under well-watered and drought stress conditions. Industrial Crops and Products, 122, 119-132. https://doi.org/10.1016/j.indcrop.2018.05.064

Nadjafi, F., Mahdavi Damghani, M., Tabrizi, L., Nejad Ebrahimi, S. 2014. Effect of biofertilizers on growth, yield and essential oil content of thyme (*Thymus vulgaris* L.) and sage (*Salvia officinalis* L.). Journal of Essential Oil Bearing Plants, 17, 237-250. https://doi.org/10.1080/0972060X.2013.813235

Nouri, M., Homaee, M., Pereira, L.S., Bybordi, M. 2023. Water management dilemma in the agricultural sector of Iran: A review focusing on water governance. Agricultural Water Management, 288, 108480. https://doi.org/10.1016/j.agwat.2023.108480

Özsevinç, A., Alkan, C. 2023. Polyurethane shell medicinal lavender release microcapsules for textile materials: An environmentally friendly preparation. Industrial Crops and Products, 192, 116131. https://doi.org/10.1016/j.indcrop.2022.116131

Paśmionka, I.B., Bulski, K., Boligłowa, E. 2021. The participation of microbiota in the transformation of nitrogen compounds in the soil-A review. Agronomy, 11, 977. https://doi.org/10.3390/agronomy11050977

Peçanha, D.A., Freitas, M.S.M., Cunha, J.M., Vieira, M.E., de Jesus, A.C. 2023. Mineral composition, biomass and essential oil yield of french lavender grown under two sources of increasing potassium fertilization. Journal of Plant Nutrition, 46, 344-355. https://doi.org/10.1080/01904167.2022.2068430

Peymaei, M., Sarabi, V., Hashempour, H. 2024. Improvement of the yield and essential oil of fennel (*Foeniculum vulgare* Mill.) using external proline, uniconazole and methyl jasmonate under drought stress conditions. Scientia Horticulturae, 323, 112488. https://doi.org/10.1016/j.scienta.2023.112488

Phares, C.A., Amoakwah, E., Danquah, A., Afrifa, A., Beyaw, L.R., Frimpong, K.A. 2022. Biochar and NPK fertilizer co-applied with plant growth promoting bacteria (PGPB) enhanced maize grain yield and nutrient use efficiency of inorganic fertilizer. Journal of Agriculture and Food Research, 10, 100434. https://doi.org/10.1016/j.jafr.2022.100434

Pokajewicz, K., Białoń, M., Svydenko, L., Fedin, R., Hudz, N. 2021. Chemical composition of the essential oil of the new cultivars of *Lavandula angustifolia* Mill. Bred in Ukraine. Molecules, 26, 5681. https://doi.org/10.3390/molecules26185681

Rodríguez-Pérez, L., Ñústez L, C.E., Moreno F, L.P. 2017. Drought stress affects physiological parameters but not tuber yield in three Andean potato (*Solanum tuberosum* L.) cultivars. Agronomía Colombiana, 35, 158-170. https://doi.org/10.15446/agron.colomb.v35n2.65901.

Sałata, A., Buczkowska, H., Nurzyńska-Wierdak, R. 2020. Yield, essential oil content, and quality performance of *Lavandula angustifolia* leaves, as affected by supplementary irrigation and drying methods. Agriculture, 10, 590. https://doi.org/10.3390/agriculture10120590

Sharma, M., Shilpa, Kaur, M., Sharma, A.K., Sharma, P. 2023. Influence of different organic manures, biofertilizers and inorganic nutrients on performance of pea (*Pisum sativum* L.) in North Western Himalayas. Journal of Plant Nutrition, 46, 600-617https://doi.org/10.1080/01904167.2022.2071735

Sheteiwy, M.S., Ali, D.F.I., Xiong, Y.-C., Brestic, M., Skalicky, M., Hamoud, Y.A., Ulhassan, Z., Shaghaleh, H., AbdElgawad, H., Farooq, M. 2021. Physiological and biochemical responses of soybean plants inoculated with Arbuscular mycorrhizal fungi and Bradyrhizobium under drought stress. BMC Plant Biology, 21, 1-21. https://doi.org/10.1186/s12870-021-02949-z

Siahbidi, A., Rrezaizad, A. 2018. Effect of deficit irrigation and super absorbent application on physiological characteristics and seed yield of new Iranian sunflower (*Helianthus annuus* L.) hybrids. Iranian Journal of Crop Sciences, 20(3), 222-236. http://agrobreedjournal.ir/article-1-942-en.html

Singh, D., Thapa, S., Geat, N., Mehriya, M.L., Rajawat, M.V.S. 2021. Biofertilizers: Mechanisms and application. in *Biofertilizers* (Elsevier). https://doi.org/10.1016/B978-0-12-821667-5.00024-5

Soumare, A., Diedhiou, A.G., Thuita, M., Hafidi, M., Ouhdouch, Y., Gopalakrishnan, S., Kouisni, L. 2020. Exploiting biological nitrogen fixation: a route towards a sustainable agriculture. Plants, 9, 1011. https://doi.org/10.3390/plants9081011

Sun, W., Shahrajabian, M.H. 2023. The application of arbuscular mycorrhizal fungi as microbial biostimulant, sustainable approaches in modern agriculture. Plants, 12, 3101. https://doi.org/10.3390/plants12173101

Ullah, N., Ditta, A., Khalid, A., Mehmood, S., Rizwan, M.S., Ashraf, M., Mubeen, F., Imtiaz, M., Iqbal, M.M. 2020. Integrated effect of algal biochar and plant growth promoting rhizobacteria on physiology and growth of maize under deficit irrigations. Journal of Soil Science and Plant Nutrition, 20, 346-356. https://doi.org/10.1007/s42729-019-00112-0

Wahab, A., Abdi, G., Saleem, M.H., Ali, B., Ullah, S., Shah, W., Mumtaz, S., Yasin, G., Muresan, C.C., Marc, R.A. 2022. Plants' physio-biochemical and phyto-hormonal responses to alleviate the adverse effects of drought stress: A comprehensive review. Plants, 11, 1620. https://doi.org/10.3390/plants11131620

Wahab, A., Muhammad, M., Munir, A., Abdi, G., Zaman, W., Ayaz, A., Khizar, C., Reddy, S.P.P. 2023. Role of arbuscular mycorrhizal fungi in regulating growth, enhancing productivity, and potentially influencing ecosystems under abiotic and biotic stresses. Plants, 12, 3102. https://doi.org/10.3390/plants12173102

Yadav, R., Ror, P., Rathore, P., Ramakrishna, W. 2020. Bacteria from native soil in combination with arbuscular mycorrhizal fungi augment wheat yield and biofortification. Plant Physiology and Biochemistry, 150, 222-233. https://doi.org/10.1016/j.plaphy.2020.02.039

Yu, X., Keitel, C., Zhang, Y., Wangeci, A.N., Dijkstra, F.A. 2022. Global meta-analysis of nitrogen fertilizer use efficiency in rice, wheat and maize. Agriculture, Ecosystems & Environment, 338, 108089. https://doi.org/10.1016/j.agee.2022.108089

Zhang, C., Li, X., Yan, H., Ullah, I., Zuo, Z., Li, L., Yu, J. 2020. Effects of irrigation quantity and biochar on soil physical properties, growth characteristics, yield and quality of greenhouse tomato. Agricultural Water Management, 241, 106263. https://doi.org/10.1016/j.agwat.2020.106263

Zhang, W., Cao, Z., Xie, Z., Lang, D., Zhou, L., Chu, Y., Zhao, Q., Zhang, X., Zhao, Y. 2017. Effect of water stress on roots biomass and secondary metabolites in the medicinal plant *Stellaria dichotoma* L. var. lanceolata Bge. Scientia Horticulturae, 224, 280-285. https://doi.org/10.1016/j.scienta.2017.06.030

Zhu, X., Ros, G.H., Xu, M., Cai, Z., Sun, N., Duan, Y., de Vries, W. 2023. Long-term impacts of mineral and organic fertilizer inputs on nitrogen use efficiency for different cropping systems and site conditions in Southern China. European Journal of Agronomy, 146, 126797. https://doi.org/10.1016/j.eja.2023.126797

Zollinger, N., Kjelgren, R., Cerny-Koenig, T., Kopp, K., Koenig, R. 2006. Drought responses of six ornamental herbaceous perennials. Scientia Horticulturae, 109, 267-274. https://doi.org/10.1016/j.scienta.2006.05.006

Italian Journal of Agrometeorology
Rivista Italiana di Agrometeorologia

Firenze University Press
https://riviste.fupress.net/index.php/IJAm

OPEN ACCESS

Citation: Nabati, E., Farnia, A., Jafarzadeh Kenarsari, M., & Nakhjavan, S. (2024). Impact of reduced irrigation on physiological, photosynthetic, and enzymatic activities in wheat (*Triticum aestivum* L.) exposed to water stress at varying plant densities. *Italian Journal of Agrometeorology* (2): 23-35. doi: 10.36253/ijam-2774

Received: June 9, 2024

Accepted: Novemeber 22, 2024

Published: December 30, 2024

© 2024 Author(s). This is an open access, peer-reviewed article published by Firenze University Press (https://www.fupress.com) and distributed, except where otherwise noted, under the terms of the CC BY 4.0 License for content and CC0 1.0 Universal for metadata.

Data Availability Statement: All relevant data are within the paper and its Supporting Information files.

Competing Interests: The Author(s) declare(s) no conflict of interest.

ORCID:
EN: 0009-0009-0051-0063
AF: 0009-0009-7575-5807
MJK: 0009-0001-4759-6476

Impact of reduced irrigation on physiological, photosynthetic, and enzymatic activities in wheat (*Triticum aestivum* L.) exposed to water stress at varying plant densities

Ezatollah Nabati, Amin Farnia*, Mojtaba Jafarzadeh Kenarsari, Shahram Nakhjavan

Department of Agronomy, Borujerd Branch, Islamic Azad University, Borujerd, Iran
*Corresponding author. E-mail: aminfarnia1401@gmail.com

Abstract. Drought stress is one of the most critical factors reducing the performance of crop plants in arid and semi-arid regions globally, and understanding underlying mechanisms is important to be able to implement measures for alleviating the negative impacts of drought on yield and yield quality. The present experiment aimed to investigate the effect of drought stress and planting density on the physiological characteristics, photosynthetic pigments, and enzymatic activity of wheat plants exposed to water stress. The experiment was conducted in a factorial arrangement based on a completely randomized block design with three replications. The treatments included irrigation cessation at three levels (control, i.e., full irrigation, irrigation until flowering (IUF), and irrigation until the dough stage (IUD)), and plant density (300, 400, 500, and 600 plants m^{-2}). The results indicate that leaf relative water content, soluble sugars, cell membrane stability index, chlorophyll a, b, and carotenoids significantly decreased under IUF, while these parameters increased at higher plant densities. Additionally, the interaction of drought stress and plant density significantly affected leaf proline and flavonoid content, total chlorophyll, and catalase activity. The highest leaf proline content (3.88 mg g^{-1} FW) was observed in IUF and a density of 600 plants m^{-2}, representing a 192% increase compared to the control. Additionally, the highest total chlorophyll content (3.66 mg g^{-1} FW) was recorded at no-stress conditions at a density of 500 plants m^{-2}. The activity of antioxidant enzymes increased under water stress. Overall, our results indicate that a density of 500 plants m^{-2} is optimal for maintaining stable growth conditions in wheat in the semi-arid to arid climate of Iran. These findings provide valuable insights to develop agronomic strategies for coping with drought in wheat cultivation, particularly in arid and semi-arid regions.

Keywords: drought stress, proline, soluble sugar, wheat, flavonoid.

HIGHLIGHTS

- Drought stress negatively affects the productivity of crop plants
- Plants are more sensitive to water stress during the flowering stage compared to the dough phase

– Optimal plant densities, such as 500 plants m^{-2}, can help mitigate drought stress.

1. INTRODUCTION

Wheat is cultivated on a large scale worldwide and ranks first among other cereals in terms of production and acreage, due to its high genetic flexibility and diversity (van Frank et al., 2020). Notably, wheat plays a vital role in Iran's food security as it is a staple food consumed daily, making it essential to the national diet (Dadrasi et al. 2023). Furthermore, Iran's policy of self-sufficiency in wheat production aims at ensuring a stable food supply and reducing dependency on imports (Ghaziani et al. 2023). The country cultivates 6 million hectares of wheat, with 2 million hectares being irrigated and 4 million hectares rain-fed. The total wheat production stands at 13.5 tons ha^{-1}, with an average yield of 4.44 tons ha^{-1}in rain-fed wheat cultivation (Dadrasi et al. 2023). In Iran, winter wheat is cultivated using three different cultivation methods: conventional, semi-mechanized, and mechanized Rain-fed cultivation, which enables economically viable production at lower costs, is found in areas with high rainfall, such as the Zagros and Alborz mountain ranges. Local irrigated wheat varieties, which are grown mainly in the temperate climate zones of the country, are Baharan, Pishgam, Sirvan, Mihan, and Heydari, while rainfed wheat varieties sare Azar, Karaj and Zagros. In addition, some international varieties such as Sultan and Kalyansona (which originate from Turkey and India, respectively) are also grown in Iran. Typical sowing dates are between November 1 and 20, and what is usually harvested in early July (Ghahremaninejad et al. 2021). The usual plant density is 450 to 500 seeds per m^2, which is about 10% below the optimal density (Ghahremaninejad et al. 2021).

The performance and physiological characteristics of wheat are influenced by factors such as water availability and plant density (Safar-Noori et al., 2018). Climate change has caused an increase in drought events, salinity problems, heat waves, and the occurrence of excessive radiation, all of which have worsened the conditions for wheat cultivation in many regions of the world (Ghadirnezhad Shiade et al., 2020; Taghavi Ghasemkheili et al., 2023) and has been responsible for a significant decline in agricultural productivity and quality (Brito et al., 2019). Given the fact that Iran is characterized by arid and semi-arid climatic conditions, droughts occur in decadal cycles (Hamarash et al. 2022). Prolonged and successive droughts significantly influence wheat yield and production, such that the country's production in dry years declines to 9 million tons, a much lower level than the 15 million tons typically harvested in wetter years (Ghaziani et al. 2023). Hence, irrigated wheat cultivation has gained importance to alleviate droughts and improve yield components (Zhao et al., 2020).

Drought stress negatively affects the growth, yield, biochemical, and physiological characteristics of crop plants (Safar-Noori et al., 2018). it impacts yield through various physiological processes, with the effects differing depending on the plant species (and cultivars), as well as the timing and severity of the drought (Seleiman et al., 2021). Water deficiency leads to reduced plant growth and yield due to increasing osmotic pressure, increased plant respiration, reduced photosynthesis, and consequently reduced cell division (Seleiman et al., 2021). In addition, various types of reactive oxygen species (ROS) are produced under stress conditions, acting as secondary messengers and playing an important role in transmitting stress signals (Ghadirnezhad Shiade et al., 2020; Ghadirnezhad Shiade et al., 2022). Plants possess antioxidant systems to mitigate the damages caused by increased production of ROS. These antioxidant systems in plants include non-enzymatic antioxidants such as proline, ascorbic acid, alpha-tocopherol, anthocyanins, phenols, flavonoids and some antioxidant enzymes such as catalase (CAT), peroxidase (POD), superoxide dismutase (SOD) and glutathione reductase (GR), which are responsible for scavenging ROS under various conditions (Møller et al., 2007; Ghadirnezhad Shiade et al., 2020). Plants with high levels of enzymatic antioxidants exhibit further resistance to oxidative damage (Kibria et al., 2017). Nasirzadeh et al., (2021) exposed wheat plants to three three levels of water stress, i.e., no stress (control), medium stress (volumetric soil water content at 40% of Field capacity (FC)), and severe stress (volumetric soil water content at 25% of FC). They noted that drought stress led to reduced relative water content (RWC), enhanced proline content, and antioxidant enzyme activities (catalase (CAT), superoxide dismutase (SOD), ascorbate peroxidase (APX)). Similarly, increased soluble sugar and proline content, while decreased RWC, photosynthetic pigments content, and the membrane stability index (MSI) were observed in wheat plants subjected to various irrigation deficit patterns (Amoah & Seo, 2021).

One of the influential factors for increasing plant performance in agricultural management is the alteration of plant density, as this can lead to changes in crop yield and yield components (Li et al., 2020). In fact, plant density is one of the most critical factors in the ability of crops to utilize environmental resources because it affects the biochemical and physiological

characteristics of the plant (D. Li et al., 2020). Optimal planting density varies depending on local or regional settings, planting date, climatic conditions (especially rainfall distribution), soil type, and wheat variety (Elhani et al., 2007). Previous studies have shown that adjusting plant density can help mitigate the adverse effects of drought. For instance, Li et al., (2020) conducted field experiments with three plant densities (480–570, 360–390, and 240–270 10^4 plants hm^{-2}) and three irrigation levels (no irrigation, 80.0 mm only at the jointing stage, and 60.0 mm each at the jointing and flowering stages). They found that increasing plant density can compensate for the adverse effects of water deficit under limited irrigation. The authors explained this result by suggesting that higher plant density enhances competition for resources, prompting the plants to optimize their use of water and nutrients.

To effectively identify the mechanisms of drought-tolerant plants, a comprehensive understanding of the physiological and antioxidant processes occurring in the crop under drought conditions is essential. These traits can used as valuable selection markers. Previous studies have largely overlooked the effects of drought stress on physiological parameters, photosynthetic pigments, and enzymatic activity of wheat at different planting densities. To fill this gap, this study aimed to: 1) Examine antioxidant levels in wheat exposed to different water stress levels and investigate the physiological, photosynthetic, and antioxidant mechanisms underlying drought tolerance in wheat; and, 2) Determine the optimal planting density to maximize yield under drought conditions.

2. MATERIALS AND METHODS

2.1. Experimental area and design

The experiment was conducted at the Agricultural Research Station of Borujerd County (48°8'E, 33°9'N, 1550 m above sea level), located in the Agricultural and Natural Resources Research Center of Lorestan Province, Iran (Figure 1). The seasonal evolution of average rainfall and temperature in the study area is shown in Figure. 2. The experiment ran from October 2020 to September 2021. The planting date was November 6, and the harvest date was June 26. The approximate flowering date was May 4, and the dough stage occurred on June 4. The experiment was carried out in a factorial design based on a completely randomized block design with three replications. The experimental treatments contained three levels of irrigation (control, i.e., full irrigation, irrigation until flowering (IUF), and irrigation until the dough stage (IUD)), and four plant densities (300, 400, 500, and 600 plants per m^2). Plants were irrigated by flood irrigation, which in IUF and IUD was discontinued based on when the corresponding developmental stages were reached. Irrigations were applied on a weekly basis when soil water fell below field capacity (FC) (i.e., between 20% and 30% of the soil's volume). The physical and chemical analysis of the soil in study area are (0–30 cm depth) presented in Table 1.

Figure 1. Map of Iran indicating the geographical location of the Borujerd County (Lorestan Province).

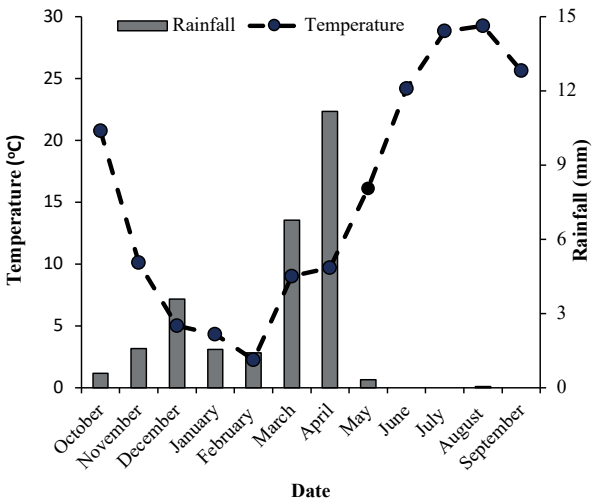

Figure. 2 Average rainfall (bars; scale on the right-hand side) and temperature (dashed line with dots; scale on the left-hand side) in the study area of Borujerd county.

Table 1. Physicochemical properties of the soil in areas of Borujerd, Iran.

Sand	Silt	Clay	Fe	NH_4	K	P	OC	EC	pH
	%			ppm			%	ds m^{-1}	
16.11	34.75	49.14	7.11	5.14	278	10.4	1.17	0.51	7.91

Fe: Iron;.NH4: Ammonium, K: potassium; P: phosphorus; OC: organic carbon; EC: electrical conductivity.

2.2. Measured physiological parameters

2.2.1. Cell membrane stability index (CMSI)

Three plants were randomly selected from each plot and the upper third part of their leaves were harvested. These leaves were individually wrapped in plastic bags and transferred to the laboratory. Leaf discs were prepared from the samples. Next, each sample (0.1 g) was mixed with distilled water (10 mL) and autoclaved at 100 °C for 15 minutes. Similarly, another set of samples was placed in Falcon tubes and kept at 40 °C for 30 min. Then, the samples were maintained in the laboratory environment until their temperature reached 25°C. Subsequently, the EC (electrical conductivity) of each Falcon tube was measured using an EC meter, and finally, the membrane stability index was calculated using Eq. (1) (Amoah & Seo, 2021):

$$CMSI = [(1- c_1/c_2) \times 100] \quad (1)$$

where, c_1 and c_2 represent the EC values at 40 and 100 °C, respectively.

2.2.2. Relative Water Content (RWC) of the leaves

Three plants were randomly selected from each plot and the upper third of their leaves were harvested at the same age. These leaves were individually packed in plastic bags and transferred to the laboratory. Each leaf was measured (fresh weight (FW)) and then placed in distilled water at 4 °C in the refrigerator for 24 hours. The leaves were then removed from the distilled water, dried with filter paper, and weighed again (saturation weight (TW)). They were then placed in an oven at 75 °C for 48 hours and weighed again (dry weight (DW)). The relative water content was calculated using Equation 2 (Ghadirnezhad Shiade et al., 2023)

$$RWC = [(FW - DW)/(TW - DW)] \times 100 \quad (2)$$

2.2.3. Measurement of soluble sugars

Dried plant samples were powdered and mixed with 80% ethanol (8 mL) and incubated for 30 minutes at 80 °C in a water bath. Afterward, the tubes were allowed to cool, followed by centrifugation at 2000 rpm for 20 minutes. The extraction process was repeated three times. To the collected liquid phase, 5.3 mL of 5% zinc sulfate ($ZnSO_4$) and 5.3 mL of 0.3 N barium hydroxide ($Ba(OH)_2$) were sequentially added to remove pigments. The liquid phase was then centrifuged again at 2000 rpm for 20 minutes. The liquid phase was transferred to a volumetric flask of 100 mL, and 2 mL of the resulting solution was used to determine the concentration of soluble sugars using the phenol-sulfuric acid method. The absorption of samples was measured using a spectrophotometer (model 6305 Jenway), at 485 nm. According to (Amoah & Seo, 2021).

2.2.4. Measurement of proline

Proline content was measured using the method described by Bates et al. (1973). The leaf sample (1 g) was homogenized with 10 mL of 3% sulfosalicylic acid in a mortar and centrifuged at 4000 rpm for 10 minutes. Then, 2 mL glacial acetic acid and 2 mL ninhydric acid were added and incubated in a boiling water bath at 100 °C for one hour. Then 4 mL of toluene was added to the sample and the optical absorbance was measured at 520 nm using a spectrophotometer.

2.2.5. Measurement of anthocyanin and flavonoids

The measurement of anthocyanins and flavonoids in the leaves was performed spectrophotometrically using the method described by (Wagner, 1979) and (Krizek et al., 1998).

2.3. Leaf chlorophyll and carotenoids

The leaf samples were randomly taken from three plants in each plot. The measurement of chlorophyll (chlorophyll a, chlorophyll b, and total chlorophyll) and

carotenoids was carried out using a non-destructive method. Leaf samples (0.5 g) were placed in 5 mL of dimethyl sulfoxide at 65 °C for 4 hours. Then, chlorophyll was measured using a spectrophotometer. The absorption levels at wavelengths of 665 (A665), 645 (A645), and 470 (A470) nm were recorded, respectively. Subsequently, the amounts of chlorophyll a (Chl a), chlorophyll b (Chl b), total chlorophyll (Total Chl), and carotenoids were calculated using Eqs. 3-6 (Ghadirnezhad Shiade et al., 2023):

$$\text{Chl a} = (12.19 \times A665) - (3.45 \times A645) \quad (3)$$

$$\text{Chl b} = (21.99 \times A645 - 5.32 \times A665) \quad (4)$$

$$\text{Total Chl} = \text{Chl a} + \text{Chl b} \quad (5)$$

$$\text{Carotenoeid} = (1000 \times A470 - 2.14 \times \text{Chla} - 70.16 \times \text{Chlb}) / 220 \quad (6)$$

2.4. Measurement of enzymatic activity

To measure the activity of the catalase (CAT) enzyme, a leaf sample (1 g) was mixed with 3 mL of buffer, extracted, and then centrifuged. Absorbance at 240 nm wavelength was measured for two minutes, and the initial minute data, with an extinction coefficient of 0.0394/0 mM cm^{-1}, was utilized to calculate catalase activity (Chance & Maehly, 1955). For peroxidase (POD) enzyme activity, a leaf sample (2 g) was mixed with 4 mL of buffer, extracted, and after centrifugation, absorbance at 470 nm wavelength was measured for 4 minutes. The initial minute data, with an extinction coefficient of 47.2 mMol cm^{-1}, was used to calculate POD (Chance & Maehly, 1955). The assay for superoxide dismutase (SOD) activity included 0.055 M of nitroblue tetrazolium, 1.42% Triton X-100, 0.1 mM of Ethylenediaminetetraacetic Acid (EDTA), and 16 mMol pyrogallol. After adding tissue sample extract, the change in absorbance at 560 nm wavelength was evaluated using a spectrophotometer (Masayasu & Hiroshi, 1979). Moreover, the assay for Glutathione Reductase (GR) activity on the sample containing 100 mMol potassium phosphate, 1 mMol EDTA, 2.0 polyvinyl phosphate, 2 mMol EDTA, 1.5 mMol magnesium chloride, 5.0 mMol oxidized glutathione, and 50 mMol of Nicotinamide adenine dinucleotide, reduced form (NADH) was read at 340 nm wavelength (Sgherri et al. 1994).

2.5. Data analysis

Data analysis was performed using SAS software, and the graphs were plotted using Origin Pro 2021 software. The Least Significant Difference (LSD) method at a 5% significance level was employed for mean data comparison.

3. RESULTS

The analysis of variance revealed that the main effects of drought stress and planting density significantly impacted all studied traits. Furthermore, the interaction effects of these factors influenced proline content, flavonoid levels, total chlorophyll, and catalase activity (Table 2).

3.1. Physiological parameters

The study findings indicated that the CMSI was affected by drought stress treatment (Table 3). Specifically, the highest value (85.8%) was observed in the control treatment, decreasing by 23% when terminating irrigation at the IUF stage, and by 16% when irrigation was terminated at the IUD stage. Additionally, the highest value of this parameter (82.21%) was recorded at a plant density of 500 plants m^{-2}, whereas the lowest value (69.35%) was reported at a density of 300 plants m^{-2} (Table 3). Similarly, the highest RWC value (81.21%) was observed in the control, decreasing by 19% and 11% under IUF and IUD, respectively (Table 3). Moreover, a plant density of 500 plants m^{-2} resulted in the highest RWC (76.89%), while the lowest value was observed at a density of 300 plants m^{-2}, at 59.25% (Table 3).

In addition, the study revealed an increase in the soluble sugar content of wheat under water stress at different growth stages (Table 3). Initially, the highest concentration of 1.95 μg g^{-1} FW was observed under the IUF treatment, which subsequently decreased by 45% to 1.52 μg g^{-1} FW under the IUD treatment. Additionally, a plant density of 600 plants m^{-2} triggered the highest parameter value (1.72 μg g^{-1} FW), which then reduced by 44% to the lowest value (0.95 μg g^{-1} FW) at a density of 500 plants m^{-2} (Table 3). The lab data showed that the highest level of leaf proline (3.88 mg g^{-1} FW) was achieved in the IUF and 600 plants m^2 density, which was statistically significantly different from the other experimental treatments. The lowest amount was recorded at the interaction effect of control and 500 plants m^{-2} density (1.41 mg g^{-1} FW) (Figure 3).

Besides, it was observed that the anthocyanin content in wheat was at its lowest level under non-water deficit conditions (34.1 mg g^{-1}). However, with increasing drought stress severity, the production of anthocyanins increased, with the highest level of anthocyanin production (2.34 mg g^{-1}) under the IUF treatment, decreasing

Table 2. Analysis of variance for physiological parameters, photosynthetic pigments, and enzymatic activity of wheat plants under drought stress and different plant densities.

SOV	df	CMSI	RWC	Soluble sugars	Proline content	Anthocyanin	Flavonoid	Chlorophyll a	Chlorophyll b	Total chlorophyll	Carotenoid	Catalase	Peroxidase	Superoxide dismutase	Glutathione reductase
Block	2	8.59	49.11	0.04	0.15	0.007	0.02	0.021	0.0009	0.001	0.006	58028	5.7	0.001	0.005
Irrigation	2	959*	659**	1.33**	4.11*	2.98**	10.5**	3.31*	0.81**	9.33**	4.24*	17144743**	336*	3.54**	3.63**
Density	3	99**	139**	0.10**	0.85*	0.1**	0.57**	1.11*	0.091*	1.2**	0.46*	169692**	198	0.04**	0.05*
Irrigation × Density	6	11.33	1.11	0.005	0.19*	0.005	0.03*	0.031	0.006	0.44**	0.021	51199*	40	0.005	0.01
Error	18	39.26	8.11	0.011	0.03	0.003	0.009	0.028	0.004	0.021	0.008	13165	58	0.003	0.008
CV		9.21	8.66	12.2	7.5	3.07	1.85	10.11	9.11	10.11	8.12	5.57	19	5.43	9.77

ns: no significant, * significant at 5% level, ** significant at 1% level.

Table 3. Physiological traits for the examined irrigation treatments and plant densities.

Treatments	CMSI (%)	RWC (%)	Soluble sugars (μg g^{-1} FW)	Anthocyanin (μg g^{-1} FW)
Irrigation				
Control	85.8 a	81.2 a	1.12 c	13.4 c
IUF	65.1 c	65.32 c	1.95 a	2.34 a
IUD	71.2 b	71.68 b	1.52 b	1.77 b
Plant density				
300 plant m^{-2}	69.35 c	59.25 d	1.40 b	1.71 b
400 plant m^{-2}	71.16 bc	64.41 c	1.11 bc	1.83 ab
500 plant m^{-2}	82.21 a	76.89 a	0.95 c	1.97 a
600 plant m^{-2}	75.15 ab	69.15 b	1.72 a	1.76 b

CMSI: cell membrane stability index, RWC: relative water content.

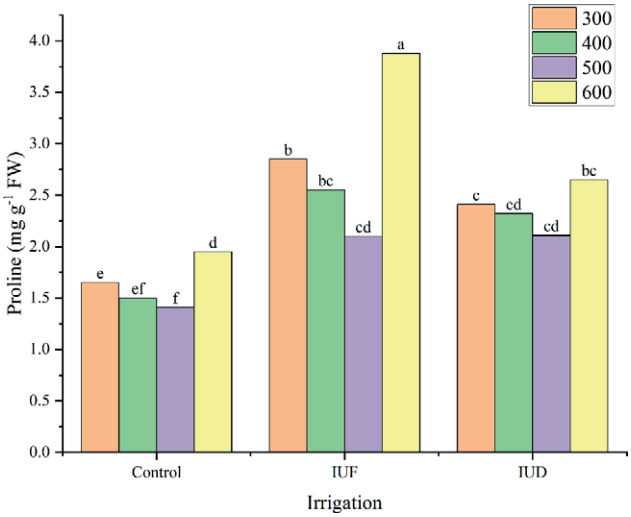

Figure 3. Interaction effects of irrigation practices (control, IUF and IUD) and plant densities (300-600 plant m^{-2}; colors) on proline content. IUF (Irrigation until the flowering stage), IUD (Irrigation until the dough stage).

(1.77 mg g^{-1}) under the IUD treatment (Table 3). Furthermore, the highest value of this parameter (1.97 mg g^{-1}) was observed at 500 plant m^{-2}, while no significant difference was observed in other treatments (all showing approximately 1.80 mg g^{-1}). On the other hand, flavonoid content in wheat leaves was influenced by the interactive effects of drought stress and plant density per unit area (Figure 4). Under non-drought stress conditions, the flavonoid content was higher at all plant densities than in the water deficit stress treatments. Additionally, the results showed that increasing plant density up to 500 plants m^{-2} led to an increase in flavonoid content in all drought stress treatments, while at a density of 600 plants

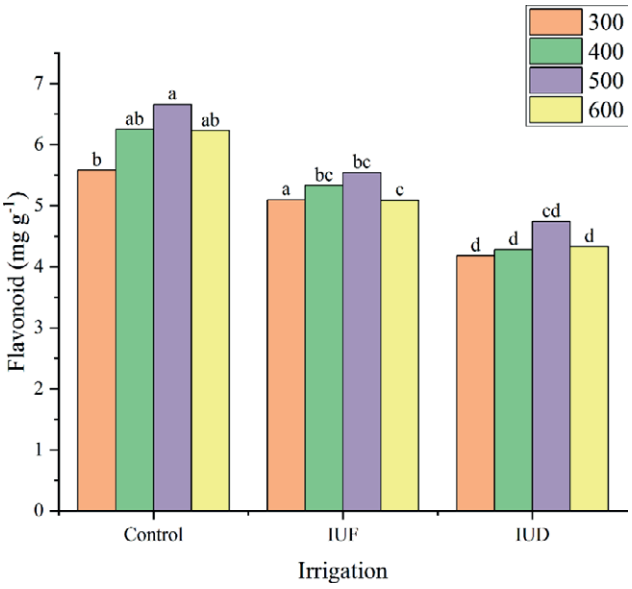

Figure 4. Interaction effects of irrigation practices (control, IUF and IUD) and plant densities (300-600 plant m^{-2}; colors) on flavonoid content. IUF (Irrigation until the flowering stage), IUD (Irrigation until the dough stage).

m^{-2}, there was a noticeable decrease in flavonoid content across all drought stress levels. The highest flavonoid content (6.6 mg g^{-1}) was observed under non-drought stress conditions and a plant density of 500 plants m^{-2}. This treatment differed significantly from other experimental treatments except for plant densities of 400 and 600 plants m^{-2} under the same level of drought stress. When irrigation continued until IUD, the flavonoid content in leaf tissues reached its lowest level across various plant densities (4.38 mg g^{-1}), (Figure 4).

3.2. Photosynthetic pigments

Our results revealed that chlorophyll a content was highest under the control treatment (1.92 mg g^{-1} FW), decreasing by 50% under IUF (0.95 mg g^{-1} FW)Under IUD, a less severe reduction of 23% was observed (1.46 mg g^{-1} FW) (Table 4). Furthermore, the chlorophyll a content increased with increasing plant density up to 500 plants m^{-2} (1.72 mg g^{-1} FW), but it decreased again at a density of 600 plants m^{-2} by 52% (1.34 mg g^{-1} FW). The lowest chlorophyll a content (1.11 mg g^{-1} FW) was observed at a density of 300 plants m^{-2} (Table 4). The same trend was recorded for Chl b under both drought and plant density treatments. Accordingly, the highest value (0.88 mg g^{-1} FW) was observed in the control treatment, decreasing by 60% under the IUF and 40% under IUD treatments. In relation to plant density, the

Table 4. Photosynthetic pigments for the examined irrigation treatments and plant densities.

Treatments	Chlorophyll a(mg g^{-1} FW)	Chlorophyll b (mg g^{-1} FW)	Carotenoid (mg g^{-1} FW)
Irrigation			
Control	1.92 a	0.88 a	2.11 a
IUF	0.95 c	0.35 c	0.92 c
IUD	1.46 b	0.52 b	1.52 b
Plant density			
300 plant m^{-2}	1.11 c	0.42 d	1.25 d
400 plant m^{-2}	1.59 ab	0.62 b	1.39 c
500 plant m^{-2}	1.72 a	0.73 a	1.48 b
600 plant m^{-2}	1.34 b	0.51 c	1.71 a

highest value (0.73 mg g^{-1} FW) was recorded at 500 plants m^{-2}, while the lowest value (0.51 mg g^{-1} FW) was recorded at 600 plants m^{-2}.

As for catenoid content, the highest level (2.11 mg g^{-1} FW) was obtained under conditions of no drought stress (Table 4). Additionally, the results indicated that with irrigation cut-off, the level of leaf carotenoids decreased 0.92 mg g^{-1} FW in IUF and 1.52 mg g^{-1} FW in IUD, respectively (Table 4). Furthermore, it was shown that the leaf carotenoid content was higher (1.71 mg g^{-1} FW) at 600 plants m^{-2} than at other densities. Decreasing the plant density from 600 to 300 plants m^{-2} resulted in a reduction in leaf carotenoid content by 18% (Table 4).

Our data indicate that the total chlorophyll content was influenced by the interaction of drought stress and plant density (Figure 5). Although the IUF treatment resulted in a greater reduction in this parameter compared to the IUD and control treatments, the highest value (3.66 mg g^{-1} FW) was measured at a plant density of 500 plants m^{-2}. Under IUF, the total chlorophyll content decreased for all studied plant densities. Accordingly, the lowest total chlorophyll content (1.52 mg g^{-1} FW) was observed in the treatment with a plant density of 300 plants m^{-2} at the IUD stage (Figure 5).

3.3. Enzymatic activity

The results indicated that in all planting densities, the CAT enzyme activity increased with the severity of drought stress (Figure 6). The increase in enzyme activity was significantly greater under IUF compared to both IUD and the control treatment. Additionally, further increasing the plant density contributed to this enhanced enzyme activity. The highest CAT activity (3956 nmol/g/min) was observed under IUF and a plant density of 600 plants m^{-2}, significantly differing from

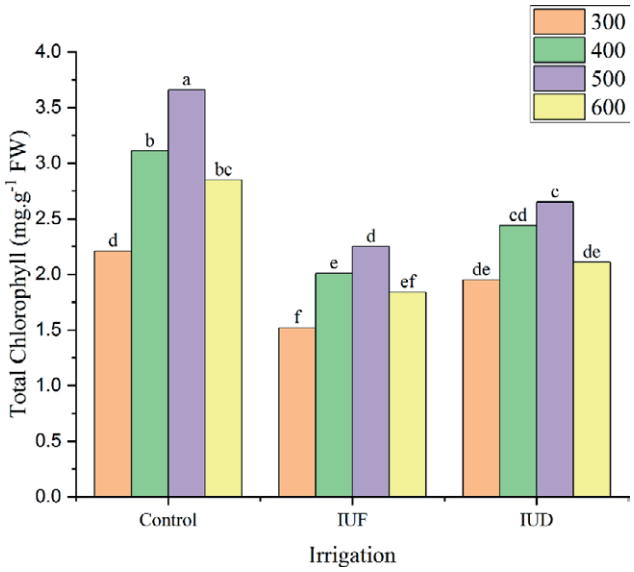

Figure 5. Interaction effects of irrigation practices (control, IUF and IUD) and plant densities (300-600 plant m^{-2}; colors) on total chrophyll content. IUF (Irrigation until the flowering stage), IUD (Irrigation until the dough stage).

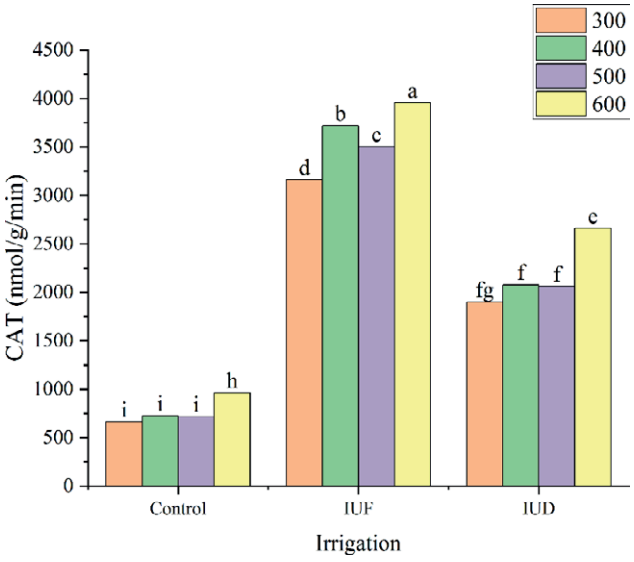

Figure 6. Interaction effects of irrigation practices (control, IUF and IUD) and plant densities (300-600 plant m^{-2}; colors) on Catalase (CAT) activity. IUF (Irrigation until the flowering stage), IUD (Irrigation until the dough stage).

other treatments, whereas the lowest value (660 nmol/g/min) was found in the control treatment and at a plant density of 300 plants m^{-2} (Figure 6).

The results reported in Table 5 indicate that the drought conditions led to an increase in the POD activity with the highest value (43 nmol/g/min) obtained under the IUF treatment. On the other hand, the lowest POD activity was observed under IUD (31 nmol/g/min). Additionally, the results showed that this enzyme activity was lower at a plant density of 300 m^{-2} (33.8 nmol/g/min) than under the other experimental treatments. Although no statistically significant difference was observed among the three densities of 400 - 600 plants m^{-2}, the results show that the highest activity of the POD enzyme was achieved at a density of 500 m^{-2} (45 nmol/g/min) (Table 5). As for SOD enzyme activity, the data show that it was lower under control conditions (61 µmol/g/min) than in conditions of water stress. Furthermore, under both IUF and IUD, the activity of this enzyme increased, with the highest increase observed in IUD (1.75 µmol/g/min) (Table 5). Similar changes were recorded for GR, with the highest activity (1.61 µmol/g/min) in IUD, and the lowest activity (0.35 µmol/g/min) in the control experiment (Table 5).

Table 5. Enzymatic activity for the examined irrigation treatment and plant densities.

Treatments	POD (nmol/g/min)	SOD (µmol/g/min)	GR (nmol/g/min)
Irrigation			
Control	39 a	0.61 b	0.35 c
IUF	43 a	0.73 b	0.84 b
IUD	31 b	1.75 a	1.61 a
Plant density			
300 plant m^{-2}	33.8 b	0.96 b	0.87 b
400 plant m^{-2}	43 a	1.1 a	1.02 a
500 plant m^{-2}	45 a	1.4 a	1.06 a
600 plant m^{-2}	37.5 ab	1.02 b	0.92 b

DISCUSSION

This study aimed to evaluate the effects of irrigation and plant densities on the physiological characteristics of wheat. The results revealed that both the individual treatments as well as their interactions significantly impacted the studied parameters. Our results indicated a considerable reduction of the CMSI under water stress conditions. Accordingly, water deficit stress increased electrolyte leakage from the cell walls and decreased cell membrane stability. In addition, our study showed a positive relation between increased cell membrane stability and other traits such as proline and soluble sugars. Specifically, we found that wheat leaves grown at a density of 500 plants m^{-2} had the highest cell membrane

stability. Interestingly, these plants had the lowest levels of soluble sugars and proline. This suggests that higher plant densities might create conditions that better maintain cell membrane stability, possibly by optimizing resource use and reducing stress at the cellular level. Our results are consistent with those of Amoah & Seo, (2021) who documented reduced CMSI under drought stress in wheat plants.

According to our results, the RWC of the leaves was reduced under water deficit. Water deprivation starting at the flowering stage (IUF) compared to water deprivation starting at the dough stage (IUD) resulted in longer-lasting water deficit exposure of the wheat plants, leading to more severe drought stress and a greater reduction in RWC in IUF than IUD. The imbalance between water supply and demand in plants is the most probable reason for the reduction in RWC under drought conditions. Similar results were reported by (Amoah & Seo, 2021) on wheat and Ghadirnezhad Shiade et al., (2023) on rice under salinity stress. Furthermore, Nasiri et al., (2017) observed similar results regarding RWC in higher plant densities (60 and 80 plants m^{-2}) on RWC. RWC is a critical parameter for assessing plant water status, quantifying the ratio of current water content to the plant's maximum water-holding capacity. Under drought conditions, a further decrease in RWC often signifies a substantial disruption in plant water relations. This disruption occurs because the plant's capacity to absorb and retain water from the soil is compromised, leading to reduced turgor pressure and impaired physiological processes. Consequently, the plant's water content diminishes, which points to the plant's difficulty in maintaining homeostasis. This decline in RWC can significantly impact various aspects of plant health, including nutrient uptake, photosynthetic efficiency, and overall growth. Additionally, under water deficit conditions, the roots cannot compensate for the water lost through transpiration, leading to a reduction in leaf water potential. Leaf relative water content directly correlates with leaf turgidity and plant water potential.

The increased anthocyanin content in wheat leaves under drought stress conditions can be attributed to the role of anthocyanins as UV-absorbing pigments in the leaf epidermis, protecting plant tissues from damage caused by these radiations (Hatier & Gould, 2008). Furthermore, it has been suggested that anthocyanin compounds accumulate in vacuoles or bind to the cuticle wall, serving as a protective response of plants against UV radiation (Carvalho et al., 2010). Additionally, the results of this study showed that the anthocyanin content in wheat leaves increased with density plant density increasing from 300 to 500 plants m^{-2}, decreasing again when plant density was further increased to 600 plants m^{-2}. The increase in anthocyanin content for plant densities up to 500 plants m^{-2} can be attributed to enhanced light absorption efficiency and improved protection of the photosynthetic system, thereby positively affecting dry matter production. Further increasing the plant density up to 600 plants m^{-2} appears to enhance shading within the wheat canopy. This reduced UV penetration into the canopy lowers anthocyanin production in the plants. Similar results were documented by Onjai-uea et al., (2022) who studied plant spacing, variety, and harvesting age effects on purple Napier grass.

Moreover, we observed that drought stress and plant density interactions also influenced the flavonoid content of wheat leaves. Under control conditions, the flavonoid content of leaves was higher in denser plant habitats compared to those under drought stress treatments. Moreover, flavonoid content increased with plant density up to 500 plants m^{-2} under drought stress but decreased significantly when plant density was further increased to 600 plants m^{-2}. Flavonoids play a crucial role in plant stress responses, including antioxidant activity and protection against oxidative stress caused by droughts (Taheri Asghari& Hossein, 2014; Onjai-uea et al., 2022). Under no drought stress, higher plant densities promote flavonoid accumulation due to efficient resource use. Under drought conditions, moderate densities (up to 500 plants m^{-2}) trigger stress responses that enhance flavonoid production, whereas excessive densities (600 plants m^{-2}) lead to reduced flavonoid content due to heightened competition and resource scarcity. Similar results were reported by Taheri Asghari& Hossein, (2014) who noted enhanced Kaempferol (a kind of flavonoid) content in Chicory (*Cichorium intybus* L.) which was exposed to water deficit conditions and cultivated at various planting densities. The antioxidative property of flavonoids, conferred by the hydroxyl group attached to a ring structure, involves the transfer of an electron to free radicals, reducing their potential. Flavonoids serve as effective scavengers for peroxide radicals, reducing the potential of alkyl peroxide radicals and ultimately acting as potent inhibitors of lipid peroxidation (Molor et al., 2016).

This study not only found that drought stress leads to an increase in proline content in the leaves, but also that an increase in plant density up to 500 plants m^{-2} leads to a decrease in proline content in the leaves at all drought stress levels. However, with an increase in plant density to 600 plants m^{-2}, the proline content of the leaves increased significantly. Regardless of drought stress effects, optimal plant growth conditions were achieved with an increase in plant density of up to 500 plants m^{-2}, leading to a decrease in leaf proline content.

However, at the higher density, stressful conditions were created due to increased competition between plants for water and nutrients as well as shading from overlapping plants, resulting in higher proline content. In this respect, our results are consistent with those of Nasiri et al., (2017).

In this study, discontinuing irrigation at different growth stages of wheat enhanced soluble sugar content. This phenomenon can be attributed to the establishment of osmotic regulation, with enhanced soluble sugar content resulting in reduced water loss from the plant and aiding in maintaining the stability of plant cells under drought-stress conditions (Shiade et al., 2024). Compatible solutes such as soluble sugars do not interfere with normal biochemical reactions of the cell and act as osmotic protectants during osmotic stress (Shiade et al., 2024). Similar results were reported by Li et al., (2014). Furthermore, it was found that increasing plant density from 300 to 500 plants m^{-2} decreased soluble sugar content, while further increasing plant density to 600 plants m^{-2} resulted in a greater increase in this compound. This can be attributed to the plant's resilient condition at 500 plants m^{-2} density.

Both the IUF and IUD treatments adversely affected the synthesis and stability of photosynthetic pigments, resulting in decreased content. Similar reductions in chlorophyll content under drought stress conditions have been reported in other studies (Nasiri et al., 2017). Taheri Asghari & Hossein (2014) also reported a reduction in chlorophyll content under drought stress conditions, noting that plants not suffering from drought stress present fewer damages from free radicals and higher leaf chlorophyll content. The negative effect of drought stress on chlorophyll content in wheat plants can be explained by the destruction of thylakoid membranes in chloroplasts and the photo-destruction of chlorophyll due to increased activity of oxygen species and chlorophyllase enzymes (Naroui Rad et al., 2012). Additionally, the activity of chlorophyllase is stimulated by the increase in some growth regulators such as ethylene and abscisic acid under drought stress (Amoah & Seo, 2021). An increase in plant density of up to 500 plants m^{-2} led to elevated photosynthetic pigment content, but the level of photosynthetic pigments was reduced under higher plant densities (600 plants m^{-2}). This phenomenon can be attributed to internal factors within the plant resulting from competition between plants for nutrient uptake in the soil. Another reason could be the reduction in leaf area due to excessive plant density, which leads to a decrease in photosynthetic pigment content. Similar results were reported by Nasiri et al., (2017) and Amoah & Seo, (2021).

The IUF treatment exposed plants to a prolonged water deficit compared to the IUD treatment. This phenomenon resulted in lipid peroxidation in the plants, caused by increased production of ROS and subsequent destruction of the cell membrane. Therefore, lant's reduced access to water availability, especially at higher densities, led to an increased antioxidant enzyme activity to scavenge ROS. Kibria et al., (2017) documented that under severe stress conditions, the CAT activity increased due to the higher lipid peroxidation and the increased production of hydrogen peroxide, as this enzyme is mainly contributing to hydrogen peroxide decomposition. Also, in other studies, an increase in CAT enzyme activity has been reported under stressful conditions (Ghadirnezhad Shiade, et al., 2023). POD enzymes play a very important role in deactivating ROS in plant cells during various stress situations, such as drought, and their activity level changes depending on the plant species and the intensity of stress in plants (Sharma et al., 2019). The increase in plant density (beyond optimal levels) was associated with increased intra-species competition, which led to the creation of stress conditions in the plant, and as a result, increased activity of antioxidant enzymes (Gao et al., 2018).

CONCLUSION

In the present study, it was found that the physiological characteristics and photosynthetic pigments of wheat are influenced by both drought stress and plant density. The results show that drought stress led to a decrease in chlorophyll content, carotenoids, relative water content, and cell membrane stability index, while it increased the levels of proline and soluble sugars. Furthermore, enzymatic activities were enhanced at higher drought stress and plant densities. Overall, our results indicated that a density of 500 plants m^{-2} can be optimal to maintain stable growth conditions in wheat under the drought conditions simulated in our field experiment. This optimal density establishes a balance between plant competition and resource utilization and allows for improved underlying responses and resilience to water scarcity.

In general, our findings reveal that the flowering stage was more sensitive to water deficit conditions than the dough stage. Accordingly, it is recommended to prioritize irrigation during the flowering stage, as wheat can better tolerate water stress afterward. Considering the limitations of water availability in Iran, continuous irrigation is not feasible in this country. Therefore, to balance water use with crop performance, irrigation should ideally be applied until the end of the flowering

stage, after which moderate drought stress can be tolerated without severe yield penalties.

It is notable that inadequate irrigation and suboptimal plant density significantly impact wheat quality and yield, with water stress leading to reduced grain size and quality, and increased susceptibility to pests and diseases, which further diminishes marketability and crop productivity. On the other hand, high plant density can cause excessive competition for resources, resulting in stunted growth and poor grain quality, while low density can lead to inefficient use of resources.

The broader significance of this study lies in its implications for managing water scarcity in arid and semi-arid regions. Our findings emphasize the fact that optimizing irrigation practices along with plant density can enhance resource efficiency and crop resilience. Current climate change scenarios for Iran indicate for the future more frequent and intense droughts, along with shifts in precipitation patterns toward less frequent but heavier rainfall events. Our findings stress the importance of targeted irrigation during sensitive phases for adapting wheat production to these changes and helping farmers cope with increased drought incidence. It is recommended that future studies should explore additional strategies for managing drought, including breeding to enhance drought resistance and resilience and selecting varieties with shorter growing stages, which could help avoid water stress conditions particularly around and after flowering. Further research into the molecular responses of plants under drought stress is also needed to better prepare wheat cultivation for the expected consequences of climate change in Iran and elsewhere.

REFERENCES

Amoah, J.N. & Seo, Y.W. (2021). Effect of progressive drought stress on physio-biochemical responses and gene expression patterns in wheat. 3 Biotech 11(10): 440. Retrieved from https://doi.org/10.1007/s13205-021-02991-6

Bates, L.S., Waldren, R.P. & Teare, I.D. (1973). Rapid determination of free proline for water-stress studies. Plant and soil 39(1): 205–207.

Brito, C., Dinis, L.-T., Moutinho-Pereira, J. & Correia, C. (2019). Kaolin, an emerging tool to alleviate the effects of abiotic stresses on crop performance. Scientia Horticulturae 250: 310–316. Retrieved from https://linkinghub.elsevier.com/retrieve/pii/S0304423819301529

Carvalho, R.F., Quecini, V. & Peres, L.E.P. (2010). Hormonal modulation of photomorphogenesis-controlled anthocyanin accumulation in tomato (*Solanum lycopersicum* L. cv Micro-Tom) hypocotyls: Physiological and genetic studies. Plant Science 178(3): 258–264. Retrieved from https://linkinghub.elsevier.com/retrieve/pii/S0168945210000294

Chance, B. & Maehly, A.C. (1955). [136] Assay of catalases and peroxidases.

Dadrasi A, Chaichi M, Nehbandani A, et al (2023) Addressing food insecurity: An exploration of wheat production expansion. PLoS One 18:e0290684. https://doi.org/10.1371/journal.pone.0290684

Gao, Y., Jiang, H., Wu, B., Niu, J., Li, Y., Guo, F., … Blakney, A.J.C. (2018). The effects of planting density on lodging resistance, related enzyme activities, and grain yield in different genotypes of oilseed flax. Crop Science 58(6): 2613–2622. Retrieved from https://acsess.onlinelibrary.wiley.com/doi/10.2135/cropsci2017.08.0498

Ghadirnezhad Shiade, Seyede Roghie;, Esmaeili, M., Pirdashti, H. & Nematzade, G. (2020). Physiological and biochemical evaluation of sixth generation of rice (*Oryza sativa* L.) mutant lines under salinity stress. Journal of plant process and function 9(35): 57–72.

Ghadirnezhad Shiade, Seyede Roghie, Fathi, A., Taghavi Ghasemkheili, F., Amiri, E. & Pessarakli, M. (2023). Plants' responses under drought stress conditions: Effects of strategic management approaches—a review. Journal of Plant Nutrition 46(9): 2198–2230. Retrieved from https://doi.org/10.1080/01904167.2022.2105720

Ghadirnezhad Shiade, Seyede Roghie, Pirdashti, H., Esmaeili, M.A. & Nematzade, G.A. (2023). Biochemical and physiological characteristics of mutant genotypes in Rice (*Oryza sativa* L.) Contributing to Salinity Tolerance Indices. Gesunde Pflanzen 75(2): 303–315. Retrieved from https://link.springer.com/10.1007/s10343-022-00701-7

Ghahremaninejad F, Hoseini E, Jalali S (2021) The cultivation and domestication of wheat and barley in Iran, brief review of a long history. Bot Rev 87:1–22. https://doi.org/10.1007/s12229-020-09244-w

Ghaziani S, Dehbozorgi G, Bakhshoodeh M, Doluschitz R (2023) Unraveling On-Farm Wheat Loss in Fars Province, Iran: A Qualitative Analysis and Exploration of Potential Solutions with Emphasis on Agricultural Cooperatives. Sustainability 15:12569. https://www.mdpi.com/2071-1050/15/16/12569#

Hamarash H, Hamad R, Rasul A (2022) Meteorological drought in semi-arid regions: A case study of Iran. J Arid Land 14:1212–1233. https://doi.org/10.1007/s40333-022-0106-9

Hatier, J.-H.B. & Gould, K.S. (2008). Anthocyanin Function in Vegetative Organs. In Anthocyanins. New

York, NY: Springer New York. Retrieved from http://link.springer.com/10.1007/978-0-387-77335-3_1

Kibria, M.G., Hossain, M., Murata, Y. & Hoque, M.A. (2017). Antioxidant defense mechanisms of salinity tolerance in rice genotypes. Rice Science 24(3): 155–162. Retrieved from https://linkinghub.elsevier.com/retrieve/pii/S1672630817300203

Krizek, D.T., Britz, S.J. & Mirecki, R.M. (1998). Inhibitory effects of ambient levels of solar UV-A and UV-B radiation on growth of cv. New Red Fire lettuce. Physiologia Plantarum 103(1): 1–7. Retrieved from https://onlinelibrary.wiley.com/doi/10.1034/j.1399-3054.1998.1030101.x

Li, D., Zhang, D., Wang, H., Li, H., Fang, Q., Li, H. & Li, R. (2020). Optimized planting density maintains high wheat yield under limiting irrigation in north China Plain. International Journal of Plant Production 14(1): 107–117. Retrieved from http://link.springer.com/10.1007/s42106-019-00071-7

Li, F., Xie, Y., Zhang, C., Chen, X., Song, B., Li, Y., … Hu, J. (2014). Increased density facilitates plant acclimation to drought stress in the emergent macrophyte Polygonum hydropiper. Ecological Engineering 71: 66–70. Retrieved from https://www.sciencedirect.com/science/article/pii/S092585741400319X

Mahdi, T.A. & Hossein, A.F. (2014). Changes in Kaempferol content of Chicory (*Cichorium intybus* L.) under water deficit stresses and planting densities. Journal of Medicinal Plants Research 8(1): 30–35. Retrieved from http://academicjournals.org/journal/JMPR/article-abstract/99D05CA42447

Maria Sgherri, C.L., Loggini, B., Puliga, S. & Navari-Izzo, F. (1994). Antioxidant system in *Sporobolus stapfianus*: Changes in response to desiccation and rehydration. Phytochemistry 35(3): 561–565. Retrieved from https://linkinghub.elsevier.com/retrieve/pii/S0031942200905612

Masayasu, M. & Hiroshi, Y. (1979). A simplified assay method of superoxide dismutase activity for clinical use. Clinica Chimica Acta 92(3): 337–342. Retrieved from https://www.sciencedirect.com/science/article/pii/0009898179902110

Møller, I.M., Jensen, P.E. & Hansson, A. (2007). Oxidative modifications to cellular components in plants. Annual Review of Plant Biology 58(1): 459–481. Retrieved from https://www.annualreviews.org/doi/10.1146/annurev.arplant.58.032806.103946

Molor, A., Khajidsuren, A., Myagmarjav, U. & Vanjildorj, E. (2016). Comparative analysis of drought tolerance of *Medicago spp* L. plants under stressed conditions. Mongolian Journal of Agricultural Sciences 19(3): 32–40.

Naroui Rad, M.R., Kadir, M.A. & Yusop, M.R. (2012). Genetic behaviour for plant capacity to produce chlorophyll in wheat ('*Triticum aestivum*') under drought stress. Australian Journal of Crop Science 6(3): 415–420.

Nasiri, A., Samdaliri, M., Rad, A.S. & Shahsavari, N. (2017). Effect of plant density on yield and physiological characteristics of six canola cultivars 249–253.

Nasirzadeh, L., Sorkhilaleloo, B., Majidi Hervan, E. & Fatehi, F. (2021). Changes in antioxidant enzyme activities and gene expression profiles under drought stress in tolerant, intermediate, and susceptible wheat genotypes. Cereal Research Communications 49(1): 83–89. Retrieved from https://doi.org/10.1007/s42976-020-00085-2

Onjai-uea, N., Paengkoum, S., Taethaisong, N., Thongpea, S., Sinpru, B., Surakhunthod, J., … Paengkoum, P. (2022). Effect of cultivar, plant spacing and harvesting age on yield, characteristics, chemical composition, and anthocyanin composition of Purple Napier Grass. Animals 13(1): 10. Retrieved from https://www.mdpi.com/2076-2615/13/1/10

Safar-Noori, M., Assaha, D.V.M. & Saneoka, H. (2018). Effect of salicylic acid and potassium application on yield and grain nutritional quality of wheat under drought stress condition. Cereal Research Communications 46(3): 558–568. Retrieved from https://www.akademiai.com/doi/10.1556/0806.46.2018.026

Seleiman, M.F., Al-Suhaibani, N., Ali, N., Akmal, M., Alotaibi, M., Refay, Y., … Battaglia, M.L. (2021). Drought stress impacts on plants and different approaches to alleviate its adverse effects. Plants 10(2): 259.

Sharma, P., Jha, A.B. & Dubey, R.S. (2019). Oxidative stress and antioxidative defense system in plants growing under abiotic stresses. In Handbook of Plant and Crop Stress, Fourth Edition. CRC press.

Shiade, S.R.G., Zand-Silakhoor, A., Fathi, A., Rahimi, R., Minkina, T., Rajput, V.D., … Chaudhary, T. (2024). Plant metabolites and signaling pathways in response to biotic and abiotic stresses: Exploring bio stimulant applications. Plant Stress 12: 100454. Retrieved from https://linkinghub.elsevier.com/retrieve/pii/S2667064X24001088

Taghavi Ghasemkheili, F., Jenabiyan, M., Ghadirnezhad Shiade, S.R., Pirdashti, H., Ghanbari, M.A.T., Emadi, M. & Yaghoubian, Y. (2023). Screening of some endophytic fungi strains for zinc biofortification in Wheat (*Triticum aestivum* L.). Journal of Soil Science and Plant Nutrition 23(4): 5196–5206. Retrieved from https://link.springer.com/10.1007/s42729-023-01392-3

van Frank, G., Rivière, P., Pin, S., Baltassat, R., Berthellot, J.-F., Caizergues, F., … Goldringer, I. (2020). Genetic diversity and stability of performance of wheat population varieties developed by participatory breeding. Sustainability 12(1): 384. Retrieved from https://www.mdpi.com/2071-1050/12/1/384

Wagner, G.J. (1979). Content and vacuole/extravacuole distribution of neutral sugars, free amino acids, and anthocyanin in protoplasts. Plant Physiology 64(1): 88–93. Retrieved from https://academic.oup.com/plphys/article/64/1/88-93/6077573

Zhao, W., Liu, L., Shen, Q., Yang, J., Han, X., Tian, F. & Wu, J. (2020). Effects of water stress on photosynthesis, yield, and water use efficiency in winter wheat. Water 12(8): 2127. Retrieved from https://www.mdpi.com/2073-4441/12/8/2127

Italian Journal of Agrometeorology
Rivista Italiana di Agrometeorologia

Firenze University Press
https://riviste.fupress.net/index.php/IJAm

OPEN ACCESS

Citation: Tortorici, N., Iacuzzi, N., Alaimo, F., Schillaci, C., & Tuttolomondo, T. (2024). Durum wheat irrigation research trends on essential scientific indicators: a bibliometric analysis. *Italian Journal of Agrometeorology* (2): 37-54. doi: 10.36253/ijam-2784

Received: May 28, 2024

Accepted: November 22, 2024

Published: December 30, 2024

© 2024 Author(s). This is an open access, peer-reviewed article published by Firenze University Press (https://www.fupress.com) and distributed, except where otherwise noted, under the terms of the CC BY 4.0 License for content and CC0 1.0 Universal for metadata.

Data Availability Statement: All relevant data are within the paper and its Supporting Information files.

Competing Interests: The Author(s) declare(s) no conflict of interest.

Durum wheat irrigation research trends on essential scientific indicators: a bibliometric analysis

Noemi Tortorici[1], Nicolò Iacuzzi[1,*], Federica Alaimo[1], Calogero Schillaci[2], Teresa Tuttolomondo[1]

[1] *Department of Agricultural, Food and Forest Sciences, University of Palermo, Viale delle Scienze 13, Building 4, 90128 Palermo, Italy*
[2] *European Commission, Joint Research Centre, Via E. Fermi, 274-21027 Ispra Italy*
*Corresponding author. E-mail: nicolo.iacuzzi@unipa.it

Abstract. Nowadays irrigation of durum wheat represents a key point to provide food security in a context of climate change. Although this topic has caught on particular attention from the global scientific community, many issues and aspects remains understudied. To fill the knowledge gap and collate present evidences, this analysis used a combined bibliometric and thematic approach to synthesize the peer-review literature from SCOPUS main collection, covering the period 1977-2023, resulting in including 332 documents. The main findings of this work are as follows:
(1) Spain and Tunisia hosts the most productive institutions in this field;
(2) the journal Agricultural Water Management emerged as the most prolific, with the largest number of articles and citations;
(3) a wide range of topics and approaches on durum wheat irrigation has been identified, with particular emphasis on controlled water deficit and remote sensing driven management;
(4) the mapping of bibliographic data coupling with co-occurrence map remains a poorly examined area of study.
The results suggest the need of strengthened institutional partnerships and synergize the research on durum wheat irrigation, particularly in the most vulnerable areas where climate change are acting heavily. Future studies should aim to contribute to the understanding of the impacts of climate change through innovative techniques in order to improve our understanding of the durum wheat water needs and their application in crop management, while ensuring ongoing updates to the existing collection of knowledge to face future challenges.

Keywords: bibliographic coupling, co-authorship and citation networks, durum wheat, durum wheat irrigation, PRISMA protocol, Scopus.

1. INTRODUCTION

Durum wheat (*Triticum turgidum* subsp. *durum* (Desf.) Husnot) is the tenth most cultivated cereal in the world (Ayed et al., 2021), with about 13.7

million hectares cultivated and a production of 34.3 million tons (2018-2022 average) (International Grains Council (IGC)), with wide variations from 30 to 39 million tons caused mainly by abiotic factors (drought, high temperatures, low temperatures or pre-budding) and biotic stress (fungal and viral diseases, weeds or harmful insects) (Blanco, 2024).

Durum wheat is an important food source with a significant role in the human diet, providing carbohydrates, proteins, B vitamins, minerals, and energy (Onipe et al., 2015). Worldwide it is mainly used to produce dry pasta and other staple foods such as couscous and bulgur, the latter in particular in North Africa and the Middle East (Troccoli et al., 2000).

The main concern in the regions of durum wheat cultivation, characterized by arid and semi-arid climates, is the potential water deficit in rainfed conditions and the scares availability of freshwater, therefore there is the need to optimize its use (Oweis T. et al., 1999). In fact, water is one of the main factors limiting wheat yield and protein quality and quantity (Flagella et al., 2010). Drought periods usually coincide with the most sensitive growth phases of the crop. The water stress from the anthesis to the ripening, especially if accompanied by high temperatures, accelerates the leaf senescence, reduces the duration and the speed of the grain-filling, as well as the duration of the phase of translocation of carbohydrate reserves in the caryopsis (Oweis et al., 2000), which reduces the average weight of caryopsis (Acevedo et al., 2002). Furthermore, the water stress around the anthesis can lead to a yield loss due to the reduction of the number of spikes and spikelet and for the fertility of those produced (Giunta et al., 1993). The availability of water also influences nitrogen management in agriculture. In fact, an adequate water supply increases the efficiency of nitrogen use (NUE), improving the assimilation and translocation of N in the caryopses (Wang et al., 2015), with significant effects on quality. Nitrogen and irrigation management are crucial in the production of irrigated durum wheat with high protein content in arid and semi-arid regions (Mon et al., 2016).

The obtaining of high yields and high protein content in durum wheat is also limited by the ongoing climate change, which is intensifying and extending dryness with further reduction of precipitation (IPCC, 2014), more frequent exposure to high temperatures and change in precipitation regimes (Fahad et al., 2017). In addition, to meet the food demand of a projected global population of about 10 billion people by 2050, it is necessary to increase food production compared to the current level (Neupane et al., 2022).

In many growing areas, durum wheat is mainly cultivated in rainfed conditions (Bassi et al., 2017). However, irrigation is an important agronomic practice to meet the demand for grain production (Meena et al., 2019).

The improvement of water use efficiency (WUE) could be achieved through different strategies, some of which, still today, are under investigation such as the selection of genotypes with high photosynthetic capacity and low stomatal conductance (Van den Boogaard et al., 1997; Ashraf & Bashir, 2003; Morgan & LeCain, 1991; Condon et al., 2002) and sustainable agronomic practices such as the adoption of regulated water deficit strategies, the application of biostimulants, non-conventional water resources, etc (Mohammadi, 2024; Ben-Jabeur et al., 2022; Werfelli et al., 2021).

The bibliometric analysis adopted in this study was first introduced by Pritchard (Pritchard, 1969), but its diffusion is more recent (Donthu et al., 2021). It is based on the identification of the body of literature, that is publications in their broadest sense, within the specific thematic area (Ellegaard et al., 2015). Rivera et al. (2015) state that, when academic output grows in a scientific domain, it becomes critical for researchers to employ quantitative review approaches to understand the structure of knowledge of the domain itself, identify what topics are being studied and potential research directions. According to Durieux et al. (2010), three types of indicators can be found in bibliometric studies: quantitative indicators relating to productivity, quality indicators concerning the publication impact, and structural indicators measuring the established connections.

Currently, bibliometrics has been widely used as a method of quantitative analysis in many fields of scientific research, such as agronomy. Some of these studies considered the most widespread crops, including wheat, as "Trends in research on durum wheat and pasta, a bibliometric mapping approach" (Cecchini et al., 2020), "Global Research Trends for Unmanned Aerial Vehicle Remote Sensing Application in Wheat Crop Monitoring" (Nduku et al., 2023), "Research trends and status of wheat (Triticum aestivum L.) based on the Essential Science Indicators During 2010-2020: a bibliometric analysis" (Yuan et al., 2021), "Worldwide Research Trends on Wheat and Barley: A Bibliometric Comparative Analysis" (Giraldo et al., 2019).

Specifically, this bibliometric analysis aimed at: (1) provide a list of durum wheat irrigation research and identifying geographic-temporal patterns within the literature; (2) analyse the dynamics of the main research topics; and (3) analyse the global relationships between researchers and countries through the analysis of co-existence, co-occurrence, citation and bibliographic coupling.

2. MATERIALS AND METHODS

2.1. Methodology design

In this work a bibliometric analysis has been conducted as a systematic search for peer-review articles (Nduku et al., 2023), to analyse the relevance of research output on durum wheat irrigation, exploring the state and trend of research in existing literature globally.

The PRISMA 2020 (Preferred Reporting Items for Systematic review and Meta-Analyses) protocol was adopted to retrieve the relevant articles. PRISMA is a consolidated methodology to carry out systematic reviews and meta-analyses (Galvão et al., 2015; Page et al., 2021).

SCOPUS was chosen as the only database for the collection of documents, as it is considered, together with Web of Science, the leader platform of abstracts and citations of the world's literature (Zhu & Liu, 2020).

SCOPUS was used to search for and identify relevant publications related to durum wheat irrigation. By using advanced search filters, we were able to narrow down the results based on specific keywords, publication types, and date ranges to capture the most comprehensive dataset.

The search queries TITLE-ABS-KEY ("durum wheat" AND "irrigation") were used for collecting academic documents and patents including "durum wheat" and "irrigation" terms in the title, abstract and/or keywords.

The obtained metadata were imported and analysed using the open-source software VOSviewer (v 1.6.19) to build and display bibliometric maps.

2.2. Data collection

To carry out the bibliometric analysis the documents were collected following the PRISMA protocol (Fig. 1). The data search on Scopus was completed in one day (November 2023) to avoid distortions. The keywords "durum wheat" and "irrigation" were used to explore the database and collect documents that included terms in the title, abstracts and/or keywords, regardless of the year of publication and the subject area. The research generated a total of 356 documents, including articles, conference papers, reviews, book chapters, data papers and conference reviews. Our analysis was limited to research articles and reviews, written in English. Finally, the complete records were exported as .csv file and then used in the VOSviewer software for the descriptive statistics, graphics and the co-occurrence citation analysis.

2.3. Data analyses

The selected publications were subjected to performance analysis and scientific mapping. The first considers the contributions of the research components, while the second focuses on the relations between those components (Donthu et al., 2021).

Regarding the performance analysis, the selected publications were evaluated considering the following factors: total publications, number of documents per year, author, institution of which the authors are members, country, subject area, journal name, keywords, and number of citations.

Keywords have been cleaned by omitting country terms, duplicate words, and plural words.

The analysis of the co-citation was realized with the program VOSviewer, included: analysis of co-authors, to show the collaborations between authors, organizations, and countries; analysis of co-occurrences of all keywords; bibliographic coupling, which allowed to separate the publications into thematic clusters based on shared references.

The maps generated contain nodes that represents an element (e.g. document, author, country, institution, keyword, journal) and whose size reflects its magnitude (the number of times it occurs). Some items are not displayed to avoid overlapping. The colours in the network view (text maps) describe groups of similar elements calculated by the program. The link between nodes indicates the existence of the bond, while the distance or thickness of the link refers to the force of the relations (number of times it occurs) (Donthu et al., 2021). The period considered starts from the year in which the first indexed documents on the issue of study date back to today.

3. RESULTS AND DISCUSSIONS

3.1. Evolution of the scientific production and distribution by countries, institutions, and authors

The search terms "durum wheat" and "irrigation" produced a total of 356 documents, of which only 332 were used in this study, falling into the category of articles and reviews.

The first indexed documents on Scopus related to the research on durum wheat irrigation date back to 1977 and both come from the USA: "Remote-sensing of crop yields" (Idso et al., 1977), review published in Science and, "Wheat canopy temperature: A practical tool for evaluating water requirements" (Jackson et al., 1977), article published in Water Resources Research.

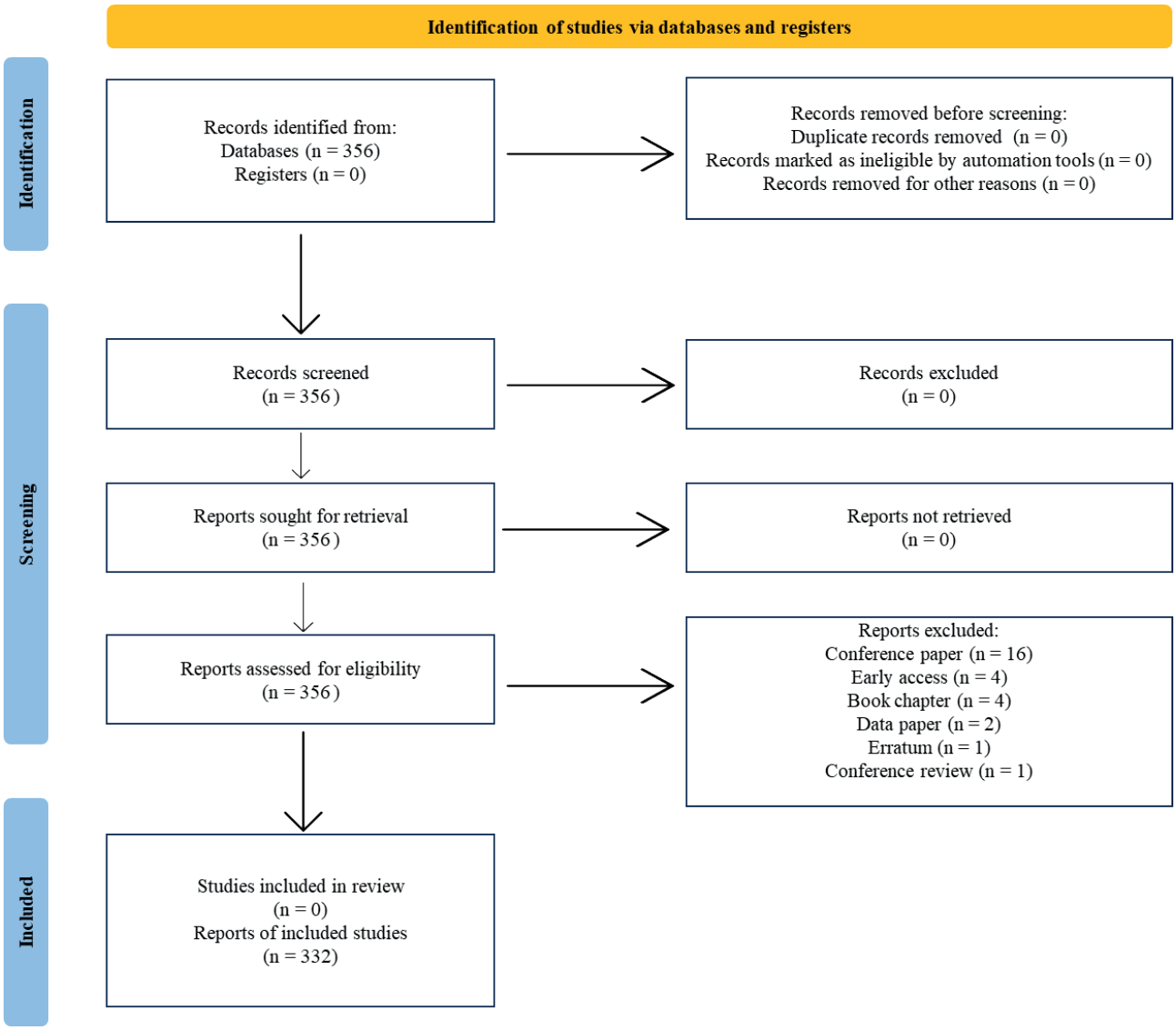

Figure 1. Procedure applied for document selection for the bibliometric review and thematic analysis (PRISMA protocol).

From 1977 to 2000, 49 articles were published (about 15% of total production), with a generally low annual production rate, since no documents were found in 1979, 1980, 1982, 1984, 1991 and 1996. On the other hand, only 27 articles were published between 1997 and 2000 (Fig. 2).

The growth of publishing production has continued from 2007 until today, where there are at least 10 publications annually, indicating the growing interest in this topic. However, during the last period, this trend has been discontinuous, as can be seen from the variability in the number of publications among years (Fig. 2). The peak was reached in 2022 with a total of 21 publications. In 2023 there were 13 documents (until 14 November), but the number could still grow.

In relation to the contributions of countries, Figure 3 shows the spatial distribution of the documents published on irrigated durum wheat from 1977 to 2023.

The results show that the interest in this topic of research is widely diffused, confirming that durum wheat is one of the most important crops cultivated worldwide (Kabbaj et al., 2017). However, the number of scientific publications is not steadily distributed among the 49 countries that contributed to the research. The largest contribution comes from countries in Southern Europe, Asia, North Africa and North America.

In particular, the top 10 countries with the best performance in terms of scientific production (Fig. 4) contributed 92% to the reference literature. Most of these

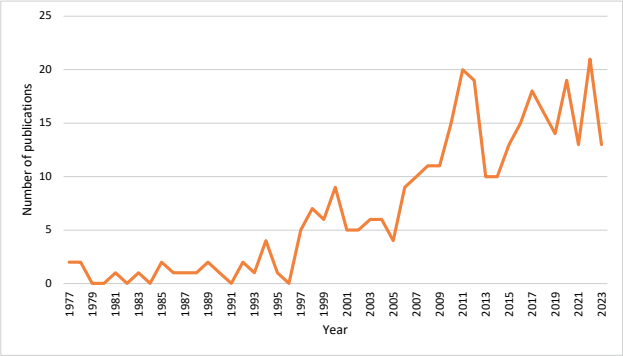

Figure 2. Annual distribution of publications.

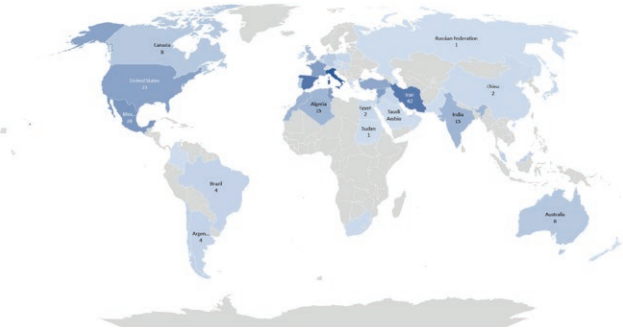

Figure 3. Spatial distribution map of scientific production on irrigation of durum wheat from 1977 to 2023.

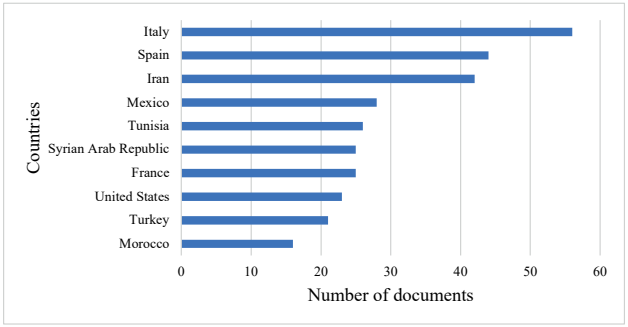

Figure 4. Top ten countries with the highest scientific production.

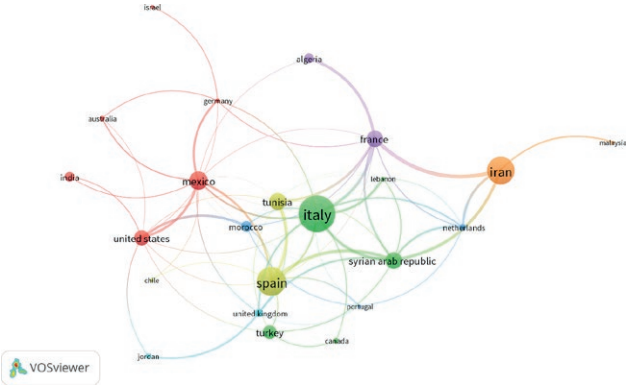

Figure 5. Co-authorship networks of countries. 1st cluster: red; 2nd cluster: green; 3rd cluster: blue; 4th cluster: yellow; 5th cluster: purple; 6th cluster: light blue; 7th cluster: orange.

countries are also among the main producers of durum wheat. Currently, the Mediterranean basin is the largest area of production of durum wheat in the world, as well as the largest consumer of durum wheat products enough to activate a very significant import market (Xynias et al., 2020). The countries of the Mediterranean basin, which are among the top ten countries with the most publications on this topic, are Italy, Spain, Tunisia, France, Syria, and Turkey (Fig. 4).

However, despite Iran doesn't appear among the biggest producers of durum wheat, several articles have been found, representing the third country in the number of scientific productions, constituted by 42 works.

Figure 5 shows the co-authorship network map between countries. It allows us to analyse the possible interaction between researchers from different countries and thus understand the dynamics of research production.

A minimum number of 5 documents for country has been set as a threshold for map creation. The software identified 23 nodes, 7 clusters and 72 links. The largest nodes identified countries with multiple publications. According to the map the first cluster (red) is the most numerous and includes Australia, Germany, India, Israel, Mexico, United States. The second cluster (green) consists of five countries Canada, Italy, Lebanon, Syria, Turkey. The third cluster (blue) includes Morocco, Netherlands, and Portugal. The fourth cluster (yellow) consists of Chile, Spain, and Tunisia. The fifth cluster (purple) consists of Algeria and France. The sixth cluster (light blue) is formed by Jordan and United Kingdom. The seventh cluster (orange) consists of Iran and Malaysia. From the map it is also visible that the countries of the same cluster have collaborations with other countries of different clusters.

Table 1 shows the top 15 most productive institutions in terms of publishing production that have carried out research on durum wheat irrigation. Fourteen of the fifteen main institutions belong to the countries with the highest publishing output: Spain (4), Italy (3), Iran (3), Tunisia (2), Mexico (1), Syria (1). Moreover, only seven are universities while the others are non-academic institutions.

The University of Barcelona with 26 publications, to which belong 2 researchers listed in Table 2 of the 10 most productive authors (Araus J.L. and Serret M.D.),

Table 1. Main universities/research institutes and their editorial production.

Affiliations	Country	Records
University of Barcelona	Spain	26
University of Carthage, Institut National de la Recherche Agronomique	Tunisia	26
International Center for Agricultural Research in the Dry Areas Syria (ICARDA)	Lebanon	25
International Maize and Wheat Improvement Center (CIMMYT)	Mexico	24
Council for Agricultural Research and Economics (CREA)	Italy	15
University of Carthage	Tunisia	15
Institute of Agrifood Research and Technology (IRTA)	Spain	13
Mediterranean Agronomic Institute of Bari (CIHEAM Bari)	Italy	11
Islamic Azad University	Iran	9
Italian Nnational Research Council (CNR)	Italy	8
Agrotecnio. Centre for Food and Agriculture Research	Spain	8
Wageningen University & Research (WUR)	Netherlands	7
Isfahan University of Technology	Iran	7
University of Lleida	Spain	7
Dryland Agricultural Research Institute, Maragheh	Iran	7

Table 2. Number of publications and citation metrics of the most influential authors. The affiliation of author was retrieved from Scopus database through 'author search'. Legend: TC-total citation; NP-number of publications.

Authors	h-index	g-index	m-index	TC	NP	Period	Affiliation	Country
Araus J.L.	56	96	1.81	418	28	1997-2023	University of Barcelona	Spain
Oweis T.	34	70	1.42	129	11	1999-2012	International Center for Agricultural Research in the Dry Areas Syria	Lebanon
Serret MD.	31	53	2.38	108	10	2010-2023	University of Barcelona	Spain
Royo C.	46	84	2	230	9	2000-2021	Institute of Agrifood Research and Technology	Spain
Trifa Y.	13	26	1.62	18	9	2015-2022	University of Carthage, Institut National de la Recherche Agronomique	Tunisia
Villegas D.	34	60	1.48	132	8	2000-2020	Institute of Agrifood Research and Technology	Spain
Aparicio N.	21	41	0.91	71	7	2000-2023	Castile-Leon Agriculture Technology Institute (ITACyL)	Spain
Govaerts B.	42	83	3.5	70	7	2011-2021	International Maize and Wheat Improvement Center	Mexico
Nachit M.M.	31	57	1.19	118	7	1997-2008	International Center for Agricultural Research in the Dry Areas Syria	Lebanon
Verhulst N.	25	55	2.08	49	7	2011-2021	International Maize and Wheat Improvement Center	Mexico

is among the busiest istitutions to work in this field of research.

As regards the number of authors, a total of 1122 authors contributed to the 332 documents analysed. However, only 3 authors had 10 or more publications in this field of research: Araus J.L. (28), Oweis T. (11) and Serret M.D. (10). About 98% had 5 or fewer publications (Table 2).

Table 2 shows also the first 10 authors who contributed to the research on durum wheat irrigation.

Figure 6 shows the network of collaborations between authors. Collaborative networks are formed between authors working together to produce an article. Having set a threshold of 5 for the minimum number of documents per author, only 31 of them met the requirement. However, some of these were not connected to each other and, therefore, they weren't listed on the map. The network consists of 25 nodes, 5 clusters and 78 links. From this analysis it emerges that the authors of the same country tend to have a close collaboration with each other.

The first cluster (red) includes 7 authors, all from Spain, such as Araus, Bort and Serret. The second cluster (green) consists of 5 authors affiliated with Tunisian universities or research institutes such as Ayadi, Chamekh, Karmous, Trifa and Sahli. Cluster 3 (blue) is represented by 4 Spanish researchers such as Aparicio, Villegas, Royo, Garcia del Moral, and by Rharrabti who belongs

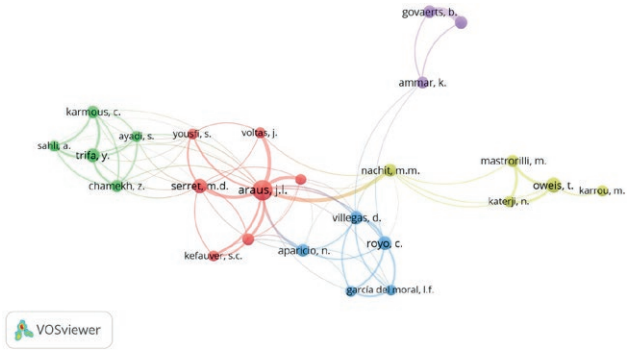

Figure 6. Author co-authorship network visualization map.. 1st cluster: red; 2nd cluster: green; 3rd cluster: blue; 4th cluster: yellow; 5th cluster: purple.

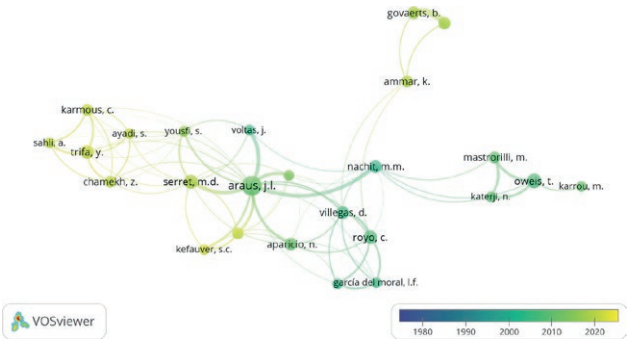

Figure 7. Temporal distribution of collaborations.

to Moroccan institutions. The fourth cluster (yellow) is always made up of 5 authors coming from different countries: Oweis and Nachit of Lebanon, Karrou from Morocco, Katerji from France, and Mastrorilli from Italy. Finally, the fifth cluster (purple) is represented by 3 researchers from Mexico such as Ammar, Govaerts and Verhulst.

In addition, the overlay visualization map (Fig. 7) shows the development through time of collaborations between authors. The authors of cluster 2 present the latest collaborations dating back to 2018, while the older ones concern clusters 1 and 4.

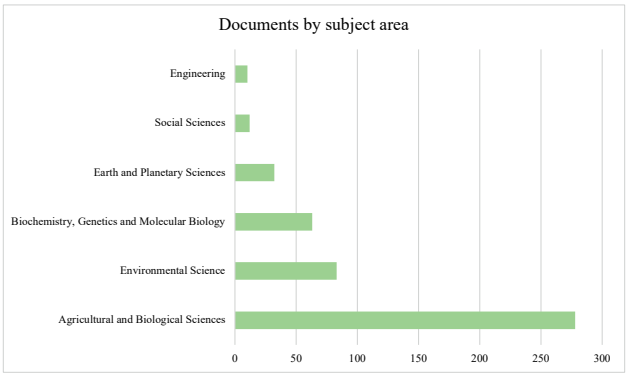

Figure 8. Number of scientific papers on durum wheat irrigation by thematic area.

3.2. Thematic areas of research and scientific sources

Scientific papers on durum wheat irrigation have been distributed in 22 thematic areas according to the Scopus classification. Figure 8 shows the thematic areas with a minimum of 10 records.

With 51%, the largest number of documents (278) is included in the Agricultural and Biological Sciences area, followed by Environmental Science (83), Biochemistry, Genetics and Molecular Biology (63), Earth and Planetary Sciences (32),Social Sciences (12) and Engineering (10)

It is evident that the same document can be assigned to several thematic areas; for example, many of the documents included in the Environmental Science area are also present in the first Agricultural and Biological Sciences area.

All 332 documents were published in 149 journals and only 6 of them had a minimum number of records of 5.

Table 3 lists the top 5 major journals that are all international and belong to the Agricultural and Biological Sciences scientific category. The table 3 also shows the Impact Factor (IF 2022) which measures the average number of times the journal articles published in the last two years have been cited in the current year (Dong P. et al., 2005).

Table 3. Number of publications and citation metrics of sources. The impact factor of the journal was retrieved from the 2022 Journal Citation Reports. Legend: TC-total citation; NP-number of publication; SYP-start of the year of publication; AC-average citation; IF-impact factor.

Sources	h-index	g-index	m-index	TC	NP	SYP	AC	IF	Country	Publisher
Agricultural Water Management	152	236	3.30	1073	19	1999	56.47	6.7	Netherlands	Elsevier
Field Crops Research	174	51	3.87	1021	19	1986	53.74	5.8	Netherlands	Elsevier
European Journal of Agronomy	131	221	4.37	525	14	1998	37.5	5.2	France	Elsevier
Italian Journal of Agronomy	29	45	1.93	100	10	2009	10	2.2	Italy	PagePress
Cereal Research Communications	37	53	1.23	108	7	1998	15.43	1.6	Germany	Cereal Research NonProfit Company

The top 3 journals rank in the first quartile (Q1), while the others in the second quartile (Q2) according to the Journal Citation Reports 2022. This distinction indicates that they are high impact factor journals, in fact, the Journal Impact Factor (JIF) published by Thomson Reuters' Journal Citation Reports is a widely used indicator for assessing the importance or visibility of a journal in its field (Liu et al., 2016).

Agricultural Water Management with 19 publications ranks first among the journals that have contributed most to research on durum wheat irrigation, immediately followed by the journal Field Crops Research with 19 papers and the European Journal of Agronomy with 14 papers. These three journals were among the main ones also in other bibliometric analyses that dealt with issues similar to the ones of this work (Sun et al., 2020; Velasco-Muñoz et al., 2018).

Both Agricultural Water Management and Field Crops Research publish only articles related to science, economics, and water management policy in agriculture. Conversely, the European Journal of Agronomy deals with several topics concerning the selection and genetics of crops, the physiology of harvesting and production as well as crop management, including irrigation, fertilization, and soil management. It also addresses aspects of agroclimatology and modelling, plant-soil relations, crop quality and post-harvest physiology, farming and cultivation systems, agroecosystems and the environment, interactions and weed management. The Italian Journal of Agronomy (IJA) is the official journal of the Italian Society of Agronomy, which deals with all aspects of Agricultural and Environmental Sciences, the interactions between cultivation systems and sustainable development. Cereal Research Communications publishes articles presenting new scientific findings on selection, genetics, physiology, pathology and mainly production of wheat, rye, barley, oats, and corn.

Further analysis shows that the most influential journal in this field by number of citations is Australian Journal of Agricultural Research (1578) (not shown in the table), although the journal accounts for only 3 documents; follow Agricultural Water Management (1073) and Field Crops Research (1021), which are the journals with more publications (Tab. 3).

Figure 9 describes the progress of scientific production of the first five journals over the years. Overall, each journal has published 12 articles per year. Agricultural Water Management released the first article in 2004, peaking in 2009 with 3 papers. Field Crops Research is the journal with the first oldest publication in this field, dating back to 1986. The first article on Italian Journal of Agronomy dates back to 2009, peaking the following year with 4 papers. The first article published on the irrigation of durum wheat in the European Journal of Agronomy dates back to 1998 and reached 3 publications in 2023. Cereal Research Communications published only 7 papers on the topic and no more than one article a year.

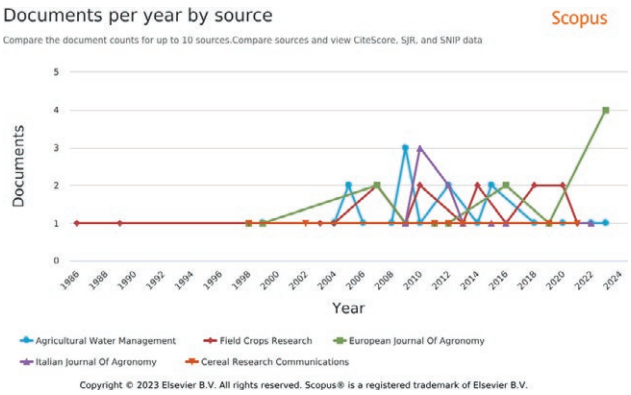

Figure 9. Trend of the scientific production of the top five journals over the years.

3.3. Keywords of the authors and co-occurrence network

The analysis of co-occurrences is a technique that allows to examine the content of the publication, since it assumes that words that frequently appear together have a thematic relationship with each other (Donthu et al., 2021).

The study gathered all the keywords of the documents under investigation to conduct the analysis of keywords and co-occurrences. For this reason, networks of co-occurrences have been created to show the relationships between keywords in the search field.

Table 4 shows the first most recurring words in documents.

Table 4. Keywords and number of occurrences.

Keyword	Occurrences (n)
durum wheat	545
Triticum aestivum	138
irrigation	143
crop yield	90
grain yield	63
drought stress	61
crops	38
genotype	36
nitrogen	36
water use efficiency	29

The keyword with the greatest number of occurrences was "durum wheat" (545), followed by "*Triticum aestivum*" (138), while "irrigation" is in third place (143). In the list were frequent keywords that are used to classify wheat. The top keywords include "grain yield" (63), "drought stress" (61), "nitrogen" (36), "water use efficiency" (29). They are therefore the most indexed words and represent the most discussed topics in this search domain.

Some of these keywords ("yield", "nitrogen", "irrigation", "drought", "climate change") were also recurrent in other bibliometric analyses of wheat (Giraldo et al., 2019; Cecchini et al., 2020; Yuan & Sun, 2021). These words refer to environmental issues that affect agricultural production, some of which are explored in the context of crop sustainability (Giraldo et al., 2019).

In a bibliometric analysis on the efficiency of water use in agriculture (Velasco-Muñoz et al., 2018), the terms "wheat", "irrigation", "irrigation system" and "crop" appeared among the top 10 keywords. Part of the documents analysed, in fact, focused their research on the use and efficiency of water irrigation to maximize production in some crops, including wheat.

Words with at least 10 occurrences have been considered to create the keyword co-occurrence network. Among the 2122 keywords identified only 51 have reached this threshold. The software then identified 51 nodes, 4 clusters and 1000 links (Fig. 10).

Cluster 1 (red) includes keywords such as irrigation, climate change, crop yield, evapotranspiration, fertilizer application, nitrogen, protein, soil water, supplemental irrigation, water use efficiency. In this network it is possible to notice how many keywords relating to the management of water resources recur. The production of durum wheat (*Triticum durum* L.) in semi-arid regions is limited by an inadequate water supply that occurs especially during the end of the harvest season (Karam et al., 2009). As a result, the planning of an adequate irrigation and nitrogen fertilization strategy, which considers the phenology of crops, allows to produce optimal wheat yields (Karam et al., 2009). This problem, which is widespread in the areas of cultivation of durum wheat, is intensified by the ongoing climate change (IPCC, 2014; Fahad et al., 2017). In fact, many studies have simulated the effects of climate change on the agronomic and productive performance of both durum wheat and other crops (Rharrabti et al., 2003; Ventrella et al., 2012; Ventrella et al. 2015; Muleke et al., 2022). Supplemental irrigation has been widely recognized as one of the most feasible means of increasing cereal yield and water efficiency in arid areas (De Vita et al., 2007; Campbell et al., 1993; Oweis et al., 1999). Oweis (1997) defines supplementary irrigation as "the addition to essentially rainfed crops of small amounts of water during times when rainfall fails to provide sufficient moisture for normal plant growth, in order to improve and stabilize yields". However, more recent studies suggest replacing additional watering with a deficit level of irrigation (regulated deficit irrigation) which should be determined considering the availability of water in the soil and the specific response of the crop (Chai et al., 2016). Consequently, understand the mechanism of the physiological process regulation of wheat relating to different irrigation regimes and, therefore, the effect of water stress on yield, would optimize water saving irrigation technology for sustainable wheat production. The amount of water can be planned already at the beginning of the anthesis and of the grain-filling, while in dry years irrigation may be necessary already in the stem elongation phase to ensure a flourishing development of the crop (Oweis et al., 1999; Chen et al., 2003).

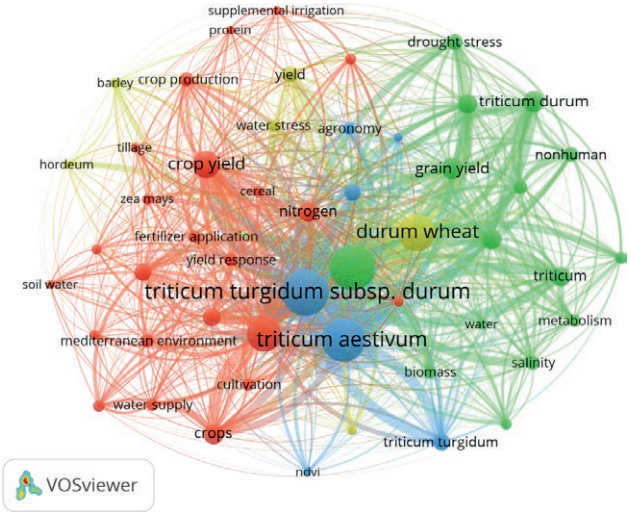

Figure 10. Trend analysis and co-occurrence network of authors' keywords. 1st cluster: red; 2nd cluster: green; 3rd cluster: blue; 4th cluster: yellow.

Cluster 2 (green) includes words such as "drought", "drought stress", "genotype", "grain yield", "photosynthesis", "salinity", "*triticum durum*", "water", "physiology", "metabolism". These words express two of the main environmental stresses, drought, and salinity, to which durum wheat is continuously subjected in semi-arid cultivation environments, such as the Mediterranean one (Guidi and Calatayud 2014; Chairi et al. 2020). Both salinity and drought reduce soil water availability for plants (Rhoades, 1972; Ayers and Westcot, 1985) causing negative effects on physiological processes resulting in loss of yield (Nowicka et al., 2018). Moreover, both salinity and drought are often present in the same envi-

ronment so many studies investigate the effects of the interaction between the two stresses (Katerji et al., 2009; Yousfi et al., 2012; Yousfi et al., 2016; Yaghoubi Khanghahi et al., 2021).

Cluster 3 (blue) consists of words such as "cultivar", "NDVI", "*Triticum turgidum*", "*Triticum aestivum*". The growing interest in the use of vegetation indices, derived from Unmanned Aerial Vehicle (UAV) or satellite images, is linked to their great potential use. Both proximal and remote sensing for the detection of vegetation indices are non-destructive methods and are well correlated with the agronomic and physiological characteristics of cultures (Reynolds et al., 2015). The Normalized Difference Vegetation Index (NDVI) is one of the most studied and used vegetation indices (Huang et al., 2021). Some researchers have evaluated the NDVI to quantify grain development and yield (Fernandez-Gallego et al., 2019; Elazab et al., 2015) and for plant phenotyping in breeding programmes (Rezzouk et al., 2022; Sanchez-Bragado et al., 2020; Mzid et al., 2020).

French et al. (2020) conducted a three-year study to assess the ability of the vegetation index (VI), derived from satellite-detected images, to track grain evapotranspiration. The results indicated that, in most cases, it was possible to accurately estimate the cultural coefficient (Kc) and the cultural evapotranspiration (Etc) from the NDVI during the middle of the season until the senescence phase.

Cluster 4 (yellow) is represented by words such as "barley", "durum wheat", "hordeum", "yield", "water stress". The link between wheat and barley is evident in this cluster. Wheat and barley are the two main cereals cultivated in the Mediterranean region and represent strategic crops for the food security of the entire area (Albrizio et al., 2010). The two cereals are often studied together, or, in other cases, wheat is used as a reference for the discussion of the results of barley research and conversely (Giraldo P. et al., 2019). Albrizio R. et al. (2010), in a study conducted in southern Italy, compared the effects of the interaction of different doses of nitrogen and water supply regimes on durum wheat and barley. Katerji et al. (2009) evaluated the effect of water and salt stress on the two cereals yields.

As may be clear from the map, each of these words form links even with many other words of different clusters.

3.4. Bibliographic coupling

Bibliographic coupling occurs when two papers refer to a common third paper in their bibliographies, indicating that there is a probability that the two papers will address a related topic. The "coupling force" of two papers is greater the more citations to other papers they share (Kessler, 1963; Martyn, 1964).

The evaluation of the bibliographic coupling of countries, journals and scientific papers was carried out as a method of measuring similarities.

For the bibliographical matching of countries (Fig. 11), those with a minimum number of 10 documents were considered. The software identified for the 14 countries that met the threshold, 5 clusters and 76 links. As can be seen from Figure 10, the largest group (red) was formed by India, Mexico, Morocco, and the USA. In this cluster the highest link was observed between USA and Mexico. The second cluster (green) includes Iran, Netherlands, and Syria. The third cluster (blue) consists of Spain, Tunisia, and Turkey. The fourth cluster (yellow) consists of Algeria and France. The fifth cluster (purple) includes United Kingdom and Italy. Moreover, from the map it is evident that Spain forms strong connections with Mexico, Tunisia, and Italy.

Regarding the bibliographical coupling of journals (Fig. 12), of which a minimum threshold of 5 papers per journal was set, only 6 of them complied with the threshold. The software has calculated two clusters and 10 links. The first cluster (red) is represented by the magazines Agricultural Water Management, European Journal of Agronomy, Italian Journal of Agronomy and Field Crops Research, while the second cluster (green) by Agronomy and Cereal Research Communications. This

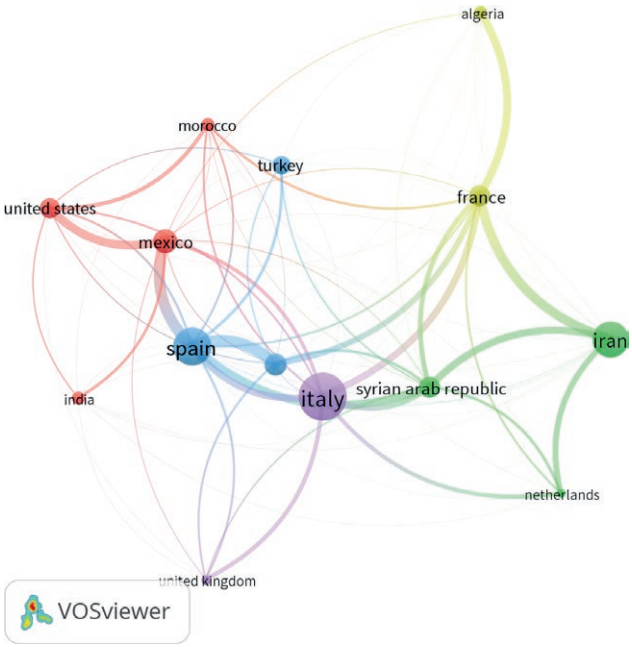

Figure 11. Bibliographic coupling of countries. 1st cluster: red; 2nd cluster: green; 3rd cluster: blue; 4th cluster: yellow; 5th cluster: purple.

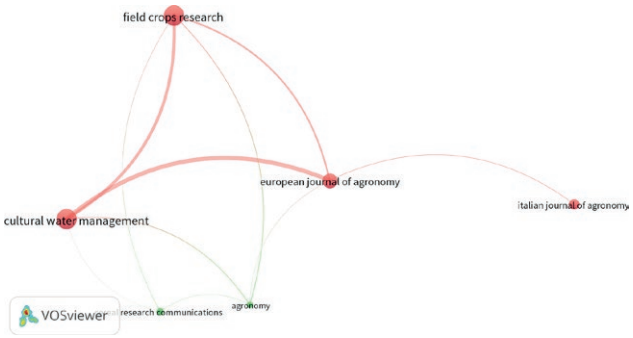

Figure 12. Bibliographic coupling of journals. 1st cluster: red; 2nd cluster: green.

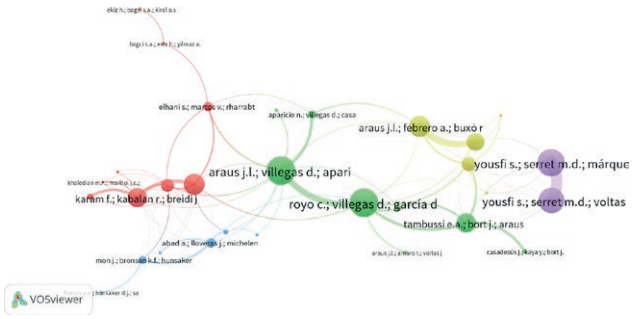

Figure 13. Bibliographic coupling of documents. 1st cluster: red; 2nd cluster: green; 3rd cluster: blue; 4th cluster: yellow; 5th cluster: purple.

analysis also shows that the journals Agricultural Water Management, Field Crops Research and European Journal of Agronomy have the greatest coupling force.

In the analysis of the bibliographic coupling of papers (Fig. 13), the minimum number of citations of a paper has been fixed at 50. Out of 332 papers, 55 reached the threshold. However, only 30 showed connections within the network. A total of 5 clusters were identified in which many of the papers had links of co-paternity.

Cluster 1 (red), more numerous, includes 9 papers which are by Albrizio et al., 2010; Bagci et al., 2007; Ekiz et al., 1998; Elhani et al., 2007; García Del Moral et al., 2003; Karam et al., 2009; Khaledian et al., 2009; Latiri-Souki et al., 1998; Zhang et al., 1999. These papers investigate the effect of water use efficiency and nitrogen fertilization on durum wheat yield.

Latiri-Souki et al. (1998) in their studies evaluated the response of durum wheat to nitrogen fertilization under conditions of different irrigation levels and in different pedoclimatic environments. Elhani et al. (2007) reported that low-yield durum wheat genotypes could be more advantageous in terms of yield compared to genotypes with high-yield capacity in non-irrigated areas.

The papers by Bagci et al. (2007) and Ekiz et al. (1998), instead, evaluated the combined effects of drought stress and Zn deficiency on yield. From this work emerged a positive correlation between the nutritional status of Zn of plants and their sensitivity to water stress (Bagci et al., 2007) in fact, plants subjected to water scarcity had a greater sensitivity to Zn deficiency (Ekiz et al., 1998).

Cluster 2 (green) comprises 8 papers by Aparicio et al., 2000; Araus et al., 1998; Araus et al., 2003; Casadesús et al., 2007; Peleg et al., 2005; Royo et al., 2002; Tambussi et al., 2007; Fischer et al., 1978. In these studies emerges one of the main issues that concerns the countries that produce durum wheat and, consequently, the scientific community. In fact, drought stress, as a combination of water deficit and high temperatures, is the main bond that limits the cultivation of durum wheat in semi-arid environments of cultivation (Araus et al., 2002). Researchers from cluster 2 selected durum wheat genotypes that could adapt to semi-arid conditions and withstand rising high temperatures while maintaining a satisfactory yield. Some have used vegetation indices (VI) (Casadesús et al., 2007; Aparicio et al., 2000) as a tool for plant phenotyping, others the discrimination of carbon isotopes (Royo et al., 2002; Peleg et al., 2005) and crown temperature (Royo et al., 2002).

Moreover, the analysis shows that the paper "Comparative performance of carbon isotope discrimination and canopy temperature depression as predictors of genotype differences in durum wheat yield in Spain" (Royo et al., 2002) formed strong links with "Environmental factors determining carbon isotope discrimination and yield in durum wheat under Mediterranean conditions" (Araus et al., 2003).

Cluster 3 (blue) consists of 6 papers produced by Abad et al., 2004, French 2020, Katerji et al., 2009, Masoni et al., 2007, Mon et al., 2016, Rharrabti et al., 2003. In some of these papers, the effect of the interaction of nitrogen fertilization and irrigation on yield components and the quality of durum wheat was evaluated. As is well known, the management of water and nitrogen influences the characteristics of durum wheat, such as protein content, which plays a key role in the final use of the product (De Santis et al., 2021). In fact, an adequate water supply, in terms of quantity and timing of distribution, can generally increase the yield of cereals and the use efficiency of nitrogen (NUE) in durum wheat by improving its assimilation and translocation in the plant, as well as minimising nitrogen losses (Lu et al., 2015).

Cluster 4 (yellow) consists of 5 articles, of which 4 show as the first author Araus (Araus, Febrero et al.,

1997a; Araus, Febrero, et al., 1997b; Araus, Amaro et al., 1997; Araus, Febrero et al., 1999), while an article is by Knight et al. (1994). These studies analysed the stable isotopic carbon composition in the dry matter of leaves and/or caryopsis, related to both photosynthetic efficiency and water use and plant yield. In addition, the analysis of the carbon isotopes discrimination in the remains of cultivated plants from archaeological sites, was used to assess the availability of water during the dawn of agricultural activity. The isotopic composition of carbon has also been extensively studied as a selection tool in cereal genetic improvement programs, both to select genetic loci associated with drought tolerance and as a measure of increased yield in good agricultural condition (Rebetzke et al., 2008). According to more recent studies, Araus et al. (2013) have shown that the stable isotopic composition of carbon is positively related to the efficiency of water use.

Cluster 5 (purple) consists of only two articles, both by Yousfi et al. (2010; 2012), "Combined use of δ13C, δ18O and δ15N tracks nitrogen metabolism and genotypic adaptation of durum wheat to salinity and water deficit" (Yousfi et al., 2010) and "Effect of salinity and water stress During the Reproductive stage on growth, ion concentrations, Δ13C, and δ15N of durum wheat and related amphiploids" (Yousfi et al., 2012).

3.5. Citation analysis

The number of citations represents, together with the number of scientific papers produced, one of the indicators reflecting the success of the research and the academic authority of a country, institution, journal, and author, relative to a given research domain (Nduku et al., 2023).

Table 5 shows the first 10 most cited scientific publications since 1977, which are therefore the most influential in the field of research covered by this analysis.

The most cited paper with 1478 citations is "Drought resistance in spring wheat cultivars. I. Grain yield responses" (Fischer et al., 1978), published by the Australian Journal of Agricultural Research. The normalized citation (TCY) demonstrates that this research still represents an important basis for studies on durum wheat irrigation. This study, conducted in Mexico for three growing seasons, investigated the effect of drought on the yield of a wide range of cereal cultivars, including durum wheat genotypes. Detailed measurements were made of the water status of the plants, leaf area, dry matter production, date of the anthesis, grain yield and its components. The drought levels were such that the average yield of all cultivars, varied from 37 to 86% compared to the control yield (irrigated thesis). Furthermore, the results of their research showed that durum and triticale wheat were more sensitive to drought than common wheat and barley. The second paper by number

Table 5. Most cited documents. Legend: TC-total citation; TCY-total citation per year.

Authors	Title	DOI	TC	TCY
Fischer R.A. et al. (1978)	Drought resistance in spring wheat cultivars. 1. Grain yield responses	10.1071/AR9780897	1478	32.84
Jackson R.D. et al. (1977)	Wheat canopy temperature: A practical tool for evaluating water requirements	10.1029/WR013i003p00651	657	14.28
Zhang H. et al. (1999)	Water-yield relations and optimal irrigation scheduling of wheat in the Meditenanean region	10.1016/S03783774(98)00069-9	370	15.41
Aparicio N. et al. (2000)	Spectral vegetation indices as nondestructive tools for determining durum wheat yield	10.2134/agronj2000.92183x	327	14.21
Garcia del Moral L.F. et al. (2003)	Evaluation of grain yield and its components in durum wheat under Mediterranean conditions: An ontogenic approach	https://doi.org/10.2134/agronj 2003.2660	276	13.80
Idso S.B. et al. (1977)	Remote-sensing of crop yields	10.1126/scienza.196.4285.19	273	5.93
Araus J.L. et al. (2003)	Environmental factors determining carbon isotope discrimination and yield in durum wheat under Mediterranean conditions	10.2135/cropsci2003.1700	203	10.15
Tambussi E.A. et al. (2007)	Water use efficiency in C3 cereals under Mediterranean conditions: A review of physiological aspects	10.1111/117447348.2007.00143.x	172	10.75
Masoni A. et al. (2007)	Post-anthesis accumulation and remobilization of dry matter, nitrogen and phosphoms in durum wheat as affected by soil type	10.1016/j.eja.2006.09.006	163	10.19
Blum A. et al. (1989)	Yield stability and canopy temperature of wheat genotypes under drought-stress	10.1016/03784290(89)90028-2	154	4.53

of citations (657) is "Wheat canopy temperature: A practical tool for evaluating water requirements" (Jackson et al., 1977) published in the journal Water Resources Research. The results of this work led to the elaboration of an indicator called "Stress Degree Day" (SDD), obtained from the sum of the differences between the crown temperature and the air temperature (Tc - Ta) measured during the test on irrigated durum wheat plots with different water levels. An equation relating evapotranspiration (ET) to net radiation and SDD was also tested. The purpose was to use SDD as an indicator to determine the timing and the number of irrigations to be applied. The third paper "Water-yield relations and optimal irrigation scheduling of wheat in the Mediterranean region" (Zhang h. et al., 1999) has 370 citations and was published in Agricultural Water Management. In the work, ten years of experiments on supplementary irrigation (SI) in Syria were conducted to assess the relationship between durum wheat (*Triticum durum* L.) and soft wheat (*Triticum aestivum* L.) with water consumption to plan and optimize irrigation at different rainfall conditions. During the test, the sensitivity of the cultures to water stress was analyzed in the different growth phases, the most sensitive of which were the raising phases, followed by the anthesis and the caryopsis-filling phase. It was found that crop yields increased linearly with increased evapotranspiration (ET), however, in conditions of limited water resources, the study identified the volumes of irrigation that allowed to optimize the use of water without compromising the yield and profits of the company.

4. CONCLUSIONS

This bibliometric analysis provided a broad analysis of research topics related to durum wheat irrigation from 1977 to 2023. The adoption of different bibliometric techniques has allowed us to gain a better understanding of the intellectual structure of the research field, allowing us to explore the main contributions and the respective relationships.

It is important to note that this revision focused only on papers in which the term "durum wheat" and "irrigation" appeared in the title, abstract or keywords. In the examination, rigorous efforts were made to follow the PRISMA protocol accurately. The survey allowed 332 papers indexed on the Scopus database to be examined.

The results of this bibliometric analysis found a steady increase in scientific publication of peer-review articles since 2007, but it is still limited to provide tools for the policy stakeholder and decision maker to act in this very crucial field crop in southern european agricultural systems.

Italy and Spain are the leading countries for the number of papers published. This trend is reflected in the institutions to which they belong, in fact among the first fifteen, four are represented by Spain and three by Italy. The analysis of the co-existence network demonstrates a wide collaboration between countries around the world. However, authors in the same country tend to have closer cooperation with each other. The journals Agricultural Water Management and Field Crops Research, each with 19 papers, represent those in which the authors published the most. The analysis of keywords, co-occurrence network and bibliographic coupling allowed to identify the focal areas of research in the literature related to durum wheat irrigation. In particular, they concerned i) the management of water resources, ii) the effect of salt and water stress on production, iii) vegetation indices and other indices for plant phenotyping. Finally, the analysis of the references highlighted the most influential publications in the field of research under study, including those of Fischer et al., 1978, Jackson et al., 1977 and Zhang et al., 1999. Considering that the year of publication, not recently, has also contributed to the greater number of citations, this does not exclude that more recent papers, but with fewer citations, are equally important.

The results suggest the need to strengthen institutional partnerships and to increase research on the irrigation of durum wheat, especially in the most vulnerable areas where climate change has the most evident impacts.

ACKNOWLEDGMENTS:

This paper and related research have been conducted during the PhD course in Biodiversity in Agriculture and Forestry.

AUTHOR CONTRIBUTIONS:

Noemi Tortorici: Conceptualization, Formal analysis, Writing- Original draft. Nicolò Iacuzzi: Conceptualization, Methodology, Formal analysis, Visualization, Writing- Original draft, Writing- Reviewing and Editing. Federica Alaimo: Formal analysis, Visualization, Writing- Original draft. Calogero Schillaci: Visualization, Writing- Reviewing and Editing, Supervision. Teresa Tuttolomondo: Conceptualization, Supervision, Writing- Reviewing and Editing.

REFERENCES

Abad, A., Lloveras, J., & Michelena, A. (2004). Nitrogen fertilization and foliar urea effects on durum wheat yield and quality and on residual soil nitrate in irrigated Mediterranean conditions. Field Crops Research, 87(2-3), 257-269.

Acevedo, E., Silva, P., & Silva, H. (2002). Wheat growth and physiology. Bread wheat, improvement and production, 30, 39-70.

Albrizio, R., Todorovic, M., Matic, T., & Stellacci, A. M. (2010). Comparing the interactive effects of water and nitrogen on durum wheat and barley grown in a Mediterranean environment. Field Crops Research, 115(2), 179-190.

Aparicio, N., Villegas, D., Casadesus, J., Araus, J. L., & Royo, C. (2000). Spectral vegetation indices as nondestructive tools for determining durum wheat yield. Agronomy Journal, 92(1), 83-91.

Araus, J. L., Amaro, T., Zuhair, Y., & Nachit, M. M. (1997). Effect of leaf structure and water status on carbon isotope discrimination in field-grown durum wheat. Plant, Cell & Environment, 20(12), 1484-1494.

Araus, J. L., Febrero, A., Buxó, R., Rodrıguez-Ariza, M. O., Molina, F., Camalich, M. D., … & Voltas, J. (1997). Identification of ancient irrigation practices based on the carbon isotope discrimination of plant seeds: a case study from the South-East Iberian Peninsula. Journal of Archaeological Science, 24(8), 729-740.

Araus, J. L., Febrero, A., Buxó, R., Camalich, M. D., Martín, D., Molina, F., … & Romagosa, I. (1997). Changes in carbon isotope discrimination in grain cereals from different regions of the western Mediterranean Basin during the past seven millennia. Palaeoenvironmental evidence of a differential change in aridity during the late Holocene. Global Change Biology, 3(2), 107-118.

Araus, J. L., Amaro, T., Casadesús, J., Asbati, A., & Nachit, M. M. (1998). Relationships between ash content, carbon isotope discrimination and yield in durum wheat. Functional Plant Biology, 25(7), 835-842.

Araus, J. L., Febrero, A., Catala, M., Molist, M., Voltas, J., & Romagosa, I. (1999). Crop water availability in early agriculture: evidence from carbon isotope discrimination of seeds from a tenth millennium BP site on the Euphrates. Global change biology, 5(2), 201-212.

Araus, J. L., Slafer, G. A., Reynolds, M. P., & Royo, C. (2002). Plant breeding and drought in C3 cereals: what should we breed for? Annals of botany, 89(7), 925-940.

Araus, J. L., Villegas, D., Aparicio, N., Del Moral, L. G., El Hani, S., Rharrabti, Y., … & Royo, C. (2003). Environmental factors determining carbon isotope discrimination and yield in durum wheat under Mediterranean conditions. Crop science, 43(1), 170-180.

Araus, J. L., Cabrera-Bosquet, L., Serret, M. D., Bort, J., & Nieto-Taladriz, M. T. (2013). Comparative performance of δ13C, δ18O and δ15N for phenotyping durum wheat adaptation to a dryland environment. Functional Plant Biology, 40(6), 595-608.

Ashraf, M., & Bashir, A. (2003). Relationship of photosynthetic capacity at the vegetative stage and during grain development with grain yield of two hexaploid wheat (Triticum aestivum L.) cultivars differing in yield. European Journal of Agronomy, 19(2), 277-287.

Ayed, S., Othmani, A., Bouhaouel, I., & Teixeira da Silva, J. A. (2021). Multi-environment screening of durum wheat genotypes for drought tolerance in changing climatic events. Agronomy, 11(5), 875.

Ayers, R. S., & Westcot, D. W. (1985). Water quality for agriculture (Vol. 29, p. 174). Rome: Food and agriculture organization of the United Nations.

Bagci, S. A., Ekiz, H., Yilmaz, A., & Cakmak, I. (2007). Effects of zinc deficiency and drought on grain yield of field-grown wheat cultivars in Central Anatolia. Journal of Agronomy and Crop Science, 193(3), 198-206.

Bassi, F. M., & Sanchez-Garcia, M. (2017). Adaptation and stability analysis of ICARDA durum wheat elites across 18 countries. Crop Science, 57(5), 2419-2430.

Ben-Jabeur, M., Chamekh, Z., Jallouli, S., Ayadi, S., Serret, M. D., Araus, J. L., … & Hamada, W. (2022). Comparative effect of seed treatment with thyme essential oil and Paraburkholderia phytofirmans on growth, photosynthetic capacity, grain yield, δ15N and δ13C of durum wheat under drought and heat stress. *Annals of Applied Biology*, *181*(1), 58-69.

Blanco, A. Structure and Trends of Worldwide Research on Durum Wheat by Bibliographic Mapping. Int. J. Plant Biol. 2024, 15, 132-160. https://doi.org/10.3390/ijpb15010012

Campbell, C. A., Selles, F., Zentner, R. P., & McConkey, B. G. (1993). Available water and nitrogen effects on yield components and grain nitrogen of zero-till spring wheat. Agronomy Journal, 85(1), 114-120.

Casadesús, J., Kaya, Y., Bort, J., Nachit, M. M., Araus, J. L., Amor, S., … & Villegas, D. (2007). Using vegetation indices derived from conventional digital cameras as selection criteria for wheat breeding in water-limited environments. Annals of applied biology, 150(2), 227-236.

Cecchini, C., Menesatti, P., Antonucci, F., & Costa, C. (2020). Trends in research on durum wheat and pas-

ta, a bibliometric mapping approach. Cereal Chemistry, 97(3), 581-588.

Chai, Q., Gan, Y., Zhao, C., Xu, H. L., Waskom, R. M., Niu, Y., & Siddique, K. H. (2016). Regulated deficit irrigation for crop production under drought stress. A review. Agronomy for sustainable development, 36, 1-21.

Chairi, F., Aparicio, N., Serret, M. D., & Araus, J. L. (2020). Breeding effects on the genotype× environment interaction for yield of durum wheat grown after the Green Revolution: The case of Spain. The Crop Journal, 8(4), 623-634.

Chen, C., Payne, W. A., Smiley, R. W., & Stoltz, M. A. (2003). Yield and water-use efficiency of eight wheat cultivars planted on seven dates in northeastern Oregon. Agronomy Journal, 95(4), 836-843.

CIMMYT. Available online: https://www.cimmyt.org/es/ (accessed on 20 November 2023).

Condon, A. G., Richards, R. A., Rebetzke, G. J., & Farquhar, G. (2002). Improving intrinsic water-use efficiency and crop yield. Crop science, 42(1), 122-131.

De Santis, M. A., Soccio, M., Laus, M. N., & Flagella, Z. (2021). Influence of drought and salt stress on durum wheat grain quality and composition: A review. Plants, 10(12), 2599.

De Vita, P., Nicosia, O. L. D., Nigro, F., Platani, C., Riefolo, C., Di Fonzo, N., & Cattivelli, L. (2007). Breeding progress in morpho-physiological, agronomical and qualitative traits of durum wheat cultivars released in Italy during the 20th century. European Journal of Agronomy, 26(1), 39-53.

Dong, P., Loh, M., & Mondry, A. (2005). The" impact factor" revisited. Biomedical digital libraries, 2(1), 1-8.

Donthu, N., Kumar, S., Mukherjee, D., Pandey, N., & Lim, W. M. (2021). How to conduct a bibliometric analysis: An overview and guidelines. Journal of business research, 133, 285-296.

Du, T., Kang, S., Zhang, J., & Davies, W. J. (2015). Deficit irrigation and sustainable water-resource strategies in agriculture for China's food security. Journal of experimental botany, 66(8), 2253-2269.

Durieux, V., & Gevenois, P. A. (2010). Bibliometric indicators: quality measurements of scientific publication. Radiology, 255(2), 342-351.

Ekiz, H., Bagci, S. A., Kiral, A. S., Eker, S. E. L. İ. M., Gültekin, I., Alkan, A. Y. F. E. R., & Cakmak, I. (1998). Effects of zinc fertilization and irrigation on grain yield and zinc concentration of various cereals grown in zinc-deficient calcareous soils. Journal of plant nutrition, 21(10), 2245-2256.

Elazab, A., Bort, J., Zhou, B., Serret, M. D., Nieto-Taladriz, M. T., & Araus, J. L. (2015). The combined use of vegetation indices and stable isotopes to predict durum wheat grain yield under contrasting water conditions. Agricultural Water Management, 158, 196-208.

Elhani, S., Martos, V., Rharrabti, Y., Royo, C., & Del Moral, L. G. (2007). Contribution of main stem and tillers to durum wheat (Triticum turgidum L. var. durum) grain yield and its components grown in Mediterranean environments. Field Crops Research, 103(1), 25-35.

Ellegaard, O., & Wallin, J. A. (2015). The bibliometric analysis of scholarly production: How great is the impact? Scientometrics, 105, 1809-1831.

Fahad, S., Bajwa, A. A., Nazir, U., Anjum, S. A., Farooq, A., Zohaib, A., … & Huang, J. (2017). Crop production under drought and heat stress: plant responses and management options. Frontiers in plant science, 1147.

Fernandez-Gallego, J. A., Kefauver, S. C., Vatter, T., Gutiérrez, N. A., Nieto-Taladriz, M. T., & Araus, J. L. (2019). Low-cost assessment of grain yield in durum wheat using RGB images. European Journal of Agronomy, 105, 146-156.

Fischer, R. A., & Maurer, R. (1978). Drought resistance in spring wheat cultivars. I. Grain yield responses. Australian Journal of Agricultural Research, 29(5), 897-912.

Flagella, Z., Giuliani, M. M., Giuzio, L., Volpi, C., & Masci, S. (2010). Influence of water deficit on durum wheat storage protein composition and technological quality. European Journal of Agronomy, 33(3), 197-207.

French, A. N., Hunsaker, D. J., Sanchez, C. A., Saber, M., Gonzalez, J. R., & Anderson, R. (2020). Satellite-based NDVI crop coefficients and evapotranspiration with eddy covariance validation for multiple durum wheat fields in the US Southwest. Agricultural Water Management, 239, 106266.

Galvão, T. F., Pansani, T. D. S. A., & Harrad, D. (2015). Principais itens para relatar Revisões sistemáticas e Meta-análises: A recomendação PRISMA. Epidemiologia e serviços de saúde, 24, 335-342.

García Del Moral, L. G., Rharrabti, Y., Villegas, D., & Royo, C. (2003). Evaluation of grain yield and its components in durum wheat under Mediterranean conditions: an ontogenic approach. Agronomy journal, 95(2), 266-274.

Giraldo, P., Benavente, E., Manzano-Agugliaro, F., & Gimenez, E. (2019). Worldwide research trends on wheat and barley: A bibliometric comparative analysis. Agronomy, 9(7), 352.

Giunta, F., Motzo, R., & Deidda, M. (1993). Effect of drought on yield and yield components of durum

wheat and triticale in a Mediterranean environment. Field Crops Research, 33(4), 399-409.

Guidi, L., & Calatayud, A. (2014). Non-invasive tools to estimate stress-induced changes in photosynthetic performance in plants inhabiting Mediterranean areas. Environmental and experimental botany, 103, 42-52.

Huang, S., Tang, L., Hupy, J. P., Wang, Y., & Shao, G. (2021). A commentary review on the use of normalized difference vegetation index (NDVI) in the era of popular remote sensing. Journal of Forestry Research, 32(1), 1-6.

Idso, S. B., Jackson, R. D., & Reginato, R. J. (1977). Remote-Sensing of Crop Yields: Canopy temperature and albedo measurements have been quantitatively correlated with final harvests of wheat. Science, 196(4285), 19-25.

Intergovernmental Panel on Climate Change (IPCC) 2014. Available online: https://www.ipcc.ch/report/ar5/syr/ (accessed on 20 November 2023).

International Grains Council (IGC). Available online: https://www.igc.int/en/default.aspx (accessed on 20 November 2023).

Jackson, R. D., Reginato, R. J., & Idso, S. (1977). Wheat canopy temperature: a practical tool for evaluating water requirements. Water resources research, 13(3), 651-656.

Kabbaj, H., Sall, A. T., Al-Abdallat, A., Geleta, M., Amri, A., Filali-Maltouf, A., … & Bassi, F. M. (2017). Genetic diversity within a global panel of durum wheat (Triticum durum) landraces and modern germplasm reveals the history of alleles exchange. Frontiers in plant science, 8, 1277.

Karam, F., Kabalan, R., Breidi, J., Rouphael, Y., & Oweis, T. (2009). Yield and water-production functions of two durum wheat cultivars grown under different irrigation and nitrogen regimes. Agricultural water management, 96(4), 603-615.

Katerji, N., Mastrorilli, M., Van Hoorn, J. W., Lahmer, F. Z., Hamdy, A., & Oweis, T. (2009). Durum wheat and barley productivity in saline–drought environments. European Journal of Agronomy, 31(1), 1-9.

Kessler, M. M. (1963). Bibliographic coupling between scientific papers. American documentation, 14(1), 10-25.

Khaledian, M. R., Mailhol, J. C., Ruelle, P., & Rosique, P. (2009). Adapting PILOTE model for water and yield management under direct seeding system: The case of corn and durum wheat in a Mediterranean context. Agricultural water management, 96(5), 757-770.

Knight, J. D., Livingston, N. J., & Van Kessel, C. (1994). Carbon isotope discrimination and water-use efficiency of six crops grown under wet and dryland conditions. Plant, Cell & Environment, 17(2), 173-179.

Latiri-Souki, K., Nortcliff, S., & Lawlor, D. W. (1998). Nitrogen fertilizer can increase dry matter, grain production and radiation and water use efficiencies for durum wheat under semi-arid conditions. European Journal of Agronomy, 9(1), 21-34.

Li, Q., Liu, M., Zhang, J., Dong, B., & Bai, Q. (2009). Biomass accumulation and radiation use efficiency of winter wheat under deficit irrigation regimes. Plant Soil Environ, 55(2), 85-91.

Liu, W., Hu, G., & Gu, M. (2016). The probability of publishing in first-quartile journals. Scientometrics, 106, 1273-1276.

Lu, D., Lu, F., Pan, J., Cui, Z., Zou, C., Chen, X., … & Wang, Z. (2015). The effects of cultivar and nitrogen management on wheat yield and nitrogen use efficiency in the North China Plain. Field Crops Research, 171, 157-164.

Martyn, J. (1964). Bibliographic coupling. Journal of documentation, 20(4), 236-236.

Masoni, A., Ercoli, L., Mariotti, M., & Arduini, I. (2007). Post-anthesis accumulation and remobilization of dry matter, nitrogen and phosphorus in durum wheat as affected by soil type. European Journal of Agronomy, 26(3), 179-186.

Meena, R. P., Karnam, V., Sendhil, R., Sharma, R. K., Tripathi, S. C., & Singh, G. P. (2019). Identification of water use efficient wheat genotypes with high yield for regions of depleting water resources in India. Agricultural water management, 223, 105709.

Mohammadi, R. (2024). Effects of post-flowering drought and supplemental irrigation on grain yield and agro-phenological traits in durum wheat. *European Journal of Agronomy*, *156*, 127180.

Mon, J., Bronson, K. F., Hunsaker, D. J., Thorp, K. R., White, J. W., & French, A. N. (2016). Interactive effects of nitrogen fertilization and irrigation on grain yield, canopy temperature, and nitrogen use efficiency in overhead sprinkler-irrigated durum wheat. Field Crops Research, 191, 54-65.

Morgan, J. A., & LeCain, D. R. (1991). Leaf gas exchange and related leaf traits among 15 winter wheat genotypes. Crop Science, 31(2), 443-448.

Muleke, A., Harrison, M. T., De Voil, P., Hunt, I., Liu, K., Yanotti, M., & Eisner, R. (2022). Earlier crop flowering caused by global warming alleviated by irrigation. Environmental Research Letters, 17(4), 044032.

Mzid, N., Cantore, V., De Mastro, G., Albrizio, R., Sellami, M. H., & Todorovic, M. (2020). The application of ground-based and satellite remote sensing for estimation of bio-physiological parameters of wheat

grown under different water regimes. Water, 12(8), 2095.

Neupane, D., Adhikari, P., Bhattarai, D., Rana, B., Ahmed, Z., Sharma, U., & Adhikari, D. (2022). Does climate change affect the yield of the top three cereals and food security in the world?. Earth, 3(1), 45-71.

Nduku, L., Munghemezulu, C., Mashaba-Munghemezulu, Z., Kalumba, A. M., Chirima, G. J., Masiza, W., & De Villiers, C. (2023). Global research trends for unmanned aerial vehicle remote sensing application in wheat crop monitoring. Geomatics, 3(1), 115-136.

Nowicka, B., Ciura, J., Szymańska, R., & Kruk, J. (2018). Improving photosynthesis, plant productivity and abiotic stress tolerance–current trends and future perspectives. Journal of plant physiology, 231, 415-433.

Onipe, O. O., Jideani, A. I., & Beswa, D. (2015). Composition and functionality of wheat bran and its application in some cereal food products. International Journal of Food Science & Technology, 50(12), 2509-2518.

Oweis, T. (1997). Supplemental irrigation: A highly efficient water-use practice. ICARDA.

Oweis, T., Pala, M., & Ryan, J. (1999). Management alternatives for improved durum wheat production under supplemental irrigation in Syria. European Journal of Agronomy, 11(3-4), 255-266.

Oweis, T., Zhang, H., & Pala, M. (2000). Water use efficiency of rainfed and irrigated bread wheat in a Mediterranean environment. Agronomy journal, 92(2), 231-238.

Page, M. L., Nicholson, C. C., Brennan, R. M., Britzman, A. T., Greer, J., Hemberger, J., … & Williams, N. M. (2021). A meta-analysis of single visit pollination effectiveness comparing honeybees and other floral visitors. American Journal of Botany, 108(11), 2196-2207.

Peleg, Z., Fahima, T., Abbo, S., Krugman, T., Nevo, E., Yakir, D., & Saranga, Y. (2005). Genetic diversity for drought resistance in wild emmer wheat and its ecogeographical associations. Plant, Cell & Environment, 28(2), 176-191.

Pritchard, A. (1969). Statistical bibliography or bibliometrics. Journal of documentation, 25, 348.

Rebetzke, G. J., Van Herwaarden, A. F., Jenkins, C., Weiss, M., Lewis, D., Ruuska, S., … & Richards, R. A. (2008). Quantitative trait loci for water-soluble carbohydrates and associations with agronomic traits in wheat. Australian Journal of Agricultural Research, 59(10), 891-905.

Reynolds, A. G., Brown, R., Kotsaki, E., & Lee, H. S. (2015, May). Utilization of proximal sensing technology (greenseeker) to map variability in ontario vineyards. In Proceedings of the 19th International Symposium GiESCO, Gruissan, France (pp. 593-597).

Rezzouk, F. Z., Gracia-Romero, A., Kefauver, S. C., Nieto-Taladriz, M. T., Serret, M. D., & Araus, J. L. (2022). Durum wheat ideotypes in Mediterranean environments differing in water and temperature conditions. Agricultural Water Management, 259, 107257.

Rharrabti, Y., Villegas, D., Royo, C., Martos-Núñez, V., & Del Moral, L. G. (2003). Durum wheat quality in Mediterranean environments: II. Influence of climatic variables and relationships between quality parameters. Field Crops Research, 80(2), 133-140.

Rhoades, J. D. (1972). Quality of water for irrigation. Soil Science, 113(4), 277-284.

Rivera, M. A., & Pizam, A. (2015). Advances in hospitality research:"from Rodney Dangerfield to Aretha Franklin". International Journal of Contemporary Hospitality Management, 27(3), 362-378.

Royo, C., Villegas, D., Del Moral, L. G., Elhani, S., Aparicio, N., Rharrabti, Y., & Araus, J. L. (2002). Comparative performance of carbon isotope discrimination and canopy temperature depression as predictors of genotype differences in durum wheat yield in Spain. Australian Journal of Agricultural Research, 53(5), 561-569.

Sanchez-Bragado, R., Vicente, R., Molero, G., Serret, M. D., Maydup, M. L., & Araus, J. L. (2020). New avenues for increasing yield and stability in C3 cereals: exploring ear photosynthesis. Current Opinion in Plant Biology, 56, 223-234.

Sun, J., & Yuan, B. Z. (2020). Mapping of the world rice research: A bibliometric analysis of top papers during 2008–2018. Annals of Library and Information Studies (ALIS), 67(1), 55-66.

Tadesse, W., Sanchez-Garcia, M., Assefa, S. G., Amri, A., Bishaw, Z., Ogbonnaya, F. C., & Baum, M. (2019). Genetic gains in wheat breeding and its role in feeding the world. Crop Breeding, Genetics and Genomics, 1(1).

Tambussi, E. A., Bort, J., & Araus, J. L. (2007). Water use efficiency in C3 cereals under Mediterranean conditions: a review of physiological aspects. Annals of Applied Biology, 150(3), 307-321.

Troccoli, A., Borrelli, G. M., De Vita, P., Fares, C., & Di Fonzo, N. (2000). Mini review: durum wheat quality: a multidisciplinary concept. Journal of Cereal Science, 32(2), 99-113.

Van den Boogaard, R., Alewijnse, D., Veneklaas, E. J., & Lambers, H. (1997). Growth and water-use efficiency of 10 Triticum aestivum cultivars at different water availability in relation to allocation of biomass. Plant, Cell & Environment, 20(2), 200-210.

Velasco-Muñoz, J. F., Aznar-Sánchez, J. A., Belmonte-Ureña, L. J., & López-Serrano, M. J. (2018). Advances in water use efficiency in agriculture: A bibliometric analysis. Water, 10(4), 377.

Ventrella, D., Charfeddine, M., Moriondo, M., Rinaldi, M., & Bindi, M. (2012). Agronomic adaptation strategies under climate change for winter durum wheat and tomato in southern Italy: irrigation and nitrogen fertilization. Regional Environmental Change, 12, 407-419.

Ventrella, D., Giglio, L., Charfeddine, M., & Dalla Marta, A. (2015). Consumptive use of green and blue water for winter durum wheat cultivated in Southern Italy. Italian Journal of Agrometeorology, 1, 33-44.

Wang, X., Shi, Y., Guo, Z., Zhang, Y., & Yu, Z. (2015). Water use and soil nitrate nitrogen changes under supplemental irrigation with nitrogen application rate in wheat field. Field Crops Research, 183, 117-125.

Werfelli, N., Ben Ayed, R., Abassi, M., & Béjaoui, Z. (2021). Contamination assessment of durum wheat and barley irrigated with treated wastewater through physiological and biochemical effects and statistical analyses. Journal of Food Quality, 2021(1), 6626184.

Xynias, I. N., Mylonas, I., Korpetis, E. G., Ninou, E., Tsaballa, A., Avdikos, I. D., & Mavromatis, A. G. (2020). Durum wheat breeding in the Mediterranean region: Current status and future prospects. Agronomy, 10(3), 432.

Yaghoubi Khanghahi, M., Leoni, B., & Crecchio, C. (2021). Photosynthetic responses of durum wheat to chemical/microbiological fertilization management under salt and drought stresses. Acta Physiologiae Plantarum, 43, 1-14.

Yousfi, S., Serret, M. D., Voltas, J., & Araus, J. L. (2010). Effect of salinity and water stress during the reproductive stage on growth, ion concentrations, Δ13C, and δ15N of durum wheat and related amphiploids. Journal of Experimental Botany, 61(13), 3529-3542.

Yousfi, S., Serret, M. D., Márquez, A. J., Voltas, J., & Araus, J. L. (2012). Combined use of δ13C, δ18O and δ15N tracks nitrogen metabolism and genotypic adaptation of durum wheat to salinity and water deficit. New Phytologist, 194(1), 230-244.

Yousfi, S., Márquez, A. J., Betti, M., Araus, J. L., & Serret, M. D. (2016). Gene expression and physiological responses to salinity and water stress of contrasting durum wheat genotypes. Journal of Integrative Plant Biology, 58(1), 48-66.

Yuan, B. Z., & Sun, J. (2021). Research trends and status of wheat (Triticum aestivum L.) based on the Essential Science Indicators during 2010–2020: a bibliometric analysis. Cereal Research Communications, 1-12.

Zhang, H., Wang, X., You, M., & Liu, C. (1999). Water-yield relations and water-use efficiency of winter wheat in the North China Plain. Irrigation Science, 19, 37-45.

Zhu, J., & Liu, W. (2020). A tale of two databases: The use of Web of Science and Scopus in academic papers. Scientometrics, 123(1), 321-335.

Italian Journal of Agrometeorology
Rivista Italiana di Agrometeorologia

Firenze University Press
https://riviste.fupress.net/index.php/IJAm

OPEN ACCESS

Citation: Negash, T.W., Tefera, A.T., & Bayisa, G.D. (2024). Maize (*Zea mays* L., 1753.) evapotranspiration and crop coefficient in semi-arid region of Ethiopia. *Italian Journal of Agrometeorology* (2): 55-63. doi: 10.36253/ijam-2777

Received: May 25, 2024

Accepted: November 1, 2024

Published: December 30, 2024

© 2024 Author(s). This is an open access, peer-reviewed article published by Firenze University Press (https://www.fupress.com) and distributed, except where otherwise noted, under the terms of the CC BY 4.0 License for content and CC0 1.0 Universal for metadata.

Data Availability Statement: All relevant data are within the paper and its Supporting Information files.

Competing Interests: The Author(s) declare(s) no conflict of interest.

ORCID:
ATT: 0000-0002-3051-6767

Maize (*Zea mays* L., 1753.) evapotranspiration and crop coefficient in semi-arid region of Ethiopia

Tatek Wondimu Negash*, Abera Tesfaye Tefera, Gobena Dirirsa Bayisa

Ethiopian Institute of Agricultural Research (EIAR), Melkassa Agricultural Research Center (MARC), P.O. Box 436, Adama, Ethiopia
*Corresponding author. E-mail: tatek.wondimu456@gmail.com

Abstract. Maize (*Zea mays* L.,1753.) plays an important role in the economy of maize-growing nations. Supplying the right amount of water to a crop based on its needs is the main agenda for implementing water-saving agriculture. Non-weighting lysimeters were used to determine the actual crop evapotranspiration and crop coefficient of maize at the experimental farmland of the Melkassa Agricultural Research Center, Ethiopia. Soil-water balance approaches were applied to obtain actual crop evapotranspiration, while the Penman-Monteith technique was used to compute reference evapotranspiration. The growth stages-wise crop coefficient was calculated as the ratio of the actual crop evapotranspiration ratio to the reference evapotranspiration. The total seasonal maize actual crop evapotranspiration during the 2017 and 2018 experimental years was 503.7 and 511.06 mm, respectively. The 2-year average maize actual crop evapotranspiration was 507.4 mm. The mean locally developed actual crop coefficient values of 0.55, 1.19, and 0.56 were observed for the initial, mid, and end seasons, respectively. The FAO-adjusted crop coefficient for the mid-season was 1.15. The developed Kc values differed considerably from the FAO-adjusted Kc values. Therefore, the determination of actual crop evapotranspiration and crop coefficients for crop growth under local climatic conditions is vital for decision-making concerning agricultural water management in areas where irrigation is practiced.

Keywords: maize, crop coefficient, crop evapotranspiration, soil-water balance, reference evapotranspiration, non-weighing lysimeter.

1. INTRODUCTION

Currently, there is competition for water among various sectors, such as industrial, municipal, and agricultural. Globally, agriculture is a major consumer of water. It accounts for more than 80% of the available water (Dingre & Gorantiwar, 2020). Nevertheless, this share continually decreases in developing countries because of the increasing demand for industries and domestic water supply (Dingre & Gorantiwar, 2020; Hamdy *et al*., 2003). Technical and economic limitations, the expense of developing new water resources,

and the occurrence of extreme events due to climate change are other factors that reduce the share of existing water resources. This is a major challenge for the agricultural sector regarding food production. Therefore, the precise use of irrigation water is crucial for reducing water scarcity in global agriculture.

Maize (*Zea mays* L.,1753.) is an important food crop in Ethiopia. It covered about 2.53 million hectares of land. With this mass of land, a total yield of 1055709.36 tons was produced, with an average yield of 4.179 tons/ha (Haile *et al*., 2022). The yields of these crops are affected by inadequate water supply and inappropriate irrigation scheduling. Knowledge of crop evapotranspiration and stage-wise crop coefficients is crucial for enhancing crop production in agricultural fields. This information is vital for enhancing irrigation water management under both full and limited irrigation scenarios. Crop evapotranspiration is a crucial variable in agricultural research. Accurate measurement of actual crop evapotranspiration (ETa) is essential for managing irrigation water during the growing season, water resource allocation, and conducting hydrologic balance analyses, especially in arid and semiarid areas (Djaman & Irmak, 2013). Therefore, it is important to quantify the ETa under different climatic conditions, irrigation techniques, and agronomic practices.

Actual crop evapotranspiration (ETa) can be measured using the soil water balance technique with the help of a lysimeter. Lysimeters are devices, typically tanks or containers, that define a specific boundary to contain soil water and permit the measurement of either the soil-water balance or the volume of water percolating vertically. It can measure the major components of the hydrological water balance. Lysimeters can be broadly classified into two types: weighing and non-weighing. Both can serve the purpose of determining the soil-water balance, vertical percolation flux (drainage), and chemistry of percolating water. Non-weighing lysimeters may be installed to determine the vertical soil-water flux (drainage) within the soil at a defined boundary. It can be used with a soil-water profile measurement method to estimate water use in evaporative processes. Weighing lysimeters permit the mass or volumetric soil water content change to be determined by weighing the lysimeter and determining its mass change over time. A non-weighing-type Lysimeter can measure long-term ETa on a weekly, decadal, and monthly basis and can be used to manage and plan irrigation systems (Allen *et al*., 1998). Weighing-type lysimeters can measure ETa values for short periods; however, their installation and maintenance costs are high (Srinivas & Tiwari, 2018). Moreover, actual crop evapotranspiration (ETa) can be estimated by utilizing a two-step method that relates the crop-specific coefficient Kc to ETo. This method is highly convenient for computing ETa and is primarily employed in real-world scenarios by technicians and irrigation professionals. Nevertheless, to facilitate irrigation planning, the crop coefficient (Kc) is necessary when utilizing the measured ETa. The crop coefficient (Kc) signifies the crop's unique water consumption, which varies throughout the growing period and is attributable to physiological changes in the crop. In 1968, Jensen introduced the crop coefficient methodology for ETa estimation, which was further improved by various researchers (Doorenbos and Pruitt, 1977; Allen *et al*., 1998). Kc is developed with a ratio of actual crop evapotranspiration (ETa) to reference evapotranspiration (ETo). Numerous approaches are available to calculate reference evapotranspiration. In 1948, Penman introduced the original reference evapotranspiration (ETo) equation, which was subsequently modified by several researchers (Doorenbos and Pruitt, 1977; Hargreaves and Samani, 1985; Watson and Burnett, 1995; Allen *et al*., 1998). The FAO-56 Penman-Monteith technique, after modification, is the only standardized approach capable of yielding satisfactory ETo outcomes across diverse climatic scenarios.

Globally, many researchers have reported maize crop coefficients. For instance, Doorenbos & Kassam (1979) proposed Kc values for maize range between 0.3 – 0.5, 0.7 – 0.85, 1.05 – 1.2, 0.8 – 0.9, and 0.55 – 0.6 for initial, development, mid-season, late-season, and harvesting, respectively. Nevertheless, these values depend on the global average Kc. The authors emphasized the importance of local calibration of Kc under given climate conditions. Allen *et al*. (1998) further proposed maize Kc values at standard climate conditions (RHmin = 45% and u2 = 2 m s^{-1}) of kc_{ini} = 0.3, kc_{mid} = 1.2, and kc_{end} = 0.35 – 0.6 (the lower value is maize harvested after complete filed drying and the upper-value harvesting at high grain moisture). They also recommended a local adjustment of Kc based on a given climatic condition when the wind speed and RHmin differed from 2 m s^{-1} and 45%, respectively, Rosa *et al*. (2012) and Zhang *et al*. (2013) developed a mid-stage maize basal crop coefficient of 1.05 and 1.15, respectively using the SIMDualKc model. Suyker & Verma (2009) obtained Kc values for maize of 0.27, 1.03, and 0.33 during the initial, mid, and end seasons, respectively, using the eddy covariance method in eastern Lincoln, Nebraska, USA. In lysimeter studies, Abedinpour (2015) in New Delhi, India, obtained maize seasonal Kc values of 0.5, 0.75, 1.2, and 0.6 for the initial, development, mid, and late seasons, respectively. Similarly, Piccinni *et al*. (2009) reported maize Kc values in

the range of 0.2–1.2 from the initial to mid-stages in the Wintergarden region of Texas, USA.

The studies mentioned above indicate a critical need for the development of Kc for local weather conditions because the scales at which the climate and its effects on crops are experienced vary. The crop coefficient for computing maize evapotranspiration was not obtained for the semi-arid region of Ethiopia; therefore, this study was conducted. This study aimed to determine the actual crop evapotranspiration (ETa) and crop coefficient (Kc) of maize under local climatic conditions using a non-weighting lysimeter.

2. MATERIAL AND METHODS

2.1. Study site

The field trial was conducted at the Melkassa Agricultural Research Center, Ethiopia. It is located at 8^0 24'N latitude and 39^0 21'E longitude at an elevation of 1550 m a.s.l (Figure 1). The climate of the study area is classified as semi-arid, with irregular and unequal rainfall patterns. Between January 01, 1977, and December 31, 2018, the average daily minimum and maximum temperatures varied from 13.8 °C to 28.7 °C. The area receives a mean annual rainfall of 825 mm during the same period. July, August, and September received the highest rainfall. From January 01, 1977, to December 31, 2018, the area's average daily wind speed and ETo ranged between 0.3 - 2.71 m s^{-1} and 3.8 - 5.42 mm day^{-1}, respectively. The daily trends and monthly climate parameters for the maize growing periods of 2017 and 2018 are presented in Figure 2 and Table 1, respectively. The soil in the study area belongs to the clay loam soil texture class. The soil had an average bulk density of 1.13 g cm^{-3}, field capacity (FC) of 0.32 m^3 m^{-3}, and permanent wetting point (PWP) of 0.22 m^3 m^{-3}. The average soil pH and electrical conductivity (EC) were 6.50 and 1.64 dS m^{-1}, respectively. The total nitrogen content was 0.09%.

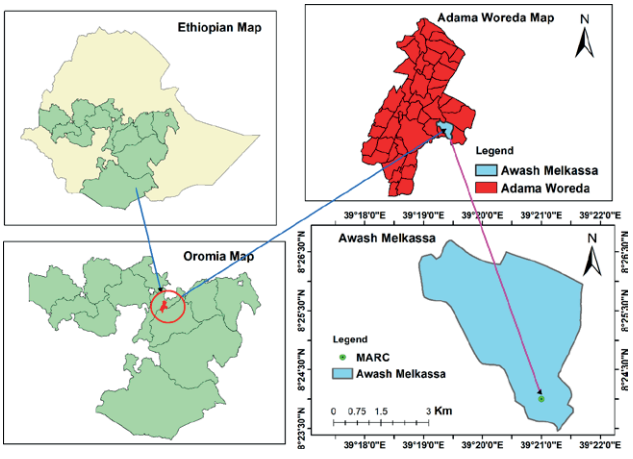

Figure 1. Study area map.

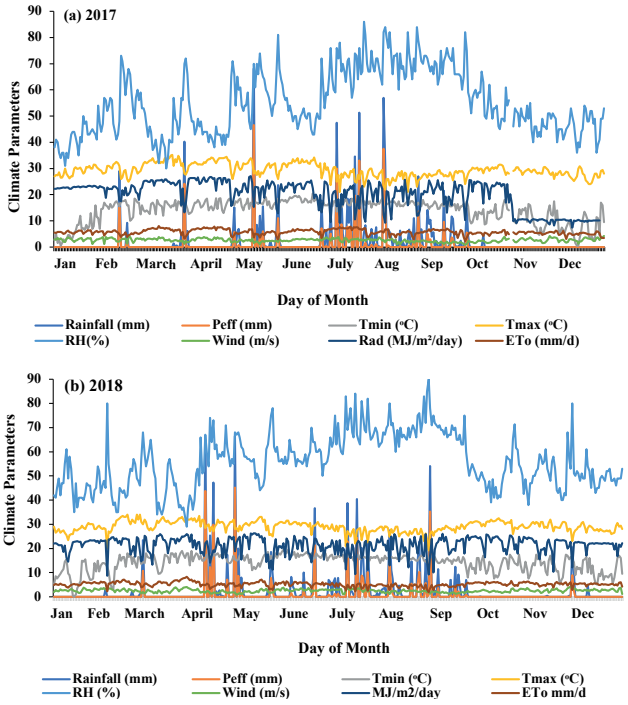

Figure 2. Daily trends of climate parameters during (a) 2017, and (b) 2018 maize growing seasons.

2.2. The Experimental setup

Two lysimeters (non-weighing-type) were used to measure ETa and Kc for maize. The first lysimeter had an internal planting area of 2 m^2, whereas the second had a larger planting area of 4 m^2. The overall depth of the lysimeters measured 2.6 m, comprising a 1 m effective soil depth along with an extra 1 m layer, 0.2 m of rock, 0.2 m of gravel, and 0.2 m of sand pack underneath. The total area of the lysimeter was 36 m^2 (6 × 6 m), including the internal area. To drain excess water, each lysimeter access chamber was linked to an underground steel pipe. The lysimeter rims were placed 0.1 m above the soil surface to prevent surface runoff from entering the lysimeter during rainy days. Access tubes were inserted to an effective root depth of 1 m to monitor the soil moisture level inside the lysimeters.

2.3. Crop agronomic practice

Maize (*Zea mays* L., 1753.), Melkassa II variety, was sowed on July 13, 2017, and July 16, 2018, within the lysimeter and in the surrounding area. Plant densities of 24 and 168 plants were sown inside and outside the lysimeter, respectively, with a lysimeter having an internal area of 4 m^2. Plant densities of 12 and 180 plants were sown inside and outside the lysimeter, respectively, with a lysimeter having an internal area of 2 m^2. The spacing between rows and plants was 75 and 25 cm, respectively. All recommended agronomic practices (fertilization, weed management, pest control, etc.) were consistently applied within the lysimeter as well as in the surrounding area. The plot was fertilized with urea at a split rate of 50 kg ha^{-1} and diammonium phosphate (DAP) at a rate of 100 kg ha^{-1}. The first application of urea and DAP was at the time of sowing (July 13, 2017, and July 16, 2018), and the second application of urea was on August 16, 2017, and August 19, 2018, when the crop reached knee height. Other agronomic practices, such as weed management and pest control, were applied based on the occurrence of weeds and pests. Over two successive experimental seasons, maize was harvested on November 9, 2017, and November 13, 2018.

2.4. Irrigation application and soil moisture monitoring

Before and after each irrigation, soil moisture was measured within the lysimeter at intervals of 15–100 cm. A neutron moisture meter (CPN503) was utilized to measure the soil moisture at depths ranging from 15 to 100 cm in the lysimeter. The gravimetric (oven method) was employed to quantify the soil moisture level in the top 0 –15 cm of the soil. The soil particle size distribution was determined using the Bouyoucos hydrometer method. The core method was used to collect undisturbed soil samples to compute the soil bulk density in the experimental field. The total available soil water (TASW) was computed by subtracting the permanent wilting point (PWP) from the field capacity (FC) after measuring the soil water content at Fc and PWP using a pressure plate apparatus. Irrigation water was provided to the crop when the main rooting layer had depleted 55 % of the available soil water. A watering can was used to apply a known volume of irrigation water to the crops. Irrigation was stopped when the crop showed signs of maturity. The following (equation (1) Brouwer *et al*., 1985) was used to compute the volume of applied irrigation water to the crop:

$$V = A * D \quad (1)$$

where: V = Quantity of applied water (m^3); A = Lysimeter area (m^2); and D = Applied depth (m).

2.5. Crop evapotranspiration and reference evapotranspiration

The following soil water balance approach (equation (2) Jensen *et al*., 1990) was employed to calculate the daily crop evapotranspiration.

$$ETa = \left[\frac{I + P - D \pm \Delta S}{\Delta t}\right] \quad (2)$$

where: ETa = Actual crop evapotranspiration (mm day^{-1}), P = effective rainfall (mm), I = applied irrigation depth (mm), D = drainage depth (mm), and t = time between two consecutive observations in days. ΔS = Change in soil moisture storage (mm), ΔS for a specific period at a specific depth (d_z) was computed as:

$$\Delta S_2 = (\theta_{z,\,final} - \theta_{z,\,initial}) * d_z \quad (3)$$

where: $\theta_{z,\,initial}$ and $\theta_{z,\,final}$ are the initial and final water content in the soil profile in a discrete time interval. Graduated cylindrical was used to measure the drainage depth (D) in the underground room. The amount of irrigation depth needed to fill the root zone to field capacity was equal to the moisture deficit in the soil when no precipitation was anticipated and the soil was not saline. The following (equation (4) Mishra and Ahmed, 1990) was used to calculate the moisture deficit (d) in the effective root zone of the crop.

$$d = \sum_{i=1}^{n} \frac{(Fci - Pwi)}{100} * ASi * Di \quad (4)$$

where: Fci = Field capacity on a weight basis; Pwi = Actual soil moisture on a weight basis; ASi = apparent specific gravity; Di = depth of i^{th} layer and, n = number of layers in the root zone.

The cropwat8.0 model was employed to compute daily ETo using the FAO Penman-Monteith equation. The model inputs consisted of weather data including daily minimum and maximum air temperatures, wind speed at a height of 2 m, relative humidity, and sunshine hours.

2.6. Crop Coefficient (Kc)

The following equation (5) was used to compute the stage-wise maize Kc values:

$$Kc_{act} = \frac{ETa}{ETo} \quad (5)$$

where: Kc_{act} = actual crop coefficient (dimensionless); ETa = actual crop evapotranspiration (mm day^{-1}), and ETo = reference evapotranspiration (mm day^{-1}).

In FAO-56 (Table 12), the maize Kc values for the initial, mid, and end seasons were 0.3, 1.2, and 0.35 - 0.6, respectively. These values were derived under conventional climatic conditions (RHmin = 45% and u_2 = 2 m s^{-1}). These numbers must be modified to account for the local climate, when the wind speed and RHmin are different from 2 m s^{-1} and 45%, respectively. The Kc values > 0.45 for the mid and end seasons were adjusted to account for the climatic conditions of the area and plant height, as follows (Allen *et al*., 1998).

$$Kc_{mid\text{-}FAO} = Kc_{mid}\ (Tab) + [0.04\ (u_2 - 2) - 0.004\ (RH_{min} - 45)] * (h/3)^{0.3} \quad (6)$$

where $Kc_{mid\text{-}FAO}$ = FAO-adjusted Kc for the mid-season, Kc_{mid} (Tab) = tabulated Kc for the mid-season gained from FAO-56, RHmin = average relative humidity during the mid-season (%), u_2 = average wind speed at 2 m height during the mid-season (m s^{-1}), and h = Mean plant height during the mid-season (m). $Kc_{\text{-end-FAO}}$ was calculated using some method.

3. RESULTS AND DISCUSSIONS

3.1. Climate parameters

Climate parameters such as mean air temperature, relative humidity (RH%), wind speed (u2), solar radiation (Rs), rainfall, and ETo for the 2017 and 2018 study seasons are presented in Table 1. These climate variables were similar to some extent in both growing seasons, except for some differences in rainfall distribution. For instance, the average temperature was 21.3°C in 2017 and 21.4°C in the 2018 maize growing season. The mean values of relative humidity (RH%), wind speed, solar radiation, and ETo were also comparable in both growing periods (Table 1). Total accumulated effective rainfall amounts of 460.1 mm in 2017 and 344.4 mm in 2018 were observed. Higher rainfall amounts were observed in July (201.12 mm) and August (146.32 mm) in 2017, while 150.9 mm of rainfall was received in August 2018 (Table 1). The total amount of rainfall recorded in 2018 was less than 25.84% of that recorded in 2017. The daily ETo values over the maize growing season ranged from 2.18 to 6.54 mm day^{-1} in 2017 and from 1.92 to 6.51 mm day^{-1} in 2018 (Figure 3).

3.2. Maize actual crop evapotranspiration

The Maize Melkassa II variety could take approximately 120 days to mature under Melkassa climate

Table 1. Selected Weather Variables for the Maize Growing Periods of 2017 and 2018.

Month	Mean Temperature (°C)	Mean Relative humidity, RH (%)	Average wind speed, u2 (m s^{-1})	Average Radiation, RS (MJ m^2 day^{-1})	Effective Rainfall (mm)	Average reference evapotranspiration, ETo (mm day^{-1})
2017						
July	21.98	68.9	2.88	17.2	201.12	4.48
August	21.47	72.1	2.36	17.3	146.32	4.26
September	21.80	69.57	1.82	18.6	91.04	4.42
October	21.37	55.06	2.36	20.9	7.20	5.29
November	19.94	47.93	2.81	22.4	14.4	5.54
Average	21.3	62.7	2.4	19.3	-	4.80
Total					**460.1**	
2018						
July	21.6	69.0	2.9	20.07	141.6	4.63
August	21.3	71.0	2.2	20.08	150.9	4.35
September	21.5	71.0	2.2	22.29	44.8	4.96
October	21.6	50.0	2.5	22.75	3.68	5.62
November	21.1	48.0	2.8	22.81	3.40	5.56
Average	**21.4**	**61.8**	**2.5**	**21.60**	-	**5.02**
Tota1					**344.4**	

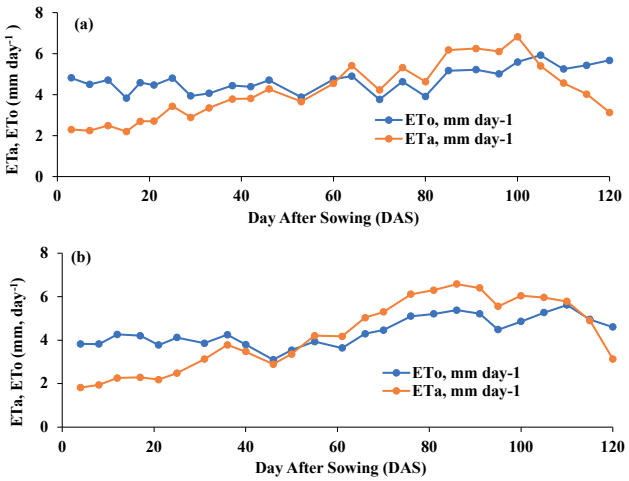

Figure 3 Actual Crop Evapotranspiration (ETa) Vs. Day After Sowing (DAS) for Maize during (a) 2017 and (b) 2018.

conditions, as presented in Table 2. At the study site, the division of maize growth stages depended on the number of plant leaves. The initial stage (Kc_{ini}) is from planting until the seedling is visible above the soil surface, the crop development stage (Kc_{dev}) is from four to five leaf numbers to tassel, the mid-season stage (Kc_{mid}) is from the initiation of ears (8-10 leaf stage) to flowering, and the late-season stage (Kc_{late}) is from full development to harvest. The seasonal maize crop evapotranspiration (ETa) during the 2017 and 2018 experimental years were 503.7 mm and 511.06 mm, respectively, with an average of 507.4 mm (Table 2). In the 2017 and 2018 experimental years, the maximum average maize daily ETa was 6.83 mm day^{-1} and 7.2 mm day^{-1}, respectively, whereas, the minimum average maize daily ETa was 2.2- and 1.82-mm day^{-1}, respectively (Figure 3). The maximum average daily crop evapotranspiration was observed at 100 DAS in 2017 and 95 DAS (midseason) in 2018, whereas the minimum mean daily ETa was observed at 15 DAS and 4 DAS (initial stages) in 2017 and 2018, respectively (Figure 3). The pattern of the average daily ETa for each maize growing season observed in the study area was comparable to the trend described in FAO-56. This trend generally shows a gradual increase in ETa from the initial value, reaching a peak at midseason and starting to decline toward the end of the season. The variation in ETa was due to the combined effects of crop development, changes in the evaporative demand of the atmosphere, and differences in energy absorption characteristics. The increase in ETa from the initial to the crop development stages can be explained by changes in evaporative demand and rapid crop growth. The decline in ETa toward the end-season stage was due to senescence and less physiological activities of the leaves because of aging (Allen *et al.*, 1998). Researchers have reported actual maize evapotranspiration in different parts of the world using different irrigation methods. Kang *et al.* (2003) obtained a maize ETa value of 424 mm under surface irrigation conditions in northwestern China. Similar studies by Zhao & Nan (2007) reported a maize ETa value of 611.5 mm using a dual-crop coefficient in northwestern China. Djaman & Irmak (2013) recorded average seasonal evapotranspiration values of 530 mm and 627 mm under rainfall and full irrigation conditions, respectively. Similarly, Suyker & Verma (2009) reported average maize season ETa values of 548 and 482 mm under surface-irrigated and rainfed conditions, respectively, in eastern Nebraska, USA. Piccinni *et al.* (2009), in South Texas, USA, reported actual maize evapotranspiration in the range of 441–609 mm under sprinkler irrigation using a weighing lysimeter. Similarly, Abedinpour (2015) observed a maize ETa value of 411 mm using a weighing lysimeter. In another study, Trout *et al.* (2018) reported an average maize ETa value of 666 mm under drip irrigation conditions in the west-central Great Plain, USA. Udom & Kamalu (2019) in Port Harcourt, Nigeria recorded a maize ETa value of 456.9 mm using Blaney-Criddle and Standard Class A Pan Evaporation data. Tariq & Usman (2009) reported an actual maize evapotranspiration of 451 mm under farmer irrigation.

3.3. Maize crop coefficient (Kc)

The computed daily actual crop coefficient values expressed as a function of the day after sowing (DAS) for the maize growing seasons of 2017 and 2018 are presented in Figure 4. The result indicates a gradual increase in Kc values from the initial, reaching a peak at the midseason and starting to decline toward the end of the season. This result was similar to the trend described in FAO-56. The seasonal Kc values during the initial (0.57), midseason (1.17), and end season (0.55) were recorded in 2017, while Kc values of 0.53, 1.2, and 0.56 for initial, mid, and end-season, respectively were obtained in 2018 (Table 3). The average maize seasonal Kc values over the two experimental years were 0.55, 1.19, and 0.56 for the initial, mid, and end-season, respectively (Table 3). The evolution of Kc values reflected crop growth, development, and physiology effects on ETa. As the crop develops and shades the ground to the effective full cover and reaches full size, the amount of water abstraction increases, increasing the ETa. The maximum Kc value of 1.17 and 1.2 was obtained during the mid-season of 2017 and 2018, respectively when ETa reached its highest

Table 2. Water balance components (cm) for maize growth periods observed at the experimental site in a semi-arid area of Ethiopia.

Crop stages	Days	2017					2018					Average				
		Pe	I	D	ΔS	ETa	Pe	I	D	ΔS	ETa	Pe	I	D	ΔS	ETa
Initial	25	186.1	5.8	124.3	-3.1	64.5	98	13.5	29.2	-28	54.3	142.1	9.7	76.8	-15.6	59.4
Development	36	105.5	70.5	9.9	-29.2	136.9	131.6	55.2	22.6	-40.6	123.6	118.6	62.9	16.3	-34.9	130.3
Mid-Season	39	57.9	172	5.1	8.4	216.7	20.8	214.5	-	-	235.3	39.4	193.4	2.6	4.2	226.0
End-Season	20	0.16	85.4	-	-	85.6	0.2	97.7	-	-	97.9	0.2	96.1	-	-	91.7
Total	120	349.7	334	139.3	-23.9	503.7	250.6	380.9	51.8	-68.6	511.06	300.2	358.5	94	-47.7	507.4

Note: ETa = actual crop evapotranspiration; I = applied irrigation depth; Pe = effective rainfall; D = drainage depth; S = change in soil moisture; and t = the amount of time between two observations in days.

Table 3. Locally Developed Kc-Values for Maize in the 2017 and 2018 experimental years.

Experimental Year	Kc-ini-Local	Kc-mid-Local	Kc-end-Local
Year I -2017	0.57	1.17	0.55
Year II -2018	0.53	1.20	0.56
Average Kc	0.55	1.19	0.56

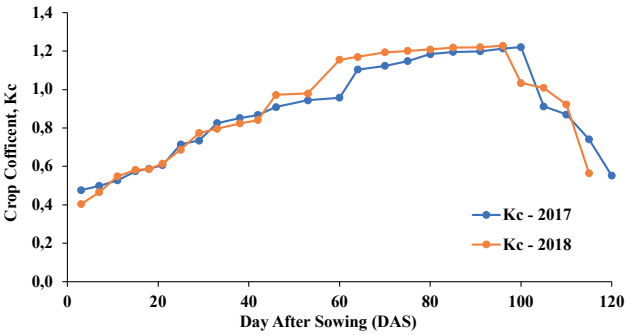

Figure 4. Crop Coefficient (Kc) Values Vs. Days After Sowing (DAS) for 2017, and 2018 maize growing periods.

demand. The Kc-mid value recorded in 2017 was lower than the Kc-mid value recorded in 2018.

3.4. Comparison with FAO Adjusted and other studies

Table 4 presents the Kc values of mid and end-season for maize, which have been adjusted by FAO and locally developed. It is clear that for these maize growth stages, the mean locally derived Kc values of the two seasons were different from the FAO-adjusted Kc (Table 4) and those reported in other publications. In comparison, the Kc_{-mid-}FAO-adjusted value of 1.15 was less than the average locally developed value of 1.19. The average $Kc_{-mid-local}$ for this study was also lower than the reported maize Kc_{-mid} values of: 1.2, 1.26, 1.43, and 1.21 by Allen *et al.* (1998); Li *et al.* (2003); Ding *et al.* (2013); and Abedinpour (2015), respectively. The mean locally developed $kc_{-mid-local}$ values were greater than the Kc_{-mid} values 1.16, 1.0, 1.13, and 1.15 reported by Gao *et al.* (2009); Facchi *et al.* (2013); Martins et al. (2013) and Giménez *et al.* (2016), respectively. However, the $Kc_{-mid-local}$ value of 1.19, observed in this study, was comparable to the Kc_{-mid} of 1.18 obtained by Miao *et al.* (2016). The average $Kc_{-end-local}$ value over two years was 0.56 and was greater than the Kc_{-end-}FAO-56. The maize's mean $Kc_{-end-local}$ values, produced locally, were found to be comparable to the Kc values reported by Irmak & Irmak (2008) and Ding *et al.* (2013), which were Kc_{-mid} = 0.54 and 0.6, respectively. The $Kc_{-ini-local}$ value developed in this study, with a mean of 0.55, is higher than the Kc_{-ini} values reported by Allen *et al.* (1998); Piccinni *et al.* (2009); Suyker & Verma (2009); Gao *et al.* (2009) which were 0.3, 0.27, 0.2, and 0.37, respectively. Nonetheless, it is comparable to the Kc initial value of (kc-ini = 0.5) developed by Li *et al.* (2003). In general, this variation of Kc values between the locally developed, the FAO adjusted and other stud-

Table 4. FAO-adjusted and Locally Developed Kc-Values for Maize in the 2017 and 2018 experimental periods.

Experimental Year	$Kc_{-mid-(Local)}$ ($Kc_{-mid(adj)}$)	$Kc_{-end-(Local)}$ ($Kc-_{end(adj)}$)
Year I (2017)	1.17 (1.13)	0.55 (**)
Year II (2018)	1.20 (1.17)	0.56 (**)
Average Kc	1.19 (1.15)	0.56 (**)

Note: ($Kc_{-mid(adj)}$) and $Kc-_{end\ (adj)}$ represent the FAO adjusted Kc for the mid and end-season, respectively, when wind speed and RHmin differ from 2 m s^{-1} and 45%. $Kc_{-mid-Local}$ and $Kc_{-end-Local}$ refer to locally developed Kc for the mid and end-season, respectively. (**) is a non-adjusted value of Kc because the maize end-season kc value found in FAO-56 was 0.35, which was less than 0.45. Therefore, it could not be adjusted to the local climate conditions. For more information refer to section 2.6 in this paper.

ies could be attributable to the difference in local climatic conditions, growing window, soil texture, and management practice.

4. CONCLUSIONS

Maize plays an important role in the economy of maize-growing nations. Underestimating actual crop evapotranspiration might result in yield penalties attributable to water stress, whereas overestimation can lead to excessive water application, thereby lowering the available water for other uses. Knowing the stage-specific Kc of maize is crucial because Kc is a critical factor in the computation of ETa for any crop. To enhance irrigation practices in the semi-arid region of Ethiopia, this study produced knowledge-based data on maize ETa and Kc using the water balance technique and a non-weighing lysimeter under local climate conditions. In 2017 and 2018, seasonal maize ETa values were 503.7 mm and 511.06 mm, respectively, with an average of 507.4 mm. In 2017, the developed maize Kc values for the initial, mid, and end seasons were 0.57, 1.17, and 0.55, respectively. In contrast, the Kc values for the initial, mid, and end of the season in 2018 were 0.53, 1.20, and 0.56, respectively. The average seasonal maize Kc values for the initial, mid, and end seasons across the two experimental years were 0.55, 1.19, and 0.56, respectively. Throughout the growth period, the Kc values obtained locally were higher than the FAO-adjusted Kc values. Using FOA-adjusted Kc values may result in an underestimation of maize irrigation scheduling in the semi-arid region of Ethiopia. The actual water use of maize can be corrected using the Kc values developed in this study. In general, this study provides useful information on the exact water applications and efficient management of irrigation water for countries that cultivate maize in semiarid areas of the world.

ACKNOWLEDGMENT

The authors express their gratitude to the Ethiopian Institute of Agricultural Research, Melkassa Agricultural Research Center, for their generous financial support and technical assistance in experimenting.

AUTHORS CONTRIBUTIONS

Tatek Wondimu Negash: Field data collection, data analysis, methodology, writing original draft, writing-review, and editing. Abera Tesfaye Tefera: Field Data collection, writing- review and editing. Gobena Dirirsa Bayisa: Writing- review and editing.

REFERENCES

Abedinpour, M. (2015). Evaluation of Growth-Stage-Specific Crop Coefficients of Maize Using Weighing Lysimeter. 2015(2), 99–104. https://doi.org/10.17221/63/2014-SWR.

Allen, R.G., Pereira, L.S., Raes, D., Smith, M. (1998). Crop evapotranspiration. In: Guidelines for Computing Crop Water Requirements, FAO Irrig. Drain. Paper 56. FAO. http://www.fao.org/docrep/x0490e/x0490e00.htm.

Brouwer, C., Goffeau, A. and Heibloem, M. (1985). Irrigation Water Management: Training Manual No.1. FAO (Food and Agriculture Organization) of the United Nations, Rome, Italy. Draft document1.

Ding, R., Kang, S., Zhang, Y., Hao, X., Tong, L., Du, T. (2013). Partitioning evapotranspiration into soil evaporation and transpiration using a modified dual crop coefficient model in irrigated maize field with ground-mulching. Agricult. Water Manag., 127, 85–96.

Dingre, S. K., & Gorantiwar, S. D. (2020). Determination of the water requirement and crop coefficient values of sugarcane by field water balance method in a semiarid region. Agricultural Water Management, 232(August 2019), 106042. https://doi.org/10.1016/j.agwat.2020.106042.

Djaman, K., & Irmak, S. (2013). Actual Crop Evapotranspiration and Alfalfa- and Grass-Reference Crop Coefficients of Maize under Full and Limited Irrigation and Rainfed Conditions. Journal of Irrigation and Drainage Engineering, 139(6), 433–446. https://doi.org/10.1061/(asce)ir.1943-4774.0000559.

Doorenbos, J., and Kassam, A. H. (1979). Yield response to water. Irrigation and Drainage Paper, 33, 257.

Facchi, A., Gharsallah, O., Corbari, C., Masseroni, D., Mancini, M., Gandolfi, C. (2013). Determination of maize crop coefficients in humid climate regime using the eddy covariance technique. Agricult. Water Manag., 130, 131–141.

Gao, Y., Duan, A., Sun, J., Li, F., Liu, Z., Liu, H., & Liu, Z. (2009). Crop coefficient and water-use efficiency of winter wheat/spring maize strip intercropping. Field Crops Research, 111(1–2), 65–73.

Giménez, L., García-Petillo, M., Paredes, P., Pereira, L. (2016). Predicting maize transpiration, water use, and productivity for developing improved supplemen-

tal irrigation schedules in western Uruguay to cope with climate variability. Water, 8(309). https://doi.org/http://dx.doi.org/10.3390/w8070309.

Haile, K., Gebre, E., & Workye, A. (2022). Determinants of market participation among smallholder farmers in Southwest Ethiopia : double - hurdle model approach. Agriculture & Food Security, 1–13. https://doi.org/10.1186/s40066-022-00358-5.

Hamdy, A., Ragab, R., & Scarascia-Mugnozza, E. (2003). Coping with water scarcity: Water saving and increasing water productivity. Irrigation and Drainage, 52(1), 3–20. https://doi.org/10.1002/ird.73.

Hargreaves G.H and Samani, Z. A. (1985). Reference crop evapotranspiration from temperature. Appl. Eng. Agric. 1 (2).

Irmak, A., & Irmak, S. (2008). Reference and crop evapotranspiration in South Central Nebraska. II: Measurement and estimation of actual evapotranspiration for corn. Journal of Irrigation and Drainage Engineering, 134(6), 700–715.

J. Doorenbos and W.O.Pruitt. (1977). Crop water requirements. FAO irrigation and drainage paper, 24.

Jensen, M.E., Burman, R.D., Allen, R. G. (1990). Evaporation and irrigation water requirements. ASCE Manuals and Reports on Eng.

Kang, S., Gu, B., Du, T., & Zhang, J. (2003). Crop coefficient and ratio of transpiration to evapotranspiration of winter wheat and maize in a semi-humid region. Agricultural Water Management, 59(3), 239–254. https://doi.org/10.1016/S0378-3774(02)00150-6.

Li, Y. L., Cui, J. Y., Zhang, T. H., & Zhao, H. L. (2003). Measurement of evapotranspiration of irrigated spring wheat and maize in a semi-arid region of north China. Agricultural Water Management, 61(1), 1–12.

Martins, J.D., Rodrigues, G.C., Paredes, P., Carlesso, R., Oliveira, Z.B., Knies, A.E., Petry, M.T., Pereira, L. (2013). Dual crop coefficients for maize in southern Brazil: model testing for sprinkler and drip irrigation and mulched soil. Biosyst. Eng., 115, 291–310.

Miao, Q., Rosa, R.D., Shi, H., Paredes, P., Zhu, L., Dai, J., Gonçalves, J.M., Pereira, L. (2016). Modeling water use, transpiration, and soil evaporation of spring wheat–maize and spring wheat–sunflower relay intercropping using the dual crop coefficient approach. Agricult. Water Manag., 165, 211–229.

Mishra, R.D. and Ahmed, M. (1990). Manual on Irrigation Agronomy. Oxford and IBH Publishing Co. PVT. LTd. New Delhi, Bombay, Calcutta.

Piccinni, G., Ko, J., Marek, T., & Howell, T. (2009). Determination of growth-stage-specific crop coefficients (KC) of maize and sorghum. Agricultural Water Management, 96(12), 1698–1704. https://doi.org/10.1016/j.agwat.2009.06.024.

Rosa, R. D., Paredes, P., Rodrigues, G. C., Alves, I., Fernando, R. M., Pereira, L. S., & Allen, R. G. (2012). Implementing the dual crop coefficient approach in interactive software. 1. Background and computational strategy. Agricultural Water Management, 103, 103, 8-24.

Srinivas, B., & Tiwari, K. N. (2018). Determination of Crop Water Requirement and Crop Coefficient at Different Growth Stages of Green Gram Crop by Using Non-Weighing Lysimeter. International Journal of Current Microbiology and Applied Sciences, 7(09), 2580–2589. https://doi.org/10.20546/ijcmas.2018.709.321.

Suyker, A. E., & Verma, S. B. (2009). Evapotranspiration of irrigated and rainfed maize-soybean cropping systems. Agricultural and Forest Meteorology, 149(3–4), 443–452. https://doi.org/10.1016/j.agrformet.2008.09.010.

Tariq, J. A., & Usman, K. (2009). Regulated Deficit Irrigation Scheduling of Maize Crop. Sarhad Journal of Agriculture, 25(3), 441–450.

Trout, T. J., Asce, F., & Dejonge, K. C. (2018). Crop Water Use and Crop Coefficients of Maize in the Great Plains. 70(Asce 2005), 1–13. https://doi.org/10.1061/(ASCE)IR.1943-4774.0001309.

Udom, B. E., & Kamalu, O. J. (2019). Crop Water Requirements during Growth Period of Maize (Zea mays L.) in a Moderate Permeability Soil on Coastal Plain Sands. 9(1), 1–7. https://doi.org/10.5923/j.plant.20190901.01.

Watson, I., Burnett, A. (1995). Hydrology: An Environmental Approach. CRC Press, Boca Raton, FL.

Zhang, B., Liu, Y., Xu, D., Zhao, N., Lei, B., Rosa, R. D. & Pereira, L. S. (2013). The dual crop coefficient approach to estimate and partitioning evapotranspiration of the winter wheat–summer maize crop sequence in North China Plain. Irrigation Science . Irrigation Science, 31, 1303–1316.

Zhao, C. Y., & Nan, Z. R. (2007). Estimating water needs of maize (Zea mays L.) using the dual crop coefficient method in the arid region of northwestern China. African Journal of Agricultural Research, 2(7), 325–333.

Italian Journal of Agrometeorology
Rivista Italiana di Agrometeorologia

Firenze University Press
https://riviste.fupress.net/index.php/IJAm

OPEN ACCESS

Citation: Author (2024). IoT technology as a support tool for the calculation of Crop Water Stress Index in a *Vitis vinifera* L. cv. Chardonnay vineyard in Northern Italy. *Italian Journal of Agrometeorology* (2): 65-80. doi: 10.36253/ijam-2747

Received: May 2, 2024

Accepted: October 22, 2024

Published: December 30, 2024

© 2024 Author(s). This is an open access, peer-reviewed article published by Firenze University Press (https://www.fupress.com) and distributed, except where otherwise noted, under the terms of the CC BY 4.0 License for content and CC0 1.0 Universal for metadata.

Data Availability Statement: All relevant data are within the paper and its Supporting Information files.

Competing Interests: The Author(s) declare(s) no conflict of interest.

ORCID:
CM: 0009-0004-6271-1200
MR: 0000-0003-3228-4557
RZ: 0000-0003-3832-6033

IoT technology as a support tool for the calculation of Crop Water Stress Index in a *Vitis vinifera* L. cv. Chardonnay vineyard in Northern Italy

Cecilia Mattedi[1], Mirco Rodeghiero[2], Roberto Zorer[3]

[1] *Agrometeorology and Irrigation Unit, Technology Transfer Center, Fondazione Edmund Mach, Via E. Mach 1, 38098 San Michele all'Adige (TN), Italy*
[2] *C3A - Center Agriculture Food Environment, University of Trento, 38098 San Michele all'Adige (TN), Italy*
[3] *Digital Agriculture Unit, Research and Innovation Centre, Fondazione Edmund Mach, Via E. Mach 1, 38098 San Michele all'Adige (TN), Italy*
*Corresponding author. E-mail: cecilia.mattedi@fmach.it

Abstract. Nowadays agriculture is one of the main sectors affected by climate change. The continuous increase of temperature and drought periods are posing serious problems in terms of shift of plants' phenological phases and a reduction of crop yield quantity and quality. Among the indexes used to assess plant water status, the Crop Water Stress Index (CWSI) is one of the most studied due to its ease of calculation. We performed a study in a vineyard in Trentino (San Michele all'Adige, Northern Italy) where we took advantage of IoT Technology to build a device to measure leaf temperature and automatically calculate the CWSI. Parameters necessary to determine the CWSI were the temperature of a non-transpiring leaf, (artificial 3D printed black leaf), and the temperature of a fully-transpiring leaf (wet bulb temperature of the air). We compared various types of thermometers to measure temperatures of the real leaves, and with repeated measuring campaigns performed during the summer of 2022 we could obtain spatial maps of CWSI that could highlight the stress levels of the vineyard and therefore address the irrigation management in a context of precision agriculture.

Keywords: drought stress, precision agriculture, leaf temperature, irrigation management, CWSI.

HIGHLIGHTS

- An IoT based approach was tested to assess leaf temperature in order to calculate the real time Crop Water Stress Index.
- A prototype was tested during summer 2022 in a vineyard in San Michele all'Adige (TN) during a period of strong drought.
- Different thermometers were compared to measure leaf temperature.

– The derived data allowed the creation of maps of CWSI which can be used in precision agriculture to save water and increase WUE.
– Some weak points of the system are discussed in order to improve the accuracy in the estimation of CWSI.

1. INTRODUCTION

Year 2022 has been one of the warmest years on record in Europe since 1950 (Global Climate Highlights 2023, 2024), with a temperature anomaly of +0.85 °C with respect to the 1991-2020 reference period average. The consequences of the ongoing Climate Change are heavily affecting human systems and ecosystems, and one of the hardest hit sectors is agriculture. The increase in air temperature has proven to be responsible for a shift in the phenological phases of the crops: for grapevine cultivation, the anticipation of the onset of the growing season and bud break has been observed in different areas of Italy and has been highlighted by several studies (Caffarra and Eccel, 2011; Venios et al., 2020). On one hand, the anticipation of the onset of the growing season can bring farmers to cultivate longer-maturing crops or more crop cycles altogether. On the other hand, temperature increases are more likely responsible for a reduction in yield and crop quality (Adams et al., 1998). Another consequence of a rapidly changing climate is the imbalance of the water regime, that is showing a decrease in annual rainfall and a higher frequency of extreme events like floods and droughts. According to the 6th Assessment Report of the IPCC (Intergovernmental Panel On Climate Change - IPCC, 2023), in the dry summer climates characterizing the Mediterranean area drought phenomena will be enhanced. Thus, responsible management of the water resource is one of the main challenges for the next few years, in order to provide crops with the right amount of irrigation without compromising crop yield and quality.

Plants are organisms directly affected by changes in atmospheric variables such as temperature and precipitation. Droughts are often linked to periods with particularly high temperatures (Mathur et al., 2014), and the effects of these phenomena are mainly appreciable in leaves and roots, which are the most sensible plant organs (Wu et al., 2022). The first-line plant defense against periods of water scarcity or high temperatures is stomatal closure (Venios et al., 2020), that prevents an excessive loss of water vapor through the leaf stomata. This is followed by a decrease in stomatal conductance (Buckley, 2019) and gas exchange (both water vapor and CO_2), that leads to a reduction of photosynthetic activity, plant growth and lower crop production and yield quality (Zhao et al., 2020).

Another consequence of stomatal closure is the increase of leaf temperature. Most of the solar radiation absorbed by the leaf is usually dissipated through sensible (responsible for temperature rise) and latent (transpiration) heat fluxes, but with limited stomatal conductance the latter is drastically reduced and the leaf overheats due to insufficient heat loss (Chaves et al., 2016). The overheating then compromises the photosynthetic processes, and the quality of the crops (Venios et al., 2020) is negatively affected. Plants can activate tolerance mechanisms to overcome short periods of stress, without reporting serious damages (Chaves et al., 2016), but repeated overheating can lead to leaf damage, visible as bleaching, up to desiccation and phylloptosis. As heatwaves accompanied by dry periods will become more frequent, Precision Agriculture practices can be implemented to improve the water use efficiency through irrigation time scheduling and modifying the irrigation rate depending on soil and plant characteristics (Nair et al., 2013; Bwambale et al., 2022). The Internet of Things (IoT) is one of the emerging technologies that complement Precision Agriculture practices, consisting in a network of physical objects interconnected via the Internet, that collects and stores the data recorded by the sensors (Esposito et al., 2022). It allows real-time collection and analysis of useful environmental information, which can be transmitted back to farmers

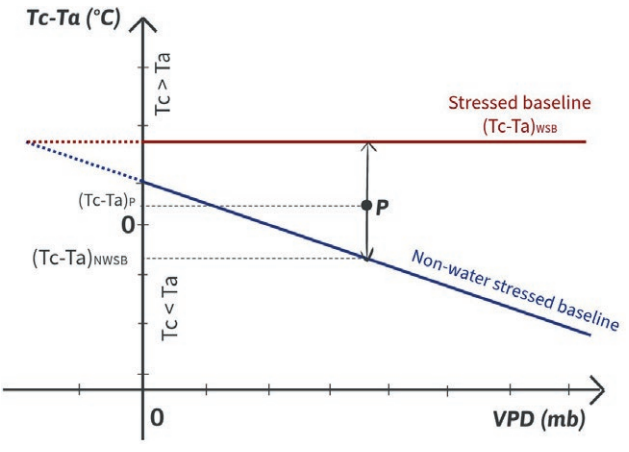

Figure 1. Schematic representation of CWSI (Crop Water Stress Index). Point *P* represents the current crop status, the "Non-Water Stressed Baseline" (NWSB) denotes the crop at potential evapotranspiration and the "Stressed Baseline" (WSB) denotes the crop in a fully stressed condition. T_c and T_a are canopy and air temperature respectively. VPD is the Vapor Pressure Deficit between the canopy and the air (plot adapted from Nanda et al., 2018).

via the Internet, acting as a support for the control of growing conditions of the crops and managing irrigation practices.

Many indexes have been developed to assess plant water status. The CWSI (Crop Water Stress Index) was first introduced in 1981 (Idso et al., 1981; Jackson et al., 1981) as an extension of the stress-degree-day concept, in order to have an index that could be independent of environmental factors other than soil moisture (like air vapor pressure, net radiation and wind speed). The expression was developed based on leaf temperature values taken in three different crop states: potential evapotranspiration, stress conditions and current conditions (Idso et al., 1981). These temperatures were plotted in a graph with the difference between canopy temperature (T_c) and air temperature (T_a) ($T_c - T_a = CATD$) on the y-axis and vapor pressure deficit (VPD) on the x-axis (Fig. 1). The measurements taken in the optimal state of potential evaporation followed a linear pattern (non-water stress baseline, NWSB), whereas the measurements taken in stress conditions were aligned along a horizontal line (stressed baseline, WSB). At a specific VPD and CATD value (point P in Fig. 1), the CWSI was defined as the ratio of 2 vertical segments: the distance between point P and the NWSB (blue line) and the total path between NWSB and WSB (red line):

$$CWSI = \frac{(T_c - T_a)_P - (T_c - T_a)_{NWSB}}{(T_c - T_a)_{WSB} - (T_c - T_a)_{NWSB}} \quad (1)$$

The CWSI value ranges from 0 to 1, representing respectively the state of no water stress (potential evapotranspiration) and the state of severe stress (suppressed transpiration).

The determination of the baselines is not straightforward, as they vary with respect to plant species and the crop growth stages (Idso, 1982). A theoretical formulation was developed from the energy balance of a crop canopy (Jackson et al., 1981):

$$CWSI_t = \frac{\gamma\left(1 + \frac{r_c}{r_a}\right) - \gamma\left(1 + \frac{r_{cp}}{r_a}\right)}{\Delta + \gamma\left(1 + \frac{r_c}{r_a}\right)} \quad (2)$$

$$(T_c - T_a)_{NWSB} = \frac{r_a\, R_n\, \gamma\, VPD}{\rho\, C_p(\Delta + \gamma)^2} \quad (3)$$

$$(T_c - T_a)_{WSB} = \frac{r_a R_n}{\rho C_p} \quad (4)$$

being γ the psychrometric constant, r_c and r_a the canopy resistance and the aerodynamic resistance to vapor transport respectively, r_{cp} the canopy resistance evaluated at full canopy transpiration, Δ the slope of the saturation vapor pressure-temperature relation, R_n the net radiation, ρ the air density, and VPD the Vapor Pressure Deficit.

In an easier calculation approach CWSI was formulated based only on infrared temperature measurements of individual leaves and of reference surfaces, specifically of wet and dry reference surfaces (T_{wet} and T_{dry}; Jones, 1999; Katimbo et al., 2022).

$$(T_c - T_a)_{NWSB} = T_{wet} - T_a \quad (5)$$

$$(T_c - T_a)_{WSB} = T_{dry} - T_a \quad (6)$$

$$CWSI = \frac{(T_c - T_a)_P - (T_c - T_a)_{NWSB}}{(T_c - T_a)_{WSB} - (T_c - T_a)_{NWSB}} = \frac{T_c - T_{wet}}{T_{dry} - T_{wet}} \quad (7)$$

With this formulation the CWSI could be calculated in an easier way and with a restricted amount of variables, by measuring at the same time the canopy temperature T_c, the temperature of a reference wet surface) T_{wet} and the temperature of a dry reference surface T_{dry} (Eq. 7).

A consistent number of studies investigated possible methods to determine these reference values. They have been determined by covering real leaves with a layer of coating like petroleum jelly or Vapor Gard to block evapotranspiration for the measurement of T_{dry}, and with a thin layer of water to measure T_{wet} (Leinonen and Jones, 2004; Ouerghi et al., 2014; Poblete-Echeverr´ıa et al., 2017). Artificial reference surfaces mimicking real leaves have also been realized using water absorbing cloths (Maes et al., 2016), or soaked fabric and dry fabric made of Styrofoam to determine respectively T_{wet} and T_{dry} (Katimbo et al., 2022). Other tests mimicking artificial leaves used cellulose paper-based surfaces (Apolo-Apolo et al., 2020), green plastic-made hemispherical surfaces (Jones et al., 2018) and wet viscose-polyester fabric covering a polystyrene float (Meron et al., 2010).

More recent experimentation tested also neural network models to determine the lower baseline and develop a CWSI based IoT irrigation DSS (Decision Supporting System), obtaining a very reliable DSS but way too much expensive for the practical commercial application (King and Shellie, 2023). This is a common problem for this kind of sperimentations, as they bring valuable results but are not affordable for a systematic use in the field. On the other hand, sensors are usually expensive and do not allow a continuous, low cost and wide monitoring of the CWSI equation parameters (Fuentes-Peñailillo et al., 2024).

This study was aimed to 1) compare different instruments to measure leaf temperature (T_{leaf}) and 2) figure out the best method to assess the dry and wet reference temperatures (T_{wet} and T_{dry}) for the computation of the Crop Water Stress Index (CWSI). Subsequently, the relation between CWSI and stomatal conductance g_{sw} was investigated. Finally, a spatial interpolation of CWSI measured during the mapping experiments was performed in Geographic Information System (GIS) software to analyze the spatial variability of the plant water stress degree in the different parts of the vineyard. The final goal of this study was to develop an IoT station for an implementation of the Crop Water Stress Index that could be affordable for the continuous monitoring of the crop water status, by means of low cost sensors and the connection to a LoRaWan network.

2. MATERIALS AND METHODS

2.1. Study site

The present research work was conducted at the Molini Bassi vineyard (Fig. 2a) of the Fondazione Edmund Mach (FEM), former Istituto Agrario di San Michele all'Adige (Trento, Italy). It is located on the eastern side of the Adige Valley, at an altitude varying between 220 and 230 m a.s.l. It is oriented in the South-West direction (about 241° North) and, due to the hilly landscape and the North-South extension of the Adige Valley, the vines can benefit from the sunlight for about 10.4 hours on average over the growing season. The vineyard has an extension of 8400 m^2 with 77 rows oriented 15° to the North-East/South-West direction. *Vitis vinifera* L. cv. Chardonnay, grafted onto SO4 rootstock, was planted during 2020. Vines are spaced to a fixed distance of 0.8 × 2 m VSP trained with guyot-type pruning system. In particular, this research work was performed in rows going from number 8 to 13 with Chardonnay (clone 809) and from 14 to 17 with clone 78 (Fig. 2a). During 2021, the vineyard was provided with a series of facilities aimed at the installation of prototype instruments developed by FEM or in collaboration with national and international companies and research institutes. At the moment, the vineyard is equipped with 220 V AC mains power and low-voltage (12V DC) power supply lines, WiFi and LoRaWAN coverage for receiving data via long-distance radio signals from Internet of Things-IoT sensors, dataloggers, and microcontrollers.

2.2. Leaf temperature measurements

The assessment of leaf temperature was a crucial aspect of this work and therefore several independent sensors were used to measure leaf temperature:

- **CWSI slave station (IRMLX, Fig. 3)**: it is a prototype of Crop Water Stress Index device, designed and assembled by FEM researchers, consisting in a portable box (WP11-15-4 G Takachi Electric Industrials enclosure of dimensions 110×150×40 mm) equipped with a MLX90614 infrared sensor (MELEXIS, Ypres, Belgium) for non-contact temperature measurements connected to an Arduino MKR WAN 1310 microcontroller. It is also supplied with an Arduino MKR GPS shield that provides the coor-

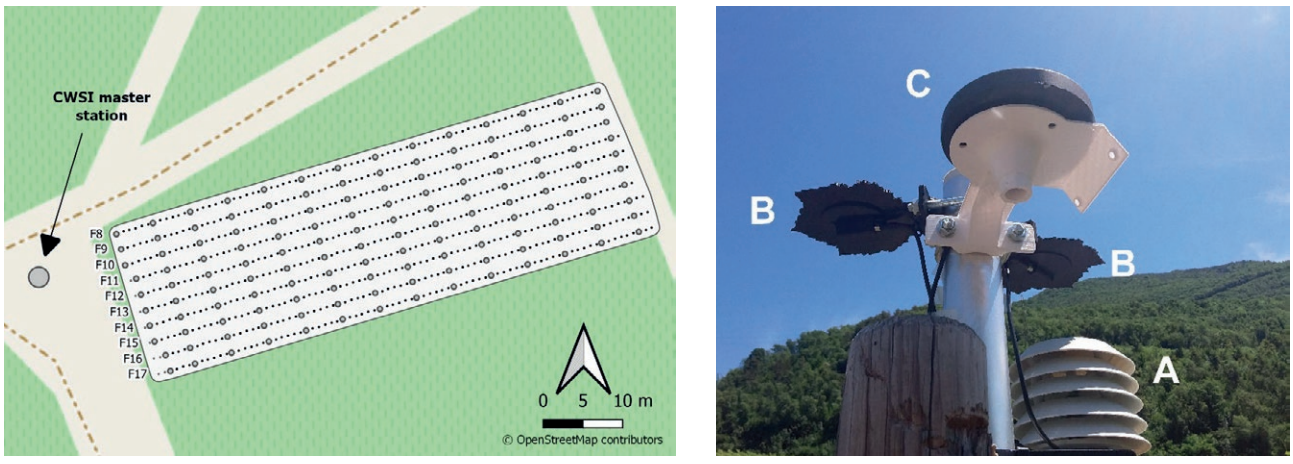

Figure 2. (a) Map of the study site (white area). The grey dots correspond to the poles and the black dots indicate the position of each vine plant. Numbers of the plant rows are shown on the left side. (b) CWSI master station equipped with: A) a thermo-hygrometer; B) two black artificial leaves; C) an aluminum oxide disk.

Figure 3. (a) Setup of CWSI slave station. (b) CWSI slave station measurements.

dinates of the sampling position. In addition the leaf temperature is sent back in the data array (payload) to the LoRaWAN Gateway by means of radio transmission (868 MHz). A GT-P3100 Samsung Galaxy Tab 2 7.0 tablet is mounted on top of the box, allowing the instrument to be powered and displaying via a serial monitor app the measured variables: temperature of the target (the leaf), the temperature of the sensor itself and its GPS coordinates. The infrared sensor has an accuracy of 0.5 °C and a resolution of 0.02 °C. The sensor is activated by pressing a red button located on the right side of the box, holding the position of the sensor for a couple of seconds to properly register the temperature value.

- **Licor LI-600 (Li600) Porometer/Fluorometer (LI-COR Inc., Lincoln, NE, USA)**: Leaf temperature was measured at the same time as stomatal conductance (g_{sw}) by means of an infrared thermal sensor integrated in the instrument itself; the data were recorded in a file together with the time of acquisition, therefore allowing the synchronization with the measurements made with the other instruments.
- **A spare Type E thermocouple (TCext) (Li6400-04; LI-COR Inc., Lincoln, NE, USA)**: part of the Li6400-40 leaf chamber fluorometer, with a 10 cm cable length and connected to a CR10X Datalogger (Campbell Scientific, Logan, UK) acquiring leaf temperature values every minute and averaging them every 15 minutes.
- **Type T thermocouple (TCint) (1m length cable, 1/0.2 mm Diameter, RS Pro Components, Belgium)**: was connected to the CR10X Datalogger as well; values were recorded every 60 seconds and averaged every 15 minutes.
- a portable **62 MAX Mini Infrared Thermometer (IR62)** (Fluke Corporation, Everett, WA, USA) was used to get leaf temperature values in the same leaf previously measured by the Licor LI-600.

2.3. CWSI master station

An essential part of the setup was represented by the CWSI Master station, consisting of an Arduino MKR WAN 1310 microcontroller and several sensors mounted on a 2.3 m high pole located at a distance of about 7 meters from the north-western corner of the vineyard (Fig. 2a). The sensors included a digital thermo-hygrometer (AM2315 - Encased I2C Temperature/Humidity Sensor; Adafruit Industries, NY, USA) recording temperature and relative humidity of the surrounding air, hosted in a 3D printed (white Co-PolyEster CPE) radiation shield (Fig. 2b, A); 3 encapsulated DS18B20 digital

temperature sensors (DFR0198, DFRobot, Shanghai) installed into 3 different artificial media, which should best mimic the state of a non transpiring leaf: the first in a black painted 3D printed leaf made of PolyAmide 12 (PA12; Fig. 2b, B), the second into a black 3D printed leaf made of black CPE (Fig. 2b, B), and, finally, the third (DS18B20 temperature probe) was placed in a black painted aluminum oxide disk, part of an Everest Interscience Model 1000 Calibration Source (Fig. 2b, C).

Other meteorological variables were derived through some simple calculations starting from the measured air temperature (T_{air}) and relative humidity (RH):

- Dew point temperature: following the derivation of Lawrence (2005):

$$T_{dew} = \frac{B\ \alpha(T_{air}, RH)}{A - \alpha(T_{air}, RH)} \tag{8}$$

where A = 17625 and B = 243.04°C are constants and α is defined as a function of T_{air} and RH (Lawrence, 2005):

$$\alpha(T_{air}, RH) = \ln\left(\frac{RH}{100}\right) + \frac{A\ T_{air}}{B + T_{air}} \tag{9}$$

- Wet bulb temperature: computed with the Stull formula (Stull, 2011):

$$T_{wb} = T_{air} \arctan(0.151977(RH + 8.313659)^{0.5}) + \arctan(T_{air} + RH) - \arctan(RH - 1.6763311) + 0.00391838\ RH^{1.5} + \arctan(0.23101\ RH) - 4.686035 \tag{10}$$

2.4. Data transmission

The CWSI master station was equipped with an Arduino MKR WAN 1310 microcontroller, adding a LoRa/LoRaWAN connectivity to the station (license-free radio frequency bands of 868 MHz) and allowing a LoRa communication with the CWSI Slave station, together with the use of a LoRaWAN protocol to send back the data to both the gateway and the online IoT-service. In fact, the Crop Water Stress Index station was registered into a cloud service provided by The Things Stack (The Things Industries), an open source LoRaWAN Network Server which offers a set of open tools and a global, open network to build IoT applications at low cost, featuring maximum security and ready to scale. The presence of a nearby registered gateway (The Things Indoor Gateway - TTIG, The Things Industries) connected to the internet through a 4G LTE WiFi router (RUT240, Teltonika Networks, Vilnius, Lituania) was required for the transmission of the data. Whenever the red button of the CWSI Slave station was pressed, a LoRa digital radio signal containing the data (leaf and sensor temperature, time and device position) was sent to the CWSI master station, activating all the sensors of the CWSI master station. The registered data were then sent as an encoded array of bytes (payload) through LoRaWAN protocols to the TTIG gateway and back to The Things Stack-TTS IoT-cloud service. The Things Stack offers a cloud storage service with a data retention period of 24 hours, an Hypertext Transfer Protocol (HTTP) integration and Message Queuing Telemetry Transport (MQTT) service to grant access and download of the data.

2.5. Field monitoring activities

Two types of field activities were performed during the summer of year 2022, between July and August: mapping sessions and calibration sessions. The mapping campaigns were executed on July 19th , July 25th , August 9th and consisted in monitoring the state of a vineyard subplot, with the aim to create spatial maps of CWSI. For every session a total of 130 leaf temperatures were recorded, choosing 13 representative leaves of the south-facing side of each row (i.e. one located in the middle between two poles). The sampling sequence started on the western side of row number 8 of the vineyard, going to the east direction; the following row was sampled going backward in the opposite direction, continuing in this way for all the 10 vineyards rows.

The target leaf was chosen according to the following criteria: mature stage, well-developed, healthy and lit by the sun. The leaf temperature was measured in the same way on the superior lamina, between the mid-vein and the superior lateral vein. For every leaf, three temperature values were collected, using three different instruments: LI-600 Porometer/Fluorometer (acronym: Li600), CWSI Slave station (acronym: IRMLX), IR thermometer (acronym: IR62). In order to have the most reliable values of temperature, they were measured in the same spot of the leaf area, the sequence of the instruments was kept constant and the time of measurement was kept as short as possible, to avoid sensible changes in leaf temperature.

The measurements were performed in days with clear sky conditions (Poirier-Pocovi and Bailey, 2020) and in the warmest hours of the day (Idso et al., 1981), i.e. an hour and a half after solar noon. At this time of the day plants usually reach their maximum stress condition and the lowest stomatal conductance, therefore being a good time

for quantifying the crop water stress (Jackson et al., 1981).

An additional mapping session was executed on August 23rd , to assess the spatial variability of air temperature and relative humidity within the vineyard as compared to the master station, positioned just outside the rows in an open position. MP100A thermo-hygrometer (Rotronic Italia S. R. L., Rho, Milano) was brought to the field, installed on a 1.5 m portable rod and connected to a Datalogger (CR10x, Campbell Scientific, Logan, UK) programmed to record temperature and relative humidity values every minute. During the measurement of the leaf temperature, the rod was leaned against the canopy in the proximity of the measured leaf with the aim of characterizing the micro-climate of the canopy. After the end of the mapping session the collected data were synchronized (based on time) with those of the CWSI master station in order to compare the climate inside and outside the vineyard. The second type of field activity consisted in calibration campaigns to compare the accuracy in leaf temperature measurement of the instruments used during the mapping session. The calibration campaigns were conducted on August 25th and August 29th following the same procedure: one representative leaf (healthy, mature and sun-lit) was selected and monitored during both days. It was located in row number 10 of the vineyard, between the third and the fourth pole. Leaf temperatures were measured with two thermocouples: one of them (RS PRO type T thermocouple, referred as internal thermocouple, TCint) was inserted in the mid-vein of the inferior lamina of the leaf, and the other one (LI-6400/XT type E thermocouple, referred as external thermocouple, TCext) was positioned in contact with the inferior lamina. The thermocouples were both connected to a CR10X Datalogger that was set to log data with an interval of 1 minute. Leaf temperatures were collected also with the instruments used in the mapping sessions with a time interval of 15 minutes as well. The two sessions started around 9:30 (CEST) in the morning and ended in the afternoon, when the leaf got shaded by the canopy and a stormy cloud was approaching.

Further details about the start and end time of the mapping sessions are given in Table 1.

2.6. Leaf temperature correction

According to the literature, the instrument which best approximates the real leaf temperature is the internal thermocouple (Halbritter et al., 2020): being inserted in the inferior lamina of the leaf, it does not affect other parameters influencing leaf temperature such as solar radiation, leaf angle or the boundary layer. Every instrument was compared to TCint with a scatter plot and a linear regression fit (Martínez et al., 2017; Kim et al., 2018), calculating also the coefficient of determination (R^2) and the statistical significance ($p < 0.05$). New temperature values for each instrument were calculated (y_{new}) based on the coefficients of the regression line:

$$y_{new} = x_{old} = (y_{old} - b)/a \tag{11}$$

where a is the slope and b the intercept of the linear regression line. This process was repeated for both the mapping and the calibration sessions.

2.7. Crop Water Stress Index calculation

The Crop Water Stress Index was calculated using Eq. 7 replacing the canopy temperature T_c with a single leaf temperature T_{leaf}

$$CWSI = \frac{T_{leaf} - T_{wet}}{T_{dry} - T_{wet}} \tag{12}$$

being T_{wet} the wet reference temperature, expressed by the wet bulb temperature of the air (Eq. 10) and T_{dry} the dry reference temperature measured by the black reference devices on the CWSI master station. Every T_{leaf}, calculated with the instruments listed previously, was

Table 1. Field activities calendar, with start and end time of each measuring session and type of instruments used. Li600 (LI-600 Porometer/Fluorometer); IR62 (IR thermometer); IRMLX (CWSI Slave station); TCint (RS PRO type T thermocouple); TCext (LI-6400/XT type E thermocouple). The "X" indicates that the measurement was taken with the corresponding instrument/sensor.

Date	Aim	Start	End	Li600	IR62	IRMLX	TCint	TCext
19/07/2022	Mapping	12:12	13:32	X	X	X	-	-
25/07/2022	Mapping	12:27	15:02	X	X	X	-	-
09/08/2022	Mapping	14:30	15:22	X	X	X	-	-
25/08/2022	Calibration	9:37	16:30	X	X	X	X	X
29/08/2022	Calibration	9:32	15:45	X	X	X	X	X

associated with a correspondent value of T_{wet} and T_{dry} collected by the CWSI master station, resulting in a CWSI value for every sampled leaf.

2.8. Mapping

The measurements collected during the mapping session were associated with the corresponding leaf and position in the vineyard. For every corrected leaf temperature the CWSI value was calculated and plotted in QGIS (Quantum GIS software, QGIS Development Team 2024). Maps of the vineyard for every instrument were created through interpolation using the Inverse Distance Weighting method (IDW) function, available in the QGIS software. The colors of the resulting maps were then divided into intervals to better highlight the distribution of stressed and non-stressed vines.

3. RESULTS

3.1. Dry and wet reference leaf temperatures

The comparison between the different dry reference temperatures is shown in Fig. 4. The dry reference temperatures chosen for the analysis were the maximum values between the two 3D printed leaves, since the two lines were quite similar, and T_{dry} should resemble the temperature of a leaf in a non-transpiring state:

$$T_{dry} = \max(T_{CPE}, T_{PA12}) \quad (13)$$

The aluminum disk was discarded because its heat capacity (880 J kg^{-1} K^{-1}) was much lower than the typical heat capacity of a real leaf which usually ranges between 1287 J kg^{-1} K^{-1} and 2267 J kg^{-1} K^{-1} (Jayalakshmy and Philip, 2010). Therefore, the heat capacity values of the 3D printed leaves (2100 J kg^{-1} K^{-1} for PA12 and 1300 J kg^{-1} K^{-1} for CPE) were more similar to real leaf values.

The wet bulb temperature of the air was taken as the wet reference temperature (T_{wet}) for the calculation of the Crop Water Stress Index. The data collected during the mapping campaign of August 23rd are displayed in Fig. 5: the air temperature inside the vineyard resulted to be higher than the air temperature outside the vineyard for all the duration of the campaign and, on the contrary, relative humidity was slightly higher outside the vine rows. The wet bulb temperature of the air, being calculated as a function of these two parameters, was higher inside the vineyard except for the first minutes of the measuring campaign.

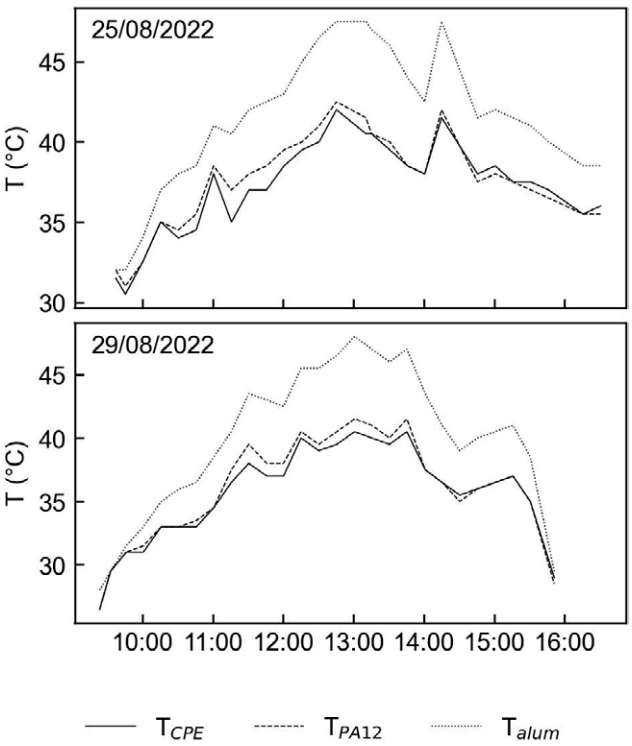

Figure 4. Dry reference temperatures measured during the calibration sessions with the CPE 3D printed leaf T_{CPE}, with the PA12 3D printed leaf (T_{PA12}) and with the aluminum oxide disk (T_{alum}), are represented respectively by the solid, dashed and dotted line.

3.2. Correction of leaf temperatures

Scatter plots of the data collected during the calibration campaigns, comparing temperatures of the different instruments with the internal thermocouple are represented in Fig. 6. The gray line marks the 1:1 reference line and shows how far the measurements were compared to the reference temperature. Basically, all the instruments tended to overestimate leaf temperature especially at the lower values. TCext values almost overlap the 1:1 reference line, therefore showing a very good correspondence with the temperatures measured with the internal thermocouple. Overall, the compared instruments showed quite good slope values, around 0.77 but, in contrast, they presented high intercepts (up to 11.5 °C). All the relationships were highly significant ($p < 0.001$), with rather high coefficient of determination ($R^2 > 0.76$).

3.3. CWSI calculation

Figure 7 displays the CWSI calculated both with measured and corrected temperatures for each day

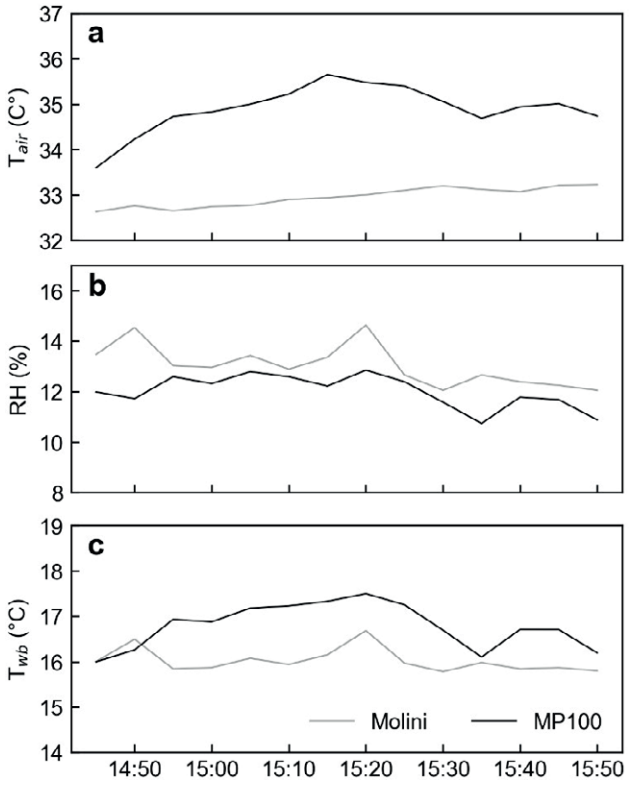

Figure 5. Air temperature (a), relative humidity of the air (b) and wet bulb temperature (c), measured with the MP100 thermohygrometer on August 23rd. Black line: values measured with the MP100 thermohygrometer; grey line: data recorded by the Molini meteorological station.

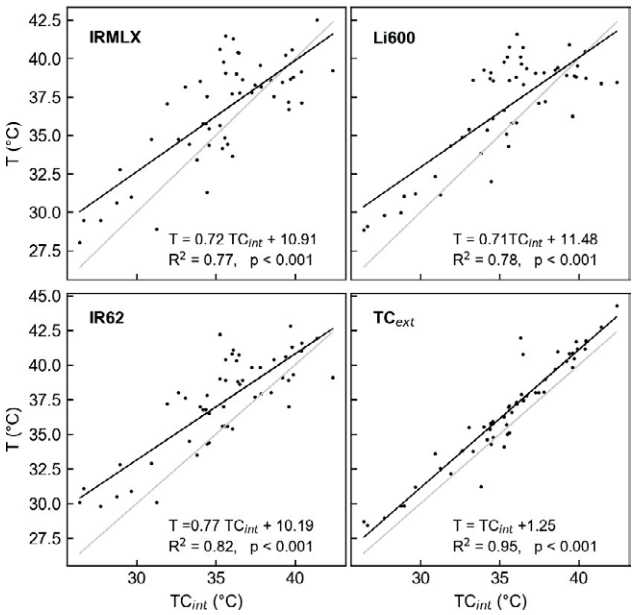

Figure 6. Linear regression between the leaf temperatures measured with the internal thermocouple and the other instruments (CWSI Slave station - IRMLX, Licor Porometer-Fluorometer - Li600, Infrared Thermometer - IR62 and thermocouple in contact with the inferior lamina of the leaf - TCext). On the bottom right of every plot are displayed the regression line equation (black line), the coefficient of determination R^2 and the significance p-value. The gray line is the 1:1 reference line. Each statistic is conducted on a sample of 54 temperature data.

of calibration. It is presented as a temporal sequence of CWSI, calculated for the same leaf during the two calibration sessions. On both days all the instruments showed high CWSI values. In some cases, especially during the afternoon, the CWSI values overcame the upper theoretical limit of the index, which is equal to 1. The lowest values of CWSI were recorded on August 25th (0.57) and on August 29th (0.47). The different temperatures used in the calculation of the CSWI are reported in Fig. 8.

3.4. Relation between CWSI and stomatal conductance g_{sw}

The time series of stomatal conductance g_{sw} and CWSI for the calibration days are reported in Fig. 9. During early morning hours CWSI presented lower values (about 0.6) compared with respect to the central hours of the day, where it varied between 0.8 and 1. The stomatal conductance instead presented higher values around 10:00 (g_{sw} = 0.08 mol m^{-2} s^{-1} on August 25th ,

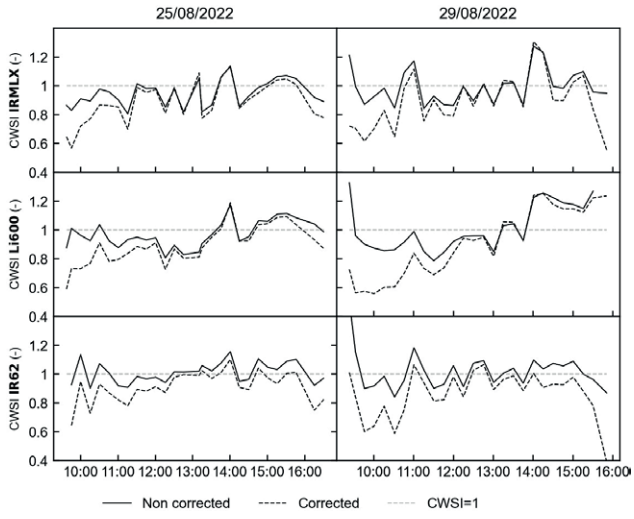

Figure 7. CWSIs calculated with the measured temperature (solid line) and with the corrected temperatures (dashed line) of the instruments used in the monitoring sessions for each day of the calibration campaign. The horizontal, dotted line marks the upper theoretical CWSI limit.

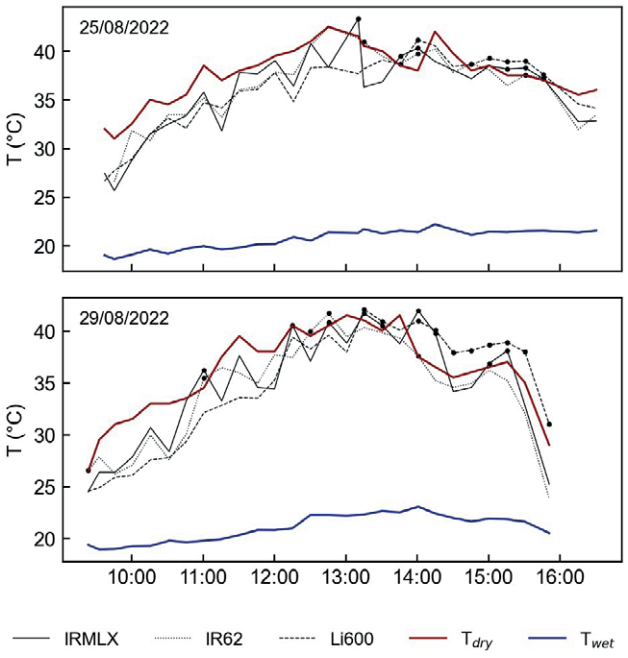

Figure 8. Comparison between the two reference baselines T_{dry} (red) and T_{wet} (blue) and the leaf temperatures recorded by IRLMX, Li600 and IR62. The dots mark the leaf temperatures higher than T_{dry}.

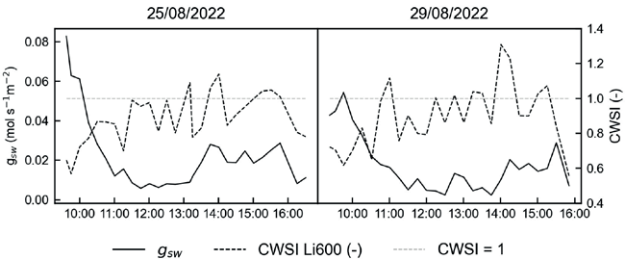

Figure 9. Temporal pattern of stomatal conductance g_{sw} (solid line) and CWSI (dashed line) during the days of calibration. The horizontal dashed line marks the upper theoretical value of CWSI. The values were measured and calculated with the Li600 porometer.

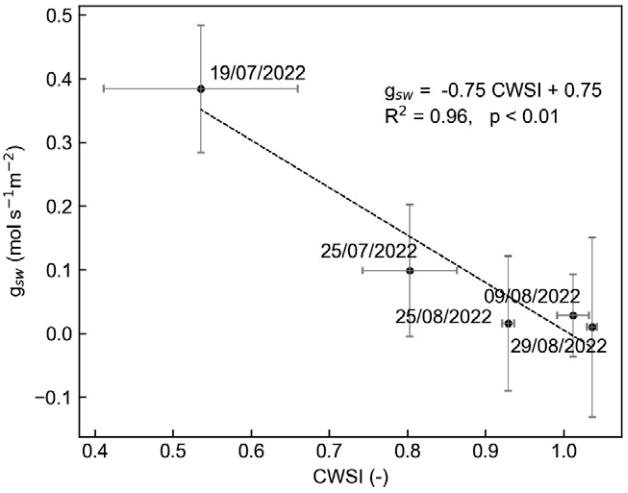

Figure 10. Relationship between CWSI (Crop Water Stress Index) and g_{sw} (stomatal conductance to water vapor) during the summer period of year 2022. Every dot represents an average of both CWSI and g_{sw} (between 12:00 and 15:00) on a specific day of measurement. Data were fitted with a linear regression line (the regression equation, the coefficient of determination R^2 and significance p-value are reported on the top right of the plot). Bars indicate the error.

and g_{sw} =0.09 mol m^{-2} s^{-1} on August 29th) and gradually decreased in the following hours, approaching very low values (almost 0 mol m^{-2} s^{-1}).

The relationship between the CWSI and stomatal conductance during the drought period of the summer season came out to be negative (Fig. 10). With CSWI increasing and decreasing g_{sw}. Every dot in the graph represents the average of CWSI and g_{sw} of each day of measurement, considering both calibration and mapping sessions. For the mapping sessions the parameters were averaged over the entire vineyard, for the calibration sessions the parameters were averaged over the same leaf and only the data recorded between 12:00 and 15:00 were considered, in order to match the temporal range of the other days.

The stomatal conductance to water vapor also decreased as the summer season progressed, with higher values being recorded in July with respect to the end of August. Consequently, CWSI values appeared to be lower at the beginning of the summer season and then they increased.

3.5. QGIS mapping

Interpolation maps were produced for IRMLX and IR62, that were the more accurate instruments in terms of leaf temperature measurement according to the calibration analysis. The maps clearly show the different levels of water stress of the plants in the different areas of the vineyard (Fig. 11). On July 19th the values of CWSI remained quite low across the vineyard (Fig. 11 a, b), but the IRMLX map shows how the southern area appears to be slightly more stressed than the northern area (Fig. 11 b); this aspect is not appreciable in the IR62 map (Fig. 11 a). The blue spots (Fig. 11 c, d) represent missing data due probably to a malfunctioning of the instrument. On July 25th (Fig. 11 c, d) both maps highlighted two distinct stress areas, with the stress level increasing southward. On the contrary, the northern area of the vineyard appeared to be at a higher stress level on August 9th, with high CWSI values almost everywhere (Fig. 11 e, f). The IR62 map (Fig. 11 e) presented higher spatial vari-

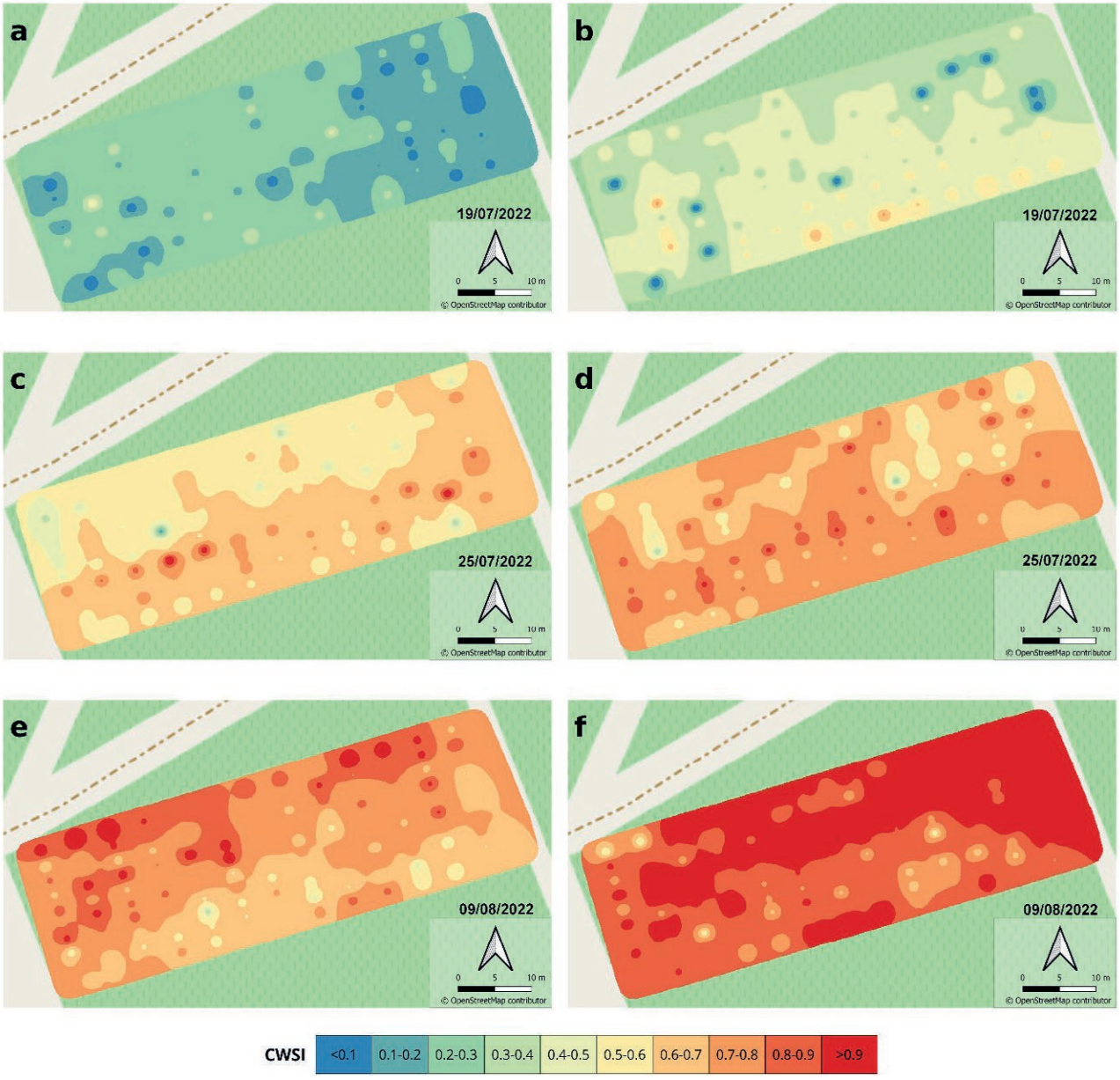

Figure 11. Maps of CWSI produced with the data collected during the mapping session of July 19th, 2022 (a, b), July 25th, 2022 (c, d) and August 9th, 2022 (e, f). Every map shows the CWSI calculated with the following instruments: a, c, e: IR62; b, d, f: IRMLX.

ability with respect to the IRMLX one (Fig. 11 f), where the CWSI was at its maximum in most of the vineyard.

4. DISCUSSION

4.1. Leaf temperature correction

The thermocouple inserted in the leaf vein (TCint) was chosen as a reference instrument for the temperature calibration because in general thermocouples are characterized by good accuracy (0.5 °C) and a short response time given by the low heat capacity of the material (L. Yu et al., 2016). The small size of the thermocouple wire (0.2 mm of diameter) allows an accurate analysis of the small target area of the leaf, also because the sensor does not interfere with the leaf environment.

Furthermore, being in contact with the leaf lamina, it is not influenced by emissivity issues that can instead affect the measurements done with infrared sensors.

Possible sources of error may be due to the absorption of radiation by the thermocouple and to the heat conduction through the wires, but these problems were overcome using low-diameter wires (0.2 mm) and assuring good contact between the wires and the leaf by stripping the insulation off the wires (Tarnopolsky and Seginer, 1999). The instruments compared in this study tended to overestimate the reference leaf temperature, especially at lower temperatures (Fig. 6), whereas there was more scattering towards higher temperatures. As a matter of fact, the three adopted instruments (Li600, IR62, IRMLX) relied on infrared sensors for the detection of object temperatures. Infrared thermometry is usually affected by leaf emission rate and environmental parameters such as dust, carbon dioxide etc. (Yu et al., 2016), or in general by the characteristics of the medium that is present between the measured object and the sensor. Moreover, if the detected temperature is averaged over a large field of view (Halbritter et al., 2020), even less accurate temperature values might be recorded. To minimize this possible source of error, the measurements with IRMLX and IR62 were taken at a distance of about 2-3 cm from the leaf surface.

Another possible reason for the higher temperatures registered by the infrared sensors could be that leaf temperature was measured on the adaxial surface of the leaf, which was directly exposed to the sun. The thermocouple was instead positioned on the abaxial side, which was shaded by the leaf lamina. The difference in radiant energy between the two sides of the leaf could have brought sensible differences in leaf temperature detection (Pallas et al., 1967). The fact that the instrument errors were minimal around solar noon, which is the time of the day when leaf temperatures are generally higher, allowed a better estimation of the water status of the crop. This aspect could be further investigated with measurement of midday leaf water potential using a pressure chamber. This is known to be an effective method to monitor the vine water state but, on the other hand, is an invasive method that relies on appropriate leaf sampling (Deloire et al., 2020). For this reason this kind of analysis was not considered appropriate for this study.

On the other hand, literature suggests that CWSI of a crop should be evaluated between 1 hour and 1:30 hours past solar noon (Idso et al., 1981; Jackson et al., 1981; Bellvert et al., 2014). Infrared thermometers and sensors are widely used nowadays in canopy monitoring (Jackson et al., 1981; Mahan et al., 2010) and are considered one of the most precise and cost-effective leaf temperature measurement methods (Yu et al., 2015; Halbritter et al., 2020). For this reason, they have been considered suitable for the CWSI computation.

4.2. CWSI, dry and wet reference temperatures

The daily trend of CWSI showed low values in the morning, then a gradual increase until 14:00, where it reached the maximum value, followed by a slight decrease in the afternoon (Fig. 10). Irregular peaks were present, probably due to the high variability of the temperature over the leaf surface.

By definition, the index should not be higher than 1, which ideally represents the maximum stressed condition of the plant, but CWSI crossed this upper limit several times in both days and in particular during the afternoon (Fig. 7 and Fig. 8). This issue arises from the empirical determination of the dry reference temperature that should represent the Water-Stressed-Baseline. Indeed, in the calculation of the index (Eq. 7), the result got higher than 1 when the numerator was greater than the denominator, therefore when the actual leaf temperature overcame T_{dry}. In both days of calibration, after 14:00, T_{dry} values were lower than the correspondent leaf temperature measured by all the instruments (IR62, IRMLX, Li600) (Fig. 8). This shows that the black 3D printed leaves lost heat faster than the real leaves. So, the dry reference temperature taken as the maximum temperature between the two black 3D-printed leaves was still not the maximum temperature that a leaf can achieve in stress conditions.

The artificial leaves were fixed horizontally, so the orientation could not allow the maximum amount of solar radiation hitting the surface. To improve the estimation of T_{dry}, a BlackGlobe temperature sensor (Blackglobe-L Campbell Scientific, Logan, UK) could be used; the spherical shape allows the solar beams to hit the surface perpendicularly regardless of the sun elevation, recording higher T_{dry} values.

Another possible source of uncertainty in the calculation of CWSI could be given by the fact that meteorological parameters measured at the CWSI Master station did not exactly match the meteorological parameters inside the vineyard. As reported in literature (e.g. Peña Quiñones et al., 2020, Matese et al., 2014 and Fig. 5) the air temperature measured inside the canopy can be sensibly higher than the one measured outside. Differences between the inner and outer part of the vineyard are usually present also in relative humidity, that together with air temperature influence the estimation of T_{wet}. One should expect higher relative humidity values inside the vineyard with respect to the surroundings, given by the transpiration of plants and the evaporation from the soil. However, in this case it was the opposite. RH values were quite low both inside and outside the vineyard, probably due to the hot and sunny meteorological condi-

tions and the fact that plant transpiration was at its minimum around noon.

In order to improve the estimation of the lower baseline temperature, it might be necessary to set the CWSI master station inside the vineyard, in order to increase the accuracy in the measurement of the microclimate of the vineyard canopy. For this study the CWSI master station was installed outside the vineyard in order not to interfere with the regular maintenance activities of the crop that have to be carried out by means of tractors and heavy machines. It was installed as close as possible to the vines, to give the most reliable picture of the microclimate in the proximity of the vineyard.

4.3. Relation between CWSI and stomatal conductance g_{sw}

The plot in Fig. 9, showing CWSI against g_{sw}, is directly comparable with the graph taken by Karaka et al. (2018), displaying seasonal averaged CWSI and g_{sw} values for soybean cultivars. Both fitting linear regression lines present negative slope (equal to −0.66 for Karaka et al. (2018) and equal to −0.75 for this analysis) and a positive intercept (of 0.75 and 0.65 for the study of Karaka et al. (2018) and this study respectively).

Stomatal conductance decreased with the progression of the growing season. In July g_{sw} measured 0.38 mol H_2O m^{-2} s^{-1} and at the end of August it approached stomatal inactivity with 0.009 mol H_2O m^{-2} s^{-1}. Similarly, Karaka et al., (2018) observed higher values of soybean g_{sw} at the beginning of the summer season (around 0.8 mol H_2O m^{-2} s^{-1}), and a gradual decline in July and August (reaching values close to 0.3 mol H_2O m^{-2} s^{-1}). This can be also a consequence of the hot and dry climate of their experimental site, that records lower values of precipitation and higher air temperatures during the growing season with respect to the San Michele all'Adige in the same period. At the study site the average precipitation of the growing season is equal to 540 ± 151 mm and the mean air temperature is 18.7 ± 6.3 °C (data were collected from the meteorological station of Fondazione E. Mach located in S. Michele all'Adige, in the time period going from April to October in the years between 1983 and 2013), whereas at the Turkish experimental site precipitation it is only 137 mm and air temperatures set on an average of 24.5 °C (calculated in the time period between 1954 and 2013 (Karaka et al., 2018)). Also Ru et al. (2020) highlighted the increasing trend of CWSI for grapevine through the growing season, that went from 0.4 to 0.8 for crops cultivated with a deficit irrigation approach. The discrepancies between the correlations could be due to the comparison between different cultivars, and the influence of external factors such as air temperature (mean air temperature during the growing season was equal to 21.5 °C), net radiation, wind speed and vapor pressure deficit of the air. Despite these correspondences in the literature, the seasonal pattern of CWSI could be studied more consistently with a higher number of measurement sessions distributed over a longer period of time during the water stressed periods of the growing season.

4.4. QGIS maps

In all the survey days the site of measurement presented spatial variability in terms of CWSI (Fig. 11). The difference in magnitude between the IR62 maps and the IRMLX maps was a common pattern observed in all the field sessions, with the IRMLX maps showing higher values of CWSI in all the mapping campaigns. All the maps in general agreed in the spatial distribution of water stress in the field.

On July 19th the IR62 recorded a low, almost uniform stress state, with CWSI < 0.5. The IRMLX map shows a slightly higher stress status on the southern side of the vineyard. The low stress state of the field was probably due to the fact that the site was under irrigation on that day and this is reflected by the high values of stomatal conductance with an average value equal to 0.4 mol H_2O m^{-2} s^{-1}), that corresponds to the mean value of non-stressed grapevine in that area (Faralli M., personal communication). The appreciable difference in spatial distribution of the maps on July 25th is probably due to the different time at which the two areas were sampled: the first 6 rows were mapped between 12:00 and 13:00 and the others were mapped starting from 14:00. As pointed out in the result section, CWSI usually reached its maximum around 14:00, so the values measured in the second part of the day could have been affected by the increase in air temperature and net radiation. The maps of August 9th presented the opposite spatial trend compared to the other days, with the northern area of the vineyard more stressed than the southern part. In this day values of CWSI were high everywhere, and this is confirmed by both maps.

To sum up, the spatial differences between the northern and southern area of the vineyard were highlighted by both the instruments for all the monitoring days. This could be a result of the length of the campaign: in fact, during a 1 hour-long campaign, a consistent variation of leaf temperature, air temperature and air relative humidity (and as a consequence of CWSI) can not be totally excluded.

The temporal variability of meteorological variables could be reduced with a faster data collection by

means of Unmanned Aerial Vehicles (UAV), that can be equipped with thermal sensors to obtain the temperature of the target object and are therefore a viable tool to monitor large field areas in a short amount of time. They have the potential to be part of an IoT network, and can give a significant contribution for the development of solutions for irrigation management (Ahansal et al., 2022). Moreover in the guyot pruning system, shoots grow mainly in the vertical direction, having only a small fraction of canopy visible from above. For this reason, the use of UAV could be more suitable for training systems with a canopy more developed in the horizontal plane (i.e. "Pergola" training system), being more easily scanned from above.

Agricultural vehicles, if equipped with thermal cameras or an array of infrared temperature sensors, can be another alternative to ground surveys, that can be time consuming especially for large vineyards (Meron et al., 2010; Zhou et al., 2022). Another viable and non-invasive alternative could be the use of remote sensing technology, which is rapidly increasing nowadays and it is often used in precision agriculture applications. The remote sensing method has the advantage of detecting the spatial variability of the vineyard water status without the need to install an elevated number of on-site sensors in the field. Furthermore, it is applicable at larger scale, and can be implemented both in mountain areas and extensively cultivated plains (Matese et al., 2018). A comparison between CWSI and soil maps could lead to more useful results in terms of irrigation needs. Different stress level areas could also reflect different soil characteristics. The soils ability to retain water is strongly related to soil particle size: sandy soils, with coarser particles, present low water retention capacity whereas deep soils of fine texture can retain higher amounts of water that can be available for plant root uptake (Saxton and Rawls, 2006). However soil maps are not always available and soil monitoring is expensive and time consuming both in terms of physicochemical characteristics and water content.

Maps provide valuable visual information about the state of the vineyard and can be of great help for farmers in the assessment of the crop water status and management of the water resource. The spatial interpolation allows to identify areas with different water stress characteristics, that could then be handled in different ways in terms of irrigation management, applying different amounts of water (Meron et al., 2010). Following the approach proposed in this study, CWSI maps could be obtained to give practical support for irrigation management, therefore saving water and increasing water use efficiency.

5. CONCLUSIONS

In a period of climate change, characterized by extreme events, prolonged drought periods are posing serious problems to the management of crops. Therefore, precision agriculture can provide the tools to optimize the use of water with the aim to increase water use efficiency. In this study, a new approach for the calculation of the Crop Water Stress Index was tested, based on the empirical formulation of the index proposed by Idso et al. (1981) and Jackson et al. (1981). Overall, the applied approach gave quite good results allowing the creation of maps by which it was possible to differentiate among areas within the vineyard presenting different levels of stress and therefore being of great help in the management of irrigation. Some technical aspects need to be improved in order to increase the accuracy in the calculation of the index: the maximum leaf temperature resulted to be slightly underestimated. Therefore, the use of a BlackGlobe sensor mimicking a non-transpiring leaf could help in the correct quantification of the radiation absorbed by a leaf at changing solar zenith angles. The IR sensors used in the measurement of the leaf temperature tended to overestimate its value: a contact thermocouple integrated into the CWSI slave station could give more reliable results. Finally, the master station should be positioned inside the vineyard in order to better represent the canopy microclimate which can be slightly different from the outside. IoT connectivity played a primary role in the present work: thanks to it, every leaf measurement performed with the IRMLX could be associated with the corresponding values of T_{dry} and T_{wet}, and the CWSI was automatically calculated. In conclusion, the present study confirmed the validity of the approach, and highlighted some weaknesses that can be solved in order to improve the estimation of the CWSI.

REFERENCES

Adams R., Hurd B., Lenhart S., Leary N., 1998. Effects of global climate change on world agriculture: an interpretive review. Climate Research 11: 19–30.

Ahansal Y., Bouziani M., Yaagoubi R., Sebari I., Sebari K., Kenny L., 2022. Towards Smart Irrigation: A Literature Review on the Use of Geospatial Technologies and Machine Learning in the Management of Water Resources in Arboriculture. Agronomy 12 (2): 297.

Apolo-Apolo O., Martínez-Guanter J., Pérez-Ruiz M., Egea G., 2020. Design and assessment of new artificial reference surfaces for real time monitoring of

crop water stress index in maize. Agricultural Water Management 240: 106304.

Bellvert J., Zarco-Tejada P.J., Girona J., Fereres E., 2014. Mapping crop water stress index in a 'Pinot-noir' vineyard: comparing ground measurements with thermal remote sensing imagery from an unmanned aerial vehicle. Precision Agriculture 15 (4): 361–376.

Buckley T.N., 2019. How do stomata respond to water status? New Phytologist 224 (1): 21–36. Bwambale E., Abagale F.K., Anornu G.K., 2022. Smart irrigation monitoring and control strategies for improving water use efficiency in precision agriculture: A review. Agricultural Water Management 260: 107324.

Caffarra A. and Eccel E., 2011. Projecting the impacts of climate change on the phenology of grapevine in a mountain area: Effects of climate change on grape phenology. Australian Journal of Grape and Wine Research 17 (1): 52–61.

Change C.C. and Services A.M., 2024. Global Climate Highlights Report 2023. English.

Chaves M., Costa J., Zarrouk O., Pinheiro C., Lopes C., Pereira J., 2016. Controlling stomatal aperture in semi-arid regions—The dilemma of saving water or being cool? Plant Science 251: 54–64.

Deloire A., Pellegrino A., Rogiers S., 2020. A few words on grapevine leaf water potential. IVES Technical Reviews, vine and wine.

Esposito M., Palma L., Belli A., Sabbatini L., Pierleoni P., 2022. Recent Advances in Internet of Things Solutions for Early Warning Systems: A Review. Sensors 22 (6): 2124.

Fuentes-Peñailillo F., Ortega-Farías S., Acevedo-Opazo C., Rivera M., Araya-Alman M., 2024. A Smart Crop Water Stress Index-Based IoT Solution for Precision Irrigation of Wine Grape. Sensors 24 (1).

Halbritter A.H., De Boeck H.J., Eycott A.E., Reinsch S., Robinson D.A., Vicca S., Berauer B., Christiansen C.T., Estiarte M., Grünzweig J.M., Gya R., Hansen K., Jentsch A., Lee H., Linder S., Marshall J., Pen˜ uelas J., Kappel Schmidt I., Stuart-Hae¨ntjens E., Wilfahrt P., the ClimMani Working Group, Vandvik V., 2020. The handbook for standardized field and laboratory measurements in terrestrial climate change experiments and observational studies (ClimEx). Methods in Ecology and Evolution 11 (1). Ed. by Freckleton R.: 22–37.

Idso, 1982. Non-water-stressed baselines: A key to measuring and interpreting plant water stress. Agricultural Meteorology 27 (1-2): 59–70.

Idso, Jackson R., Pinter P., Reginato R., Hatfield J., 1981. Normalizing the stress-degree-day parameter for environmental variability. Agricultural Meteorology 24: 45–55.

Intergovernmental Panel On Climate Change (IPCC), 2023. Climate Change 2022 – Impacts, Adaptation and Vulnerability: Working Group II Contribution to the Sixth Assessment Report of the Intergovernmental Panel on Climate Change. 1st ed. Cambridge University Press.

Jackson R.D., Idso, Reginato R.J., Pinter P.J., 1981. Canopy temperature as a crop water stress indicator. Water Resources Research 17 (4): 1133–1138.

Jayalakshmy M.S. and Philip J., 2010. Thermophysical Properties of Plant Leaves and Their Influence on the Environment Temperature. International Journal of Thermophysics 31 (11-12): 2295–2304.

Jones H.G., 1999. Use of infrared thermometry for estimation of stomatal conductance as a possible aid to irrigation scheduling. Agricultural and Forest Meteorology 95 (3): 139–149.

Jones H.G., Hutchinson P.A., May T., Jamali H., Deery D.M., 2018. A practical method using a network of fixed infrared sensors for estimating crop canopy conductance and evaporation rate. Biosystems Engineering 165: 59–69.

Karaka C., Tekelioglu B., Buyuktas D., Bastug R., 2018. Relations between Crop Water Stress Index and stomatal conductance of soybean depending on cultivars. Fresenius Environmental Bulletin 27. Edition: 27 Section: 6: 4212–4219.

Katimbo A., Rudnick D.R., DeJonge K.C., Lo T.H., Qiao X., Franz T.E., Nakabuye H.N., Duan J., 2022. Crop water stress index computation approaches and their sensitivity to soil water dynamics. Agricultural Water Management 266: 107575.

Kim Y., Still C.J., Roberts D.A., Goulden M.L., 2018. Thermal infrared imaging of conifer leaf temperatures: Comparison to thermocouple measurements and assessment of environmental influences. Agricultural and Forest Meteorology 248: 361–371.

King B.A., Shellie K.C., 2023. A crop water stress index based internet of things decision support system for precision irrigation of wine grape. Smart Agricultural Technology 4: 100202. Lawrence M.G., 2005. The Relationship between Relative Humidity and the Dewpoint Temperature in Moist Air: A Simple Conversion and Applications. Bulletin of the American Meteorological Society 86 (2): 225–234.

Leinonen I., Jones H.G., 2004. Combining thermal and visible imagery for estimating canopy temperature and identifying plant stress. Journal of Experimental Botany 55 (401): 1423–1431.

Maes W.H., Baert A., Huete A.R., Minchin P.E., Snelgar W.P., Steppe K., 2016. A new wet reference target method for continuous infrared thermography

of vegetations. Agricultural and Forest Meteorology 226-227: 119–131.

Mahan J.R., Conaty W., Neilsen J., Payton P., Cox S.B., 2010. Field performance in agricultural settings of a wireless temperature monitoring system based on a low-cost infrared sensor. Computers and Electronics in Agriculture 71 (2): 176–181.

Martínez J., Egea G., Agüera J., Pérez-Ruiz M., 2017. A cost-effective canopy temperature measurement system for precision agriculture: a case study on sugar beet. Precision Agriculture 18 (1): 95–110.

Matese A., Baraldi R., Berton A., Cesaraccio C., Di Gennaro S.F., Duce P., Facini O., Mameli M.G., Piga A., Zaldei A., 2018. Estimation of Water Stress in Grapevines Using Proximal and Remote Sensing Methods. Remote Sensing 10 (1): 159–167.

Matese A., Crisci A., Di Gennaro S.F., Primicerio J., Tomasi D., Marcuzzo P., Guidoni S., 2014. Spatial variability of meteorological conditions at different scales in viticulture. Agricultural and Forest Meteorology 189-190: 159–167.

Mathur S., Agrawal D., Jajoo A., 2014. Photosynthesis: Response to high temperature stress. Journal of Photochemistry and Photobiology B: Biology 137: 116–126.

Meron M., Tsipris J., Orlov V., Alchanatis V., Cohen Y., 2010. Crop water stress mapping for site- specific irrigation by thermal imagery and artificial reference surfaces. Precision Agriculture 11 (2): 148–162.

Nair S., Johnson J., Wang C., 2013. Efficiency of Irrigation Water Use: A Review from the Perspectives of Multiple Disciplines. Agronomy Journal 105 (2): 351–363.

Nanda M.K., Giri U., Bera N., 2018. Canopy Temperature-Based Water Stress Indices: Potential and Limitations. In: *Advances in Crop Environment Interaction*. Ed. by Bal S.K., Mukherjee J., Choudhury B.U., Dhawan A.K. Singapore: Springer Singapore, 365–385.

Ouerghi F., Ben-Hammouda M., Teixeira Da Silva J., Albouchi A., Bouzaien G., Aloui S., Cheikh-M'Hamed H., Nasraoui B., 2014. The effects of vapor gard on some physiological traits of durum wheat and barley leaves under water stress. Agriculturae Conspectus Scientificus 79 (4): 261–267.

Pallas J.E., Michel B.E., Harris D.G., 1967. Photosynthesis, Transpiration, Leaf Temperature, and Stomatal Activity of Cotton Plants under Varying Water Potentials. Plant Physiology 42 (1): 76–88.

Peña Quiñones A.J., Hoogenboom G., Salazar Gutiérrez M.R., Stöckle C., Keller M., 2020. Comparison of air temperature measured in a vineyard canopy and at a standard weather station. PLOS ONE 15 (6). Ed. by Huang M.: e0234436.

Poblete-Echeverría C., Espinace D., Sepúlveda-Reyes D., Zúñiga M., Sanchez M., 2017. Analysis of crop water stress index (CWSI) for estimating stem water potential in grapevines: comparison between natural reference and baseline approaches. Acta Horticulturae (1150): 189–194.

Poirier-Pocovi M., Bailey B.N., 2020. Sensitivity analysis of four crop water stress indices to ambient environmental conditions and stomatal conductance. Scientia Horticulturae 259: 108825.

Ru C., Hu X., Wang W., Ran H., Song T., Guo Y., 2020. Evaluation of the Crop Water Stress Index as an Indicator for the Diagnosis of Grapevine Water Deficiency in Greenhouses. Horticulturae 6 (4): 86.

Saxton K.E., Rawls W.J., 2006. Soil Water Characteristic Estimates by Texture and Organic Matter for Hydrologic Solutions. Soil Science Society of America Journal 70 (5): 1569–1578.

Stull R., 2011. Wet-Bulb Temperature from Relative Humidity and Air Temperature. Journal of Applied Meteorology and Climatology 50 (11): 2267–2269.

Tarnopolsky M., Seginer I., 1999. Leaf temperature error from heat conduction along thermo- couple wires. Agricultural and Forest Meteorology 93 (3): 185–194.

Venios X., Korkas E., Nisiotou A., Banilas G., 2020. Grapevine Responses to Heat Stress and Global Warming. Plants 9 (12): 1754.

Wu J., Wang J., Hui W., Zhao F., Wang P., Su C., Gong W., 2022. Physiology of Plant Responses to Water Stress and Related Genes: A Review. Forests 13 (2): 324.

Yu, Ding G.-D., Gao G.-L., Zhao Y.-Y., Yan L., Sai K., 2015. Using Plant Temperature to Evaluate the Response of Stomatal Conductance to Soil Moisture Deficit. Forests 6 (12): 3748–3762.

Yu L., Wang W., Xin Z., Zheng W., 2016. A Review on Leaf Temperature Sensor: Measurement Methods and Application. In: vol. 478.

Zhao W., Liu L., Shen Q., Yang J., Han X., Tian F., Wu J., 2020. Effects of Water Stress on Photosynthesis, Yield, and Water Use Efficiency in Winter Wheat. Water 12 (8): 2127.

Zhou Z., Diverres G., Kang C., Thapa S., Karkee M., Zhang Q., Keller M., 2022. Ground-Based Thermal Imaging for Assessing Crop Water Status in Grapevines over a Growing Season. Agronomy 12 (2): 322.

Italian Journal of Agrometeorology
Rivista Italiana di Agrometeorologia

Firenze University Press
https://riviste.fupress.net/index.php/IJAm

OPEN ACCESS

Citation: Mahdi, Z.S., Abu-AL Shaeer, M.J., & Al-Jiboori, M.H. (2024). Quantitative relationships among potential evapotranspiration, surface water, and vegetation in an urban area (Baghdad). *Italian Journal of Agrometeorology* (2): 81-88. doi: 10.36253/ijam-2557

Received: March 6, 2024

Accepted: October 16, 2024

Published: December 30, 2024

© 2024 Author(s). This is an open access, peer-reviewed article published by Firenze University Press (https://www.fupress.com) and distributed, except where otherwise noted, under the terms of the CC BY 4.0 License for content and CC0 1.0 Universal for metadata.

Data Availability Statement: All relevant data are within the paper and its Supporting Information files.

Competing Interests: The Author(s) declare(s) no conflict of interest.

ORCID:
MJA-AS: 0000-0003-3178-9625
MHA-J: 0000-0002-0816-3918

Quantitative relationships among potential evapotranspiration, surface water, and vegetation in an urban area (Baghdad)

Zahraa S. Mahdi[1], Mahmood J. Abu-AL Shaeer[2], Monim H. Al-Jiboori[1,*]

[1] *Atmospheric Sciences Department, College of Science, Mustansiriyah University, Baghdad, Iraq*
[2] *Al Rafidain University College, Baghdad, Iraq*
*Corresponding author. E-mail: mhaljiboori@gmail.com

Abstract. Potential evapotranspiration (PET) is the amount of water that evaporates from land, surface water and plant transpiration. Based on monthly surface water and vegetation cover areas derived from Sentinel-2 imagery and precipitation records from Baghdad station for the two years 2018 and 2019, the quantitative relationships such as PET versus water area, PET versus vegetation area and PET versus precipitation were investigated. Using Origin 9.2 program, a new multiple regression model was derived to estimate the monthly mean PET in dry and wet months. To improve the accuracy of the model, monthly errors, bias and mean absolute error were calculated to approximate reasonable estimates of PET. Based on this statistical analysis, the best value of about -1 mm/day should be added to the proposed model as a correction term.

Keywords: surface water, vegetation, potential evapotranspiration, statistical analysis, Baghdad.

1. INTRODUCTION

Surface water bodies and vegetation cover in urban areas have mostly suffered significant impacts in recent decades (Singh and Biswas, 2022) due to the effects of the continuous changes in urbanization expansion and climate conditions (Guo, Westra and Maier, 2017; Zhang et al., 2022). These natural resources are the main drivers in the study of potential evapotranspiration (PET) (Zhao and Ma, 2021), which is an important process in the hydrological cycle especially for non-limited water availability, and can be considered as one of the direct indicators of climate change in a given area (Li et al., 2022). PET represents the potential maximum amount of water that would be released from the Earth's surface into the atmosphere by the combined processes of evaporation and transpiration, if sufficient water were available. It is an input for various applications in hydrological models, so its estimation plays a key role in agricultural irrigation, dry-wet condition assessment, weather variability, water management and climate-related hazard assessment (Kirkham, 2014).

Baghdad, the capital of Iraq, has been notably suffered from the influence of global climate change and increased water demand (Jaber, Al-Saadi and Al-Jiboori, 2020) and has therefore received increased attention from many scientists and the country's central government. PET averages are generally influenced by meteorological conditions and the surrounding near-surface environment. Therefore, it can vary simultaneously with surface changes (Wang and Zheng, 2022).

To date, many studies have been conducted to investigate the spatial and temporal analysis of PET in watersheds (Zhang and Wang, 2021; Yan et al., 2017). In recent years, the trend directions of PET have also been investigated by some researchers in Iraq, such as Al-Hasani and Shahid (2022), who examined the spatial distribution of the trend of annual and seasonal scales using the modified classical Mann-Kendall test for the period 1981-2021. They found that PET has a significantly increasing trend over most of Iraq, especially in summer with an average of 0.5 mm/decade. In this paper, it is reasonable to hypothesize that PET could be affected by changes in the quantitative evolution of vegetation cover, surface water and precipitation, which still have less knowledge about the connection with the PET.

The relationship between PET and vegetation has also been established, for example in a large spatial banana plantation in Venezuela (Olivares et al., 2021). The relationship between precipitation and PET has been used to verify the possible climate type (dry or wet) and was found to vary greatly between seasons (Stefanidis and Alexandridis, 2021). Unfortunately, most empirical methods for estimating PET depend on several meteorological factors: air temperature, solar radiation, relative humidity, sunshine duration, and wind speed. These methods have shown that the weight of these variables on the estimation of PET varies between regions and spatial and temporal scales. However, it is known that vegetation, soil water content, and precipitation are directly correlated with PET as the primary causes of combined evaporation and transpiration. The main research gap is a lack of knowledge about linkage between ground-based PET estimates with cumulative precipitation, vegetation cover area and surface water area, which are jointly derived from remote sensing technologies in this paper. Therefore, the overall objective of this paper is to explore a multiple regression model formulated to estimate the mean PET in the Tigris River basin of Baghdad as a function of these variables at interannual scales in arid and semi-arid conditions. Prior to this relationship, the monthly relationships between PET estimates and influencing factors during the two years (2018 and 2021) characterized by different conditions were investigated. Finally, some statistical parameters such as bias and mean absolute error were tested to improve this model.

2. STUDY AREA AND DATA SOURCES

2.1. Briefly description of study area

This study was carried out in an urban area such as Baghdad (see Fig. 1), the capital of Iraq, which is a medium-density city and part of the Tigris River basin with several meanders, i.e. it is a low-lying and alluvial plain. It covers an area of 894.3 km^2, has an average elevation of 34 m above sea level and is located at 33° 21' N latitude and 44° 20' E longitude. Baghdad's climate is hot and dry in summer and cold in winter. The rainy season lasts from October to May, with an average annual rainfall of 140 mm. The vegetation cover often consists of palm orchards in the north, farms, parks, and domestic gardens. In addition to the Tigris, there are small permanent ponds on both sides of the river.

2.2.Briefly description of data

Monthly weather data for air temperature (Ta), solar radiation (SR), relative humidity (RH) and evaporation rates were obtained from the Baghdad meteorological station belonging to the Iraqi Meteorological Organization for two years 2018 and 2021. The reason for selecting these years was that they were characterized by completely different conditions, with 2018 being semi-arid and 2021 being severely arid (Abd Al Rukabie, Naif and Al-Jiboori, 2024). In addition, Sentinel-2 satellite images (downloaded from https://scihubcopernicus.eu) were used to identify urban surface water and vegetation by

Figure 1. Study area of the paper: left (Iraq) and right (Baghdad) in which green (vegetation), blue (water bodies) and other colours (housing districts and barren land).

calculating spectral indices for Modified Normalized Difference Water Index (MNDWI) and Normalized Difference Vegetation Index (NDVI). For more details, pre- and post-processing of the satellite images, such as clipping, compositing, merging bands and extraction of the study area, are explained through the two references Ahmed et al. (2024) and Mahdi, Tawfeek and Al-Jiboori (2024), respectively.

3. METHODOLOGY

3.1. PET estimation

To execute the objectives of this paper, the Turc method for two different ranges of relative humidity, wet: 50-100% and dry: 0-49%, was widely used to estimate PET because it is a simple and more accurate empirical equation to (Turc, 1961; Jensen, Burman and Allen, 1990). Furthermore, several studies have shown that the Turc equation is the most appropriate and has been consistently well implemented in many places around the world due to its justification for local climatic conditions (Trajkovic and Stojnic, 2007; Fisher and Pringle III, 2013; Santos et al., 2019). It is also the second best method after the Penman-Monteith method when compared to the other available methods. However, the Turc method depends on the mean Ta (in °C), SR (in $MJ.m^{-2}.day^{-1}$) and RH (in %) given by the following equation:

$$PET = 0.01333((239000 * RS) + 50)\left(\frac{Ta}{Ta+15}\right) \quad \text{for RH>50\%} \tag{1}$$

$$PET = 0.01333((239000 * RS) + 50)\left(\frac{Ta}{Ta+15}\right)\left(1 + \left(\frac{50-RH}{70}\right)\right) \quad \text{for RH<50\%} \tag{2}$$

3.2. Spectral indices of surface water and vegetation

Modified Normalized Difference Water Index (MNDWI) is a power method used to classify the urban scenes into two categories consisted of water and non-water objects given as (Chen et al., 2020)

$$MNDWI = \frac{\text{Green (Band 3)} - \text{SWIR (Band11)}}{\text{Green (Band 3)} + \text{SWIR (Band 11)}} \tag{3}$$

While the NDVI is defined as the ratio of the spectral difference between the red and near infrared (NIR) bands divided by their sum, as given by (Bannari et al., 1995):

$$NDVI = \frac{\text{NIR(band 8)} - \text{Red (band 4)}}{\text{NIR(band 8)} + \text{Red (band 4)}} \tag{4}$$

Both MNDWI and NDVI have values ranging from -1 to +1, with higher values corresponding to increased water bodies and vegetation (Abdullah et al., 2019), respectively. In this study after extracting digital images of MNDWI and NDVI, all pixels were classified into only two groups for each index separately. Pixesl with MDWI greater than 0.5 where considered surface water areas and, similarly, pixels with NDVI greater than 0.2 were considered as vegetated areas. Therefore, surface water and vegetation areas in km^2 were extracted using the r.report function in the toolbox of the QGIS program.

3.3. Statistical analysis

It is conventional to test our empirical relationship with statistical analysis. First, scatter plots were used to show the variation between PET, surface water, vegetation, precipitation and evaporation. Once the nature of the relationship was established, R^2 (or goodness of fit) was calculated, which is a statistical measure of how well the regression line approximates the real data if it follows the regression equation. Meanwhile, the Pearson correlation coefficient (r) with a range of -1 to 1 and the p-value were calculated by Student t-test to assess the level of significance at 0.95. The standard deviation (SD), represented by vertical lines and defined as a measure of the dispersion of a dataset relative to its mean, was also calculated. Overall accuracy measures the quality of the prediction by comparing the actual values with the predicted values. Other measures of accuracy were chosen, such as bias and mean absolute error (MAE). Bias refers to deviations that are not due to chance alone and MAE is a measure of how close a fitted line to the data points, which is a common measure of prediction error in time series analysis. However, they were calculated as (Al-Jiboori et al., 2020):

$$Bias = \frac{1}{n} * \sum_{i=1}^{n}(\varepsilon_i) \tag{5}$$

$$MAE = \frac{1}{n} * \sum_{i=1}^{n} |\varepsilon_i|^2 \tag{6}$$

where ε is the error due to the difference between observed and estimated values and n the total number.

4. RESULTS

4.1. Inter-annual variations of PET estimations, MNDWI and NDVI areas

Table 1 shows monthly variation of PET in the two years: 2018 and 2021 characterized with semiarid and dry conditions, respectively. Also, quantitative areas for both surface water and vegetation represented by the calculation of spectral indices for both MNDWI and NDVI respectively were displayed in this table. In addition, in order to see the annual differences in these variables between the two years, the annual means with their SD were calculated, as shown in the last row of Table 1. During the two years, the highest values of PET are found in the summer months and the lowest values in the winter months. Under arid conditions, PET has high values in the months of 2021 compared to the semi-arid year of 2018.

In general, the surface water areas in 2018 are relatively larger than those in 2021, especially in the six months (i.e., February, March, April, May, June and November). While in summer (i.e., July, August and September) the areas are about the same with an average value of 18 km^2. The only exception is January and December, where more water areas were recorded, especially in January. This distribution of water areas was mostly reflected in the growth of vegetation in Baghdad, where the total area of pixels for vegetation (NDVI) in months: January, March, April, June, October and December of 2018 were larger than those of 2021. The remaining months have almost the same NDVI areas, especially in May.

Table 1. Monthly values for PET, surface water area, and vegetation area in two years 2018 and 2021.

Months	PET (mm/day)		MNDWI area (km^2)		NDVI area (km^2)	
	2018	2021	2018	2021	2018	2021
Jan.	1.9	1.7	37	77.2	120.1	115.7
Feb.	3.2	2.2	36.9	35.4	107	118
Mar.	4.2	3.5	29	24	187.7	84.9
Apr.	4.3	5.6	28.5	22.8	201.7	150.4
May	6.3	8	29.6	19.5	197.8	197.8
June	8.8	8.9	28.5	18.7	163.5	119.3
July	8.3	8.7	18.7	20	120.1	124.8
Aug.	7.5	8.3	20	21	162.8	124.3
Sep.	6.2	6.6	18.7	21.8	122.9	139.4
Oct.	3.3	4.5	21.3	23.1	172.8	129.2
Nov.	2	2	40.7	32.1	147.4	154.8
Dec.	1.6	1.5	39.9	47.1	291.8	138.8
Aver.±SD	4.8±2.6	5.1±2.9	29.1±8.2	30.2±17	166.3± 50.9	133.1± 27.4

4.2. Relationship among PET, MNDWI, and NDVI, precipitation

To explore the nature of the relationship, the PET estimates were plotted separately against MNDWI and NDVI, and the best line fit was derived using Origin 9.2. Before that, we explored the relationship between two related parameters, monthly PET estimates with evaporation rates (Fig. 2a) and with surface water area measurements (Fig. 2b). They are represented by different symbols, with green and red dots representing semi-arid (2018) and arid (2021) conditions, respectively, as shown in the panel of the figures below. Monthly means of PET cannot exceed free water evaporation under the same weather conditions.

There is no significant difference between the two years and they have almost the same behaviour, except for a slightly higher value occurred in 2018 due to the high rainfall received in 2018 (284.2 mm). This was also explained through the annual means of PET and SD reported in Table 1, which are almost similar to values of 4.8±2.6 and 5.1±2.9 mm/day in 2018 and 2021, respectively. However, the monthly PET values and evaporation rates were very well correlated and found to have a positive relation with r=0.95 and p<0.00001. The fitted curve has been passed through the data points, which obey the exponential polynomial function with an excellent correlation (R^2=0.95).

$$PET = EXP(0.23 + 0.0071 * \text{evaporation rate} - 6.6 * 10^{-6}) \quad (7)$$

Fig. 2b shows the relationship between PET and surface water area (Aw) derived from MNDWI, where the highest PET values were concentrated around small water areas found during the non-wet months (May to October), while the lowest PET values were found in large surface water areas. Despite this decreasing behaviour, these two variables were negatively well correlated (r=-0.68) and p<0.00001. The decreasing exponential function could fit these data points with an R^2=0.7, given as

$$PET = 1.02 + 28.1 * EXP(-Aw/13.2) \quad (8)$$

where Aw is the surface water area. Ahemd et al. (2024) have recently investigated the relationship between PET and vegetation area (Av) represented by NDVI for the same Sentinel-2 images, time period, and study area. They were linearly correlated and expressed by the regression model with a R^2=0.72.

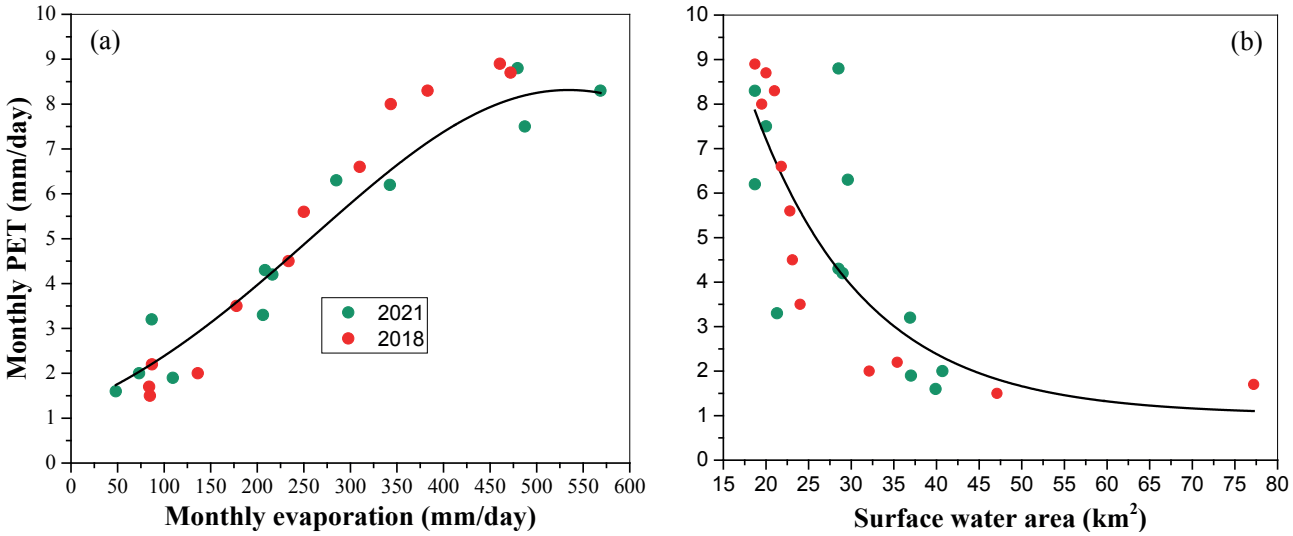

Figure 2. Monthly variations between (a) PET and evaporation, and (b) PET and surface water area.

$$PET = 1.8 + 0.03 * Av \quad (9)$$

where Av is the vegetation cover area. Al Rukabie, Salwa and Al-Jiboori (2024) have studied the impact of monthly precipitation (P) on PET for the same site, data and period and found an empirical relation describing its behavior (R^2=0.69) given below

$$PET = 2.9 + 1.5 * (EXP(-76.2 * P)) \quad (10)$$

From the above discussions, an integrated multiple regression model for PET in arid and semi-arid regions can be derived as follows:

$$PET \propto F(Aw,Av,P)$$
$$PET = \beta + F(Aw,Av,P) \mp \varepsilon \quad (11)$$

where b is a general empirical constant based on the above independent variables. As there are no directly measured observations for PET, the PET values in this paper were considered more reliable when testing this model, as shown in the next section. To obtain the mean PET predictions resulting from the ecological parameters studied in this paper, we substitute Eqs. (8), (9) and (10) in Eq. (5) with summation constants in the first terms.

$$\overline{PET} = \frac{1}{3} * [5.72 + 28.1 * EXP(-Aw/13.2) + 0.03 * Av + 1.5 * EXP(-76.2*P)] \quad (12)$$

When P approaches zero as in dry months as shown in Fig. 2, Eq. 6 becomes

$$\overline{PET} = \frac{1}{2} * (7.22 + 28.1 * EXP(-Aw / 13.2) + 0.03 * Av) \quad (13)$$

The three-dimensional graph in Fig. 3 shows the combined effect of monthly water and vegetation on PET due to free precipitation. In general, PET values were higher in 2018 due to water availability than in the dry year 2021. The highest PET values were associated with small water areas (~18 km^2) and large vegetation areas. Meanwhile, the lowest PET values were found in large water areas and low vegetation areas.

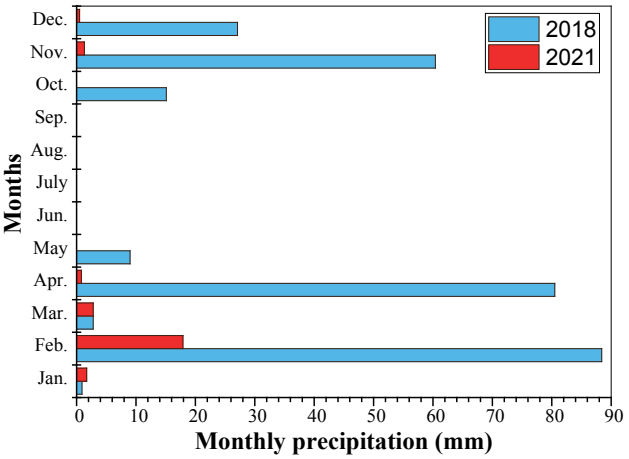

Figure 3. Monthly variation of cumulative precipitation during two years (2018 and 2021) observed at meteorological Baghdad station.

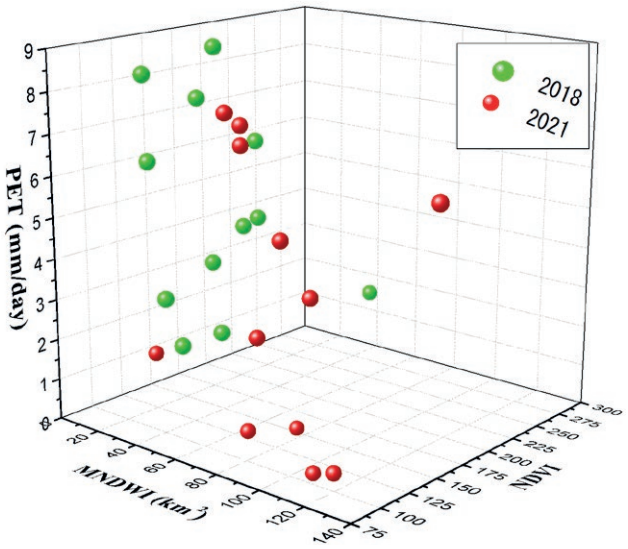

Figure 4. Monthly variations of PET with surface water and vegetation areas during 2018 and 2021.

4. DISCUSSION

This study is not the only attempt to estimate PET using remote sensing measurements, which is an alternative approach to estimating PET, but there have been several studies describing the spatial distribution of PET over a given region at different time scales (Rossato et al., 2005; Olivares et al., 2021; Gebremedhin et al., 2022). Rossato et al. (2005) in Brazil found a linear correlation between monthly PET and NDVI over the period 1981-2000. Olivares et al. (2021) also studied the Spearman coupling of NDVI with PET in a banana plantation in Venezuela under drought conditions and found that the influence of PET on NDVI was more evident with a lag of 1 month.

This paper could present a comprehensive analysis to estimate the monthly PET by using a multi-regression model of Eq. (12) or (13) including more possible factors related to the PET. The proposed model will of course improve the results of PET estimation as it depends on several factors rather than one variable, e.g., vegetation, surface water or precipitation. Also, this model can enhance the policy makers to set the relevant plans to monitor monthly or seasonal changes, especially in semi-arid environments that are characterized by low precipitation, high evaporation rates that exceed precipitation, and wide temperature ranges both daily and seasonally.

The monthly correlation analysis between PET and its factors (surface water, vegetation cover and precipitation) has a different shape depending on the prevailing climate type in a given year. For the dry year (2021), PET showed the high values especially in the summer months due to the permanent water available in the Tigris River and other water ponds, as reported by Mahdi et al. (2024), and the high amounts of solar radiation received by the surface, which primarily provides heat (or energy) for evaporation. The proposed multiple regression models (Eq. 8 and Eq. 9) reflect the combined effect of the above variables on PET estimates. It should be noted that wind speed can play a relative role in exceeding PET values (Zhang and Wang, 2021), but it is not included in this paper because the urban environments are characterized by low wind due to the high surface roughness, while it was found to be 1.2 m as reported in Haraj and Al-Jiboori (2021).

Eqs. (8) and (9) were multiplied by factors of 1/3 and ½, respectively, depending on the number of terms contributing to PET in the atmosphere. For further discussion, we divided the months of both years into two groups: wet months (14 in total) with precipitation activity (from October to May), and dry months that never have precipitation (June-September), with no rain even in two months (May and October) of 2021, as shown in Fig. 2.

Now we turn to discuss the statistical parameters such as bias or error with standard deviation, mean square deviation and root mean square deviation. Using the results of MNDWI, NDVI and precipitation presented in the previous section, the predictions of mean PET were obtained from Eqs. (8) and (9) for wet and dry months respectively. In order to improve the performance of these equations, the monthly errors between the PET values obtained from Eqs. (8) and (9) and their predictions were averaged to find the bias (using Eq. (1)) with standard deviation for both wet and dry periods. The negative bias values were 1.04 mm/day with SD=±1.3 mm/day in dry period and 1.16 mm/day with SD=±1.2 mm/day in wet period. With these results, the bias in dry months was slightly less than that in wet months. These negative values should be subtracted from the mean monthly predictions obtained by Eqs. (8) and (9) to obtain better results. To check the accuracy of these predictions, the results of the monthly MAE were also obtained from Eq. (2) for the same period, which were found to be 1.3 mm/day with SD=1.2 mm/day and 1.4 mm/day with SD=0.9 mm/day, respectively. This means that the accuracy of equation (9) has less predictable error compared to that of equation (8). This small difference between the outputs of these equations reflects the weak role of precipitation in enhancing evaporation and transpiration in arid urban environments, where high rainfall variability is a significant feature.

5. CONCLUSION

This study used monthly digital areas for both MNDWI and NDVI derived from the Sentinel-2 products reported in Mahdi et al. (2024) and Ahmed et al. (2024), respectively, for the same study area (Baghdad) and time period (2018 and 2021) associated with completely different wet and dry conditions. In addition to the monthly cumulative evaporation and precipitation rates, the monthly PET estimates calculated by the Truc method using the ground-based data for solar radiation, temperature and relative humidity were combined with the above areas to establish empirical relationships. PET estimates were closely related to evaporation with an exponential polynomial function and to MNDWI areas with a decreasing exponential function. The results showed that PET values were linearly correlated with vegetation and non-linearly correlated with evaporation, precipitation and surface water. This study could also derive a general relationship for estimating mean PET including all the above variables together. Understanding this relationship would allow for better planning of natural resources, suggesting relevant and applicable adaptation strategies to avoid adverse environmental impacts in the future.

ACKNOWLEDGEMENTS

The authors are grateful to Mustansiriyah University for acceptance this work. Finally, the authors thank anonymous reviewers especially Editor-in-Chief for constructive comments for improvement of the paper.

REFERENCES

Abd Al Rukabie J.S.A., Naif S.S. and Al-Jiboori M.H. (2024). Quantitative impact of monthly precipitation on urban vegetation, surface water and potential evapotranspiration in Baghdad under wet and dry conditions. *Nature Environment and Production Technologies, 23(4)*, 2383-2389. https://doi.org/10.46488/NEPT.2024.v23i04.041

Ahmed M.H., Mahdi Z.S., Al-Jiboori M.H. and Mahmood D.A. (2024). Interannual variations of monthly normalized difference vegetation index and potential evapotranspiration and their Relations in Baghdad. *Open agriculture*, 9. https://doi.org/10.1515/opag-2022-0386

Al-Hasani A.A.J. and Shahid S. (2022). Spatial distribution of the trends in potential evapotranspiration and its influencing climatic factors in Iraq. *Theoretical and Applied Climatology*. https://doi.org10.1007/s00704-022-04184-4

Al-Jiboori MH., Abu Al-Shaeer M.J. and Hassan A.S. (2020). Statistical forecast of daily maximum air temperature in arid areas in the summertime. *J. Mat. Fund. Sci., 52*(3), 353-365. https://doi.org10.5614/j.math.fund.sci.2020.52.3.8

Chen F., Chen X., Van de Voorde T., Roberts D., Jiang H. and Xu W. (2020). Open water detection in urban environments using high spatial resolution remote sensing imagery. *Remote Sensing of Environment, 242*. https://doi.org10.1016/j.rse.2020.111706

Fisher D.K. and Pringle III H.C. (2013). Evaluation of alternative methods for estimating reference evapotranspiration. *Agricultural Sciences, 4*(8A), pp. 51-60. https://doi.org10.4236/as.2013.48A008

Gebremedhin M. A., Lubczynski M.W., Maathuis B.H.P. and Teka D. (2022). Derving potential evapotranspiration from satellite-based reference evpotranspiration, Upper Tekeze Basin. *Journal of Hydrology: Regional Studies, 41*. https://doi.org10.1016/j.ejrh.2022.101059

Guo D., Westra S. and Maier H.R. (2017). ensitivity of potential evapotranspiration to changes in climate variables for different Australian climatic zones. *Hydrology and Earth System Sciences, 21*(4), 2107–2126. https://doi.org10.5194/hess-21-2107-2017

Haraj S.A. and Al-Jiboori M.H. (2021). Study of aerodynamic surface roughness for Baghdad City using signal-level measurements. *Baghdad Science Journal, 16*(1 supplement), 215-220. https://doi.org10.21123/bsj.2019.16.1(Suppl.).0215

Jaber, S.H., Al-Saadi, L.M. and Al-Jiboori, M.H. (2020). Spatial vegetation growth and its relation to seasonal temperature and precipitation in Baghdad. *International Journal of Agricultural and Statistical Sciences, 16*(Supplement 1). https://connectjournals.com/03899.2020.16.2021

Kirkham M.B. (2014). *Principles of Soil and Plant Water Relations: Ch. 28, Potential Evapotranspiration* (2nd ed.). Academic Press. https://doi.org10.1016/C2013-0-12871-1

Li Y., Qin Y. and Rong P. (2022). Evolution of potential evapotranspiration and its sensitivity to climate change based on the Thornthwaite, Hargreaves, and Penman–Monteith equation in environmental sensitive areas of China. *Atmospheric Research, 273*. https://doi.org10.1016/j.atmosres.2022.106178

Mahdi Z.S., Tawfeek Y.Q. and Al-Jiboori M.H. (2024). Monthly urban surface water assessment at Baghdad and their environmental effects. *Water practure and Technology*. https://doi.org10.2166/wpt.2024.098

Olivares B.O., Paredes F., Rey J.C., Lobo D. and Galvis-Causil S. (2021). The relationship between the normaized difference vegetation index, rainfall, and potential evapotranspiration in a banana plantation of Venezuela. *Sanis Tanah-Journal of Soil Sciemce and Agroclimatology, 18*(1), 58-64. https://doi.org10.20961/stjssa.v18i1.50379

Rossato L., Alvala R.C.S., Ferreira N.J. and Tomasella J. (2005). Evapotranspiration estimation in the Brazil using NDVI data. *Remote Sensing for Agriculture, Ecosystems, and Hydrology, 5976*. https://doi.org10.1117/12.626793

Santos L., Cruz G. H., Capuchinho F.F., José J.V. and dos Reis E.F. (2019). Assessment of empirical methods for estimation of reference evapotranspiration in the Brazilian. *Australian Journal of Crop Sciences, 13(7)*, pp. 1094-1104. https://doi.org10.21475/ajcs.19.13.07.p1569

Singh S. and Biswas R. (2022). Analysis of land use change effects/impacts on surface water resources in Delhi. *Urban Science, 6*(4). https://doi.org10.3390/urbansci6040092

Stefanidis S. and Alexandridis V. (2021). Precipitation and potential evapotranspiration temporal variability and their relationship in two forest ecosystems in Greece. *Hydrology, 8*(4). https://doi.org10.3390/hydrology8040160

Trajkovic S. and Stojnic V. (2007). Effect of wind speed on accuracy of Turc method in a humid climate. *Facta Universitatis series: Architecture and Civil Enggineering, 5*(2), 107-113.

Wang H. and Zheng J. (2022). Assessing the effects of surface conditions on potential evapotranspiration in a humid subtropical region of Chinal. *Frontiers in Climate, 4*. https://doi.org10.3389/fclim.2022.813787

Yan D., Xu T., Grima A., Yuan Z., Weng B., Qin T., Do P. and Yong Y. (2017). Regional correlation between precipitation and vegetation in the Huang-Huai-Hai River Basin, China. *Water, 9*. https://doi.org10.3390/w9080557

Zhang H. and Wang L. (2021). Analysis of the variation in potential evapotranspiration and surface wet conditions in the Hancang River Basin, China. *Scientific Reports, 11*. https://doi.org10.1038/s41598-021-88162-2

Zhang L., Yang L., Zohner C.M., Crowther T.W., Li M., Shen F., Guo M., Qin J., Yao L., Zhou C. (2022). Direct and indirect impacts of urbanization on vegetation growth across the world's cities. *Sciences Advances, 8*(27). https://doi.org10.1126/sciadv.abo0095

Zhao H. and Ma Y. (2021). Effects of various driving factors on potential evapotranspiration trends over the main grain-production area of China while accounting for vegetation dynamics. *Agricultural Water Management, 250*. https://doi.org10.1016/j.agwat.2021.106854

Italian Journal of Agrometeorology
Rivista Italiana di Agrometeorologia

Firenze University Press
https://riviste.fupress.net/index.php/IJAm

OPEN ACCESS

Citation: Nigatu, B., Getu, D., Getachew, T., & Getaneh, B. (2024). Effect of irrigation regime on yield component and water use efficiency of tomato at Ataye irrigation scheme, Ataye Ethiopia. *Italian Journal of Agrometeorology* (2): 89-100. doi: 10.36253/ijam-2492

Received: February 13, 2024

Accepted: Novemeber 23, 2024

Published: December 30, 2024

© 2024 Author(s). This is an open access, peer-reviewed article published by Firenze University Press (https://www.fupress.com) and distributed, except where otherwise noted, under the terms of the CC BY 4.0 License for content and CC0 1.0 Universal for metadata.

Data Availability Statement: All relevant data are within the paper and its Supporting Information files.

Competing Interests: The Author(s) declare(s) no conflict of interest.

Effect of irrigation regime on yield component and water use efficiency of tomato at Ataye irrigation scheme, Ataye Ethiopia

Belihu Nigatu*, Demisew Getu, Tsegaye Getachew, Biruk Getaneh

Amhara Agriculture Research Institute, Debre Birhan Agricultural Research Center, PO. Box 112, Debre Birhan, Ethiopia
*Corresponding author. E-mail: belihun12@gmail.com

Abstract. The importance of an irrigation regime is that it enables the irrigator to apply the exact amount of water to achieve optimum production and minimize adverse environmental impact. In the study area, the amount of irrigation and the frequency of application are not well determined, and the farmers are unaware of how much water and when to apply for tomato crops. Therefore, the objective of this study is to quantify the effects of irrigation regimes on yield and yield components of tomatoes in lowland areas of Ethiopia. The treatments were factorial combinations of five irrigation depths (50, 75, 100, 125, and 150 % of ETc) and three irrigation intervals and laid out in a randomized complete block design with three replications. The collected data were analyzed using R-software and significant treatment means separated using the least significant difference at 5 %. According to the findings, irrigation level and frequency had a significant ($P< 0.05$) effect on marketable fruit yield, water use efficiency, and plant height of tomatoes. The highest and lowest yields were 54.49 t/ha and 37.89 t/ha respectively. The optimum yield (48.5 t/ha) and water use efficiency (10.79kgm^{-3}) were obtained from 75% ETc before the 3-day interval. Therefore, for the study area and similar agro-ecologies, tomatoes can be irrigated with 376.72 mm net irrigation depth with 33.64 mm and 5-day interval, 60.54 mm and 9-das interval, 94.18 mm and 14-day interval, 94.18 mm and 14-days interval, and 94.18 mm and 14-days irrigation interval at initial, development one, development two, mid and late stages of tomatoes crop respectively and saving 3127.33 m^3 water to irrigate an additional 0.59 ha to achieve a yield of 29.00 t/ha for the user without a high yield penalty.

Keywords: irrigation regime, Tomato yield, water use efficiency, irrigation land, Ethiopia.

1. INTRODUCTION

Many regions of the world, particularly East Africa, are extremely concerned about food security. Ethiopia is a country with a total population of more than 110 million, of which about 80% of the total population is engaged in subsistence farming in rural areas (CSA, 2017). The distribution of Ethiopia's rainfall is erratic and unpredictable due to climate change is one of the most important challenges for crop production (Bezu, A., 2020). Currently,

climate change is negatively influencing the availability of water resources, crop production, and food security in the world. Raising the unit yield is one practical way to keep the food supply self-sufficient. Several studies showed that irrigation is a good way to increase yield per unit of space (Hume et al., 2021).

Tomato is an important commercial vegetable crop in the world (Costa and Heuvelink, 2018). In Ethiopia tomato is one of the most economical and widely grown vegetable crop by smallholder farmers, commercial state and private farms (Emana et al., 2017). Water availability is a major limiting factor for tomato crop growth and productivity, thus a successful production of tomatoes requires irrigation (Chand et al., 2021). Irrigation water plays a great role in vegetable production as it affects the growth, yield, and quality of the tomato crop (Kuscu et al., 2014; Abdelhady et al., 2017).

Irrigation management practices such as amount and time of application are considered as components of major limiting factors of tomato crops production. However, water resources in many parts of the world are limited and thus there is an urgent need to apply effective irrigation strategy to operate under the prevailing conditions of water scarcity (DeNicola et al., 2015; Xinchun et al., 2017).

USING the CROPWAT model to determine the amount and time of application of irrigation water suitable for practicing irrigation water management to effectively use irrigation water to optimize crop production and productivity (Hossain et al., 2017). The CROPWAT 8 program was developed by FAO from the Penman-Monteith method, based on FAO Irrigation and Drainage Paper 56 named FAO56. FAO56 adopted the P - M (Penman - Montieth) method as a global standard to estimate ETo from meteorological data (Allen et al., (1998)). The FAO CROPWAT program incorporates procedures for reference crop evapotranspiration and crop water requirements and allow the simulation of crop water use under various climates, crop, and soil conditions. ETo was calculated for every ten days (defined as a "decade" by FAO) and then cumulated to monthly data. Soil characteristics considered for the estimation of crop water requirements are available water content (mm/m) and depth of soil (cm) (Surendran et al., 2015). Temperature and irrigation water demand were found to be related to crop water needs (Surendran et al., 2014).

The majority of irrigation water management in Ethiopia is traditional, meaning that farmers irrigate their land not properly which there is water available without taking into account whether it is above or below the crop's ideal water demand. The information on the crop water requirements of the anticipated crops is typically used for major dam design purposes rather than for the actual responsibility of irrigation operation. However, the availability of the same information is severely constrained in regions where farmers practice small-scale agriculture, and more water is thought to be wasted there (Roth G., 2014). For irrigation planning and water-efficient use in an arid area, understanding crop water requirements is crucial (Levidow et al., 2014). In addition, water usage in the agriculture sector would be required due to the growing shortage of water and the increased competition for it (Flörke et al., 2018). For the creation of a sufficient water supply, it is required to forecast the water requirements for crops in irrigation.

Using known techniques for calculating crop evapotranspiration and yield responses to water stress, the CROPWAT 8.1 model simulates agricultural water stress situations and estimates yield decreases (Swelam et al., 2019).

In the study area, farmers can irrigate their crops based on traditional know-how causing nutrient leaching, waterlogging, and severe water shortage problems. The amount and scheduling of tomato irrigation are still unknown and not properly manage the agricultural water to the field. Therefore, the objective of this study was to determine the effect of the irrigation regime on the yield and water use efficiency of tomatoes in lowland areas of Ethiopia for better resource allocation and crop productivity.

2. MATERIALS AND METHODS

2.1. Description of the study area

The experiment was conducted in the Efferatana Gidim district, Amhara Region, Ethiopia. The experimental site is located at 39°54'27" Easting and 10°17'28" Northing and an altitude of 1514 m above sea level. The two main seasons in the study area are the wet and dry ones. The dry season primarily lasts from October to the end of May, while the rainy season lasts from the beginning of June to the end of September, with a mean annual rainfall of 1010 mm. The mean maximum and minimum temperatures are 27.7°C and 11.3°C respectively in Table 6. Use the CROPWAT model to determine the amount of crop water needed in the study area. The trial was conducted in the Ataye irrigation scheme (Fig. 1). The precipitation versus reference evapotranspiration (ETo) of the study area shown in Fig. 2.

2.2. Reference evapotranspiration (ETo)

The reference evapotranspiration ETo was calculated by the FAO Penman-Monteith method, using decision

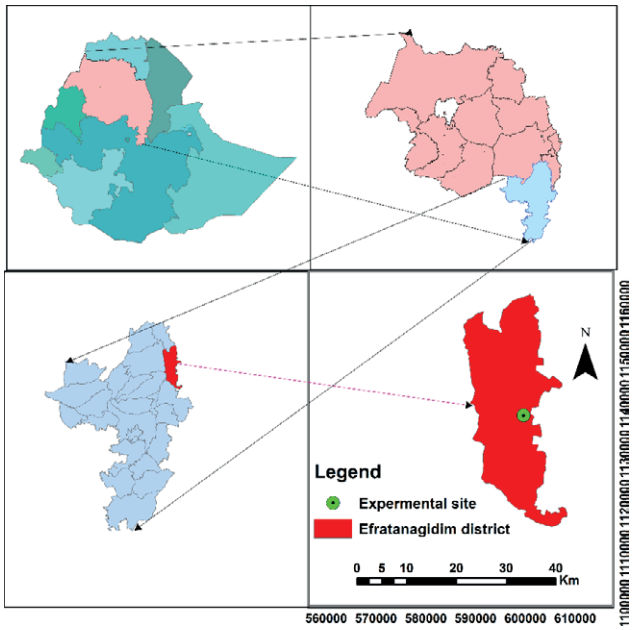

Figure 1. Location map of the experimental area.

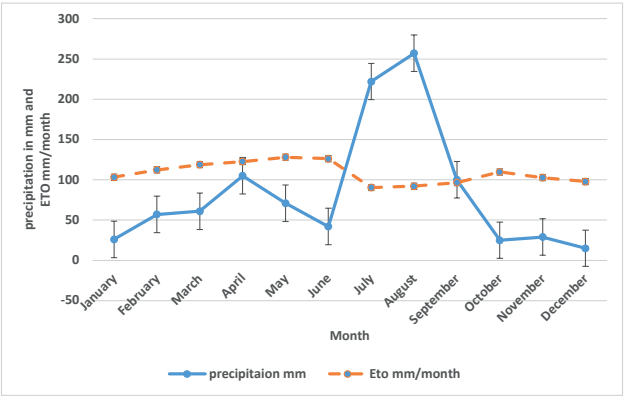

Figure 2. The precipitation and ETo of the study area.

Table 1. Crop parameters as an input for the CROPWAT model (Allen et al., 1998).

Growth stage	Initial	Development	Mid	Late	Total
Stage lengths (days)	30	40	45	30	145
Crop coefficient (Kc)	0.6	<<	1.15	0.7	
Rooting depth (m)					0.7-1.15
Depletion levels (P)	0.4	0.4	0.4	0.4	

support software CROPWAT8 developed by FAO, based on Allen et al.,(1998). The Penman-Monteith equation integrated in the CROPWAT program is expressed by the following equation 1 (FAO, 1998a).

$$ETo = \frac{0.408\Delta(Rn-G)+\gamma\frac{900}{T+273}U2(es-ea)}{\Delta+\gamma(1+00.34\ u2)} \quad (1)$$

where: ETo is reference evapotranspiration (mm day^{-1}), Rn, G, and T are net radiation values at crop surface (MJ m-2 day^{-1}) at 2 m height, soil heat flux density (MJ m^{-2} day-1) and daily mean temperature °C respectively. Also, u_2, es, ea, (es–ea), Δ and γ represent wind speed at 2 m height (m s^{-1}), the saturated vapor pressure at the given temperature (kPa), actual vapor pressure (kPa), saturation vapor pressure deficit (kPa), the slope of the saturation vapor pressure curve (Pa/°C) and psychometric constant (kPa/°C), respectively.

2.3. Determination of irrigation requirements and scheduling

Crop water use (ETc) was determined by multiplying ETo by the crop coefficient (FAO, 1998a) for initial, development, mid-season, and late stages. Irrigation water to be applied to tomatoes was determined at an allowable constant soil moisture depletion fraction (p = 0.3) (Table 1) of the total available soil water (TAW) and readily available water (RAW).

The crop water use (ETc) was calculated as equation 2:

$$ETc = ETo*kc \quad (2)$$

where ETc = crop water use (actual evapotranspiration); ETo = Reference evapotranspiration; Kc = Crop factor.

The irrigation Requirement of the crop based on long-term rainfall data estimated from study sites was as follows equation 3 (FAO, 1998a);

$$IR = ETc - Reff \quad (3)$$

where IR= Net irrigation requirement (mm); ETc = Crop water requirement (mm) and Reff = Effective rainfall (mm).

Effective rainfall is a part of rainfall that enters into the soil and is made available for crops. It can be calculated as follows equation 4 and 5 (FAO, 1998a);

$$\text{Effective rainfall (mm)} = 0.6 * RF\ (mm) - 10 \quad \text{for } RF < 70\ mm \quad (4)$$

$$\text{Effective rainfall (mm)} = 0.8 * RF\ (mm) - 24 \quad \text{for } RF > 70\ mm \quad (5)$$

where, RF = Rainfall (mm/month); Peff= Monthly decades of effective rainfall (mm).

The optimal irrigation schedule was worked out using the CROPWAT 8.0 computer model and assumed

Table 2. Method to determine chemical and physical properties of soil.

Parameters	Methods of analysis	References
pH	PH –meter	
EC	EC-meter or electrometer	
Organic carbon (OC)	Rapid titration method	(Walkley and black,1934)
Organic matter (OM)	1.724*OC	(Pribyl, 2010)
Soil texture	Hydrometer	Bouyoucous, 1962
Bulk density	Core sampler	(Hillel, 2000)
Field capacity (FC) and wilting point (PWP)	Pressure plate apparatus	

the irrigation regime applied at 100% readily available soil moisture. The RAW is the amount of water that crops can extract from the root zone without experiencing any water stress.

The TAW and RAW are calculated as follows equation 6 and 7 respectively (FAO, 1998).

$$TAW = \frac{(FC-PWP)}{100} * BD * Dz \quad (6)$$

$$RAW = TAW * P \quad (7)$$

where FC and PWP are in % on a weight basis, BD is the bulk density of the soil in gm cm^{-3}, and Dz is the maximum effective root zone depth in mm. RAW in mm, p is soil water depletion fraction for no stress in fraction and TAW is the total available soil water of the root zone in mm per root depth.

2.4. Soil sampling and analysis

Before planting, the experimental field's composite soil samples were collected using an auger at a depth of 0-20 cm. After the composite samples had been well mixed 500 grams of subsamples were taken in a plastic bag, and brought to the Debre Birhan Agricultural Research Center soil and water laboratory for analysis.

At the Debre Birhan Agricultural Research Center Soil Laboratory, physical-chemical soil characteristics were evaluated by using the manual for soil and plant analysis laboratories (Ryan et al., 2001). The soil samples were processed by permitting passage through a 2 mm sieve, grinding with a pestle and mortar, and allowing air drying at room temperature (Changwen et al., 2007). Working samples from bulk samples were taken, and they were then examined to evaluate the physicochemical characteristics of the soil, such as its texture, organic carbon content, organic matter, pH, and so on (Table 2).

Table 3. Soil physical and chemical properties in the study area.

Parameter	Value	Parameter	Value
Sand (%)	28	OC (%)	1.8
Clay (%)	38	OM (%)	3.04
Silt (%)	34	BD (g/cm^3)	1.37
pH	7.8	FC (%)	23.4
EC (ds/m)	0.23	PWP (%)	6.95
Textural class	Clay		

OC = organic carbon, OM = organic matter, BD = bulk density, PWP = permanent wilting point, FC = field capacity and EC = electric conductivity

2.5. Physical-chemical properties of soil

The physical-chemical properties of the soils of the study area are presented in Table 3. Based on the triangle of the International Soil Science Society (ISSS) methodology, the study area soil textural class was established (Rowell, 1994). Clay is the dominant soil type in the study area. The pH and EC results, which were 7.8 and 0.23 dS/m, respectively in Table 3, showed that the soil is moderately suitable for surface irrigation to the increment of commercial crop production (Hussien et al. (2019).

2.6. Experimental design and data collection

A factorial randomized complete block design (RCBD) with three replications and 15 treatments was used to experiment (Table 4). The unit plot was 2.1m by 4 m (8.4 m^2). The SAS software was used to randomly assign treatments to each experimental plot within a replication. 30 cm, 75 cm, 1 meter, and 2 meters, respectively, separated the plant, row, plot, and repetition. The layout of the treatment is shown in Table 4. As a source of NPS and urea fertilizer, phosphorus, and nitrogen were applied to the field at the suggested rates of 240

Table 4. Treatments and applied water levels.

Treatments	Applied water level
T1	50% ETC
T2	75% ETC
T3	100% ETC
T4	125% ETC
T5	150% ETC
T6	50% ETC before a 3-day interval
T7	75% ETC before the 3-day interval
T8	100% ETC before a 3-day interval
T9	125% ETC before a 3-day interval
T10	150% ETC before a 3-day interval
T11	50% ETC after a 3-day interval
T12	75% ETC after a 3-day interval
T13	100% ETC after a 3-day interval
T14	125% ETC after a 3-day interval
T15	150% ETC after a 3-day interval

T= Treatment, ETC= evapotranspiration of the crop.
The amount of water and frequency in each growth stage during the tomato growth period is represented in table 5.

kg per hectare and 100 kg per hectare, respectively. The water application method was a surface irrigation technique that was applied through furrow and a siphon hose was used for measuring the amount of water we applied using a constant head. The flow rate was estimated using the volumetric method. This has been done by collecting water in a tank of known volume. Q = V/t where, V = volume of the container (m^3), t = time taken (hr), and Q = discharge of irrigation water (m^3 hr–1) for both experimental sites (Gore and Banning, 2017).

The crop data that were collected from the experimental location for analysis included yield characteristics (fruit yield), marketable and non-marketable yield, amount of water, and frequency (interval) during the application period.

2.7. Water productivity

Rasul and Thapa (2004) claim that the ratio between the amount of agricultural yield used for selling and the amount of water used to grow the crops can be used to calculate water productivity. It can be calculated as shown in equation 8.

$$Eu = \frac{Y}{WR} \quad (8)$$

where; Eu = water use efficiency (t/ha-mm); Y = crop yield (t/ha); WR = Water requirement of the crop (ha-mm).

2.8. Statistical analysis

Using R 4.2.2 software, an analysis of variance (ANOVA) was performed on the gathered data. The least significant difference (LSD) test was used to make a mean separation in cases when the treatment effect was significant at a 5% level of probability. Using Pearson correlation, correlation analyses of particular factors were also carried out.

3. RESULTS AND DISCUSSION

3.1. Reference evapotranspiration and crop water requirement of the experimental area

The simulated result of the metrological data for reference evaporation of the study area is summarized concerning each month and the average ETO is shown in Table 6.

The highest monthly ETO for the study area is observed in May (4.74 mm/day), while the lowest is observed in August 2.65 mm/day in Table 6. According to this finding, ETO was higher in the dry season and lower in the wet season. This finding is supported by FAO (1998a), the ETo that rises with rising temperature during the dry season. In the study area, the average ETO is 3.93 mm/day (Table 6) determine the amount of water needed and when to apply it presented in *Table 7*. Depending on the location, climate, type of soil, cultivation technique, etc., crops have various water needs, and the total amount of water needed for crop growth is not distributed evenly throughout the crop's life (Some et al., 2006).

Early in the development process, the ETc values were lower than ETo in Table 7, but as the canopy grew over time, they eventually surpassed ETo close to the end of the crop season. Early in January, when there were few leaves to contribute to evapotranspiration and most evapotranspiration was caused by soil evaporation, low ETc rates were observed. Water use by plants during the vegetative stage was the main reason for the rise in water use from February to March. Water use increased after the last day of April, with the peak demands occurring during the flowering stage or in April (mid-stage) (fruit set stage) in Table 7. Daily ET crop varied from 2.34 millimeters per day at crop establishment to 2.65 millimeters per day during early

Table 5. The amount of water and frequency in each growth stage during the tomato growth period.

Treatment	Initial		dev. 1		dev.2		Mide		Late	
	depth(mm)	interval	depth(mm)	interval	depth(mm)	interval	depth(mm)	interval	depth(mm)	interval
50% ETc	36	8	53.69	12	76.75	17	76.75	17	76.75	17
75% ETc	54	8	80.53	12	115.12	17	115.12	17	115.12	17
100% ETc	72	8	107.37	12	153.49	17	153.49	17	153.49	17
125% ETc	90	8	134.22	12	191.86	17	191.86	17	191.86	17
150% ETc	108	8	161.06	12	230.24	17	230.24	17	230.24	17
50% ETc before 3-day interval	22	5	40.27	9	63.20	14	63.20	14	63.20	14
75% ETc before 3-day interval	33.64	5	60.40	9	94.80	14	94.80	14	94.80	14
100% ETc before 3-day interval	45	5	80.53	9	126.40	14	126.40	14	126.40	14
125% ETc before 3-day interval	56	5	100.66	9	158.00	14	158.00	14	158.00	14
150% ETc before 3-day interval	67	5	120.80	9	189.60	14	189.60	14	189.60	14
50% ETc after 3-day interval	49.5	11	67.11	15	90.29	20	90.29	20	90.29	20
75% Etc after a 3-days interval	74.25	11	100.67	15	135.44	20	135.44	20	135.44	20
100% ETc after 3-day interval	99	11	134.22	15	180.58	20	180.58	20	180.58	20
125% ETc after 3-day interval	123.75	11	167.78	15	225.73	20	225.73	20	225.73	20
150% ETc after 3-day interval	148.5	11	201.33	15	270.87	20	270.87	20	270.87	20

Note: 100% ETC means Application of 100% CROPWAT model generated depth with respective interval in each stage, 100% ETc before 3-day interval means Application of 100% CROPWAT generated depth with 3 day before generated the CROPWAT model interval, and 100% ETc after 3-days interval means Application of 100% of CROPWAT generated depth with 3 days after generated CROPWAT model interval and the other treatments are the same meaning.
Dev.1=development stage one, dev.2= development stage two.

Table 6. The reference evapotranspiration (ETO) values in the study area.

Month	Min Temp °C	Max Temp °C	Humidity %	Wind km/day	Radiation MJ/m²/day	ETo mm/day
January	12.1	25.7	60	156	18.2	3.9
February	12.8	27	60	173	21.1	4.59
March	13.6	26.7	59	173	18.5	4.4
April	13.6	27.7	69	156	19.9	4.45
May	14	27.2	62	173	21.2	4.75
June	13.8	26.1	76	104	18.1	3.73
July	11.8	21.1	88	104	15	2.82
August	12	20.8	90	104	14.9	2.77
September	12.8	22.5	83	112	16.9	3.24
October	12.6	24.6	64	190	19.8	4.23
November	11.3	25	62	190	21.1	4.3
December	11.5	25.2	60	173	18.9	3.97
Average	12.7	25	69	150	18.6	3.93

vegetative growth to 4.85 millimeters per day during late vegetative growth, with a peak of 5.1 millimeters per day during flowering. The ET crop was reduced to 4.96 mm/day in the ripening stage (late stage) (Table 7). According to FAO (1986), the flowering stage is when tomato crop growth requires more water than the other growth stage.

The total crop water requirement for tomatoes was 463 mm/dec (Table 7). The findings are supported by Ahmed et al. (2020) and Casals et al. (2021)), a tomato crop cultivated in the field for 90 to 120 days after transplanting, depending on the climate.

Table 7. Crop water and irrigation requirement for tomatoes.

Month	Decade	Stages	KcCoefff	ETcrop mm/day	ETcrop mm/dec	Ir. Req. mm/day	Ir. Req. mm/dec
Jan	2	Init	0.6	2.34	11.7	2.34	11.7
Jan	3	Init	0.6	2.48	27.3	2.48	27.3
Feb	1	In/De	0.61	2.65	26.5	2.65	26.5
Feb	2	Dev.t	0.69	3.18	31.8	3.18	31.8
Feb	3	Dev.t	0.84	3.78	30.2	3.78	30.2
Mar	1	Dev.t	0.98	4.36	43.6	4.36	43.6
Mar	2	De/Mi	1.1	4.85	48.5	4.85	48.5
Mar	3	Mid	1.15	5.08	55.8	5.08	55.8
Apr	1	Mid	1.15	5.1	51	5.1	51
Apr	2	Mi/Lt	1.11	4.96	49.6	4.96	49.6
Apr	3	Late	1.01	4.6	46	4.6	46
May	1	Late	0.87	4.1	41	4.1	41
Total					463		463

3.2. Effect of irrigation regime on Tomatoes yield components

The effect of irrigation level and frequency on the tomato growth parameters is presented in Table 8. The trend of PH, NMF, and NUMF growth yield components in the first year and second year of tomatoes was illustrated for the application of different amount levels of water depth and frequency (Table 8). The mean height of the tested tomato was in the range of 63 -95.2 cm which is in line with the observations of Zou *et al.*,(2017) and Xiao et al.,(2022) who reported that the height of tomato plants varied between the ranged from 36.80-126.7cm. In general, the higher the number of fruits the more fruit yield is happened; fruit size also determines the yield estimation (Koirala *et al.,* 2019). The mean number of fruits per plant lay between 4 and 98 (Nangare *et al.,* 2016) reported values between 10 and 1589, while in Ethiopia, Lendabo (2021) reported that the fruit number per plant was between 26 and 62. The number of fruits per plant is a character affected by genetic and environmental differences.

Based on our findings in the first year, the maximum treatment values of PH, NMF, and NUMF were, 125% ETc before the 3-day interval, 125% ETc after the 3-day interval, and 150% ETc before the 3-day interval, respectively and the minimum values were 50% ETc before the 3-day interval, 50% ETc after the 3-day interval, and 150% ETc before the 3-day interval. The yield component maximum values in the second year were 125% ETc after three days, 50% ETc, and 50% ETc, while their minimum values were 75% ETc before three days, 150% ETc before three days, and 50% ETc before three days interval. The difference is brought on by the amount of water applied and the frequency of days. The PH and NUMF are significant ($P<0.05$) influenced by water level and frequency in the first year. However, in the second year the PH, NMF, and NUMF were non-significant ($P<0.05$) influenced by water level and frequency (Table 8). The same findings were observed plant height and number of marketable fruit were affected by irrigation regime (Fawzy, 2019).

3.3. Effect of irrigation regime on tomatoes yield and water productivity

The effect of the irrigation regime on the combined two years of MYF, UNMYF, and TYF yields and water productivity for tomatoes were presented in (Table 9). The maximum values of MYF, UNMYF, and TYF were in the 125% ETc, 125% ETc before the 3-day interval, and 150% ETc, and the minimum values of the yields were in the 50% ETc, 50% ETc before 3 days interval, and 150% ETc after 3 days interval respectively. The maximum and minimum water application amount is in the 150% ETc after a 3-day interval and 50% ETc respectively due to the application difference level and the time interval (Table 9). In the research area, water level and frequency had a significant ($P <0.05$) effect on tomato marketable yield, total yield, and water use efficiency. Marketable fruit yield is the major determinant variable for selection of tomato productivity, as it directly affects commercialization and thus income generation of the farms (Koirala *et al.,* 2019). The findings reported that the irrigation regime were significant ($P<0.05$) affected on marketable fruit yield.

According to Lendabo (2021), the sunburnt, small-sized, cracked, disease-affected, and insect pest-damaged

Table 8. Effect of irrigation regime on tomatoes yield components in two years.

Treatments	First-year			Second year		
	PH cm	NMf /ha	NUMf /ha	PH cm	NMf/ha	NUMf /ha
50% ETc	63^{fgh}	479369	96428.57	84.33	338892.9	47226.19
75% ETc	65^{efgh}	478179	99607.14	75.87	267059.5	35714.29
100% ETc	77^{ab}	537702	106345.2	80.27	194440.5	25000
125% ETc	70^{cdef}	525000	142857.1	89.2	244440.5	34916.67
150% ETc	62^{gh}	490083	95238.1	85.6	319047.6	36511.9
50% ETc before the 3-day interval	60^{h}	448809	67464.29	85.47	233726.2	22226.19
75% ETc before the 3-day interval	64^{efgh}	489678	99202.38	74.93	304369	41666.67
100% ETc before a 3-day interval	76^{ab}	475797	130559.5	78.07	216666.7	26988.1
125% ETc before the 3-day interval	82^{a}	494845	130321.4	84	196273.8	36904.76
150% ETc before the 3-day interval	72^{bcd}	416512	74607.14	83.47	188571.4	28571.43
50% ETc after a 3-day interval	74^{bcd}	399202	85714.29	85.2	278964.3	36107.14
75% Etc after a 3-day interval	70^{cdef}	525000	85321.43	83.93	297619	36511.9
100% ETc after a 3-day interval	67^{defg}	402143	109916.7	67.67	244845.2	39678.57
125% ETc after a 3-day interval	65^{efgh}	473417	84607.14	95.2	311904.8	33726.19
150% ETc after a 3-day interval	68^{defg}	473012	86904.76	76.07	263488.1	32535.71
CV (%)	5.41	10.55	17.51	16.1	30.34	28.6
Mean	69	473917	99673.01	81.95	260021.2	34285.71
LSD (0.05)	2.79	NS	10.96	NS	NS	NS

Note: PH= plant height in cm, NMf= number of marketable fruit NUMF= number of unmarketable fruit.

Figure 3. The experiment performance of the irrigated tomatoes at development stage.

fruits are considered as unmarketable. Unmarketable fruit yield did not differ substantially at the 5% level of significance and was not affected by the irrigation regime. The result agreed with the study the difference in irrigation regime had significant (P<0.05) effect on the total fruit yield of tomatoes (Djurović et al., 2016). The highest and lowest yields were yield 54.49 t/ha and 37.89 t/ha respectively. The results are generally in agreement with Fawzy (2019) and Zou *et al.,* (2017) who reported that total fruit yield of tomato ranging from 6.46-82.50 t ha-1 in their study. The optimum yield with high water use efficiency was 48.5 t/ha of irrigation water at a depth of 376.71 mm and saving 3127.33 m^3 of water to irrigate an additional 0.59 ha to achieve a yield of 29.00 t/ha for

Figure 4. The irrigated tomato yield performance of the field experiment during harvesting.

the user without a high yield penalty (Table 9). The present finding clearly indicated that the irrigation regime were to determine the quantity of the Tomato production (Lovelli et al., 2017). This study lined with a decent commercial production of tomatoes under irrigation is 45–65 t/ha of fresh fruits, and the water efficiency for fresh tomato harvest is 10–12 kg/m3, according to FAO (1986). The research supported earlier findings that the fresh tomato output ranged from 45 to 65 t/ha (El-Naggar, 2020).

3.4. Water saved, additional area irrigated and possible yield to be obtained

The yield and land opportunity obtained from saving water in the application of water through time intervals is illustrated in Figure 5. The land and water levels in Treatment 15 (150% ETc after a 3-day interval) were the lowest. However, treatment seven (75% ETc before the 3-day interval) was a better land opportunity, saving 3127.33 m^3 of water and 0.59 ha of additional irrigation land to achieve a yield of 29.00 t/ha for the user without a high yield penalty. This is because of the statistical relationship between yield and land opportunity (land developed by saving water).

3.5. Tomato yield- water use function

The tomato yields rose with applied water depth up to a maximum value of 54.49 t/ha before falling with more water (Table 9). The findings of this study sup-

Table 9. Effect of irrigation regime on tomato yield and water productivity.

Treatment	MYF t/ha	UNMYF t/ha	TYF t/ha	WP kg/m^3	TW m^3/ha
50% ETc	31.11^{f}	6.78	37.89^{e}	9.42^{bc}	3931.81
75% ETc	39.39^{bcde}	5.79	45.19^{bcde}	8.46^{cd}	5244.2
100% ETc	43.00^{abcd}	6.04	49.04^{abcd}	7.39^{de}	6546.25
125% ETc	47.62^{a}	6.88	54.49^{a}	7.24^{de}	7559.27
150% ETc	44.84^{ab}	6.69	51.53^{ab}	5.87^{e}	9227.11
50% ETc before the 3-day interval	33.56^{f}	4.97	38.52^{e}	11.28^{a}	3389.96
75% ETc before the 3-day interval	41.66^{abcde}	7.29	48.95^{abcd}	10.79^{ab}	4431.94
100% ETc before a 3-day interval	38.65^{bcdef}	7.01	45.66^{bcde}	8.10^{cd}	5465.34
125% ETc before the 3-day interval	39.00^{bcdef}	7.04	46.05^{abcde}	6.97^{de}	6505.11
150% ETc before the 3-day interval	37.38^{bcdfe}	6.18	43.56^{de}	5.99^{e}	7460.39
50% ETc after a 3-day interval	35.98^{cdf}	6.26	42.25^{de}	9.27^{bc}	4473.65
75%ETc after a 3-day interval	42.78^{abcd}	6.50	49.29^{abcd}	8.52^{cd}	5641.17
100 ETc% after a 3-day interval	39.36^{bcde}	7.06	46.42^{abcde}	6.31^{e}	7624.39
125% ETc after a 3-day interval	43.57^{abc}	6.56	50.13^{abc}	5.73^{e}	9254.32
150% ETc after a 3-day interval	35.20^{def}	6.06	41.26^{cde}	3.72^{f}	10970.1
CV (%)	15.37	26.58	14.14	17.79	
mean	39.44	6.43	45.87	7.68	
LSD (0.05)	2564.1	NS	2743	0.58	

MYF=marketable fruit yield, UNMYF= unmarketable fruit yield, TYF= total fruit yield, WP=water productivity, TW= total water amount.

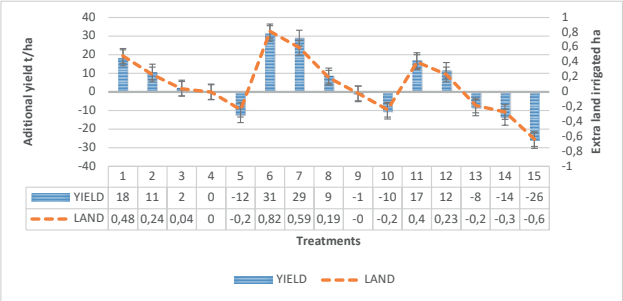

	1	2	3	4	5	6	7	8	9	10	11	12	13	14	15
YIELD	18	11	2	0	-12	31	29	9	-1	-10	17	12	-8	-14	-26
LAND	0,48	0,24	0,04	0	-0,2	0,82	0,59	0,19	-0	-0,2	0,4	0,23	-0,2	-0,3	-0,6

Figure 5. Additional area to be irrigated with the saved water and possible yield.

port those of Samui et al. (2020), who claimed that good water management directly contributes to the high quality and productivity of vegetable crops. It has been found that as water depth increases, water use efficiency also decreases.

3.6. Correlation functions of the growth and yield parameters

The correlation functions of the growth and yield components of tomatoes are presented in *Table 10*. The yield of all fruits and the number of marketable fruits are strongly positively correlated, whereas the yield of all fruits and the volume of water are medium correlated (Table 10).

4. CONCLUSIONS AND RECOMMENDATIONS

In the lowlands of Ethiopia, where water is not available for surface irrigation and farmers are not aware of irrigation management the adoption of the right amount of water and frequency is an important issue. The net irrigation requirement and gross irrigation requirement of garlic were found as 463 mm and 658 mm respectively. Up to a certain point in the experimental region increasing the depth of water applied enhanced tomato crop yield. The soil in the research area has a clay texture. The findings indicate that a 48.95 t/ha tomato yield output required a total water depth of 4431.94 m^3/ha over the tomato crop growth period in the research location, which allowed for the addition of more irrigation land without suffering a severe yield penalty. At each stage, water was used as follows: Initial measurement was 33.64 mm with a 5-day interval, Development One was 60.54 mm with a 9-day interval, Development Two was 94.18 mm with a 14-day interval, mid-stage was 94.18 mm with a 14-day interval, and late stage was 94.18 mm with a 5-day interval with net irrigation depth 376.72mm and saving 3127.33 m^3 water to irrigate an additional 0.59 ha to achieve a yield of 29.00 t/ha for the user without a high yield penalty. It is recommended that various tomato varieties and irrigation techniques be used in this study.

AUTHOR CONTRIBUTION STATEMENT

Belihu Nigatu: Conceived and designed the experiments; Performed the experiments; Analyzed and interpreted the data; wrote the paper.

Demisew Getu, Tsegaye Getachew, and Biruk Getaneh: Conceived and designed the experiments; performed the experiment.

FUNDING STATEMENT

This work was supported by the Debre Birhan Agricultural Research Center (DBARC), Amhara Agriculture Research Institute, Ethiopia.

ACKNOWLEDGMENTS

The experiment was greatly helped by Lisanu Getaneh, Getaneh Shegaw, and Zebideru Mekonen, for whom the author is grateful. I also want to express my gratitude and appreciation for the fund's support to the

Table 10. Correlation function of the parameters.

	NMY	NUMY	M Y (Kg)/ha	UNMY (Kg)/ha	TY (Kg)/ha	Water amount m^3/ha
NMY	1					
NUMY	0.809	1				
M Y (Kg)/ha	0.835	0.798	1			
UNMY (Kg)/ha	0.772	0.894	0.729	1		
TY (Kg)/ha	0.862	0.859	0.988	0.826	1	
water amount m^3/ha	0.489	0.509	0.562	0.511	0.578	1

Amhara Agricultural Research Institute and Debre Berhan Agricultural Research Center.

5. REFERENCES

Abdelhady, S.A., El-Azm, N.A.I.A. and El-Kafafi, E.S.H., 2017. Effect of deficit irrigation levels and NPK fertilization rates on tomato growth, yield and fruits quality. *Middle East J. Agric. Res*, *6*(3), pp. 587-604.

Ahmed, A., Oyebode, M.A., Igbadun, H.E. and Oiganji, E., 2020. Estimation of crop water requirement and crop coefficient of tomato crop using meteorological data in Pampaida Millennium village, Kaduna State, Nigeria. Fudma Journal of Sciences, 4(3), pp. 538-546.

Bezu, A., 2020. Analyzing impacts of climate variability and changes in Ethiopia: A review. *American Journal of Modern Energy*, *6*(3), pp. 65-76.

Bouyoucos, G.J., 1962. The hydrometer method improved for making particle size analyses of soils 1. Agronomy Journal, 54(5), pp. 464-465.

Broadbent F. 1953.The soil organic fraction. AdvAgron 5: 153–183. https://doi.org/10.1016/s0065-2113(08)60229-1

Brouwer, C. and Heibloem, M., 1986. Irrigation water management: irrigation water needs. Training manual, 3, pp. 1-5.

Casals, J., Martí, M., Rull, A. and Pons, C., 2021. Sustainable transfer of tomato landraces to modern cropping systems: the effects of environmental conditions and management practices on long-shelf-life tomatoes. *Agronomy*, *11*(3), p. 533.

Chand, J.B., Hewa, G., Hassanli, A. and Myers, B., 2021. Deficit irrigation on tomato production in a greenhouse environment: A review. *Journal of Irrigation and Drainage Engineering*, *147*(2), p. 04020041.

Costa, J.M. and Heuvelink, E.P., 2018. The global tomato industry. *Tomatoes*, *27*, pp. 1-26.

CSA (Central Statistical Agency), 2017. Agricultural Sample Survey Report on Area and Production of Crops. *Statical Bulletin* 586, April 2018, Addis Ababa.

DeNicola, E., Aburizaiza, O.S., Siddique, A., Khwaja, H. and Carpenter, D.O., 2015. Climate change and water scarcity: The case of Saudi Arabia. *Annals of global health*, *81*(3), pp. 342-353.

Djurović, N., Ćosić, M., Stričević, R., Savić, S. and Domazet, M., 2016. Effect of irrigation regime and application of kaolin on yield, quality and water use efficiency of tomato. *Scientia Horticulturae*, *201*, pp. 271-278.

El-Naggar, A., 2020. New sensing methods for scheduling variable rate irrigation to improve water use efficiency and reduce the environmental footprint: a thesis presented in partial fulfillment of the requirements for the degree of Doctor of Philosophy in Soil Science at Massey University, Palmerston North, New Zealand (Doctoral dissertation, Massey University)

Emana, B., Afari-Sefa, V., Nenguwo, N., Ayana, A., Kebede, D. and Mohammed, H., 2017. Characterization of pre-and postharvest losses of tomato supply chain in Ethiopia. *Agriculture & Food Security*, *6*, pp. 1-11.

FAO 2009. CROPWAT Version 8.0.

FAO. 1998a. Crop evapotranspiration: Guidelines for computing crop water requirements. By: Richard Allen, Luis Pereira,Dirk Raes and Martin Smith. FAO Irrigation and Drainage Paper 56. Rome, Italy.

Fawzy, Z.F., 2019. Effect of irrigation systems on vegetative growth, fruit yield, quality and irrigation water use efficiency of tomato plants (Solanum lycopersicum L.) grown under water stress conditions. *Acta Scientific Agriculture*, *3*, pp. 172-183.

Flörke, M., Schneider, C. and McDonald, R.I., 2018. Water competition between cities and agriculture is driven by climate change and urban growth. *Nature Sustainability*, *1*(1), pp. 51-58.

Food and Agricultural Organization (FAO), 1986. Yield response to water. Irrigation and Drainage Paper 33. Rome, Italy

Gore JA and Banning J (2017). Discharge measurements and streamflow analysis. In Methods in Stream Ecology, Volume 1 (Third Edition) (pp. 49-70). https://doi.org/10.1016/B978-0-12-416558-8.00003-2

Hillel, D., 2000. Salinity Management for Sustainable Irrigation: Integrating Science, Environment, and Economics. World Bank Publications.

Hossain, M.B., Yesmin, S., Maniruzzaman, M. and Biswas, J.C., 2017. Irrigation scheduling of rice (Oryza sativa L.) using CROPWAT model in the western region of Bangladesh.

Hume, I.V., summers, D.M. and Cavagnaro, T.R., 2021. Self-sufficiency through urban agriculture: Nice idea or plausible reality? *Sustainable Cities and Society*, *68*, p. 102770.

Hussien, K., Woldu, G., and Birhanu, S. (2019). A GIS-based multi-criteria land suitability analysis for surface irrigation along the Erer Watershed, Eastern Hararghe Zone, Ethiopia. East Afr. J. Sci. 13 (2), pp. 169–184.

Koirala, A., Walsh, K.B., Wang, Z. and McCarthy, C., 2019. Deep learning–Method overview and review of use for fruit detection and yield estimation. *Computers and electronics in agriculture*, *162*, pp. 219-234.

Kuscu, H., Turhan, A., Ozmen, N., Aydinol, P. and Demir, A.O., 2014. Optimizing levels of water and

nitrogen applied through drip irrigation for yield, quality, and water productivity of processing tomato (Lycopersicon esculentum Mill.). *Horticulture, Environment, and Biotechnology*, *55*, pp. 103-114.

Lendabo, G., Wulchafo, K. and Abayechaw, D., 2021. International Journal of Current Research and Academic Review. *Int. J. Curr. Res. Aca. Rev*, *9*(03), pp. 31-46.

Levidow, L., Zaccaria, D., Maia, R., Vivas, E., Todorovic, M. and Scardigno, A., 2014. Improving water-efficient irrigation: Prospects and difficulties of innovative practices. *Agricultural Water Management*, *146*, pp. 84-94.

Lovelli, S., Potenza, G., Castronuovo, D., Perniola, M. and Candido, V., 2017. Yield, quality and water use efficiency of processing tomatoes produced under different irrigation regimes in Mediterranean environment. *Italian Journal of Agronomy*, *12*(1).

Nangare, D.D., Singh, Y., Kumar, P.S. and Minhas, P.S., 2016. Growth, fruit yield and quality of tomato (Lycopersicon esculentum Mill.) as affected by deficit irrigation regulated on phenological basis. *Agricultural Water Management*, *171*, pp. 73-79.

Pribyl, D.W., 2010. A critical review of the conventional SOC to SOM conversion factor. *Geoderma* 156 (3–4), pp. 75–83.

Roth, G., Harris, G., Gillies, M., Montgomery, J. and Wigginton, D., 2014. Water-use efficiency and productivity trends in Australian irrigated cotton: a review. Crop and Pasture Science, 64(12), pp. 1033-1048.

Rowell, 1994. Based on the soil textural class determination triangle of the International Soil Science Society (ISSS) system

Samui, I., Skalicky, M., Sarkar, S., Brahmachari, K., Sau, S., Ray, K., Hossain, A., Ghosh, A., Nanda, M.K., Bell, R.W. and Mainuddin, M., 2020. Yield response, nutritional quality and water productivity of tomato (Solanum lycopersicum L.) are influenced by drip irrigation and straw mulch in the coastal saline ecosystem of Ganges delta, India. *Sustainability*, *12*(17), p. 6779.

Surendran, U., Sushanth, C.M., Mammen, G. and Joseph, E.J., 2014. Modeling the impacts of an increase in temperature on irrigation water requirements in Palakkad district: A case study in humid tropical Kerala. Journal of Water and Climate Change, 5(3), pp. 472-485.

Surendran, U., Sushanth, C.M., Mammen, G. and Joseph, E.J., 2015. Modelling the crop water requirement using FAO-CROPWAT and assessment of water resources for sustainable water resource management: A case study in Palakkad district of humid tropical Kerala, India. *Aquatic Procedia*, *4*, pp. 1211-1219.

Swelam, A., El-Marsafawy, S. and Elbana, M., 2019. Effective management of on-farm irrigation for some major crops in Egypt using the CROPWAT model. *Misr Journal of Agricultural Engineering*, *36*(1), pp. 105-122.

Walkley, A. and Black, I.A., 1934. An examination of the Degtjareff method for determining soil organic matter, and a proposed modification of the chromic acid titration method. Soil science, 37(1), pp. 29-38.

Xiao, Z., Lei, H., Jin, C., Pan, H. and Lian, Y., 2022. Relationship between the dynamic characteristics of tomato plant height and leaf area index with yield, under aerated drip irrigation and nitrogen application in greenhouses. *Agronomy*, *13*(1), p. 116.

Xinchun, C., Mengyang, W., Xiangping, G., Yalian, Z., Yan, G., Nan, W. and Weiguang, W., 2017. Assessing water scarcity in agricultural production system based on the generalized water resources and water footprint framework. *Science of the Total Environment*, *609*, pp. 587-597.

Zou, X., Niu, W., Liu, J., Li, Y., Liang, B., Guo, L. and Guan, Y., 2017. Effects of residual mulch film on the growth and fruit quality of tomato (Lycopersicon esculentum Mill.). *Water, Air, & Soil Pollution*, *228*, pp. 1-18.

Italian Journal of Agrometeorology
Rivista Italiana di Agrometeorologia

Firenze University Press
https://riviste.fupress.net/index.php/IJAm

OPEN ACCESS

Citation: Alvar-Beltrán, J., & Franceschini, G. (2024). Effect of future climate on crop production in Bhutan. *Italian Journal of Agrometeorology* (2): 101-119. doi: 10.36253/ijam-2782

Received: May 27, 2024

Accepted: October 8, 2024

Published: December 30, 2024

© 2024 Author(s). This is an open access, peer-reviewed article published by Firenze University Press (https://www.fupress.com) and distributed, except where otherwise noted, under the terms of the CC BY 4.0 License for content and CC0 1.0 Universal for metadata.

Data Availability Statement: All relevant data are within the paper and its Supporting Information files.

Competing Interests: The Author(s) declare(s) no conflict of interest.

ORCID:
JA-B: 0000-0003-2454-0629
GF: 0000-0001-8140-3706

Effect of future climate on crop production in Bhutan

Jorge Alvar-Beltrán*, Gianluca Franceschini

Food and Agriculture Organization (FAO) of the United Nations, Rome, Italy
*Corresponding author: jorge.alvarbeltran@fao.org

Abstract. Understanding the relationship between adverse weather conditions and crop productivity is the backbone of risk assessments on food security. It is paramount in countries like Bhutan, which has a limited number of impact assessment studies in agriculture. The work presented here highlights agricultural production trends under a changing climate and the attribution of yield changes to a specific weather hazard. Thus, the relationship between climate and yields is improved by running the Food and Agriculture Organization (FAO) Python Agroecological Zoning (PyAEZ) model with state-of-the-art climate projections from the Coordinated Regional Climate Downscaling Experiment (CORDEX-CORE). At the national level, we analyze climate change impacts on yields for ten crops (grain maize, foxtail millet, buckwheat, wheat, wetland rice, common beans, cabbage, white potatoes, carrots, and citrus). The main simulation findings point to higher yield variations, either a gain or a loss, under rainfed conditions for the Representative Concentration Pathway (RCP) 8.5 as opposed to irrigated conditions and RCP 2.6; for example, by +17.4% (white potatoes), +15.3% (wheat), +12.8% (cabbage), -5.8% (citrus), and -6.7% (buckwheat) under RCP 8.5 by 2070-2099. Yield results show the potential of irrigation to modulate adverse weather conditions and to improve crop performance by +43.4% on average for all crops as opposed to rainfed crops which are more exposed to weather hazards (i.e., heat stress and dry spells). This study also sheds light on the most impactful weather perils describing 28% (RCP 2.6) and 33% (RCP 8.5) of the yield variability over time. Thus, our findings support smallholder farmers, decision-makers, and project formulators in developing adaptation solutions that minimize the effects of growing adverse weather conditions on crop yields.

Keywords: agricultural meteorology, crop modelling, food security, climate change.

1. INTRODUCTION

The Kingdom of Bhutan (hereafter Bhutan) is a small landlocked country located on the eastern side of the Himalayas. Historically isolated due to challenging topography, the country's economy is dependent on climate-sensitive sectors such as agriculture, hydropower, and forestry. Subsistence farming is adversely affected by temperature changes and shifting monsoon patterns, while hydropower critically depends on anticipated and stable precipitation patterns, likely to be altered by climate change. According to the

National Environmental Commission (NEC, 2023), the country's rich biodiversity and extensive forest cover are already affected by climate change, having cascading consequences for the tourism and services sectors.

This Himalayan country is typically agrarian, with most of the population (56%) relying on agriculture for their livelihoods and accounting for 15% of the country's gross domestic product (ILO, 2019). Smallholder farmers cultivate staple crops (i.e., rice, maize, barley, wheat, and millet) for household consumption. However, from a socioeconomic standpoint, rice, maize, and potato are the most important crops in Bhutan. Smallholder farmers are particularly vulnerable to changing climatic patterns; even small variations in the departure of the summer monsoon season can have dire consequences on livelihoods. Farmers are increasingly aware of climate change because weather-related impacts represent 10 to 20% of the crop damage (Chhogyel, 2020). Additional studies on farmers' perceptions show that 94% of the farmers perceive a change in local climate, and about 86% are aware of the potential impacts of climate change on their livelihoods (Katwal et al. 2015). For most Bhutanese farmers, climate change means unpredictable weather, less or no rain, and drying of water resources. Farmers also refer to climate change as the arrival of pests and diseases, intensification of rains, less snow cover, and shorter winters.

The limited information on climate extremes in South Asian countries, including Bhutan, is often cited in the literature (Naveendrakumar et al. 2019). Although there are several impact studies assessing the effect of past and future climate on agricultural production in Bhutan, some of the existing literature suggests that weather extremes, including weather-related pests and diseases, are the main drivers of crop production losses. The latter is particularly important in Bhutan, which, for example, experienced a rice blast epidemic in 1995-96 that resulted in a yield loss of 70 to 90% in high-altitude temperate rice-growing areas. Based on the Ministry of Agriculture and Forests (MoAF, 2011) and NEC (2011) estimates, the grey leaf spot disease severely affected maize production between 2005 and 2007, and by 50% during the 2015 outbreak of maize blight disease; whereas a hailstorm event in 2012 damaged 30 to 40% of the cropland in Punakha (Chhogyel and Kumar, 2018). According to the Department of Agriculture (DoA, 2016), hailstorms and high-intensity rains negatively affected rice-producing areas in 2015 and 2016. Widespread damages to irrigation channels from landslides, triggered by heavy monsoon rains, have also been reported across the country.

Despite increasing efforts to reduce Bhutanese farmers' vulnerability to climate change, the existing policy instruments have not been adequately streamlined into the development plans. There is not yet a clear research and development agenda to mitigate and adapt farming activities to increasing climate adversities (Choden et al. 2020). It is, therefore, paramount to strengthen policy instruments that modulate climate change impacts, enhance smallholder farmers' resilience, and improve crop productivity.

Because of the reasons mentioned above, this study applies PyAEZ, which is an assistant tool for countries interested in integrating local-level data into national-level assessments. In the Asia and Pacific region, only a few countries (i.e., Laos, Thailand, and Nepal) have tested PyAEZ (FAO, 2017; Alvar-Beltrán et al. 2023). The study from Alvar-Beltrán et al. (2023), for example, describes PyAEZ simulation constraints (i.e., pests and diseases and CO_2 fertilization effect on crop growth are not considered; reliance on global climate, soil, and land cover datasets are known to be uneven across regions, among others) and various applications for agricultural development planning and for preparing rapid impact assessments in agriculture. Despite these constraints, rapid impact assessments using PyAEZ are necessary for timely decision-making, accelerated response to emergencies, policy formulation, monitoring and evaluation, and risk management. They are indeed particularly important in countries where there is scarce information or obsolete studies. Thus, this work aims to fill the information gap on climate risks in agriculture by strengthening the linkages between weather hazards and impacts on key crops sustaining national food production and the livelihoods of smallholder farmers across Bhutan. Lastly, it offers a better understanding of the changing climate dynamics and identifies weather perils likely to be harmful to national agricultural production.

2. MATERIALS AND METHODS

2.1. Area of study

According to Köppen's climatic classification, Bhutan is characterized by a humid sub-tropical climate and a sub-tropical highland oceanic climate (Cwb) along the low-lying areas (< 800 m.a.s.l.), mid-hills (800-1800 m.a.s.l.), and high-hills (1800-3000 m.a.s.l.), respectively (Beck et al. 2005). A temperate continental (Dwb), cool continental (Dwc), and tundra climate (ET) progressively appear towards the higher altitude areas of the Himalayas. As a result of a mosaic of climates, MoAF has divided the country into six agroecological zones, each with singular climatic conditions (Fig. 1). Four of them (wet sub-tropical, humid sub-tropical, dry sub-tropical, and

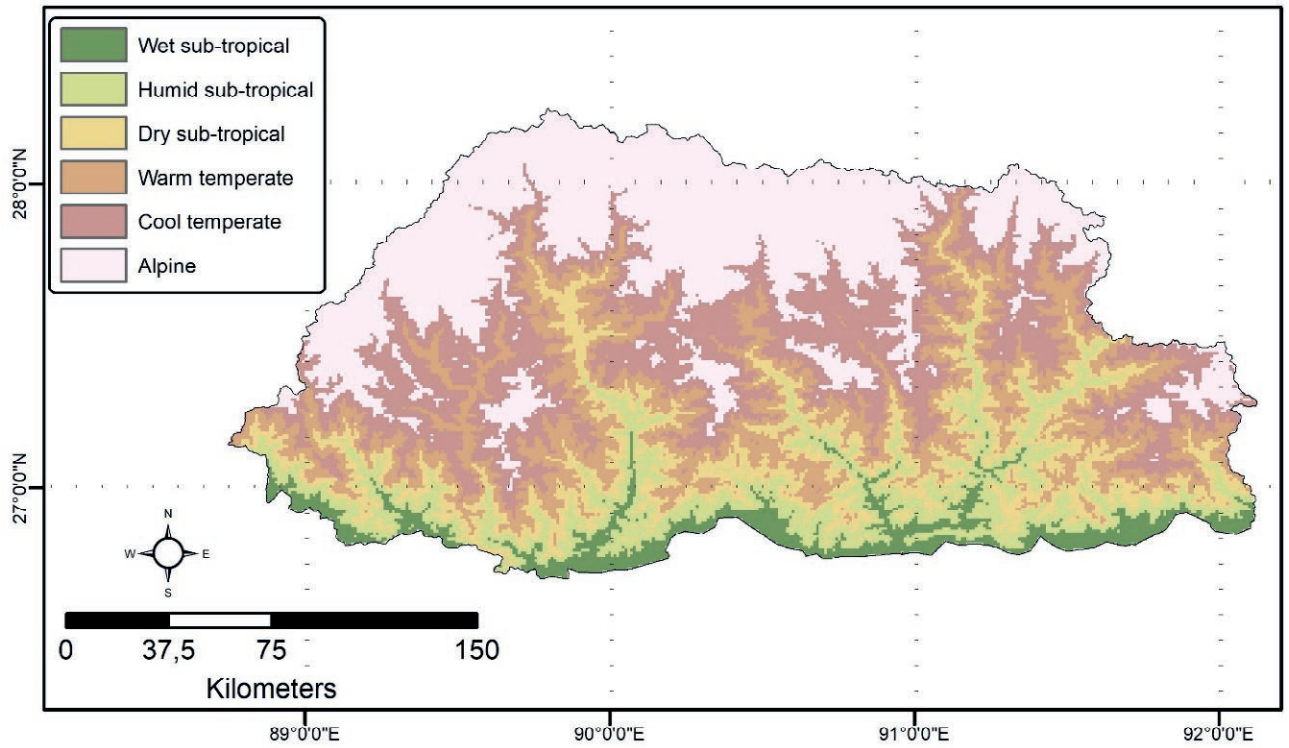

Figure 1. Agroecological zones of Bhutan.

warm temperate) are agriculturally predominant, while one (cool temperate) is considered an agricultural marginal area, and the remaining one (alpine) livestock predominant.

2.2. Climate projections

Daily minimum and maximum temperatures, and precipitation data from the Coordinated Regional Climate Downscaling Experiment (CORDEX) - Coordinated Output for Regional Evaluations (CORE) - were used in this study. Briefly, the CORDEX-CORE initiative has created a shared climate modelling framework worldwide (Giorgi et al. 2021) by providing homogeneous regional climate projections for most inhabited land regions using nine CORDEX domains at 0.22º spatial resolution (25 km). Three Global Climate Models (GCMs) for high (HadGEM2-ES), medium (MPI-ESM), and low (NorESM) equilibrium climate sensitivities, representing the full ensemble of the Coupled Model Intercomparison Project (CMIP5), were dynamically downscaled using one Regional Climate Model (RCM), namely REMO, under two Representative Concentration Pathways (RCP), RCP 2.6 and RCP 8.5 (Coppola et al. 2021; Teichmann et al. 2021). For the 1981-2010 historical period, we used the W5E5 merged dataset, which combined the WFDE5 dataset over land with the ERA5 dataset over the ocean (Cucchi et al. 2020). W5E5 is commonly used in impact assessment studies and has been adopted by the Inter-Sectoral Impact Model Intercomparison Project (ISIMIP) as the official product for the bias correction of atmospheric models. Thus, the CORDEX-CORE simulations were bias-corrected using the W5E5 reanalysis dataset for the 1980-2005 period, time slice where both datasets overlap.

2.3. Agroecological zoning (PyAEZ)

Yields were estimated based on an eco-physiological model developed by FAO (Kassam et al. 1991; Kassam, 1977). We adopted the simplified version of AEZ, implemented in Python (PyAEZ), and publicly available through a GitHub repository (https://github.com/gicait/PyAEZ). Geo-referenced global climate (see section 2.2), soil (from the Harmonized World Soil Database at 0-30 and 30-100 cm soil depth), land cover (from the Global Land Cover-SHARE), elevation, and terrain slope data (from the Shuttle Radar Topography Mission) were combined into a land resources database, which was then assembled into global grids at a resolution of 30 arc-seconds (about 0.9 by 0.9

km at the equator) (Fischer et al. 2021; Latham et al. 2014; Nachtergaele et al. 2012). Constraint-free crop biomass was accumulated during the growing season, mainly driven by incoming solar radiation, temperature, and crop-specific characteristics (i.e., growing length, maximum photosynthetic rate, leaf area index (LAI) at full development, harvest index, and crop's sensitivity to heat provision). To maximize yields, the start of the growing season was automatically determined by PyAEZ. Simulations were run on an annual basis independently for rainfed and irrigated conditions for all ten crops (buckwheat, foxtail millet, grain maize, wetland rice, wheat (subtropical cultivar), common bean, cabbage, white potatoes, carrots, and citrus) and averaged for the 2010-2039, 2040-2069, and 2070-2099 periods. Reference historical yield values (Table 1) were used to bias-correct future crop simulations. Most of the crop parameters (e.g. length of growth cycle, LAI, harvest index) were adapted from Fischer et al. (2021), using the cultivar and corresponding crop characteristics that were more common in the country.

The procedure to assess the maximum attainable yield was conducted in PyAEZ by calculating an automatic crop calendar based on the most suitable climatic and perfect management conditions. The simulations were run 365 times per year with a moving window of a day to identify the starting date when the highest final yields were obtained. This meant that the starting growing date changed each year according to the specific annual climatic conditions. While some crops may have multiple growing seasons in a year, only one simulation period was computed per crop, representing the one simulating the highest yield.

The assessment of rainfed yields was done by calculating a daily water balance and applying a yield-reduction factor (associated with yield stress) at each phenological stage. Daily soil moisture balance calculation procedures followed the methodologies outlined by Allen et al. (1998). Briefly, the quantification of a crop-specific water balance determined the crop's actual evapotranspiration (ETa), a measure used for calculating water-constrained crop yields by comparing ETa with a crop's evaporative demand. As a result, the daily reference soil water balance was calculated for each grid cell and actual evapotranspiration was estimated for each crop.

Table 1. Average crop yields (kg/ha) for 2018-2022. Yield values presented in Table 1 were usually lower than those of PyAEZ simulations which considered the maximum attainable yields. Source: FAOSTAT

Crop	Yield (kg/ha)
Maize (corn)	3492.0
Millet	1189.4
Buckwheat	1166.4
Wheat	1310.1
Rice	4240.0
Beans (dry)	1038.4
Cabbage	7146.2
Potatoes	10497.9
Carrots and turnips	10759.2
Citrus (lemons and limes)	3313.7

2.4. Attributing adverse weather conditions

Understanding the impact of adverse weather conditions on simulated crop yields required a dynamic statistical approach to (i) identify adverse weather conditions, (ii) assess the goodness of fit of the statistical model, and (iii) select the best model by dynamically repeating the process. For this reason, we developed a tailored computational and statistical framework (Fig. 2). Briefly, climate models were processed to retain climate information only for the growing period. The selected period was different every year, as PyAEZ adopted a dynamic sowing date approach (see results in supplementary section). Then, adverse weather conditions such as warm days, cold days, dry days, wet days, maximum and mean duration of dry spells were computed. Results were spatially averaged and correlated adverse weather conditions were removed. Multiple linear regression was applied to explain the predicted yield. In each case, a dynamic selection of thresholds was used for calcu-

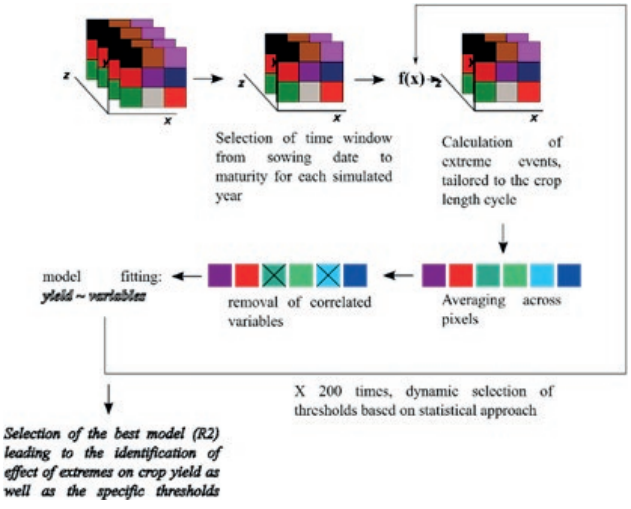

Figure 2. The statistical and computational framework used for the quantification of adverse weather conditions and to assess their impacts on crop yields.

lating weather extremes. At the end of the simulation cycle, only the best model (highest R^2) was retained. This R^2 analysis allowed us to discern the most impactful adverse weather conditions on crop yields, describing the percentual change of the output variable (yield) explained by the input variable (adverse weather condition). This approach was then repeated for each crop, year, RCP, and climate model, resulting in around 12,000 simulations.

3. RESULTS

3.1. Future climate

For projected precipitation changes, the different climate models and scenarios showed less model agreement. Briefly, total annual precipitation displayed minimal anomalies (positive/negative) in the near (2020-2039) and mid-term (2040-2069) for both RCPs. However, total annual rainfall anomalies were heightened towards the end of the century, with a decline along the low-lying and agricultural predominant areas, particularly under RCP 8.5 (-100 to -200mm) and, to a minor extent, under RCP 2.6 (0 to -100mm). Supp. Fig. 1 showed the changes in monthly precipitation across the century for both RCPs. Projected changes were minimal between November and March and peaked during the summer monsoon season. For example, the wet-subtropical and humid sub-tropical agro-ecological zones were projected to experience a decline in monthly precipitation (June, August and September) ranging from -50 to -150mm/month by 2070-2099 under RCP 8.5. Conversely, cool temperate and alpine climates, corresponding to the non-agricultural predominant areas, were thought to experience a precipitation increase during the summer monsoon season of about 50 to 100 mm/month under RCP 8.5 by 2070-2099. Additionally, the pre-monsoon months (April and May) were projected to gain in precipitation, particularly towards the southeast of Bhutan.

Mean maximum temperature (hereafter Tmax) anomalies were heightened towards the high-altitude areas from January to March (Supp. Fig. 2). Tmax was projected to increase by 1 to 2°C under RCP 2.6 and by 3 to 5°C under RCP 8.5 by 2070-2099 compared to 1980-2005. Although mean minimum temperature (hereafter Tmin) anomalies displayed a similar spatiotemporal pattern to that of Tmax, the rate of increase was higher across the century. For example, Tmin was projected to increase by 4 to 6°C, or a staggering 7 to 9°C over the Himalayas, from January to March under RCP 8.5 by 2070-2099 compared to 1980-2005 (Supp. Fig. 3). For both climatic variables (Tmax and Tmin), the spatial changes during the summer monsoon season (from June to September) were softened across Bhutan.

3.2. Crop suitability analysis

3.2.1. Cereal crops

For maize (Fig. 3a) under rainfed conditions, PyAEZ yield simulations showed no significant changes (+0.3%) over time in RCP 2.6 (from 4,064 to 4,077 kg/ha) and a slight loss (-2.1%) in RCP 8.5 (from 4,053 to 3,968 kg/ha) between 2010-2039 and 2070-2099. The shortfalls in maize production under RCP 8.5 can also be attributed to a decline in monthly precipitation over the rainy season (June to September), particularly along the mid-hills and low-lying areas of Bhutan (Supp. Fig. 1). Additionally, while all the GCMs agreed on projected yield changes under RCP 2.6, some differences were observed under RCP 8.5, with higher yields simulated in MPI-ESM (4,133 kg/ha) compared to NorESM1-M and HadGEM2-ES (3,920 kg/ha) on average across the century. For irrigated conditions, there were no major yield differences over time. Overall, the average maize yields simulated across the century under irrigated conditions were 25% higher than those simulated under rainfed conditions for both RCPs and GCMs. Lastly, under perfect management conditions, the most optimal sowing date to attain the highest yields was 117 calendar days for HadGEM2-ES, 114 for NorESM1-M, and 101 for MPI-ESM. However, the trends for the most optimal sowing date showed a delay for NorESM1-M and MPI-ESM, thus, leading to a similar sowing date as that of HadGEM2-ES towards the end of the century (Supp. Fig. 4a).

For foxtail millet (Fig. 3b) under rainfed conditions, yield simulations showed a minimal positive anomaly (+1.4%) over time in RCP 2.6 (from 1,766 to 1,790 kg/ha) and a decreasing trend (-3.4%) in RCP 8.5 (from 1,769 to 1,708 kg/ha) between 2010-2039 and 2070-2099. The monthly precipitation decline over the rainy season largely explained the losses in millet yields, particularly under RCP 8.5 (Supp. Fig. 1). Additionally, remarkable foxtail millet yield anomalies were simulated among different GCMs, especially when comparing HadGEM2-ES and MPI-ESM to NorESM1-M under RCP 2.6. Across the century, the latter two GCMs simulated higher yields (1,804 kg/ha) than NorESM1-M (1,723 kg/ha) under RCP 2.6. On the other hand, for irrigated conditions, PyAEZ simulations did not show major yield differences over time (2,092 kg/ha). However, while HadGEM2-ES and MPI-ESM displayed similar yields (2,077 kg/ha) for both RCPs, NorESM1-M projected a slightly higher yield (2,143 kg/ha) under RCP 8.5. Lastly, large differences

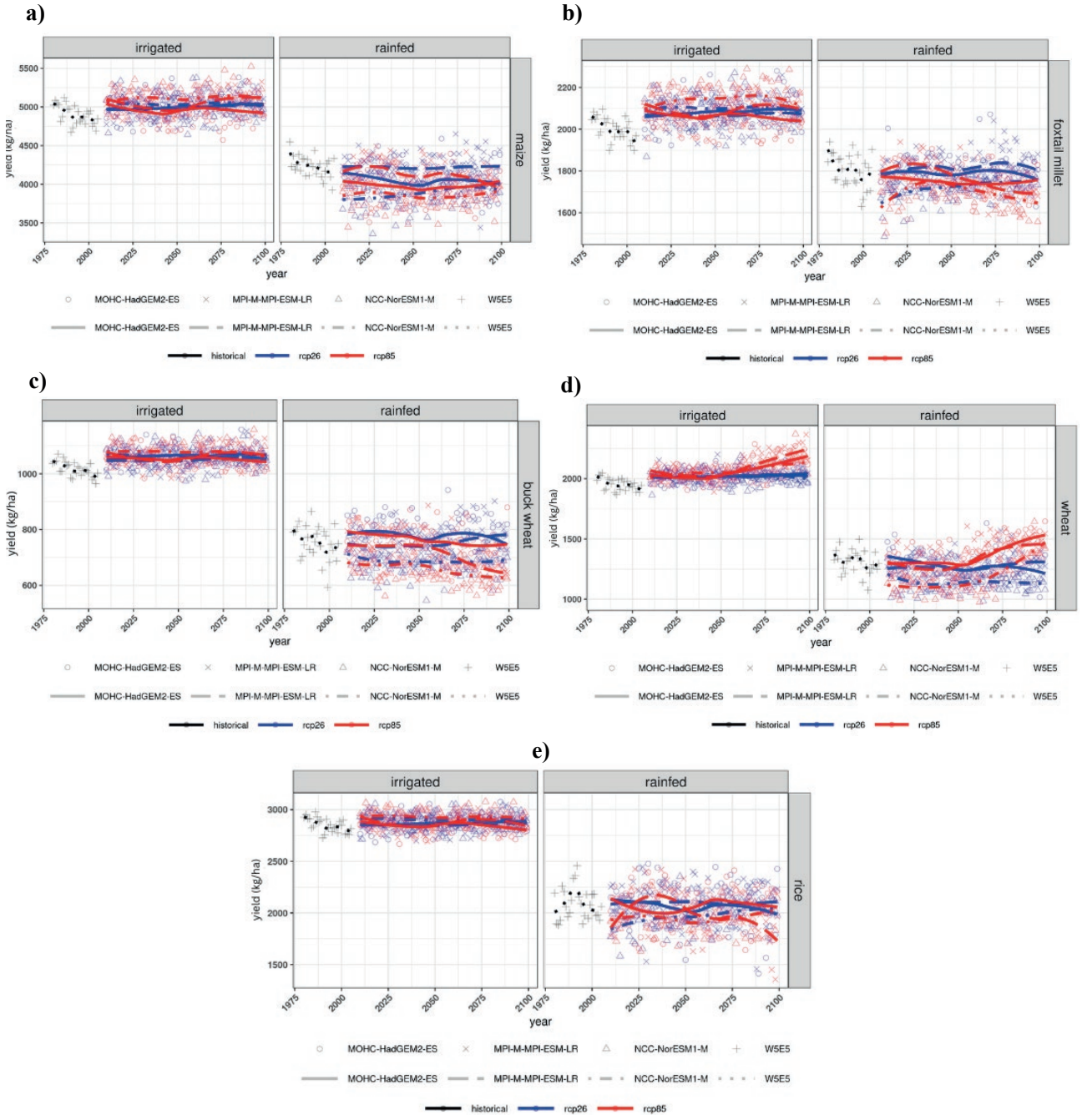

Figure 3. National level yield trends (kg/ha) for **(a)** maize, **(b)** foxtail millet, **(c)** buckwheat, **(d)** wheat, and **(e)** rice under irrigated and rainfed conditions for RCPs 2.6 and 8.5 over the 2010-2099 period. Future yield simulations were based on three GCMs and historical information on the W5E5 dataset.

were simulated for the most optimal sowing date among GCMs. While NorESM1-M simulated 134 calendar days as the most optimal sowing date, for MPI-ESM it was 112 days. Overall, all models agreed on an earlier sowing date to attain the highest yields (Supp. Fig. 4b).

For buckwheat (Fig. 3c) under rainfed conditions, PyAEZ yield simulations showed no significant anomalies (+0.1%) over time in RCP 2.6 (from 743 to 744 kg/ha) and declining trends (-6.7%) in RCP 8.5 (from 731 to 682 kg/ha) between 2010-2039 and 2070-2099. However, sig-

nificant yield differences were detected when comparing different GCMs, particularly between HadGEM2-ES and NorESM1-M. In this case, HadGEM2-ES (high sensitivity to GHG emissions) simulated higher yield trends than NorESM1-M (low sensitivity to GHG emissions). Conversely, for irrigated conditions, PyAEZ simulations did not exhibit major differences between RCPs, with an average yield of 1,062 kg/ha across the century. Overall, under irrigated conditions, buckwheat yields were approximately 46% higher compared to those simulated under rainfed conditions. Lastly, under perfect management conditions, all GCMs agreed on a similar sowing date to attain the highest yields, ranging from 152 (HadGEM2-ES) to 138 (MPI-ESM) calendar days (Supp. Fig. 4c). However, different trends on the most optimal sowing date were displayed along the century, with an earlier sowing date of about 10 days for HadGEM2-ES and NorESM1-M and a delay of about 5 days for MPI-ESM.

For wheat (Fig. 3d) under rainfed conditions, PyAEZ yield simulations displayed a slight decline (-1.0%) under RCP 2.6 (from 1,245 to 1,232 kg/ha) and a significant yield gain (+15.3%) under RCP 8.5 (from 1,227 to 1,415 kg/ha) between 2010-2039 and 2070-2099. The former yield changes can be attributed to more optimal temperatures during the winter season and to a slight precipitation increase (e.g. April and May) during the grain filling phase of wheat, particularly under RCP 8.5. Furthermore, under RCP 8.5, all three GCMs agreed on a notable yield increase over time, though with slight differences in the timing of the increase. Similarly, for irrigated conditions, higher wheat yields were simulated under RCP 8.5 (2,142 kg/ha) compared to RCP 2.6 (2,027 kg/ha) by 2070-2099. Similarly to the other crops, inter-annual yield variability under irrigated conditions was much lower than that simulated under rainfed conditions due to the high variations in soil water balance when fields were not irrigated. Lastly, all three GCMs displayed minor changes in the most suitable sowing date throughout the century. Although the main planting season usually occurs from November to December, PyAEZ simulations pointed to higher yields if sown after 71 calendar days (Supp. Fig. 4d). However, the latter sowing date overlaps with the preparation of the land of other crops, such as maize that is usually sown during the spring season.

For rice (Fig. 3e) under rainfed conditions, PyAEZ simulations showed minimal yield changes (+0.2%) under RCP 2.6 (from 2,052 to 2,057 kg/ha) and a slight decline (-1.6%) under RCP 8.5 (from 2,033 to 2,001 kg/ha) between 2010-2039 and 2070-2099. However, under RCP 8.5 for MPI-ESM, simulated yields were estimated to decrease by -7.1% (from 2,076 kg/ha to 1,928 kg/ha) between the 2010-2039 and 2070-2099 periods. For irrigated conditions, rice yields remained constant over time, with low inter-annual yield differences and similar yield values under both RCPs. Generally, large differences of up to 42% (from 2,880 kg/ha to 2,027 kg/ha) were observed when comparing the yields simulated under irrigated and rainfed conditions, respectively, across the century for both RCPs. Lastly, all GCMs agreed on a similar sowing date to attain the highest rice yields, ranging from 111 (HadGEM2-ES) to 98 (MPI-ESM) calendar days (Supp. Fig. 4e).

3.2.2. Legumes, vegetables, and tuber crops

For common beans (Fig. 4a) under rainfed conditions, PyAEZ yield simulations did not display a change (0.0%) in RCP 2.6 and a loss (-4.8%) in RCP 8.5 (from 1,126 to 1,072 kg/ha) between 2010-2039 and 2070-2099. The reported decline under RCP 8.5 was largely due to increasing number of warm days and mean dry spell duration (Fig. 8). Additionally, under RCP 8.5, the negative yield change was expected in the second half of the 21st century. Simulations for common beans showed large inter-annual yield differences between GCMs, particularly under RCP 8.5. Conversely, for irrigated conditions, similar yields (1,410 kg/ha) were projected under both RCPs across the century. However, from the mid-century onwards, the yield variability was expected to increase. Overall, the average yield differences across the century between irrigated and rainfed conditions were 26% for both RCPs and all GCMs. Additionally, simulations on the most optimal sowing date to attain the highest yields show large differences across the century (Supp. Fig. 4f). On average, HadGEM2-ES simulated the latest sowing date (124 calendar days), while MPI-ESM the earliest sowing date (104 calendar days).

For cabbage (Fig. 4b) under rainfed conditions, PyAEZ yield simulations did not show anomalies over time (-0.3%) in RCP 2.6 (from 1,893 to 1,888 kg/ha) and a moderate gain (+12.8%) in RCP 8.5 (from 1,865 to 2,104 kg/ha) between 2010-2039 and 2070-2099. Under RCP 8.5, the rate of yield enhancement was significant from mid-century until the end of the century. For irrigated conditions, yield trends for cabbage were identical to those simulated for wheat. The average cabbage yield remained constant (2,892 kg/ha) under RCP 2.6, while there was a notable increase under RCP 8.5, especially when comparing 2010-2039 (2,907 kg/ha) and 2070-2099 (3,044 kg/ha). Lastly, all GCMs agreed on a similar sowing date to attain the highest cabbage yields, ranging from 66 to 72 calendar days, as well as on a slight delay on the most optimal sowing date across the century (Supp. Fig. 4g).

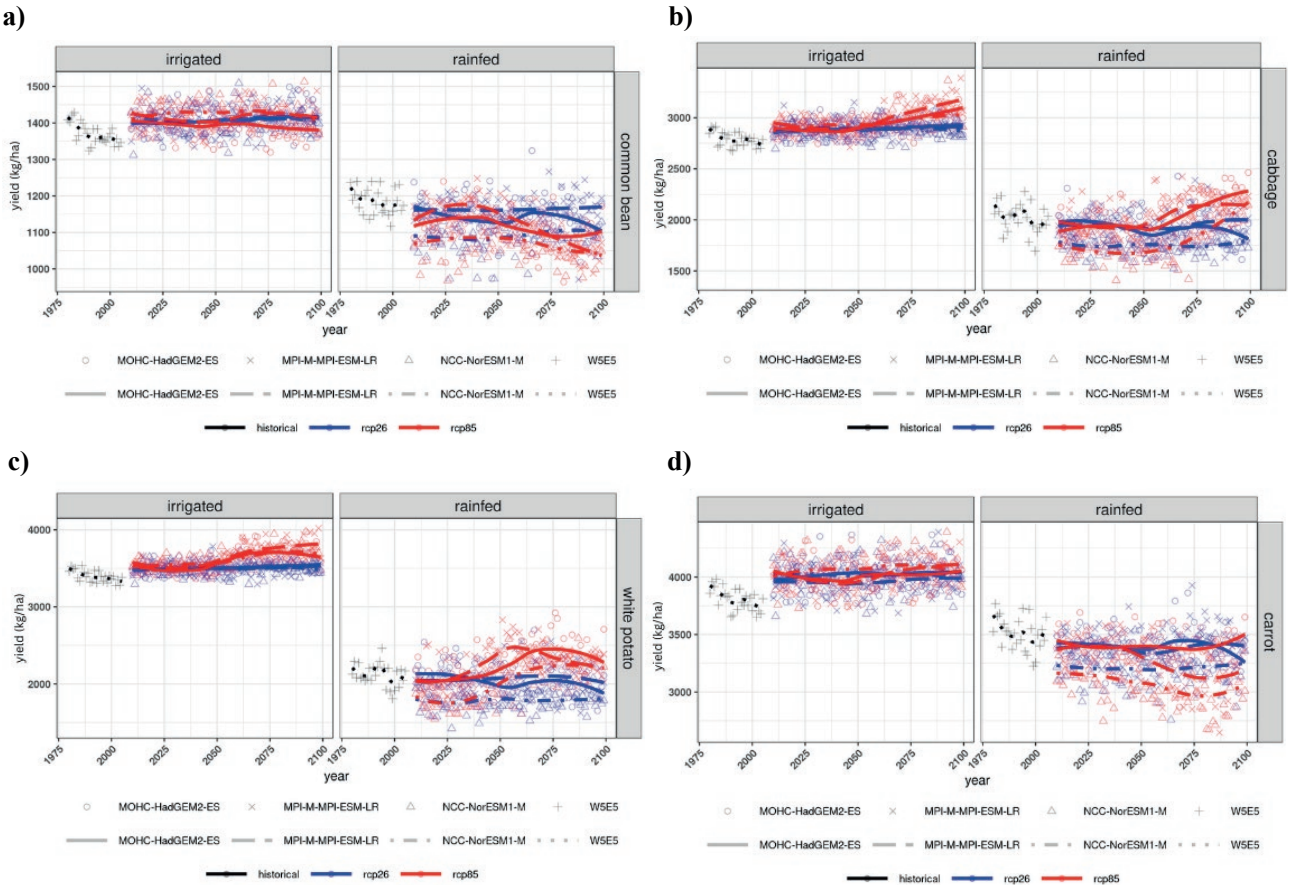

Figure 4. National level yield trends (kg/ha) for **(a)** common beans, **(b)** cabbage, **(c)** white potatoes, and **(d)** carrot under irrigated and rainfed conditions for RCPs 2.6 and 8.5 over the 2010-2099 period. Future yield simulations were based on three GCMs and historical information on the W5E5 dataset.

For white potatoes (Fig. 4c) under rainfed conditions, PyAEZ yield simulations did not display a major change (-0.6%) over time in RCP 2.6 (from 1,978 to 1,968 kg/ha) and showed a notable increase (+17.4%) in RCP 8.5 (from 1,962 to 2,303 kg/ha) between 2010-2039 and 2070-2099. Under RCP 8.5, all three GCMs showed similar yield trends over time, with a strong increase up until mid-century and a slight to moderate decrease towards the end of the century. Higher inter-annual yield variability was projected under RCP 8.5 compared to RCP 2.6. For irrigated conditions, white potato yields were likely to remain constant (+0.8%) under RCP 2.6 and increase (+5.5%) under RCP 8.5 (from 3,525 to 3,719 kg/ha) by 2070-2099 compared to 2010-2039. Overall, significantly higher yields (72%) were expected under irrigated conditions (3,562 kg/ha) compared to rainfed conditions (2,067 kg/ha) when averaged across the century for both RCPs and the three GCMs. All three GCMs displayed a similar optimal sowing date (79 calendar days) (Supp. Fig. 4h). The latter matched farmers sowing calendars, as potatoes are traditionally sown in the spring, around March to April.

For carrot (Fig. 4d) under rainfed conditions, PyAEZ yield simulations did not show a change (+0.1%) over time in RCP 2.6 (from 3,344 to 3,346 kg/ha) and a slight loss (-3.9%) under RCP 8.5 (from 3,309 to 3,181 kg/ha) between 2010-2039 and 2070-2099. However, under RCP 8.5, simulations emerging from different GCMs showed divergent behavior, leading to uncertainty over time. While MPI-ESM and NorESM1-M displayed similar yield trends over time (a decrease from 2050 onwards), HadGEM2-ES projected an increase towards the end of the century. On the other hand, under irrigated conditions, carrot yields showed similar performance under both RCPs and across all GCMs when comparing 2010-2039 and 2070-2099. Overall, higher yields (22%) were projected across the century under irrigated conditions (4,018 kg/ha) compared to rainfed conditions (3,288 kg/ha) when averaged across the century for both RCPs and the three

GCMs. Regarding the most suitable sowing date, the earliest sowing date to attain the highest yields was simulated by HadGEM2-ES (88 calendar days), while the latest by NorESM1-M (97 calendar days) (Supp. Fig. 4i). All three GCMs agreed on an earlier sowing date, 15 to 20 days than baseline values, to attain the highest yields under future climatic conditions.

3.2.3. Tree-crop

For citrus tree (Fig. 5) under rainfed conditions, PyAEZ yield simulations showed a yield loss (-1.9%) in RCP 2.6 (from 2,471 to 2,425 kg/ha) and a moderate decrease (-5.8%) in RCP 8.5 (from 2,404 to 2,264 kg/ha) between 2010-2039 and 2070-2099. The projected decline under RCP 8.5 could be attributed to the compounded effect of several weather perils such as the alternation of warm and cold days as well as dry-spells, particularly during the flowering stage (typically from March to May) (Fig. 8). Although similar yield trends were projected over time for the three GCMs in RCP 8.5, higher average yields were simulated in MPI-ESM and HadGEM2-ES (2,357 kg/ha) compared to NorESM1-M (2,170 kg/ha). For irrigated conditions, citrus yields showed similar performance across both RCPs and all GCMs, though with a slight loss (from 2,917 to 2,901 kg/ha) when comparing 2010-2039 with 2070-2099. Overall, while a high inter-annual yield variability was projected under rainfed conditions, a low variability was simulated under irrigated conditions due to minimal changes in soil water balance.

3.3. Attributing adverse weather conditions to changes in crop yields

On average, weather extremes explained 28% and 33% of the yield variability over time under RCPs 2.6 and 8.5, respectively (Fig. 6). The impacts were also crop-dependent, with a high level of uncertainty between crops, ranging from high (rice) to low (citrus and wheat). The crops most affected by adverse weather conditions were citrus and common beans under RCPs 2.6 and 8.5, respectively. Furthermore, the most impactful adverse weather condition, explaining 20% to 50% of the yield changes for all ten crops, was heat stress, followed by dry spells (Fig. 7). Nonetheless, the impact of dry spells on yields increased with higher model sensitivity to GHGs, showing an opposite trend to that of heat stress. The latter was highlighted by the transparency of the colors (e.g., high transparency in Fig. 7 corresponded to a low R^2 value).

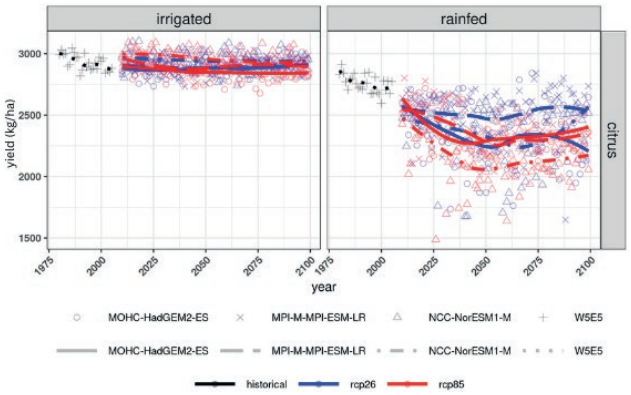

Figure 5. National level yield trends (kg/ha) for citrus trees under irrigated and rainfed conditions for RCPs 2.6 and 8.5 over the 2010-2099 period. Future yield simulations were based on three GCMs and historical information on the W5E5 dataset.

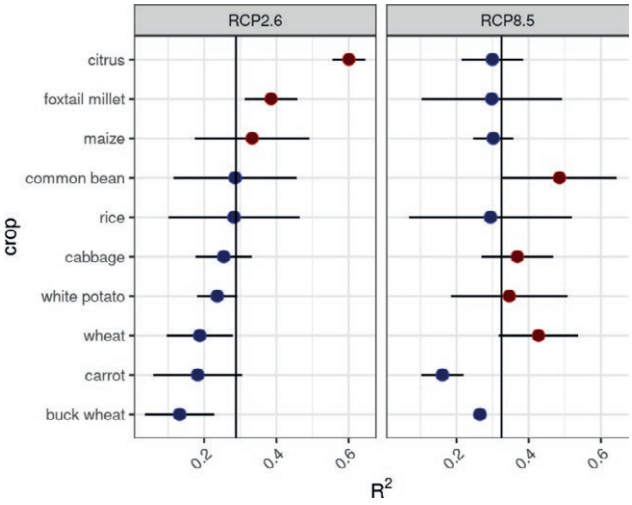

Figure 6. Impact of weather extremes on crops and associated uncertainty between GCMs.

The following analysis focuses on those crops most likely to be affected by different abiotic stresses (Fig. 8). The number of consecutive dry days will increasingly affect crop yields under RCP 8.5 compared to RCP 2.6. Although very wet days (here defined as heavy rainfall events with a dynamic threshold selected based on statistical significance) affected a small number of crops, their impact was higher under RCP 8.5. Overall, the findings suggested that erratic rainfall (e.g., heavy rainfall events followed by dry periods) will increasingly affect crop yields under RCP 8.5. Thus, under RCP 8.5, precipitation will be the main limiting factor reducing crop yields, exceeding the effect of heat stress, which was the most impactful weather hazard under RCP 2.6

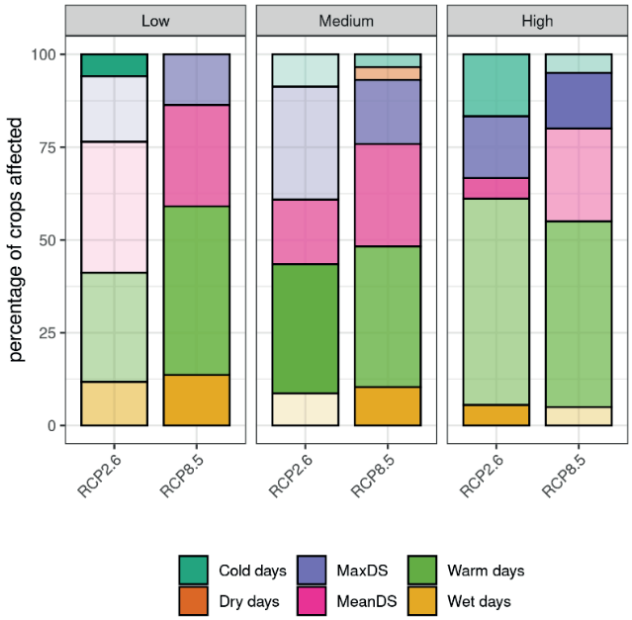

Figure 7. Percentage of crops affected by weather extremes based on different RCPs and GCMs sensitivity to GHG emissions (high: HadGEM2-ES; medium: MPI-ESM; low: NorESM1-M). The high transparency of the color indicated a low R^2 value.

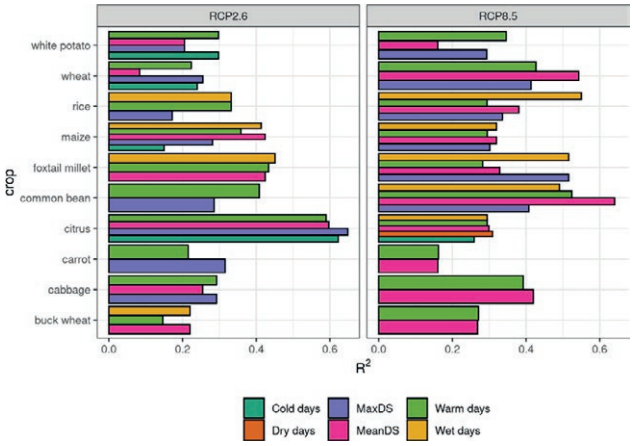

Figure 8. Impact of weather extremes on targeted crops for the ensemble of GCMs.

4. DISCUSSION

This work described the relationship between weather extremes and crop yields, explaining about 28% and 33% of the yield variation over time under RCPs 2.6 and 8.5, respectively. Heat stress and dry spells were identified as the most impactful weather hazards, accounting for 20% to 50% of the yield anomalies across the century. Thus far, there are national-level impact assessments examining the effect of elevated heat stress on crop production in Bhutan. However, regional studies have shown that yield gains due to the CO_2 fertilization effect would be offset by the negative impact of a 2°C increase in mean daily surface temperatures on irrigated rice and rainfed wheat (Lal, 2011). Studies also indicated a more significant warming during the spring and winter seasons, leading to shifting growing seasons, accelerated crop growth, increased evapotranspiration rates, affected pollination dynamics, and elevated pressure from pests and diseases on crops (e.g., wheat and maize).

Regarding precipitation indices, past climate analyses point to an increasing trend in the number of consecutive dry days during the 1996-2001 period across Bhutan (Llamo et al. 2023). While scientific studies are available on seasonal precipitation trends, little is known about precipitation extremes in Bhutan. Projections indicate an increase in total annual rainfall ranging from +10% to +30% under RCP 4.5 by 2070-2099, with a +5% to +15% increase in summer rainfall (NEC, 2020). The latter results align with this study's findings on total annual precipitation, though depending on the RCP (annual results not shown for brevity). However, conflicting findings emerged for monthly precipitation. While our findings pointed to a widespread loss in August and September, particularly under RCP 8.5, NEC (2020) suggested an increase. The compounded effect of weather perils, together with a slight increase (0 to +2 days for both RCPs) in the number of days with heavy precipitation ($R \geq 20$ mm/day) on an annual average (results not shown for brevity), are expected to have severe consequences (e.g., uprooting crops and waterlogging soils) on some of the studied crops, particularly among shallow-rooted (e.g., vegetables) and high-water-demanding crops (e.g., rice and maize).

Existing literature (e.g., NEC, 2011, 2020) on future crop yields in Bhutan, using the Decision Support System for Agrotechnology Transfer (DSSAT) model and the A1B Special Report on Emission Scenarios (SRES), showed a mean yield change for maize (without the CO_2 fertilization effect) ranging from -21% to -7% by 2040-2069. Conversely, our findings suggested stable yield trends under RCP 2.6 and a slight decline (-2.1%) under RCP 8.5. Although there is a likelihood of a decline in maize suitability areas, the reported loss is not significant (-3.4%) under RCP 4.5 by 2070 (NEC, 2020). The decline in maize yields was attributed to water deficits and accelerated crop development, which resulted in lower biomass accumulation and, consequently, in a yield decline. Similarly, in Nepal, a 20-day reduction in the growing cycle of maize was expected under RCPs 4.5 and 8.5 by the end of the century across the mid-hills

(Alvar-Beltrán et al. 2023). Furthermore, Parker et al. (2017) study, using the EcoCrop database of crop constraints and characteristics together with an ensemble of 31 GCMs, showed an increasing precipitation pattern across Bhutan. As a result, the suitability areas for maize were likely to increase in the future compared to the baseline period, particularly under RCP 8.5 and in the high-altitude areas of eastern Bhutan. However, a decline in maize yields was detected towards the southeastern parts due to hot temperatures exceeding the critical threshold for maize pollination.

For rice, a crop with a C3 photosynthetic pathway, the uncertainties were much higher with and without the CO_2 fertilization effect. Our results, which did not account for the CO_2 fertilization effect, showed an average (ensemble of GCMs for both rainfed and irrigated conditions) yield loss of -1% under RCP 8.5 by the end of the century. In contrast, NEC (2011) projected a yield change ranging from +72% to -27% by 2040-2069 depending on the climate scenario. Rice suitability may increase in the dzongkhag of Punakha, as well as in the eastern and southeastern parts of the country under RCPs 4.5 and 8.5, driven by optimal growing conditions and the CO_2 fertilization effect (Parker et al. 2017). Generally, an increase ranging from +8.9% to +13.9% in rice suitability areas was projected under RCPs 4.5 and 8.5 by 2050, with a decline (-3.3%) under RCP 8.5 by 2070 (NEC, 2020).

Similar to rice, wheat production under rainfed conditions might experience a yield gain (+15.5% for RCP 8.5 by the end of the century) in Bhutan, partially because future temperatures are not expected to exceed the critical threshold (Tmax >32°C) for pollen viability, as reported across different agroclimatic zones of Nepal (Alvar-Beltrán et al. 2023). However, the combined effect of elevated CO_2 and heat stress during meiosis can reduce pollen viability, spikelet number, and grain yield per spike (Bokshi et al. 2021). Additionally, NEC (2011) projected a positive yield trend for potatoes (+19% to +89% depending on the GCM) in Phobjikha, aligning with this study's findings (+17.7%) under rainfed conditions for RCP 8.5. Parker et al. (2017) also suggested that lower altitude areas in the south (<1000 m.a.s.l.) will no longer be suitable for potato production due to increasing temperatures, while mid- and high-altitude areas (1000-3000 m.a.s.l.) may experience an expansion in crop suitability over time, particularly under RCP 8.5 by 2050.

Although there is no scientific evidence on future climate impacts on vegetables, legumes, and tree crops in Bhutan, 10% to 20% damages in crop production (e.g., vegetables, mandarins, and apples) were already reported by the DoA between 2014 and 2016 (Chhogyel et al. 2020). Our work revealed an increase in the exposure of vegetables to weather adversities, particularly of cabbage, which is increasingly exposed and, thus, affected by a higher number of warm days and prolonged dry spells under RCP 8.5. However, citrus trees are expected to be less exposed to cold days under RCP 8.5. Under a warmer climate, citrus trees could expand to higher altitude areas (up to 1500 m.a.s.l.) in Nepal, which have similar bioclimatic characteristics to those of Bhutan (Atreya and Kaphle, 2020). However, higher temperatures and evaporation rates during flowering and fruit set could result in detrimental effects to citrus production in Bhutan.

5. CONCLUSIONS

Climate impact potential assessments on crop production are at an early stage in Bhutan. Although climate and crop and eco-physiological models and datasets can contain limitations (e.g., the quality and reliability of some of the underlying datasets of PyAEZ are known to be uneven across regions and the CO_2 fertilization effect is not considered in PyAEZ), if adequately processed, through statistical means and if their weaknesses well understood, they can be valuable for attributing adverse weather conditions to agricultural production and to assist field management decision-making in both rainfed and irrigated agriculture in Bhutan. The latter attribution allowed us to discern the weather hazards likely to be most harmful (i.e., heat stress and dry spells) to specific crops and, thus, to guide climate actions on the ground. The emerging findings of this work (see summary Table 2) can also be advantageous to identify tailored adaptation solutions, including the selection of most suitable sowing dates based on future climatic conditions, water allocation and water-related policies, which can modulate, to a certain extent, future weather perils on studied crops.

This study also showed the importance of irrigation to increase yields by +43.4% on average for all crops and RCPs across the century. In this line, adequate planning and implementation of irrigation systems recognizing the detrimental effects of climate change need to be thoroughly considered in water resource inventories aiming to strengthen the existing National Integrated Water Resource Management Plan. Agro-biodiversity is often cited in literature as one of the potential solutions to adapt to climate change in Bhutan, mainly through the development and use of biotic and abiotic tolerant varieties, strengthening the traditional seed system, and enhancing the on-farm diversity as an insurance to climate change impacts.

Table 2. Summary of yield changes (%) for selected crops under rainfed and irrigated conditions for 2070-2099 (average of all 3 GCMs) compared to 2010-2039 for RCPs 2.6 and 8.6.

Grain maize	Rainfed		Irrigated		% differences (irrigated and rainfed)
	RCP 2.6	RCP 8.5	RCP 2.6	RCP 8.5	
Grain maize	-1.9	-5.8	+0.3	-1.3	+24
Foxtail millet	+0.3	-2.1	+0.7	+0.3	+25
Buckwheat	+1.4	-3.4	+0.7	+0.2	+62
Wheat (subtropical cultivar)	+0.1	-6.7	+0.5	=	+46
Wetland rice	-1.0	+15.3	+0.7	+5.4	+62
Common beans	+0.2	-1.6	+0.4	-0.4	+42
Cabbage	=	-4.8	+0.7	-0.4	+26
White potatoes	-0.3	+12.8	+1.0	+4.7	+53
Carrots	-0.6	+17.4	+0.8	+5.5	+72
Citrus	+0.1	-3.9	+0.6	+1.0	+22

Differences between irrigated and rainfed conditions are performed for the ensemble of GCMs and RCPs across the century.

Overall, our findings not only represent an opportunity for future crop-specific modelling work assessing the most effective agricultural adaptation solutions in Bhutan but are also a novel source of information for climate risk assessments in agriculture across Bhutan. Beyond providing a snapshot of climate change impacts on agriculture production in Bhutan, the emerging findings of this study are a steppingstone to facilitate the work of project formulators, development agencies, agricultural extension, and decision-makers, among others, when developing projects, policies and strategies based on factual information that relies on the best available climate information (CORDEX-CORE) for impact assessment studies in agriculture.

ACKNOWLEDGEMENTS

The analysis was initiated under the implementation of a World Bank project "Bhutan: Climate Impacts in Bhutan's Agroecological Zones and Opportunities for Climate-Smart Agriculture Practices". The authors recognize the invaluable support provided by the World Bank (Christine Heumesser) and FAO (Riccardo Soldan) technical experts during the conceptualization of this analytical work.

REFERENCES

Allen, R.G., Pereira, L.S., Raes, D. and Smith, M., 1998. Crop Evapotranspiration (guidelines for computing crop water requirements), Drainage and Irrigation Paper N 56. Rome, Italy, Food and Agriculture Organization of the United Nations.

Alvar-Beltrán, J., Soldan, R., Vanuytrecht, E., Heureux, A., Shrestha, N., Manzanas, R., Pant, K.P. and Franceschini, G., 2023. An FAO model comparison: Python Agroecological Zoning (PyAEZ) and AquaCrop to assess climate change impacts on crop yields in Nepal. *Environmental Development*, *47*, p. 100882.

Atreya, P.N. and Kaphle, M., 2020. Visible evidence of climate change and its impact on fruit production in Nepal. *International Journal of Agriculture Environment and Food Sciences*, *4*(2), pp.200-208.

Beck, C., Grieser, J., Kottek, M., Rubel, F., and Rudolf, B. 2005. Characterizing global climate change by means of Köppen climate classification. *Klimastatusbericht*, *51*, pp. 139-149.

Bokshi, A.I., Tan, D.K., Thistlethwaite, R.J., Trethowan, R. and Kunz, K., 2021. Impact of elevated CO2 and heat stress on wheat pollen viability and grain production. *Functional Plant Biology*, *48*(5), pp. 503-514.

Chhogyel, N., Kumar, L., Bajgai, Y., and Hasan, M. K. 2020. Perception of farmers on climate change and its impacts on agriculture across various altitudinal zones of Bhutan Himalayas. *International Journal of Environmental Science and Technology*, *17*(8), pp. 3607-3620.

Chhogyel, N., and Kumar, L. 2018. Climate change and potential impacts on agriculture in Bhutan: a discussion of pertinent issues. *Agriculture & Food Security*, *7*(1), pp. 1-13.

Choden, K., Keenan, R. J., and Nitschke, C. R. 2020. An approach for assessing adaptive capacity to climate change in resource dependent communities in the Nikachu watershed, Bhutan. *Ecological Indicators*, *114*, p. 106293.

Coppola, E., Raffaele, F., Giorgi, F., Giuliani, G., Xuejie, G., Ciarlo, J.M., Sines, T.R., Torres-Alavez, J.A., Das,

S., di Sante, F. and Pichelli, E., 2021. Climate hazard indices projections based on CORDEX-CORE, CMIP5 and CMIP6 ensemble. *Climate Dynamics*, *57*, pp. 1293-1383.

Cucchi, M., Weedon, G. P., Amici, A., Bellouin, N., Lange, S., Müller Schmied, H., & Buontempo, C. 2020. WFDE5: bias-adjusted ERA5 reanalysis data for impact studies. *Earth System Science Data*, *12*(3), pp. 2097-2120.

Department of Agriculture (DoA). 2016. Agriculture statistics 2015. Thimphu. Ministry of Agriculture and Forests (MoAF), Royal Government of Bhutan.

Fischer, G., Nachtergaele, F.O., van Velthuizen, H.T., Chiozza, F., Franceschini, G., Henry, M., Muchoney, D. and Tramberend, S. 2021. Global Agro-Ecological Zones v4 – Model documentation. Rome, FAO.

Food and Agriculture Organization (FAO). 2017. National Agro-Economic Zoning for Major Crops in Thailand (NAEZ). Available online at: https://openknowledge.fao.org/server/api/core/bitstreams/7b71ea9b-4fec-4486-818a-9b13af4ca363/content

Giorgi, F., Coppola, E., Jacob, D., Teichmann, C., Abba Omar, S., Ashfaq, M., Ban, N., Bülow, K., Bukovsky, M., Buntemeyer, L. and Cavazos, T., 2021. The CORDEX-CORE EXP-I initiative: description and highlight results from the initial analysis. *Bulletin of the American Meteorological Society*, pp. 1-52.

International Labour Organization (ILO). 2019. Data, resources: statistics on employment. Available online at: https://ilostat.ilo.org/topics/employment/

Kassam, A. H., Van Velthuizen, H. T., Fischer, G. W., and Shah, M. M. 1991. Agro-ecological land resources assessment for agricultural development planning. A case study of Kenya. Resources data base and land productivity. *Technical Annex*, *1*, pp. 9-31.

Kassam, A. H. 1977. Net Biomass Production and Yield of Crops with Provisional Results for Tropical Africa. Soil Resources, Management and Conservation Service, Land and Water Development Division, FAO.

Katwal, T.B., Dorji, S., Dorji, R., Tshering, L., Ghimiray, M., Chhetri, G.B., Dorji, T.Y. and Tamang, A.M., 2015. Community perspectives on the on-farm diversity of six major cereals and climate change in Bhutan. *Agriculture*, *5*(1), pp. 2-16.

Lal, M., 2011. Implications of climate change in sustained agricultural productivity in South Asia. *Regional Environmental Change*, *11*(Suppl 1), pp. 79-94.

Latham, J., Cumani, R., Rosati, I. & Bloise, M., 2014. Global Land Cover SHARE (GLC-Share) database Beta-Release Version 1.0. Rome, Italy, FAO of the United Nations. 40 pp. Available online at: https://www.fao.org/uploads/media/glc-share-doc.pdf

Lhamo, T., Chen, G., Dorji, S., Tamang, T.B., Wang, X. and Zhang, P., 2023. Trends in Extreme Precipitation Indices over Bhutan. *Atmosphere*, *14*(7), p. 1154.

Ministry of Agriculture and Forests (MoAF). 2011. National action plan biodiversity persistence and climate change. Timphy: MoAF, Royal Government of Bhutan. Available online at: https://www.nbc.gov.bt/wp-content/uploads/2010/06/National-Paper-on-Biodiversity-and-Climate-Change-_Bhutan1.pdf

Nachtergaele, F.O., van Velthuizen, H., Verelst, L. & Wiberg, D. 2012. Harmonized World Soil Database (version 1.2). Rome, Italy, FAO, International Institute for Applied Systems Analysis (IIASA), ISRIC-World Soil Information, Institute of Soil Science – Chinese Academy of Sciences (ISSCAS), Joint Research Centre of the Europe. 50 pp. Available online at: https://www.fao.org/soils-portal/data-hub/soil-maps-and-databases/harmonized-world-soil-database-v12/en/

National Environmental Commission (NEC). 2023. National Adaptation Plan (NAP) of the Kingdom of Bhutan. Available online at: https://unfccc.int/sites/default/files/resource/NAP-Bhutan-2023.pdf

National Environmental Commission (NEC). 2020. Third National Communication to the UNFCCC, 2020. Available online at: https://unfccc.int/sites/default/files/resource/TNC of Bhutan 2020.pdf

National Environmental Commission (NEC). 2016. Water in Bhutan's economy: importance to partners. Available online at: https://wwfasia.awsassets.panda.org/downloads/water_in_the_economies__policy_brief_for_development_partners_2.pdf

National Environmental Commission (NEC). 2011. Second National Communication from Bhutan to the UNFCCC. Available online at: https://adaptation-undp.org/sites/default/files/resources/bhutan-second_national_communication.pdf

Naveendrakumar, G., Vithanage, M., Kwon, H.H., Chandrasekara, S.S.K., Iqbal, M.C.M., Pathmarajah, S., Fernando, W.C.D.K. and Obeysekera, J., 2019. South Asian perspective on temperature and rainfall extremes: A review. *Atmospheric Research*, *225*, pp. 110-120.

Parker, L., Guerten, N., Nguyen, T. T., Rinzin, C., Tashi, D., Wangchuk, D., and Penjor, S. 2017. Climate change impacts in Bhutan: challenges and opportunities for the agricultural sector. *CCAFS Working Paper*.

Teichmann, C., Jacob, D., Remedio, A.R., Remke, T., Buntemeyer, L., Hoffmann, P., Kriegsmann, A., Lierhammer, L., Bülow, K., Weber, T. and Sieck, K., 2021. Assessing mean climate change signals in the global CORDEX-CORE ensemble. *Climate Dynamics*, *57*, pp. 1269-1292.

SUPPLEMENTARY FIGURES

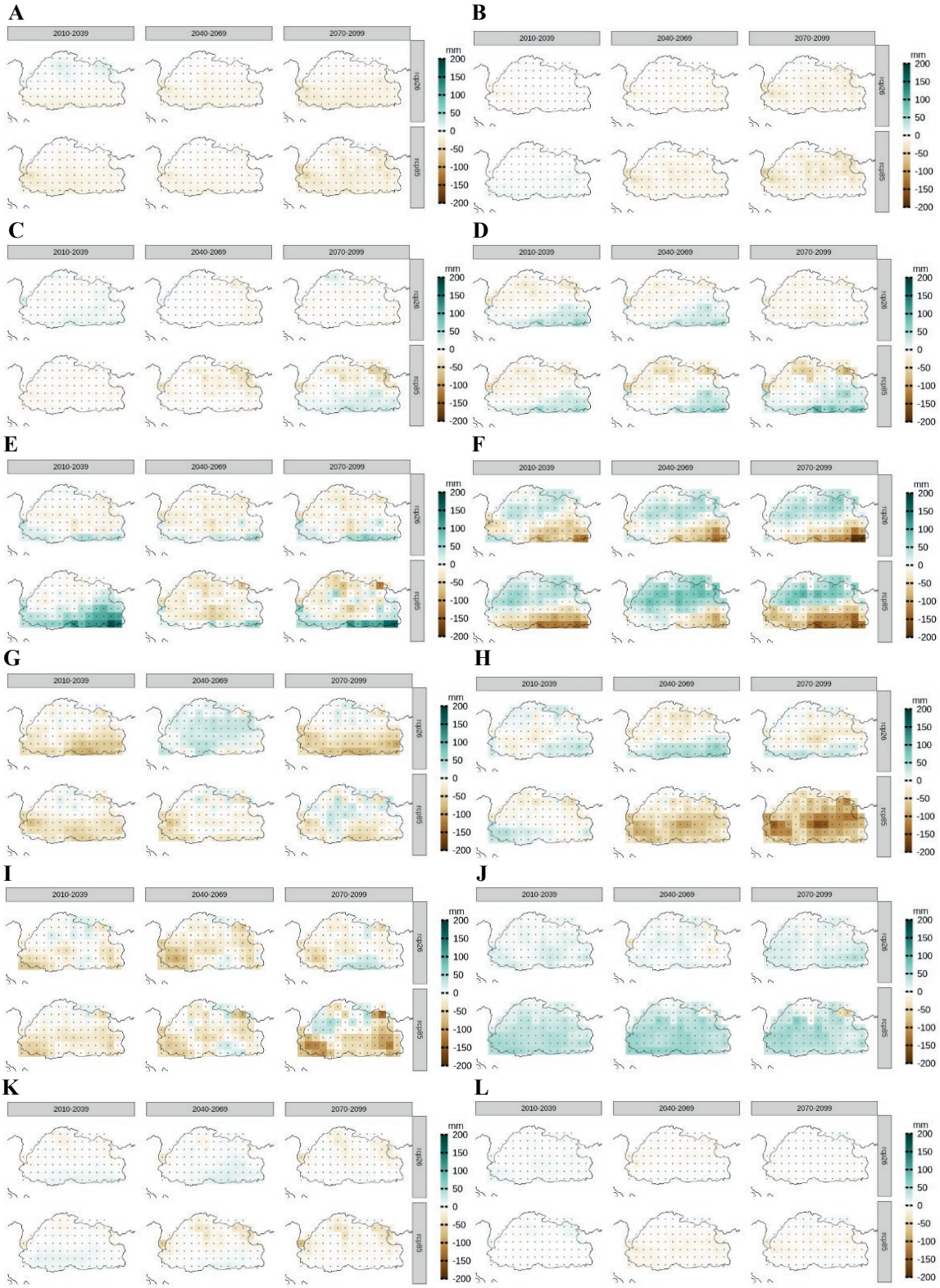

Supp. Figure 1. Climate change signals for monthly precipitation ((**A**) January, (**B**) February, (**C**) March, (**D**) April, (**E**) May, (**F**) June, (**G**) July, (**H**) August, (**I**) September, (**J**) October, (**K**) November, and (**L**) December) for the different time-periods (2010-2039; 2040-2069; 2070-2099) and RCPs (2.6 and 8.5).

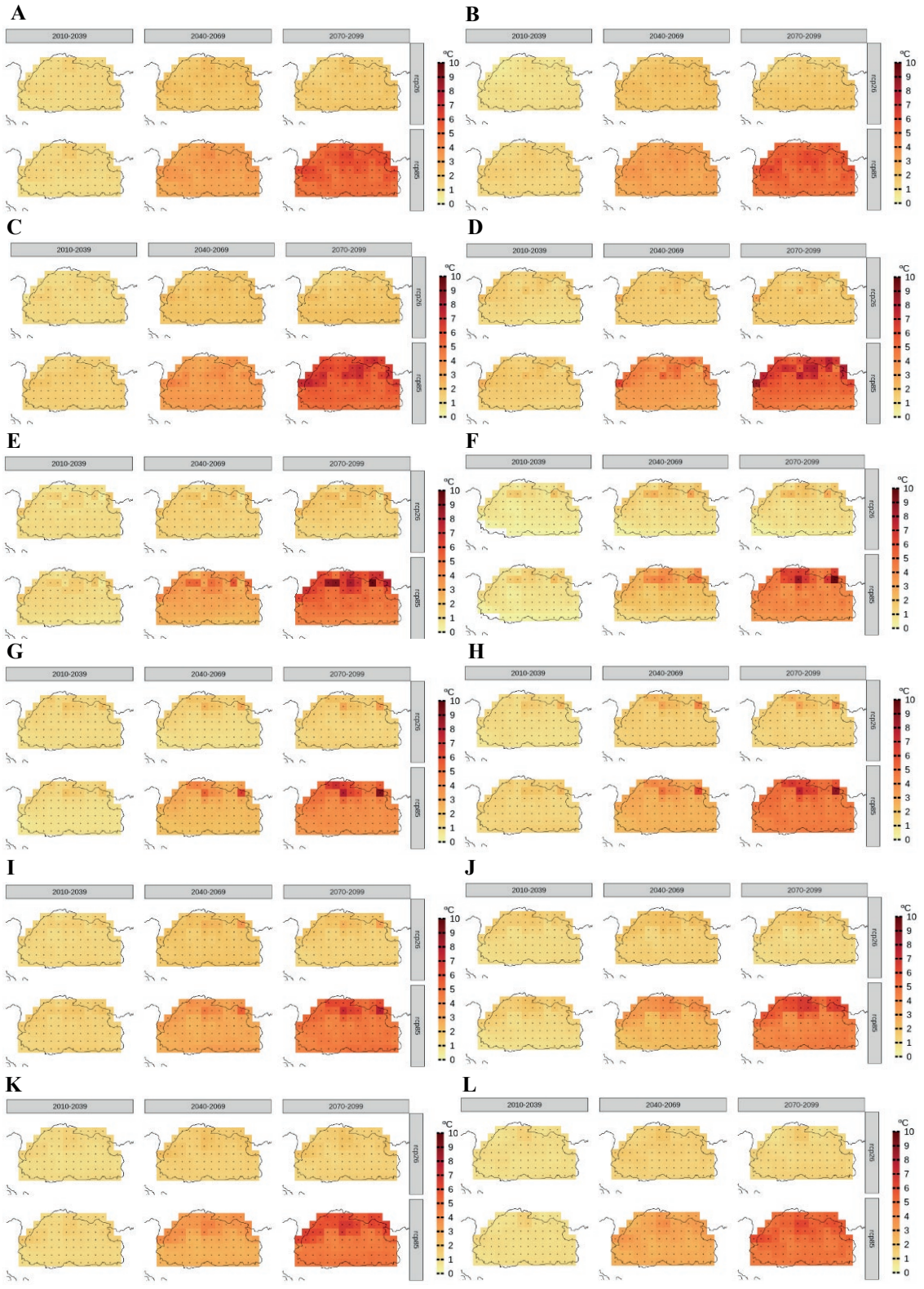

Supp. Figure 2. Climate change signals for monthly maximum temperature ((**A**) January, (**B**) February, (**C**) March, (**D**) April, (**E**) May, (**F**) June, (**G**) July, (**H**) August, (**I**) September, (**J**) October, (**K**) November, and (**L**) December) for the different time-periods (2010-2039; 2040-2069; 2070-2099) and RCPs (2.6 and 8.5).

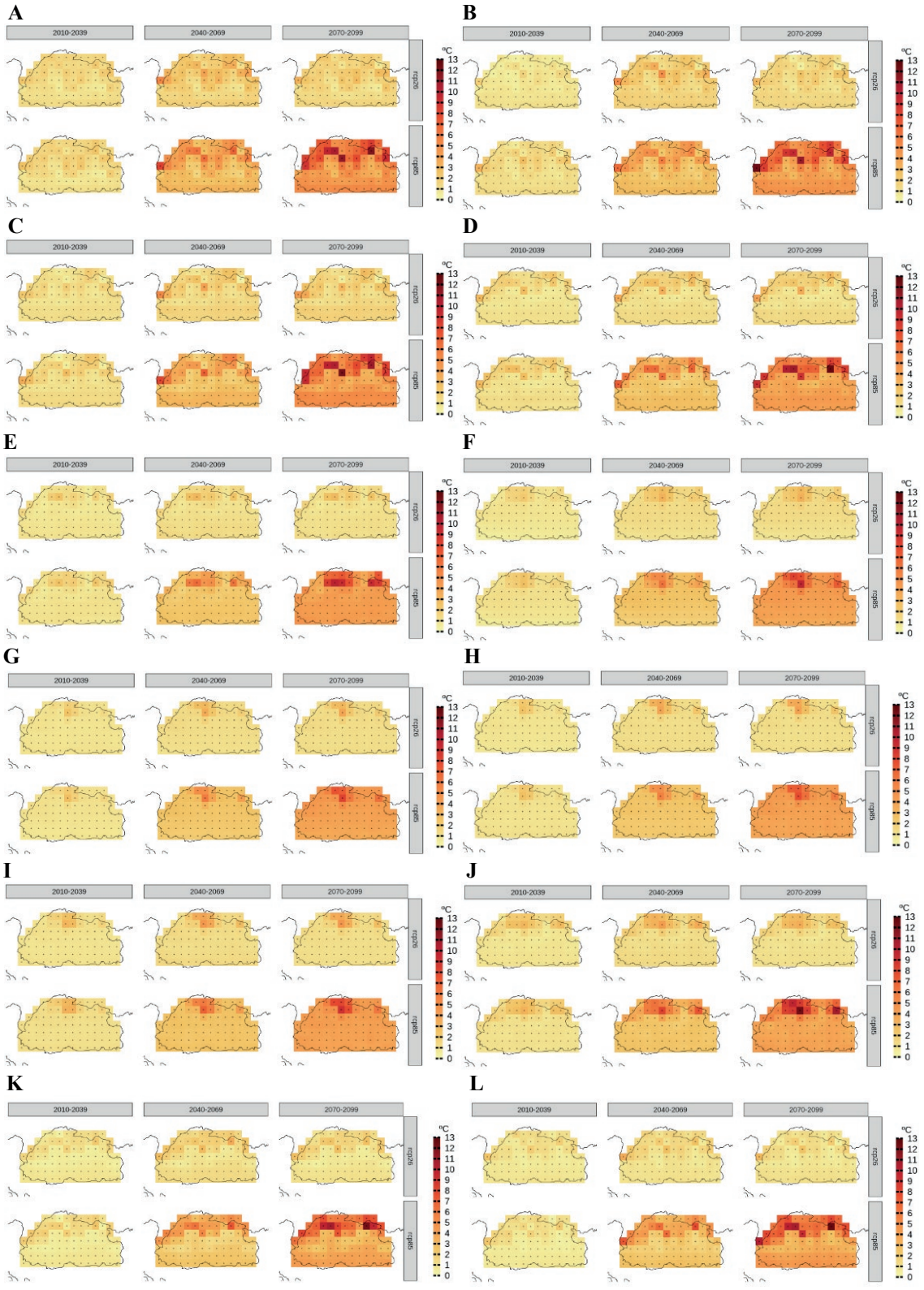

Supp. Figure 3. Climate change signals for monthly minimum temperature ((**A**) January, (**B**) February, (**C**) March, (**D**) April, (**E**) May, (**F**) June, (**G**) July, (**H**) August, (**I**) September, (**J**) October, (**K**) November, and (**L**) December) for the different time-periods (2010-2039; 2040-2069; 2070-2099) and RCPs (2.6 and 8.5).

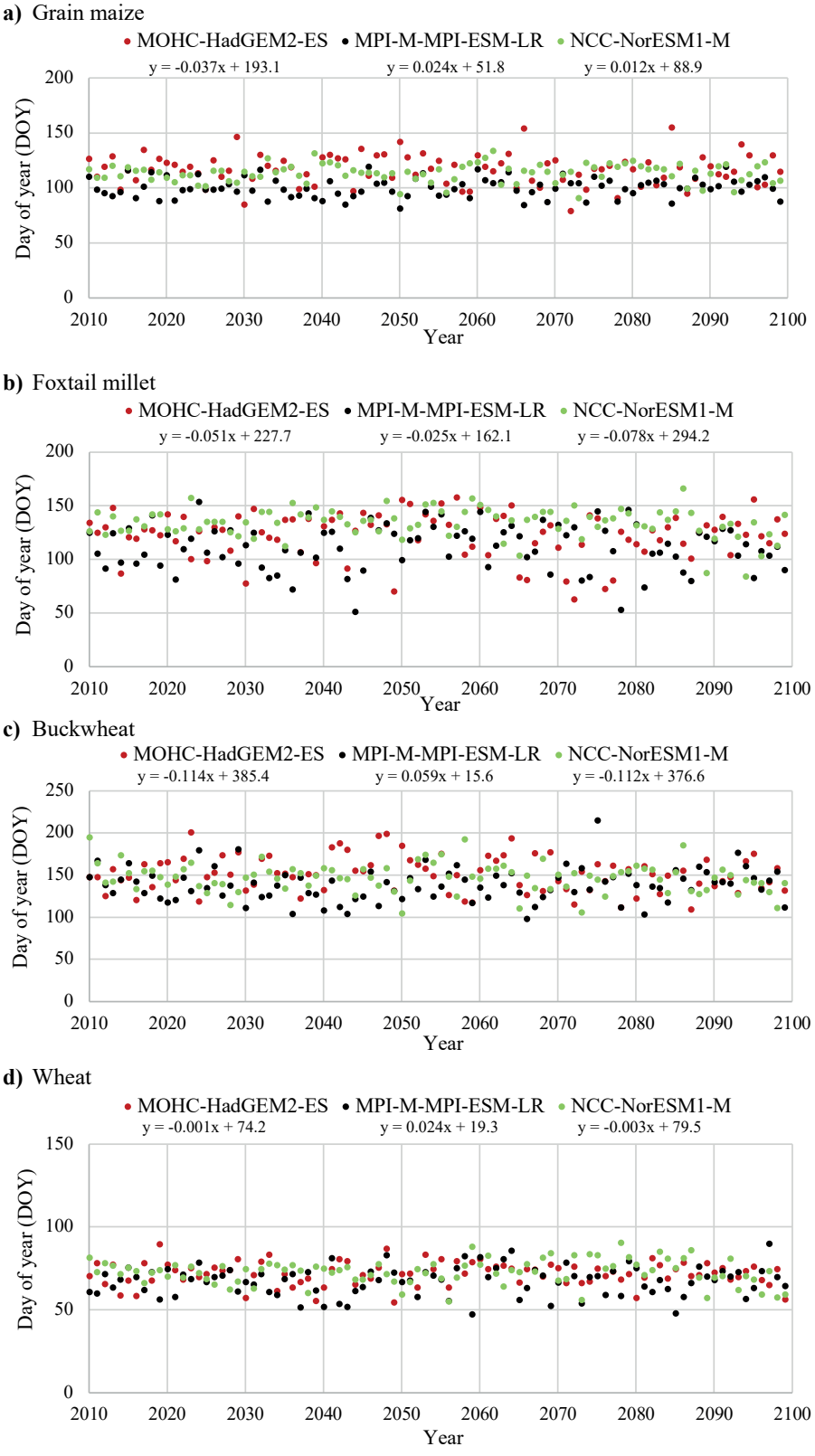

Supp. Figure 4-1. Starting date of crop growth (day of the year) and regression line for all GCMs based on PyAEZ simulations. Note: results for citrus trees were not considered in the analysis of Supp. Fig. 4.

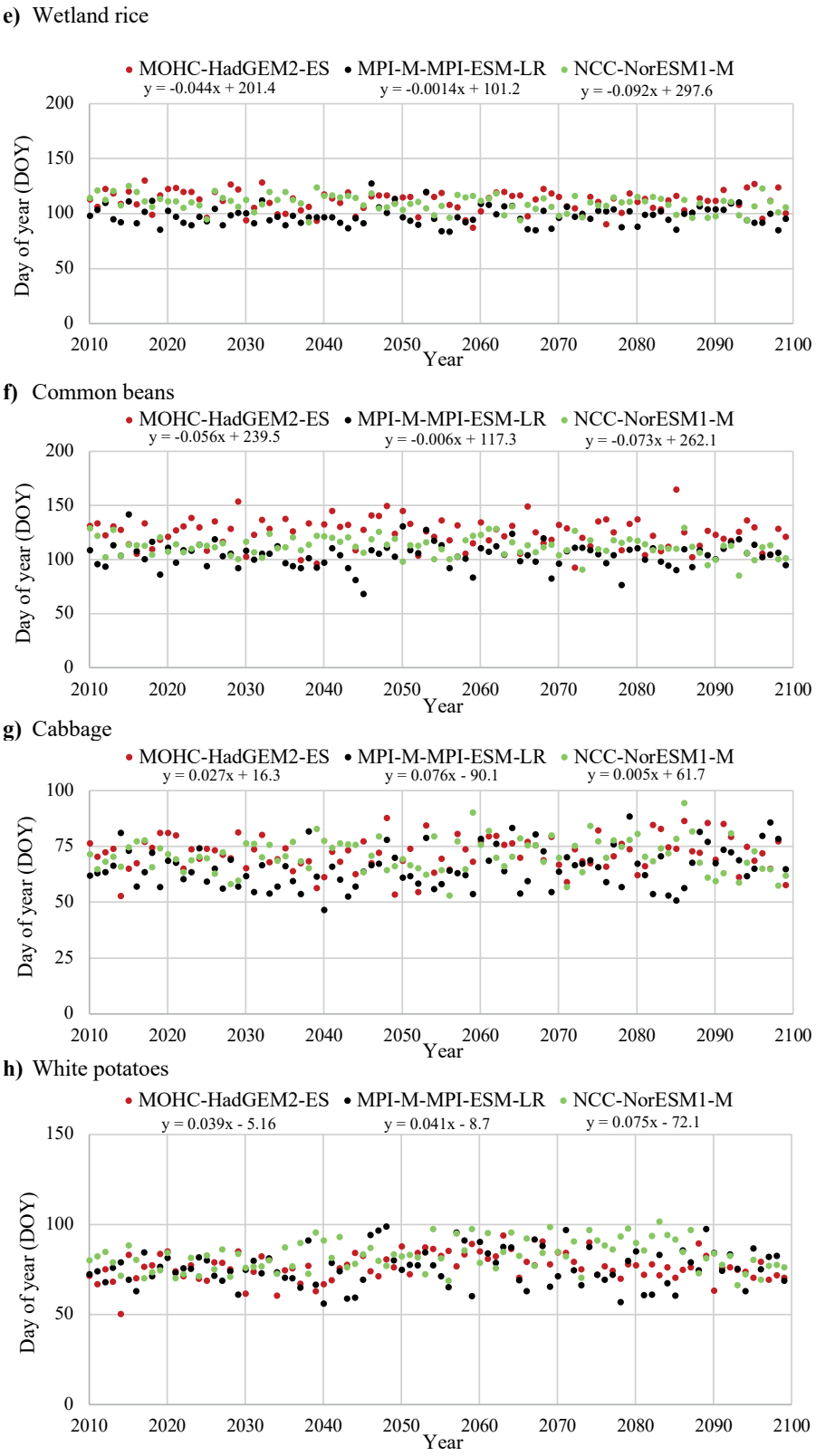

Supp. Figure 4-2. Starting date of crop growth (day of the year) and regression line for all GCMs based on PyAEZ simulations. Note: results for citrus trees were not considered in the analysis of Supp. Fig. 4.

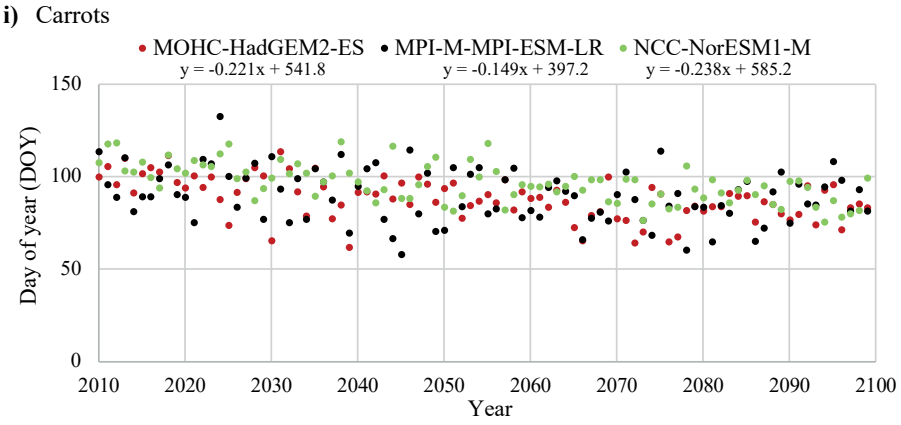

Supp. Figure 4-3. Starting date of crop growth (day of the year) and regression line for all GCMs based on PyAEZ simulations. Note: results for citrus trees were not considered in the analysis of Supp. Fig. 4.

Italian Journal of Agrometeorology
Rivista Italiana di Agrometeorologia

Firenze University Press
https://riviste.fupress.net/index.php/IJAm

OPEN ACCESS

Citation: Scanavini, J.G.V., Coelho, R.D., Barros, T.H.S., Costa, J.O., & Duarte, S.N. (2024). Irrigation strategies of sugarcane seedlings from micropropagation and biofactory methods. *Italian Journal of Agrometeorology* (2): 121-130. doi: 10.36253/ijam-2447

Received: January 20, 2024

Accepted: November 28, 2024

Published: December 30, 2024

© 2024 Author(s). This is an open access, peer-reviewed article published by Firenze University Press (https://www.fupress.com) and distributed, except where otherwise noted, under the terms of the CC BY 4.0 License for content and CC0 1.0 Universal for metadata.

Data Availability Statement: All relevant data are within the paper and its Supporting Information files.

Competing Interests: The Author(s) declare(s) no conflict of interest.

Irrigation strategies of sugarcane seedlings from micropropagation and biofactory methods

José Guilherme Victorelli Scanavini[1,*], Rubens Duarte Coelho[1], Timóteo Herculino da Silva Barros[2], Jéfferson de Oliveira Costa[3], Sergio Nascimento Duarte[1]

[1] *University of São Paulo/USP-ESALQ, Biosystems Engineering Department, C.P. 09, 13418-900 Piracicaba, SP, Brazil*
[2] *University of São Paulo/USP-CENA, Center of Nuclear Energy in Agriculture, 13416-000 Piracicaba, SP, Brazil*
[3] *Minas Gerais Agricultural Research Agency/EPAMIG, Experimental Field of Gorutuba, 39525-000 Nova Porteirinha, MG, Brazil*
*Corresponding author. E-mail: jgvs274@gmail.com

Abstract. The sugarcane industry has been suffering from unstable productivity on commercial fields. The major factors causing this problem are mechanized harvesting damage to cane clumps in the field and the slow process of releasing and adopting new sugarcane cultivars. By utilizing new micropropagation processes involving the extraction of apical meristem from new cultivars and biofactory methods for multiplying the material, it is possible to produce an extraordinary number of sugarcane seedlings to provide nurseries rapidly with new cultivars for planting on commercial fields. The goal of this study was to evaluate several irrigation strategies (IS) to determine the best one for supplying the biofactory sugarcane seedlings water requirements, under conditions of different volumes of substrate (VS): 56, 73, 93 and 125 cm^3. The irrigation management experiment comprised eight IS based on different periods of accumulated reference evapotranspiration (ET_o). We found that the irrigation application must occur at intervals below 30 mm of accumulated ET_o. IS1 (maintenance of soil moisture at field capacity) results in a larger number of tillers, longer extension of the primary stalks, and enhanced dry matter (DM) yield independent of VS. The VS factor accounted for statistical differences in sugarcane survival rate and morphological characteristics, but only for low initial soil moisture conditions. The intermediate VS of 73 cm^3 was the best option for plants to thrive in the field; larger VS (93 and 125 cm^3) produced young plants with many leaves, which transpire a lot in the field, increasing the chances of early death under water stress after planting; the smaller VS (56 cm^3) resulted in young plants with small root systems and minimal water reservoirs, resulting in lower survival under drought conditions.

Keywords: *Saccharum* spp., soil moisture, volume of substrate, agricultural water management.

HIGHLIGHTS

- Different irrigation strategies (IS) for the planting and management of micropropagated sugarcane seedlings in different volumes of substrate (VS) were evaluated.
- IS1 (maintenance of soil moisture at field capacity) resulted in a larger number of tillers, longer extensions of primary stalks, and enhanced dry matter (DM) yield independent of VS.
- VS accounted for differences in sugarcane survival rate and morphological characteristics, but only for low initial soil moisture conditions.
- The intermediate VS of 73 cm^3 was the best option for plants to thrive in the field.
- Larger VS (93 and 125 cm^3) and smaller VS (56 cm^3) resulted in young plants with similar problems surviving in the field under drought conditions.

1. INTRODUCTION

The sugarcane (*Saccharum* spp.) planting operation is defined according to the multiplication technique that is used (Rocha and Sparovek, 2021; Santos et al., 2022). When the material multiplication is carried out through the plant's own vegetative structures, a previously cultivated sugarcane field, called a nursery, is used as the source of planting material. From this nursery, seedlings can be removed manually or by mechanical harvesters adapted to the task. Other sugarcane multiplication techniques are known and used by growers to provide higher proliferation rates. The tissue culture method of in vitro micropropagation stands out as very favorable (Silva et al., 2018; Matoso et al., 2021). In addition to improving the quality of the product, it enables the propagation of plants free of viruses and other diseases, promotes the maintenance of the characteristics of the matrix plant and the optimization of productivity, while providing rapid, large-scale multiplication of seedlings in so-called biofactories (Peloia et al., 2019).

This biotechnological process needs to be well defined and to operate with appropriate technology, for production on a commercial scale. When planted in the field, micropropagation seedlings already have a good leaf area and root system contained in a substrate, while sugarcane seedlings produced vegetatively (stalks with leaf buds) can only generate new plants if conditions are favorable (Castro et al., 2019; Hu et al., 2022). The presence of leaves results in evapotranspiration that can cause stress from moisture loss. If the water available in the soil or in the substrate is too little for survival of the seedlings, there will be irreversible losses in the plant population and subsequent financial losses (Tavares et al., 2018; Maldaner et al., 2020).

Thus, whether considering nurseries for micropropagation of sugarcane seedlings or another methodology in which the plants already have aerial parts, a type of irrigation must be adopted that guarantees vegetative development of the plants and growth of the stalks, leaving sufficient water available in the soil during periods of higher temperature and longer photoperiod (Aquino et al., 2018; Farias-Ramírez et al., 2024). Given this need of the production sector to renew areas with reduced productivity by introducing new cultivars with higher productive potential (Sanches et al., 2019; Poudial et al., 2022; Barbosa et al., 2024), this research aimed to evaluate different irrigation strategies (IS) for the planting and management of micropropagated sugarcane seedlings in different volumes of substrate (VS).

2. MATERIAL AND METHODS

2.1. Location and characterization of the experimental area

The study was conducted in 2013 at the University of São Paulo, located in the municipality of Piracicaba, São Paulo State, Brazil (22°46'39" S, 47°17'45" W) at an altitude of 570 m a.s.l. The experimental units (plots) were distributed in a rain-out shelter with an area of approximately 160 m^2 containing 96 asbestos-cement boxes of 100 L each (Cherri et al., 2019), with dimensions of 0.60 x 0.40 x 0.45 m (Figure 1A), distributed in four strips spaced 0.80 m between rows and 0.50 m between boxes (Figure 1B). The soil used to fill the boxes was classified as an Oxisol (Typic Ustox) with a sandy loam texture, the predominant soil in sugarcane growing areas in Brazil. The physical-water characteristics of the soil are shown in Table 1.

The irrigation system consisted of the following components: (i) a five-hundred-liter reservoir, (ii) polyethylene pipes, (iii) a KSB-C500N motorized pump, (iv) two disk filters, and (v) four control heads with eight registers, responsible for controlling the flow of the experimental units. Two self-compensating button surface drippers of 8 L h^{-1} each were installed in each asbestos-cement box, and for better distribution of the flow of each dripper and standardization of the wetted area, a discharge divider with two rods was connected to each dripper (Figure 1C).

The following climatic elements were monitored: global solar radiation (MJ m^{-2} day^{-1}) using a pyranometer (LP02-L12, Campbell Scientific), air temperature (°C) and relative humidity (%), using sensors (Vaissala

Table 1. Physical and hydric characterization of soil in four layers.

Layers m	Granulometric fractions			U_{FC}	U_{PWP}	D_s	D_p	AWC mm	TP %
	Sand	Silt	Clay						
	%			g g^{-1}		g cm^{-3}			
0 - 0.10	75.1	7.8	17.1	0.148	0.069	1.53	2.65	12.11	42.3
0.10 - 0.20	74.5	8.0	17.5	0.151	0.065	1.50	2.65	12.81	43.4
0.20 - 0.30	74.5	8.0	17.5	0.151	0.065	1.50	2.65	12.81	43.4
0.30 - 0.40	74.4	8.6	17.0	0.143	0.078	1.69	2.64	10.88	36.0

U_{FC}: moisture at field capacity (corresponding to a matric potential of -4.85 kPa, according to Tapparo et al., 2019); U_{PWP}: moisture at the permanent wilting point (corresponding to a matric potential of -1500 kPa); AWC: available water capacity; D_s: soil bulk density. D_p: soil particle density; TP: total soil porosity.

Figure 1. Photos showing details of the experimental area. Asbestos-cement boxes (100 L) with dimensions of 0.60 x 0.40 x 0.45 m (A). Distribution of asbestos-cement boxes in four rows spaced 0.80 m between rows and 0.50 m between boxes (B). Self-compensating button surface drippers and discharge divider with two rods (C). Sensors installed in the center of the experimental area and above the crop canopy (D). Tensiometers installed at depths of 0.10, 0.20, 0.30 and 0.40 m (E). Digital vacuometer used in the experiment (F).

HMP45C-L12, Campbell Scientific). Three sensors were installed in the center of the experimental area and above the crop canopy (Figure 1D). Data were monitored by a data acquisition system (datalogger), with averages stored every 15 minutes.

2.2. Experimental design, treatments and irrigation management

A randomized block design was used in a factorial scheme (4 x 8), in three blocks, for the 96 boxes available for the experiment. Each experimental plot was represented by a box containing four micropropagated sugarcane seedlings approximately 60 days old. The treatments were four VS, 56, 73, 93 and 125 cm^3 for seedling production (Figure 2) and eight IS.

For the IS, eight treatments were defined from IS1 to IS8. In four of them, the seedlings were planted with the soil initially moist at an initial irrigation depth of 30 mm (from IS1 to IS4). The 30 mm depth was adopted because most sugarcane mills have winding reels for irrigation of the micropropagated seedling nursery. This equipment performs the application at a fixed irrigation depth and, in order to supply sufficient water to the plants, a depth of 30 mm is recommended since a large part of the water is lost through evaporation. For the other IS (from IS5 to

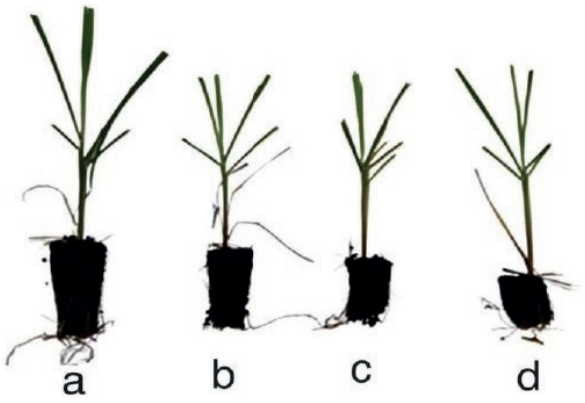

Figure 2. Seedlings produced in each type of container with different volumes of substrate (VS). Seedlings with 125 (a), 93 (b), 73 (c) and 56 cm^3 (d) of VS.

IS8), seedlings were planted in dry soil, without setting an irrigation depth after soil stabilization in the experimental unit. Subsequently, IS1 was maintained with the soil at field capacity throughout the entire experiment. The 30 mm irrigation depth applied in each pre-fixed strategy for different periods of accumulated reference evapotranspiration (ET_o) are detailed in Table 2.

As a more suitable parameter for the IS treatments based on the water demand in each period, the ET_o was estimated using the standard method (Penman-Monteith) proposed by the FAO (Allen et al., 1998). To define the irrigation dates for the treatments over time, the accumulated ET_o in mm was calculated and the fixed irrigation depth (ID_{30}) was achieved through measurements of the accumulated ET_o during different periods. Therefore, IS2 received seven ID_{30} spaced every 30 mm of accumulated ET_o, starting with 15 mm of accumulated ET_o plus the initial ID_{30}. IS3 received two ID_{30} spaced every 95 mm of accumulated ET_o plus the initial ID_{30}. IS4 received two ID_{30}, initial and another with 130 mm of accumulated ET_o. IS5 received seven ID_{30} spaced every 30 mm of accumulated ET_o and starting with 10 mm of accumulated ET_o. IS6 received five ID_{30} spaced every 40 mm of accumulated ET_o and starting with 15 mm of ET_o accumulated. IS7 received three ID_{30} spaced every 70 mm of accumulated ET_o and starting with 30 mm of accumulated ET_o. IS8 received two ID_{30} spaced every 100 mm of accumulated ET_o and starting with 40 mm of accumulated ET_o.

The irrigation management for IS1 was carried out based on soil moisture data obtained from tensiometer readings. Tensiometers were installed for all IS1 treatments (12 boxes) at depths of 0.10, 0.20, 0.30 and 0.40 m, totaling 48 tensiometers (Figure 1E). Readings were taken within a maximum interval of three days using a digital vacuometer (Figure 1F). Based on the mean readings obtained from the soil water matric potential, the irrigation necessary to bring the soil moisture to field capacity was calculated using the van Genuchten approach (van Genuchten, 1980), according to Equation 1:

$$\theta(\Psi_m) = \theta_r + \frac{(\theta_s - \theta_r)}{(1 + (\alpha \times \Psi_m)^n)^m} \quad (1)$$

where θ (ψm) is the soil volumetric water content (cm^3 cm^{-3}), θ_r is the soil residual volumetric water con-

Table 2. Irrigation strategies (IS) used in the study with applications of irrigation depths during different periods of accumulated reference evapotranspiration (ET_o).

Accumulated ET_o mm	Days after planting (DAP)	IS1	IS2	IS3	IS4	IS5	IS6	IS7	IS8
0	0	ID_{30}	ID_{30}	ID_{30}	ID_{30}				
10	4	ID_{FC}				ID_{30}			
15	6	ID_{FC}	ID_{30}				ID_{30}		
30	12	ID_{FC}						ID_{30}	
40	18	ID_{FC}				ID_{30}			ID_{30}
45	22	ID_{FC}	ID_{30}						
55	26	ID_{FC}					ID_{30}		
70	36	ID_{FC}				ID_{30}			
75	39	ID_{FC}	ID_{30}						
95	50	ID_{FC}		ID_{30}			ID_{30}		
100	53	ID_{FC}				ID_{30}		ID_{30}	
105	57	ID_{FC}	ID_{30}						
130	80	ID_{FC}			ID_{30}	ID_{30}			
135	83	ID_{FC}	ID_{30}				ID_{30}		
140	86	ID_{FC}							ID_{30}
160	100	ID_{FC}				ID_{30}			
165	104	ID_{FC}	ID_{30}						
170	107	ID_{FC}						ID_{30}	
175	110	ID_{FC}					ID_{30}		
190	121	ID_{FC}		ID_{30}		ID_{30}			
195	124	ID_{FC}	ID_{30}						

ID_{FC}: irrigation depth to maintain soil moisture at field capacity; ID_{30}: 30 mm fixed irrigation depth.

tent ($cm^3\,cm^{-3}$), θ_s is the volumetric water content of the saturated soil ($cm^3\,cm^{-3}$), m and n are the regression parameters of equation (dimensionless), α is the parameter with dimension equal to the inverse of the tension (kPa^{-1}) and ψ_m is the function of the matric potential (kPa).

2.3. Planting, crop management, and evaluated features

The sugarcane cultivar selected for the experiment was RB93509 due to its ready availability in the market. According to the Technical Bulletin of the Interinstitutional Network for the Development of the Sugar and Alcohol Sector (RIDESA), this cultivar has medium resistance to drought, good tillering in plant cane and ratoon cane. At the end of the micropropagation procedures, the seedlings were transplanted into four models of trays filled with substrate, based on pine bark and coconut fiber, into which a solution of a hydroretentive polymer was mixed with the substrate at a concentration of 5 g L^{-1}. The trays used had four VS options, 56, 73, 93 and 125 cm^3 (according the treatments).

The seedlings were transplanted with an approximately similar leaf area; pruning was performed, to reduce all plants to ~20 cm in height. This procedure of reducing the leaf area is carried out on commercial sugarcane plantations to reduce transpiration. The upper surface of each box was divided into four quadrants of equal area and a hole was made in the center of each quadrant slightly larger than the root system of the seedlings, for the seedlings to be planted.

The experiment ran from April to August, ending 141 DAP. The tillering intensity in all treatments was measured by counting the number of tillers (NT), with a complete tiller being considered the sprout formed from the planted seedling, including the primary stalk. This evaluation was done at 141 DAP. For determining the NT, the average of the four plants in the experimental unit was used. Using a measuring tape, the maximum extension of the primary stalk (MEPS) from the soil surface to the tip of the highest leaf (stretched manually) was determined at 141 DAP, this measure being representative of the total growth of the plant, both stalk and leaves. For plant survival analysis, the percentage of live clumps was determined at 30, 50, 80 and 120 DAP. A dead clump was one that did not show any green leaves, not even the cartridge leaves, or on both the tillers and the primary stalk, and no emission of new tillers. Plants were collected for dry weight determination at the end of the experiment. To measure the dry matter (DM) of the clumps, all tillers present in the experimental plot were cut. To obtain the dry weight, after the collection procedure, the material was dried in an oven with a forced hot air circulation system at a temperature of 65°C until the moisture level reached a constant value. To calculate the total DM weight, the total weight of each plant in the experimental unit was determined.

2.4. Data analysis

For the analysis of variance, we verified whether the statistical assumptions of the main effects were additive, and the independent, normally distributed errors and the homogeneous variances were satisfied. The evaluated parameters were checked for normality using the Kolmogorov-Smirnov and Shapiro-Wilk tests. The data were statistically analyzed using analysis of variance, splitting the analyses whenever the interaction was significant based on Tukey's test at a 5% probability level.

3. RESULTS AND DISCUSSION

3.1 Meteorological data and irrigation water applied

During the experimental period, the average temperature was 20.7°C and relative humidity was 72.9%. The maximum temperature was 39.7°C at 140 DAP and the minimum of 4.3°C occurred at 78 DAP. The maximum relative humidity was 98.1% at 76 DAP and the minimum was 15.2% at 127 DAP. The maximum and minimum values of global solar radiation occurred at 3 DAP (11.4 MJ m^{-2} day^{-1}) and 59 DAP (0.6 MJ m^{-2} day^{-1}), respectively. The transparent plastic cover (diffuser film), and a black screen on the sides intercepted 30% of the incident radiation as reported by Costa et al. (2015) and Chaves et al. (2021). The daily ET_o calculated by using the Penman-Monteith method ranged between 0.6 mm day^{-1} (59 DAP) and 2.7 mm day^{-1} (1 DAP). The vapor pressure deficit (VPD) fell between 0.2 kPa (59 DAP) and 2.6 kPa (118 DAP) (Figure 3).

The total amount of irrigation water applied to IS1 was 180 mm. For treatments that received fixed irrigation depth of 30 mm, the total amount of irrigation water applied was 240, 90, 60, 210, 150, 90 and 60 mm for IS2, IS3, IS4, IS5, IS6, IS7 and IS8, respectively (Figure 4). IS2 and IS5 received amounts of irrigation water greater than the treatment with irrigation management and maintenance of soil moisture at field capacity (IS1). The other treatments (IS3, IS4, IS6, IS7 and IS8) received a smaller amount of irrigation water when compared to IS1.

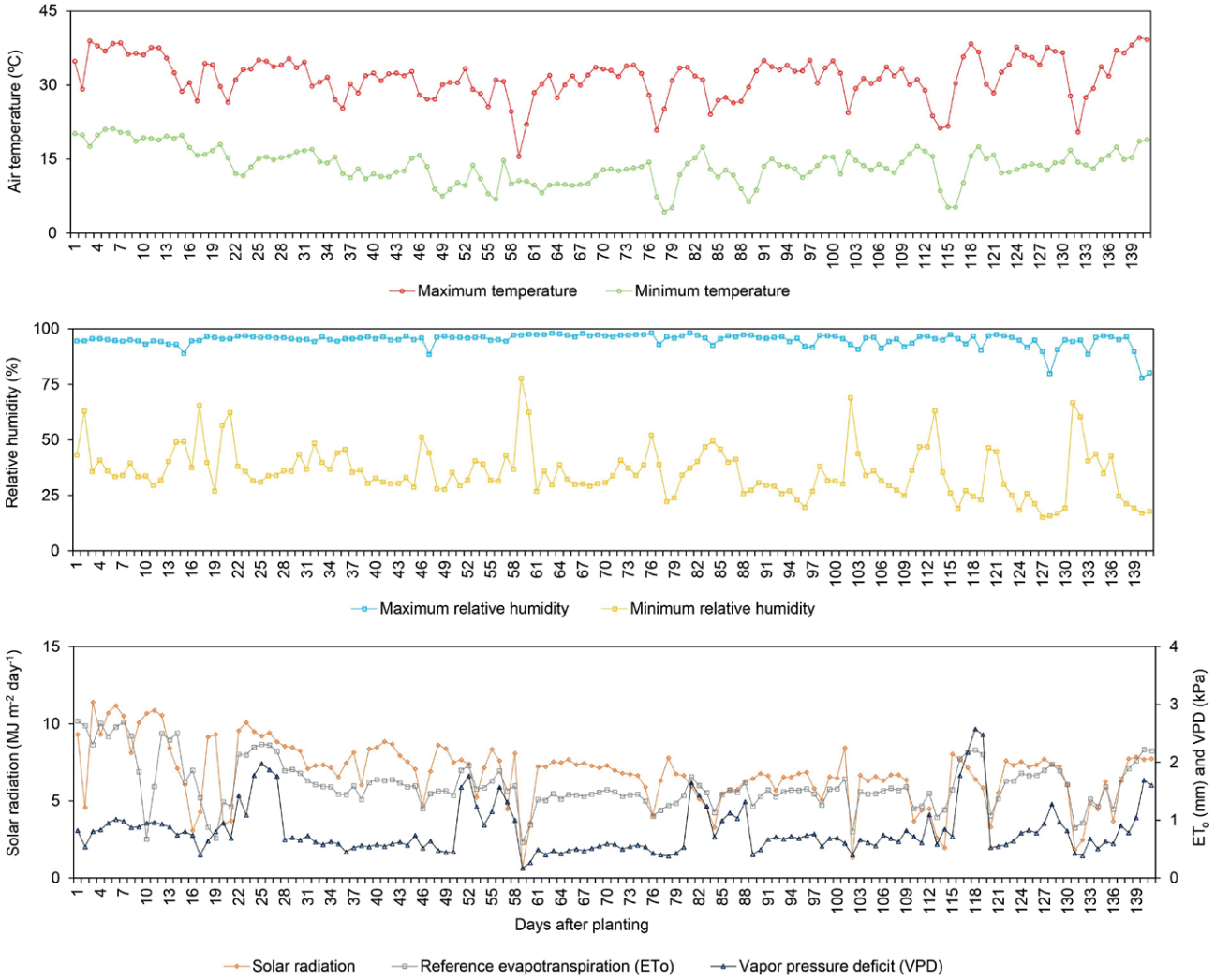

Figure 3. Daily data on meteorological variables air temperature, relative humidity, solar radiation, reference evapotranspiration (ET_o) and vapor pressure deficit (VPD).

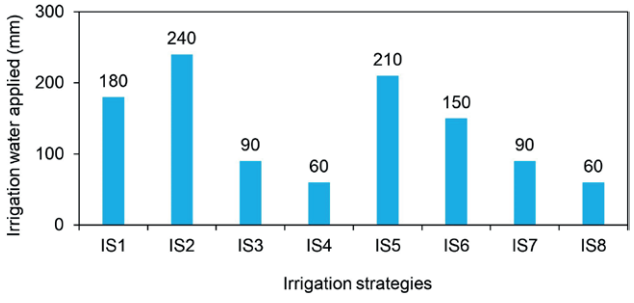

Figure 4. Irrigation water applied (mm) as a function of irrigation strategies (IS).

3.2. Responses related to plant development

Regarding the percentage of dead plants, it was found that for the interaction IS and VS there was a difference for four accumulated ET_o periods (30, 50, 80 and 120 DAP). The IS and VS factors alone showed no difference. IS3, IS4, IS7 and IS8 resulted in the highest percentages of dead plants especially in the periods of 80 and 120 DAP. IS1, IS2 and IS5 resulted in the lowest percentages of dead plants in all VS tested and in the four periods evaluated (Table 3). It can be seen that there was no difference in IS1, IS2, IS4 and IS8 for the tested VS, during the four evaluated periods. As for IS3, IS5 and IS6, there were differences in some of the periods, and the size of the VS influenced the survival of the plants.

Table 3. Percentage of dead plants (%) as a function of irrigation strategies (IS) with a specific volume of substrate (VS) for the evaluation periods of 30, 50, 80 and 120 days after planting (DAP).

Irrigation strategies	Evaluation period							
	30 DAP				50 DAP			
	Volume of substrate (cm^3)							
	56	73	93	125	56	73	93	125
IS1	0 a	0 a	0 a	0 a	0 a	0 a	0 a	0 a
IS2	0 a	0 a	0 a	0 a	0 a	0 a	0 a	0 a
IS3	0 a	0 a	0 a	0 a	58 bc	0 a	67 c	8 b
IS4	0 a	0 a	0 a	0 a	67 a	100 a	100 a	100 a
IS5	50 b	0 a	0 a	0 a	50 a	0 a	0 a	0 a
IS6	75 a	67 a	33 a	75 a	75 a	67 a	33 a	75 a
IS7	75 bc	17 a	100 c	42 ab	75 ab	25 a	100 b	50 ab
IS8	58 a	100 a	100 a	100 a	58 a	100 a	100 a	100 a
Irrigation strategies	Evaluation period							
	80 DAP				120 DAP			
	Volume of substrate (cm^3)							
	56	73	93	125	56	73	93	125
IS1	0 a	0 a	0 a	0 a	0 a	0 a	0 a	0 a
IS2	0 a	0 a	0 a	0 a	0 a	0 a	8 a	0 a
IS3	58 a	33 a	67 a	25 a	92 a	100 a	100 a	100 a
IS4	67 a	100 a	100 a	100 a	83 a	100 a	100 a	100 a
IS5	50 a	0 a	0 a	0 a	50 b	0 a	0 a	0 a
IS6	75 a	67 a	33 a	75 a	75 b	67 b	33 a	75 b
IS7	75 ab	25 a	100 b	50 ab	100 b	50 a	100 b	100 b
IS8	58 a	100 a	10 a	100 a	92 a	100 a	100 a	100 a

Mean values followed by the same letter in the row within the same evaluation period do not differ significantly by Tukey's test at 5% probability.

For planting meristem or pre-twinned seedlings, the density per linear meter was two to three plants. However, the percentage of dead plants constitutes more relevant information for decision makers to choose a certain IS and VS to be adopted in a planting nursery. Maintaining conditions to ensure the survival of all plants after planting helps to guarantee an ideal final stand in the nursery (Poja et al., 2020). On the other hand, planting gaps between 0.30 and 0.50 m do not always affect the quality of the sugarcane stand, since, under these conditions, tillering can be stimulated by greater solar radiation, thus compensating for the lower NT in the crop. However, when the failure rate is >50%, it is recommended to replant the area. This is valid for commercial stands in which 12 to 15 buds per linear meter are recommended for manual planting or 20 to 25 buds for mechanical planting. It is understood that each bud is likely to germinate and originate a new plant (Li et al., 2020; Otto et al., 2021; Rocha et al., 2022).

Throughout the entire experiment there was no increase in plant survival time with increasing VS. In IS6, for example, the highest survival rate (67%) was observed with the 93 cm^3 tray. As the VS factor is imposed at planting, plants exhibit different rates of development depending on this factor and plants with a VS of 125 cm^3 showed greater initial development. In this case, however, the plants' water consumption was higher, which increased the water deficit in the soil and caused critical water stress compared to the treatment in the 93 cm^3 tray; the same result occurred in IS7. The best performance was observed for the treatment with the 73 cm^3 tray, and this result was maintained for all evaluations.

The VS for the NT showed significance, however, the VS for total DM and MEPS was not significant. With respect to the IS factor, there was significance for total DM, MEPS and NT. For NT, it was found that treatments IS1, IS2 and IS5 presented the highest averages, with 8.3, 6.6 and 6.8 tillers, respectively, considering the four VS.

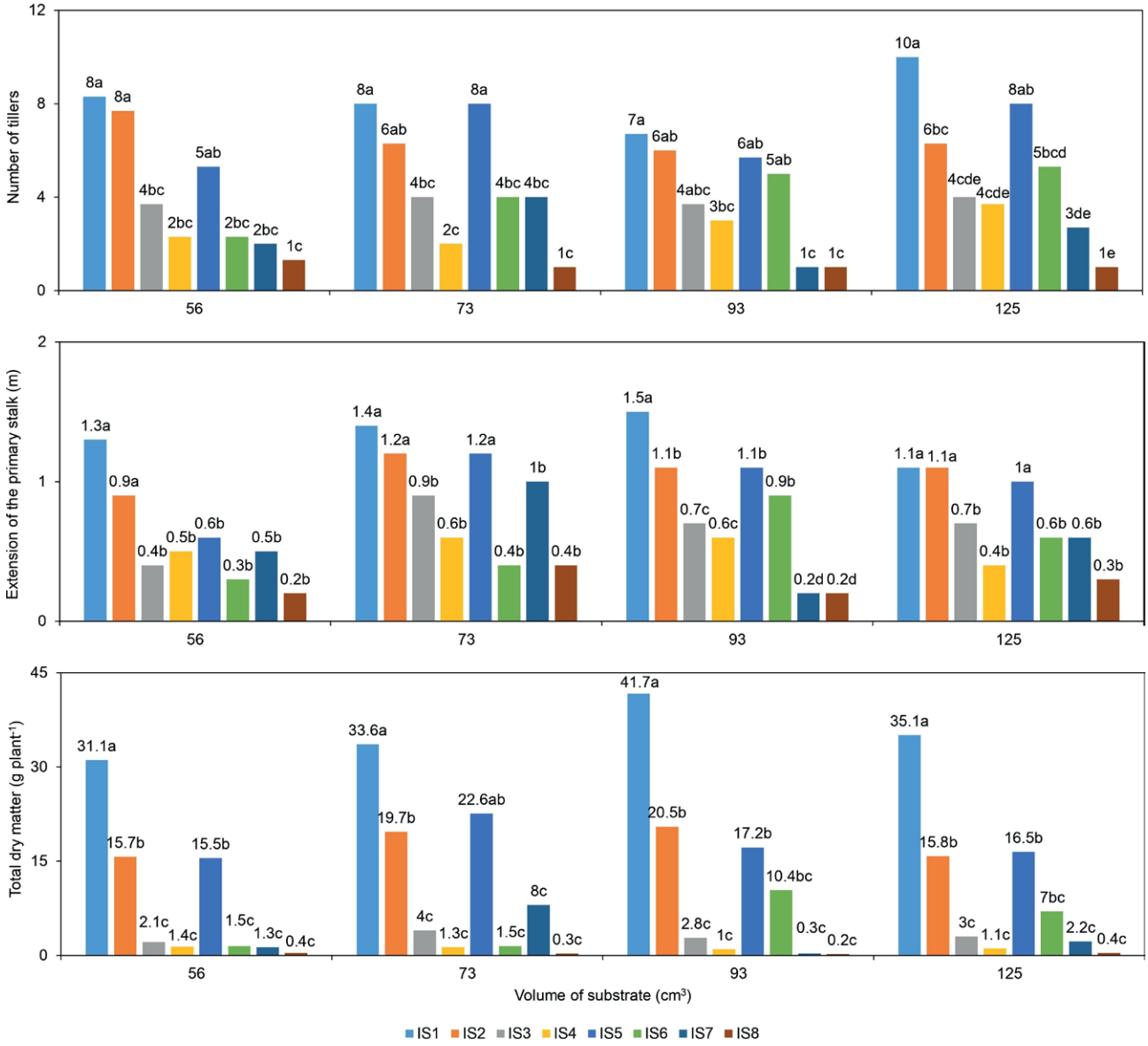

Figure 5. Number of tillers (NT), maximum extension of the primary stalk (MEPS) and total dry matter (DM) as a function of irrigation strategies (IS) with a specific volume of substrate (VS). Mean values followed by the same letter within each VS do not differ significantly by Tukey's test at 5% probability.

Treatments IS7 and IS8 had the lowest averages, 2.4 and 1.1 tillers, respectively, considering the four VS (Figure 5).

We observed that plants with larger stalk diameters generally had smaller NTs. However, because of size differences, the total weight may be the same although the NT is different. The NTs in the vegetative stage is usually higher than at the end of the crop cycle, as some tillers in the clump are lost due to competition during development (Lal et al., 2015; Santos et al., 2019). Because of this, the total DM weight and the NTs are presented and discussed together. They are considered to be related characteristics for assessing a stand of a sugarcane in a nursery area, even taking into account the vegetative phenological stage.

For MEPS, it was found that treatments IS1 and IS2 yielded the highest averages of 1.3 and 1.1 meters, respectively, for the four VS conditions, while IS6 and IS8 had the lowest averages at 0.5 and 0.3 meters, respectively. As for total DM, it was observed that IS1 and IS2 presented mean values much higher than the

other treatments, for the four VS, 35.6 and 18 g plant^{-1}, respectively. IS6, IS7 and IS8 had the lowest average values of total DM, 5.1, 2.9 and 0.3 g plant^{-1}, respectively (Figure 5).

With respect to the IS factor, there was significance for total DM and NT, which highlights the importance of an adequate water supply for the plants to establish good growth. The greater the availability of water in the soil for the plants, the more tillering occurred, and consequently there was a greater accumulation of biomass, reflected in higher DM yield.

It should be noted that there was a greater difference between the treatments for the 93 cm³ VS, in four average groups, unlike the other VS, which presented only two groups. Thus, for a VS of 93 cm³, under the conditions of the experiment, the IS with the lowest water deficit (IS1, IS2 and IS5) promoted cell growth in the plants. In contrast, the IS7 and IS8 had more severe water deficits, and the plants with the 93 cm³ VS stopped growing; IS7 showed the lowest MEPS value of 0.22 m and the largest difference between groups.

4. CONCLUSIONS

It was concluded that for planting biofactory seedlings in moist soil with a frequency of irrigation every 30 mm of accumulated ET_o, the volume of substrate is not important, as no plant death was observed with any of the strategies analyzed in this study. For planting biofactory seedlings in dry soil with irrigation frequency every 30 mm of accumulated ET_o, the minimum reserve substrate volume must be 73 cm³ (plus 20% gel), as the lower volume of 56 cm³ resulted in the death of 50% of the plants. For biofactory planting in dry soil with irrigation frequency every 30 mm of accumulated ET_o, volumes of substrate greater than 93 or 125 cm³ caused a greater initial water consumption by the plants resulting in a water deficit and a reduction in the stand.

ACKNOWLEDGEMENTS

This experiment was supported by the Brazilian Research Agency 'Fundação de Amparo à Pesquisa do Estado de São Paulo', FAPESP 2012/50083–7.

REFERENCES

Allen, R.G.; Pereira, L.S.; Raes, D.; Smith, D. 1998. Crop evaporation guidelines for computing crop water requirements. Rome, FAO. 300 p. (FAO Irrigation and Drainage Paper, 56).

Aquino, G.S.; Medina, C.C.; Silvestre, D.A.; Gomes, E.C.; Cunha, A.C.B.; Kussalva, D.A.O.; Almeida, L.F.; Shahab, M.; Santiago, A.D. 2018. Straw removal of sugarcane from soil and its impacts on yield and industrial quality ratoons. Scientia Agricola 75: 526-529. https://doi.org/10.1590/1678-992X-2017-0093

Barbosa, F.S.; Coelho, R.D.; Barros, T.H.S.; Lizcano, J.V.; Fraga Júnior, E.F.; Santos, L.C.; Leal, D.P.V.; Ribeiro, N.L.; Costa, J.O. 2024. Sugarcane Water Productivity for Bioethanol, Sugar and Biomass under Deficit Irrigation. AgriEngineering 6: 1117-1132. https://doi.org/10.3390/agriengineering6020064.

Castro, S.G.Q.; Rossi Neto, J.; Kölln, O.T.; Borges, B.M.M.N. 2019. Decision-making on the optimum timing for nitrogen fertilization on sugarcane ratoon. Scientia Agricola 76: 237-242. https://doi.org/10.1590/1678-992X-2017-0365

Chaves, S.W.P.; Coelho, R.D.; Costa, J.O.; Tapparo, S.A. 2021. Micrometeorological modeling and water consumption of tabasco pepper cultivated under greenhouse conditions. Italian Journal of Agrometeorology 1: 21-36.

Cherri, A.C.; Vianna, A.C.G.; Ramos, R.P.; Florentino, H.O. 2019. A methodology to determine size and shape of plots for sugarcane plantation. Scientia Agricola 76: 1-8. https://doi.org/10.1590/1678-992X-2017-0174

Costa, J.O.; Almeida, A.N.; Coelho, R.D.; Folegatti, M.V.; José, J.V. 2015. Estimation models of micrometeorological elements in a protected environment. Water Resources and Irrigation Management 4: 25-31.

Farias-Ramírez, A.J.; Duarte, S.N.; Moreno-Pizani, M.A.; de Oliveira Costa, J.; da Silva Barros, T.H.; Coelho, R.D. 2024. Combined effect of silicon and nitrogen doses applied to planting furrows on sugar, biomass and energy water productivity of sugarcane (*Saccharum* spp.). Agricultural Water Management 296: 108796. https://doi.org/10.1016/j.agwat.2024.108796

Hu, S.; Shi, L.; Zha, Y.; Huang, K. 2022. A new sugarcane yield model using SiPAS model. Agronomy Journal 114: 490-507. https://doi.org/10.1002/agj2.20949

Lal, M.; Tiwari, A.K.; Gupta Kavita, G.N. 2015. Commercial scale micropropagation of sugarcane: Constraints and remedies. Sugar Technology 17: 339-347. https://doi.org/10.1007/s12355-014-0345-y

Li, Y.; Mo, Y.Q.; Are, K.S., Huang, Z.; Guo, H.; Tang, C.; Wang, X. 2021. Sugarcane planting patterns control ephemeral gully erosion and associated nutrient losses: Evidence from hillslope observation. Agriculture,

Ecosystems & Environment 309: 107289. https://doi.org/10.1016/j.agee.2020.107289

Maldaner, L.F.; Molin, J.P. 2020. Data processing with rows for sugarcane yield mapping. Scientia Agricola 77: 1-8. https://doi.org/10.1590/1678-992X-2018-0391

Marchiori, P.E.R.; Machado, E.C.; Sales, C.R.G.; Espinoza-Núñez, E.; Magalhães Filho, J.R.; Souza, G.M.; Pires, R.C.M.; Ribeiro, R.V. 2017. Physiological plasticity is important for maintaining sugarcane growth under water deficit. Frontiers in Plant Science 8: 1-12. https://doi.org/10.3389/fpls.2017.02148

Matoso, G.C.; Reis, V.A.; Giacomini, S.J.; Silva, M.T.; Avancini, A.R.; Anjos e Silva, S.D. 2021. Diazotrophic bacteria and substrates in the growth and nitrogen accumulation of sugarcane seedlings. Scientia Agricola 78: 1-9. https://doi.org/10.1590/1678-992X-2019-0035

Otto, R.; Machado, B.A.; da Silva, A.C.M.; de Castro, S.G.Q.; Lisboa, I.P. 2022. Sugarcane pre-sprouted seedlings: A novel method for sugarcane establishment. Field Crops Research 275: 108336. https://doi.org/10.1016/j.fcr.2021.108336

Peloia, P.R.; Bocca, F.F.; Rodrigues, L.H.A. 2019. Identification of patterns for increasing production with decision trees in sugarcane mill data. Scientia Agricola 76: 281-289. https://doi.org/10.1590/1678-992X-2017-0239

Pooja, A.S.N.; Chand, M.; Pal, A.; Kumari, A.; Rani, B.; Goel, V.; Kulshreshtha, N. 2020. Soil moisture deficit induced changes in antioxidative defense mechanism of sugarcane (*Saccharum officinarum*) varieties differing in maturity. Indian Journal of Agricultural Sciences 90: 507–12. https://doi.org/10.56093/ijas.v90i3.101458

Poudial, C.; Costa, L.F.; Sandhu, H.; Ampatzdis, Y.; Odero, D.C.; Arbelo, O.C.; Cherry, R.H. 2022. Sugarcane yield prediction and genotype selection using unmanned aerial vehicle-based hyperspectral imaging and machine learning. Agronomy Journal 114: 2320-2333. https://doi.org/10.1002/agj2.21133

Rocha, B.M.; Fonseca, A.U.; Pedrini, H.; Soares, F. 2022. Automatic detection and evaluation of sugarcane planting rows in aerial images. Information Processing in Agriculture 10: 400-415. https://doi.org/10.1016/j.inpa.2022.04.003

Rocha, G.C.; Sparovek, G. 2021. Scientific and technical knowledge of sugarcane cover-management USLE/RUSLE factor. Scientia Agricola 78: e20200234. https://doi.org/10.1590/1678-992X-2020-0234

Sanches, G.M.; Paula, M.T.N.; Magalhães, P.S.G.; Duft, D.G.; Vitti, A.C.; Kolln, O.T.; Borges, B.M.M.N.; Franco, H.C.J. 2019. Precision production environments for sugarcane fields. Scientia Agricola 76: 10-17. https://doi.org/10.1590/1678-992X-2017-0128

Santos, L.C.; Coelho, R.D.; Barbosa, F.S.; Leal, D.P.; Fraga Júnior, E.F.; Barros, T.H.; Ribeiro, N.L. 2019. Influence of deficit irrigation on accumulation and partitioning of sugarcane biomass under drip irrigation in commercial varieties. Agricultural Water Management 221: 322-333. https://doi.org/10.1016/j.agwat.2019.05.013.

Santos, A.K.B.; Popin, G.V.; Gmach, M.R.; Cherubin, M.R.; Siqueira Neto, M.; Cerri, C.E.P. 2022. Changes in soil temperature and moisture due to sugarcane straw removel in central-southern Brazil. Scientia Agricola 79: e202000309. https://doi.org/10.1590/1678992X.2020-0309

Silva, J.A.G.; Costa, P.M.A.; Marconi, T.G.; Barreto, E.J.S.; Solís-Garcia, N.; Park, J.; Glynn, N.C. 2018. Agronomic and molecular characterization of wild germplasm *Saccharum spontaneum* for sugarcane and energy cane breeding purposes. Scientia Agricola 75: 329-338. https://doi.org/10.1590/1678-992X-2017-0028

Tapparo, S.A., Coelho, R.D., Costa, J.O., Chaves, S.W.P. 2019. Growth and establishment of irrigated lawns under fixed management conditions. Scientia Horticulturae 256: 108580. https://doi.org/10.1016/j.scienta.2019.108580

Tavares, R.L.M.; Oliveira, S.R.M.; Barros, F.M.M.; Farhate, C.V.V.; Souza, Z.M.; La Scala Junior, N. 2018. Prediction of soil CO_2 flux in sugarcane management systems using the Random Forest approach. Scientia Agricola 75: 281-287. https://doi.org/10.1590/1678-992X-2017-0095

van Genuchten, M.T. 1980. A closed-form equation for predicting the hydraulic conductivity of unsaturated soils. Soil Science Society of America Journal 44: 892-898. https://doi.org/10.2136/sssaj1980.03615995004400050002x

Finito di stampare da
Logo s.r.l. – Borgoricco (PD) – Italia

RIGOROUS PEER REVIEW
Each submission to IJAm is subject to a rigorous quality control and peer-review evaluation process before receiving a decision. The initial in-house quality control check deals with issues such as competing interests; ethical requirements for studies involving human participants or animals; financial disclosures; full compliance with IJAm's data availability policy, etc.
Submissions may be returned to authors for queries, and will not be seen by our Editorial Board or peer reviewers until they pass this quality control check.
Each paper is subjected to critical evaluation and review by Field Editors with specific expertise in the different areas of interest and by the members of the international Editorial Board.

OPEN ACCESS POLICY
The Italian Journal of Agrometeorology provides immediate open access to its content. Our publisher, Firenze University Press at the University of Florence, complies with the Budapest Open Access Initiative definition of Open Access: By "open access", we mean the free availability on the public internet, the permission for all users to read, download, copy, distribute, print, search, or link to the full text of the articles, crawl them for indexing, pass them as data to software, or use them for any other lawful purpose, without financial, legal, or technical barriers other than those inseparable from gaining access to the internet itself. The only constraint on reproduction and distribution, and the only role for copyright in this domain is to guarantee the original authors with control over the integrity of their work and the right to be properly acknowledged and cited. We support a greater global exchange of knowledge by making the research published in our journal open to the public and reusable under the terms of a Creative Commons Attribution 4.0 International Public License (CC-BY-4.0). Furthermore, we encourage authors to post their pre-publication manuscript in institutional repositories or on their websites prior to and during the submission process and to post the Publisher's final formatted PDF version after publication without embargo. These practices benefit authors with productive exchanges as well as earlier and greater citation of published work.

COPYRIGHT NOTICE
Authors who publish with IJAm agree to the following terms:
Authors retain the copyright and grant the journal right of first publication with the work simultaneously licensed under a Creative Commons Attribution 4.0 International Public License (CC-BY-4.0) that allows others to share the work with an acknowledgment of the work's authorship and initial publication in IJAm.
Authors are able to enter into separate, additional contractual arrangements for the non-exclusive distribution of the journal's published version of the work (e.g., post it to an institutional repository or publish it in a book), with an acknowledgment of its initial publication in this journal.
Authors are allowed and encouraged to post their work online (e.g., in institutional repositories or on their website) prior to and during the submission process, as it can lead to productive exchanges, as well as earlier and greater citation of published work (See The Effect of Open Access).

PUBLICATION FEES
Unlike many open-access journals, the Italian Journal of Agrometeorology does not charge any publication fee.

WAIVER INFORMATION
Fee waivers do not apply at Firenze University Press because our funding does not rely on author charges.

PUBLICATION ETHICS
Responsibilities of IJAm's editors, reviewers, and authors concerning publication ethics and publication malpractice are described in IJAm's Guidelines on Publication Ethics.

CORRECTIONS AND RETRACTIONS
In accordance with the generally accepted standards of scholarly publishing, IJAm does not alter articles after publication: "Articles that have been published should remain extant, exact and unaltered to the maximum extent possible". In cases of serious errors or (suspected) misconduct IJAm publishes corrections and retractions (expressions of concern).

Corrections
In cases of serious errors that affect or significantly impair the reader's understanding or evaluation of the article, IJAm publishes a correction note that is linked to the published article. The published article will be left unchanged.

Retractions
In accordance with the "Retraction Guidelines" by the Committee on Publication Ethics (COPE) IJAm will retract a published article if:
- there is clear evidence that the findings are unreliable, either as a result of misconduct (e.g. data fabrication) or honest error (e.g. miscalculation)
- the findings have previously been published elsewhere without proper crossreferencing, permission or justification (i.e. cases of redundant publication)
- it turns out to be an act of plagiarism
- it reports unethical research.
- An article is retracted by publishing a retraction notice that is linked to or replaces the retracted article. IJAm will make any effort to clearly identify a retracted article as such.

If an investigation is underway that might result in the retraction of an article IJAm may choose to alert readers by publishing an expression of concern.

ARCHIVING
IJAm and Firenze University Press are experimenting a National legal deposition and long-term digital preservation service.

SUBMITTING TO IJAm
Submissions to IJAm are made using FUP website. Registration and access are available at: https://riviste.fupress.net/index.php/IJAm/submission
For more information about the journal and guidance on how to submit, please see https://riviste.fupress.net/index.php/IJAm/index

Principal Contact
Simone Orlandini, University of Florence
simone.orlandini@unifi.it

Support Contact
Alessandro Pierno, Firenze University Press
alessandro.pierno@unifi.it

GUIDE FOR AUTHORS
1. Manuscript should refer to original researches, not yet published except in strictly preliminary form.
2. Articles of original researches findings are published in Italian Journal of Agrometeorology (IJAm), subsequent to critical review and approval by the Editorial Board. External referees could be engaged for particular topics.
3. Three types of paper can be submitted: original paper, review, technical note. Manuscript must be written in English. All pages and lines of the manuscript should be numbered.
4. First Name, Last Name, position, affiliation, mail address, telephone and fax number of all the Co-Authors are required. Corresponding Authors should be clearly identified.
5. The abstract should be no longer than 12 typed lines.
6. Full stop, not comma, must be used as decimal mark (e.g. 4.33 and not 4,33).
7. Figures, tables, graphs, photos and relative captions should be attached in separate files. All images must be vector or at least 300 effective ppi/dpi to ensure quality reproduction.
8. Captions should be written as: Fig. x – Caption title, Tab. x – Caption title. Images should be referred to in the text as (Fig. x), (Tab. x).
9. Proof of the paper (formatted according to the Journal style) will be sent to the Corresponding Author for proof reading just one time. Corrections can be made only to typographical errors.
10. All the references in the text must be reported in the "References" section and vice-versa. In the text, only the Author(s) last name must be present, without the name or the first letter of the name (e.g. "Rossi, 2003" and not "Federico Rossi, 2003" or "F. Rossi, 2003"). If two authors are present, refer to them as: "Bianchi and Rossi, 2003" in the text (do not use "&" between the surnames). If more than two Authors are present, refer to them as: "Bianchi et al., 2003" in the text.
For journals, references must be in the following form:
Bianchi R., Colombo B., Ferretti N., 2003. Title. Journal name, number: pages.
For books:
Bianchi R., Colombo B., Ferretti N., 2003. Book title. Publisher, publishing location, total number of pages pp.
Manuscripts "in press" can be cited.

BECOME A REVIEWER
Peer review is an integral part of the scholarly publishing process. By registering as a reviewer, you are supporting the academic community by providing constructive feedback on new research, helping to ensure both the quality and integrity of published work in your field. Once registered, you may be asked to undertake reviews of scholarly articles that match your research interests. Reviewers always have the option to decline an invitation to review and we take care not to overburden our reviewers with excessive requests.
You must login before you can become a reviewer.
If you don't want to be a reviewer anymore, you can change your roles by editing your profile.

COMPETING INTERESTS
You should not accept a review assignment if you have a potential competing interest, including the following:
- Prior or current collaborations with the author(s)
- You are a direct competitor
- You may have a known history of antipathy with the author(s)
- You might profit financially from the work

Please inform the editors or journal staff and recuse yourself if you feel that you are unable to offer an impartial review.
When submitting your review, you must indicate whether or not you have any competing interests.

Italian Journal of Agrometeorology

Rivista Italiana di Agrometeorologia

n. 2 – 2024

Table of contents